

Linearization of power amplifiers by means of digital predistortion

Linearisierung von Leistungsverstärkern mittels digitaler Vorverzerrung

Der Technischen Fakultät der
Universität Erlangen-Nürnberg
zur Erlangung des Grades

Doktor-Ingenieur

vorgelegt von
Nazim Ceylan
Erlangen - 2005

Als Dissertation genehmigt von
der Technischen Fakultät der
Universität Erlangen-Nürnberg

Tag der Einreichung: 07.04.2005
Tag der Promotion: 17.10.2005
Dekan: Prof. Dr. Alfred Leipertz
Berichterstatter: Prof. Dr. Robert Weigel
Prof. Dr. Christian Schäffer

Kurzfassung

In der neuen Generation von Mobilfunksystemen (WCDMA, CDMA2000, EDGE) werden Modulationsformate implementiert, die das jeweilige Frequenzspektrum effizient ausnutzen. Die Schlüsselvoraussetzung dafür ist eine hohe Linearität des Leistungsverstärkers (PA). Diese Komponente des Senders weist zudem den höchsten Leistungsverbrauch auf, so dass sie neben den Anforderungen an die Linearität auch über einen hohen Wirkungsgrad verfügen muss. Dieser Umstand ist besonders bei batteriebetriebenen Systemen von grosser Bedeutung.

Das Ziel, einen PA mit hoher Linearität und gleichzeitig hohem Wirkungsgrad zu entwerfen führt zu Anforderungen, die sich gegenseitig ausschließen, so dass ein Kompromiss zwischen Wirkungsgrad und Linearität eingegangen werden muss. Die Arbeitspunkte von PA's werden gewöhnlich in einem Bereich weit unterhalb der Sättigung (back-off) betrieben, um die Spezifikationen bezüglich ihrer Linearität einzuhalten, welche aber auf einen niedrigen Wirkungsgrad hinausführt. Eine mögliche Lösung ist es, PAs in der Nähe des Sättigungsbereiches zu betreiben, wo sie einen hohen Wirkungsgrad haben. Ihre Eigenschaften bzgl. der Linearität werden dann durch Linearisierungsverfahren verbessert.

Es gibt verschiedene Linearisierungsmethoden für PA, die im Wesentlichen durch die Oberbegriffe Feedback, Feedforward und Vorverzerrung klassifiziert werden können. Im Rahmen dieser Dissertation wird das weite Feld der Linearisierung von PA auf die Untersuchung sog. "Look-up-Table" (LUT) basierter gedächtnisloser digitaler Vorverzerrung (MDP) eingeschränkt. Dieses Verfahren wird favorisiert, da der PA für die hohen Anforderungen der Leistungsfähigkeit dimensioniert werden und gleichzeitig ihre Linearität mit der MDP unabhängig davon verbessert werden kann. Im Weiteren wird es im digitalen Basisband realisiert und ist vorteilhaft aufgrund seiner hohen Leistungsfähigkeit, der Einfachheit, dem niedrigen Leistungsverbrauch, der Zuverlässigkeit, der Flexibilität, den niedrigen Kosten und der Grösse. Diese Kombination ergibt eine flexible Designmethode, um PA mit guter Linearität und gleichzeitig gutem Wirkungsgrad zu entwerfen.

Digitale Vorverzerrung ist dafür bekannt, eine Linearisierungsmethode mit hohem Leistungsverbrauch und komplizierter Linearisierungsverfahren zu sein, die man in Basisstationen anwendet, wo äusserst hohe Anforderungen an die Linearität gestellt werden. Studien zu MDP zeigten, dass diese Methode auch für Mobilstationen anwendbar ist und eine signifikante Linearitätsverbesserung erreicht werden kann.

Die hauptsächlichen Leistungen dieser Arbeit sind:

- Eine genaue und einfache PA-Charakterisierungsmethode wird vorgeschlagen. Die Zahl der erforderlichen Analogbestandteile der herkömmlichen Methode wird reduziert, und ein in Systemsimulationen verwendbares Verhaltensmodell wird erstellt [1, 2].

- Der LUT basierte MDP ist im Stande, den Senderwirkungsgrad in WCDMA und EDGE Mobilstationen bedeutsam zu verbessern. Die Methode ist dazu fähig, die in einem WCDMA-System maximal erreichbare lineare Ausgangsleistung um 2 dB und den durchschnittlichen System-Wirkungsgrad um 20% zu verbessern, im Vergleich zu einem System ohne Vorverzerrung [3]. Der verwendete PA ist für ein TDMA - System dimensioniert. In EDGE ist eine Verbesserung der linearen Ausgangsleistung von 3.5 dB zu verzeichnen und der Wirkungsgrad an der maximal erreichbaren Ausgangsleistung wird von 15% auf 23% erhöht mit einem vorhandenen GSM PA [2]. Die benötigten Modifizierungen in vorhandenen Systemen wurden bestimmt, um MDP zu implementieren.
- Eine neue LUT Adressierungsmethode wird vorgeschlagen, die den Leistungsverbrauch im MDP reduzieren kann [4]. Das ist nützlich in Sendern, die ihre Basisbandsignale in kartesischer Form haben.
- Es wird geprüft, ob dass LUT basierte MDP dazu fähig ist, die Linearität der hocheffizienten Senderarchitektur Envelope-Elimination and Restoration (EER) in EDGE Mobilstationen mit PAs in Sättigung zu verbessern. Spezifikationen werden erfüllt für Ausgangsleistungsniveaus von 20 bis 29.5 dBm mit nur einer Netzspannungsabstimmung. Durch zusätzliche Bias-Modulation kann die Systemleistung weiter verbessert werden.

Abstract

In new generation mobile communication systems (WCDMA, CDMA2000, EDGE), where spectrum efficient linear modulation formats are used, power amplifier (PA) linearity is a key requirement. On the other hand the PA is one of the most power consuming components in a mobile communication system. Therefore its power added efficiency (PAE) and linearity must be simultaneously high especially in battery operated handsets. However, normally a compromise between PAE and linearity has to be accepted in a design. PAs are usually operated with a back-off in order to fulfill linearity specifications, which in turn results in lower power efficiency. One possible solution is to operate PAs near to saturation where they are highly nonlinear but efficient, and linearize them by using some external circuitry.

There are different PA linearization methods available which can be classified mainly as feedback, feedforward and predistortion. This thesis deals mainly with look-up table (LUT) based memoryless digital predistortion (MDP) realized in digital baseband due to its high performance, simplicity, low power consumption, reliability, flexibility, low cost and size. It is attractive because the PA can be designed for high efficiency and the linearity can be improved independently with MDP. The combination of both gives design flexibility for achieving good linearity and efficiency at the same time. Although digital predistortion is known to be a high power consuming and complicated linearization method applicable in base stations where extremely high linearity is required, the studies on MDP showed that with a careful design it is also applicable in handsets resulting in significant linearity improvement.

The main achievements of this thesis are:

- An accurate and simple PA characterization method is proposed. The number of required analog components in the conventional measurement setup is reduced and a behavioral model based on large signal S-parameters usable in system simulations is generated [1, 2].
- The LUT based MDP is able to improve the transmitter efficiency significantly in WCDMA and EDGE handsets. The method is proved to be capable of increasing the maximum achievable linear output power by 2 dB and average system efficiency by 20% compared to without predistortion case in WCDMA using an available linear PA designed for TDMA [3]. In EDGE the improvement in linear output power is 3.5 dB and the efficiency at maximum linear output power is increased from 15% to 23% using an available GSM PA [2]. Required modifications in available systems are determined in order to implement the system.
- A novel LUT addressing method capable of reducing power consumption in MDP systems is proposed [4]. It is useful in transmitters having baseband signals in Cartesian form.

- It is verified that LUT based MDP is able to improve the linearity of highly efficient transmitter architecture envelope elimination and restoration (EER) in EDGE handsets which uses highly efficient saturated power amplifiers. Specifications are fulfilled for 20 to 29.5 dBm output power levels by modulating just the supply voltage. The performance can be improved further using additional bias modulation.

Contents

- 1 Introduction** **1**
 - 1.1 Outline of the thesis 2

- 2 Power amplifiers** **4**
 - 2.1 Power amplifier fundamentals 4
 - 2.1.1 Gain and output power 4
 - 2.1.2 Linearity 4
 - 2.1.3 Efficiency 8
 - 2.1.4 Back-off 10
 - 2.1.5 Matching 11
 - 2.2 Amplifier classes 12
 - 2.2.1 Class A amplifiers 13
 - 2.2.2 Class B amplifiers 14
 - 2.2.3 Class AB amplifiers 15
 - 2.2.4 Class C amplifiers 17
 - 2.2.5 Class D amplifiers 17
 - 2.2.6 Class E amplifiers 18
 - 2.2.7 Class F amplifiers 19
 - 2.3 Amplifier topologies 20
 - 2.3.1 Single-ended power amplifiers 20
 - 2.3.2 Differential power amplifiers 21
 - 2.3.3 Balanced power amplifiers 21
 - 2.4 Investigated power amplifiers 22

- 3 Mobile communications** **23**
 - 3.1 Digital modulation formats 23
 - 3.1.1 Amplitude shift keying (ASK) 24

3.1.2	Phase shift keying (PSK)	24
3.1.3	Quadrature amplitude modulation (QAM)	26
3.1.4	Gaussian minimum shift keying (GMSK)	26
3.2	Cellular systems	27
3.2.1	GSM/EDGE	28
3.2.2	WCDMA/CDMA2000	30
4	RF transmitters	33
4.1	Transmitter architectures	33
4.1.1	Direct conversion (homodyne) architecture	33
4.1.2	Two-step conversion (heterodyne) architecture	35
4.1.3	Modulation loop	36
4.1.4	Polar modulator	37
4.2	Nonlinear transmitter	37
4.3	Linear transmitters	38
4.3.1	Linear transmitter with linear PA	39
4.3.2	Envelope elimination and restoration (EER) / Polar transmitter (PTx)	39
4.3.3	Polar loop transmitter (PLTx)	43
4.3.4	Envelope Follower	44
4.3.5	Power Tracking	45
5	Power amplifier linearization methods	47
5.1	Feedback	47
5.1.1	RF feedback	48
5.1.2	Polar loop	49
5.1.3	Cartesian loop	50
5.2	Feedforward	51
5.3	Predistortion	53
5.3.1	Analog predistortion	54
5.3.2	Digital predistortion	56
5.4	Memoryless digital predistortion (MDP)	58
5.4.1	Look-up table (LUT) based predistortion	59
5.4.2	Polynomial predistorter	68
5.4.3	Effects of system imperfections	71
5.5	Predistortion of PAs with memory	74

6	Memoryless digital predistortion for terminals	78
6.1	Power amplifier characterization	79
6.2	Application of MDP in EDGE	87
6.2.1	System performance	89
6.2.2	Quantization analysis	93
6.2.3	Effects of antenna mismatch	95
6.2.4	Required system modifications	97
6.3	Application of MDP in WCDMA	101
6.4	MDP for PAs with DC-DC converters	105
6.5	Symbol addressing	109
6.6	MDP implemented as open- and closed-loop	115
6.6.1	Open-loop	116
6.6.2	Closed-loop	117
6.7	Application of MDP in polar transmitter concept	120
6.7.1	PA characterization	120
6.7.2	System performance	123
7	Conclusions	125
7.1	Future work	126
	Bibliography	128

Acknowledgements

I would like to express my deep appreciation to my advisor Prof. Dr. Robert Weigel for his guidance and support throughout the study.

The work presented was supported by Infineon Technologies AG, department for RFICs, Munich. I would like to gratefully acknowledge the help, comments and guidance received from Dr. Jan-Erik Müller. I am also grateful to Stefan Beyer, Dr. Volker Thomas and Josef Fenk for making this study at Infineon possible.

I would like to express my thanks to Dr. Andreas Holm, Dr. Winfried Bakalski and Nick Shute for critical reading of the manuscript and informative discussions. My gratitude also goes to Peter Pfann and Dr. Alexander Zenzinger for valuable discussions and help during the measurements. Further I want to thank my friends Özhan Koca, Caglayan Erdem, Krzysztof Kitlinski and Martin Simon for their help and motivating discussions with them.

Finally, I would like to thank my wife Esra for her understanding and valuable support and my parents for their encouragement during my PhD studies.

List of Abbreviations

AC	Alternating Current
ACI	Adjacent Channel Interference
ACPR	Adjacent Channel Power Ratio
ACPR I	Adjacent Channel Power Ratio
ACPR II	Alternate Channel Power Ratio
ADC	Analog-to-Digital Converter
ADS	Advanced Design System
AM	Amplitude Modulation
ASK	Amplitude Shift Keying
BALUN	BALanced to Unbalanced
BER	Bit Error Rate
BPF	Band-Pass Filter
BPSK	Binary Phase Shift Keying
BS	Base Station
CDMA	Code Division Multiple Access
CMOS	Complementary Metal Oxide Semiconductor
C_p	Output power capability
DAC	Digital-to-Analog Converter
DC	Direct Current
DP	Digital Predistortion
DPCCH	Dedicated Physical Control CHannel
DPDCH	Dedicated Physical Data CHannel
DSP	Digital Signal Processing
DSSS	Direct Sequence Spread Spectrum
DUT	Device Under Test
EDGE	Enhanced Data for Gsm Evolution
EER	Envelope Elimination and Restoration
EVM	Error Vector Magnitude
FDD	Frequency Division Duplex
FDMA	Frequency Division Multiple Access
FM	Frequency Modulation
FPGA	Field Programmable Gate Array
GMSK	Gaussian Minimum Shift Keying
GSM	Global System for Mobile communications
I	Current
I_q	Quiescent current
IMD	InterModulation Distortion
IMP	InterModulation Product
IC	Integrated Circuit
IF	Intermediate Frequency
LAN	Local Area Networking

LNA	Low Noise Amplifier
LO	Local Oscillator
LPF	Low-Pass Filter
LUT	Look-Up Table
MDP	Memoryless Digital Predistortion
MMIC	Monolithic Microwave Integrated Circuit
MSK	Minimum Shift Keying
OBO	Output Back-Off
OQPSK	Offset Quadrature Phase Shift Keying
OSR	OverSampling Ratio
PA	Power Amplifier
PAE	Power Added Efficiency
PAR	Peak-to-Average Ratio
PBO	Peak Back-Off
PFD	Phase-Frequency Detector
P_{in}	Input Power
PLL	Phase-Locked Loop
PLTx	Polar Loop Transmitter
PM	Phase Modulation
P_{max}	Maximum Power
P_{out}	Output Power
P_{sat}	Saturated Output Power
PSK	Phase Shift Keying
PTx	Polar Transmitter
QAM	Quadrature Amplitude Modulation
QPSK	Quadrature Phase Shift Keying
RF	Radio Frequency
RAM	Random Access Memory
RMS	Root Mean Square
RRC	Root Raised Cosine
SAW	Surface Acoustic Wave
SDM	Sigma-Delta Modulator
SF	Spreading Factor
SMIQ	Signal generator from Rohde & Schwarz
SNR	Signal-to-Noise Ratio
TDD	Time Division Duplex
TDMA	Time Division Multiple Access
UMTS	Universal Mobile Telecommunications System
V	Voltage
VCO	Voltage Controlled Oscillator
VSWR	Voltage Standing Wave Ratio
WCDMA	Wideband Code Division Multiple Access
1G	1 st Generation
2G	2 nd Generation
2.5G	2.5 th Generation
3G	3 rd Generation

Chapter 1

Introduction

Products in the area of mobile communications became very important in our daily life in the last decade and it seems that their importance will increase further. Manufacturers try to improve their products by adding new features and services to increase the number of subscribers. This forces them to use new system topologies, reduce power consumption, increase system integration in order to increase the battery life and reduce the size and cost of the products.

Higher number of subscribers and new services require wider spectrum bandwidths which is not easily available due to current fixed spectrum allocations. The solution is to use spectrum efficient modulation schemes as in 2.5th and 3rd generation (2.5G, 3G) mobile communication systems such as EDGE (Enhanced Data for GSM Evolution) and UMTS (Universal Mobile Telecommunications System) in Europe. In 2nd generation (2G) systems such as GSM (Global System for Mobile Communications) the phase of the carrier is modulated and its envelope is kept constant whereas in the 2.5G and 3G systems the amplitude of the carrier (signal envelope) is also modulated. This is the reason for increase in spectrum efficiency (transmitted bits/Hz) compared to 2G systems.

New generation mobile communication systems are very sensitive to nonlinearities in their transmitter paths because their signals have fluctuating envelopes. The nonlinearity in a transmitter is mostly due to the PA at the end of the chain. Therefore the PA is operated with some back-off in order to obtain desired linearity. This makes the PA operate with low power efficiency which is not the case in the phase modulated constant envelope 2G systems. If the system linearity requirements are stringent, then the efficiency is worse because the PA must be operated with more back-off. Since PA is one of the most power consuming components in a mobile communication transmitter, every small change in its efficiency has a significant effect on overall system efficiency and therefore talk time. This is very important especially in battery operated mobile terminals. Moreover in low efficient systems a significant part of the power is dissipated as heat which may cause high case temperatures.

The linearity requirement in a transmitter path makes the design of PAs difficult because it must be linear and at the same time highly efficient. Linearization techniques can be applied to improve the linearity, decrease the required amount of back-off and hence increase the efficiency of PAs. There are different types of linearization techniques

which can be classified under three main groups: feedback, feedforward and predistortion. In this thesis a LUT based MDP system is investigated which is simple, low power consuming, reliable, flexible, having low cost and size, and applicable to handset (also called terminal) PAs achieving significant performance improvement.

In today's mobile communication systems the overall system performance is important. This means the individual integrated circuits (IC) must not necessarily have very high performance but the systems composed of these ICs and embedded within an adequate architectural approach require high performance in terms of linearity and efficiency. This makes digital predistortion (DP) attractive because the PA can be designed for high efficiency and the linearity can be improved with DP. The combination of both gives design flexibility for achieving good linearity and efficiency at the same time. The additional efforts for the processor benefit in the long term from a fast and continuous improvement in digital IC technology, as its performance benefits from device scaling. Power consumption decreases, achievable clock frequency increases and digital ICs are more flexible and robust compared to analog ICs. DP is a promising linearization technique because in future more and more tasks will be done in digital domain much more easily.

1.1 Outline of the thesis

In chapter 2 PAs are considered in general. The fundamental terms such as gain, linearity, efficiency etc. are explained, different PA classes and topologies are considered. The PAs used for the work are listed.

Chapter 3 explains 2G, 2.5G and 3G mobile communication systems GSM, EDGE, CDMA2000 (Code Division Multiple Access 2000) and WCDMA (Wideband CDMA). Their system capacity, advantage and disadvantages are mentioned and their specifications especially in terms of adjacent channel power ratio and error vector magnitude are explained, the effects of PA nonlinearities are discussed.

Various transmitter architectures are described in chapter 4 with respect to their benefits and drawbacks for future high efficient terminal transmitter architectures. These are nonlinear transmitters as in GSM, linear transmitters as in EDGE, WCDMA or CDMA2000 and polar transmitter which is able to handle both linear and nonlinear systems at the same time.

Linearization methods are explained in detail throughout chapter 5. They can be classified mainly as feedback, feedforward and predistortion systems, where various implementation types (polar, cartesian, digital, analog) are possible. DP systems having the capability to correct memory effects are complex and may be applicable in base stations. MDP has a good performance in terminal PAs due to small memory effects and it has been observed to be simple, low power consuming, reliable, flexible, having low cost and low size. This chapter concentrates on predistortion and explains it in detail.

In chapter 6 static and dynamic PA AM/AM and AM/PM characterization methods are compared. Application of MDP in EDGE and WCDMA terminals using linear mode

PAs is investigated. Required system modifications in available systems and possible efficiency improvement with a DC-DC converter are also investigated. A new addressing method useful in transmitters with Cartesian form baseband signals is proposed and tested successfully. Also some novel open- and closed-loop MDP implementations usable in terminal applications are proposed. Moreover the application of MDP in EER is investigated.

Chapter 7 concludes the thesis and points out possible future work for implementing the proposed method in mobile communication systems.

Chapter 2

Power amplifiers

2.1 Power amplifier fundamentals

PAs are devices used to amplify signals in order to obtain high signal powers necessary for transmission via a propagation medium. They are indispensable in wireless communications. The following section is a brief introduction of some fundamental PA features.

2.1.1 Gain and output power

In mobile communications each system has its specifications which must be fulfilled. Obtaining output powers high enough for various applications is a very important task achieved by PAs. In general the information signal is first modulated and upconverted, and then sent to a PA. This input is multiplied with a gain factor and the desired output power is obtained. Gain is handled in dB and power in dBm throughout this thesis. Fig. 2.1 (a) and (b) show example PA output and gain versus input power characteristics of a linear PA respectively. PA output versus input power characteristics shown in fig. 2.1 (a) is also called AM/AM characteristics of the PA

As it can be seen from the figures the gain is constant for low input powers and it reduces with approaching its saturation region. Saturation region is easily visible from the output power curve where the output power stays constant with further increase of the input power. In the fig. 2.1 (a) 1 dB compression point is also shown, which refers to the output power level at which the amplifier's transfer characteristics deviates from the ideal one by 1 dB [5]. This is a widely used measure of amplifier linearity revealing roughly which linear output power value is achievable with the device under test (DUT).

2.1.2 Linearity

Linearity is one of the key issues in PAs used in new generation mobile communication systems [5, 6]. The linearity of a PA is easily visible in its gain and phase characteristics.

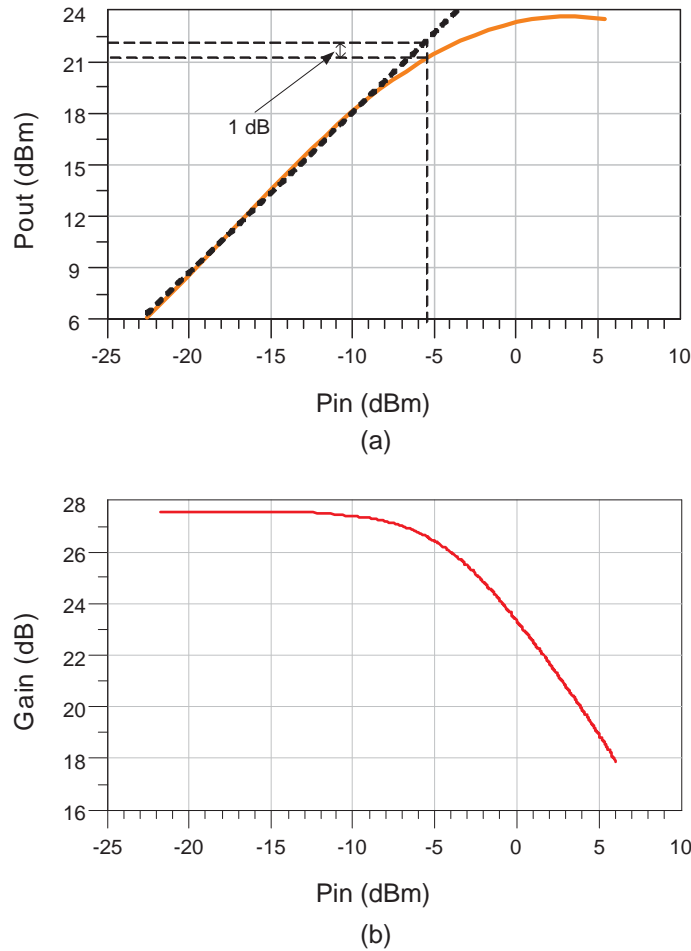


Figure 2.1: (a) Output power and (b) gain characteristics of a PA.

If an amplifier has a constant gain and phase response for an input power region, then the amplifier is said to be linear for this region. Fig. 2.2 (a) and (b) show typical and desired amplifier gain and phase characteristics respectively. Solid lines are gain and phase characteristics of a memoryless PA and dashed lines indicate the ideally linear PA gain and phase characteristics. In general after reaching a relatively high output power value the amplifier gain decreases gradually with increasing input power because the PA reaches its saturation point. Phase nonlinearity increases also with increasing input power. Amplifier phase characteristics shown in fig. 2.2 (b) is also called as AM/PM characteristics. The other way of determining PA nonlinearity is using second and third order intercept points. The advantage is that it is a fixed quantity from which the distortion level at a particular operating point may be predicted [5].

There are some conventional analog techniques used to design linear PAs by optimizing linearity and efficiency through bias and matching adjustments [7, 8]. However, these analog techniques have their limits and achieving a highly linear gain and phase response simultaneously is very difficult. Currently these methods are widely used and achievable performance is close to its limits. Therefore some other sophisticated solutions are necessary to solve the problem.

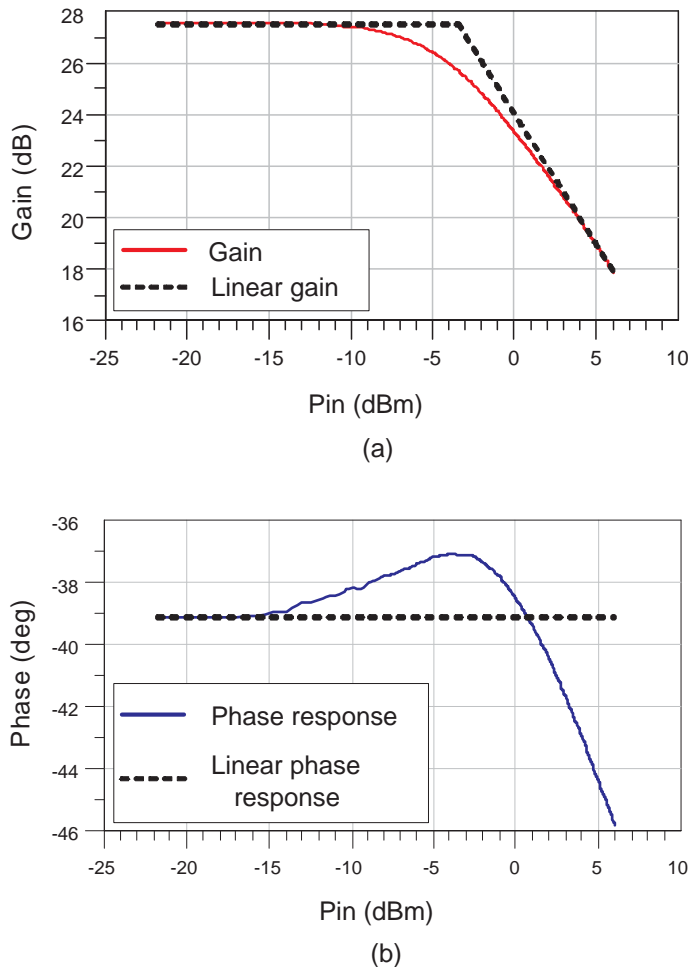


Figure 2.2: Nonlinear and ideally linear PA (a) gain and (b) phase characteristics.

The reason why the linearity is so important is the varying signal envelopes in spectrum efficient modulation types used in new generation mobile communication systems [5]. If signals have constant envelopes like in FM (Frequency Modulation) or GMSK (Gaussian Minimum Shift Keying) then PA linearity is not an important issue because the instantaneous input power stays constant and therefore there are no gain and phase variations for a specific operation point. However, if the signal envelope varies, then the instantaneous input power changes continuously. As a result the signal at the PA output is distorted if the amplifier gain and phase response are not linear. This distortion can be measured in terms of IMD (Intermodulation Distortion), ACPR (Adjacent Channel Power Ratio) or EVM (Error Vector Magnitude) [6]. Fig. 2.3 (a) and (b) show possible degradation of PA output ACPR (for WCDMA) and EVM due to its nonlinearity. If a two-tone signal is applied to a nonlinear device, then a large number of harmonics and IMPs (Intermodulation Products) are generated depending on the nonlinearity degree of the device. The odd-order IMPs (3^{rd} , 5^{th} , 7^{th} , etc) are the most important ones because they fall into the neighborhood of the main signal and therefore not easily filterable. The most commonly used measure of IMD is the ratio of the largest IMP to the amplitude of one of the two equal tones [5]. ACPR is caused by IMPs falling in

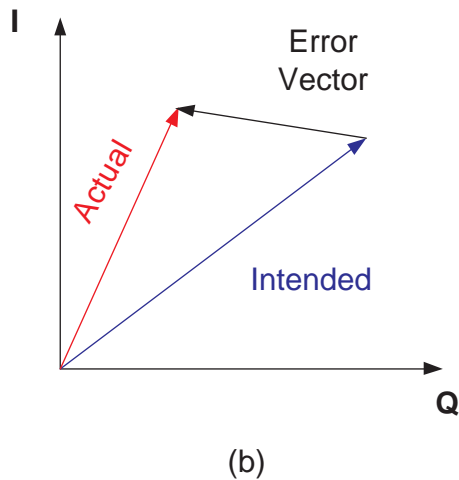
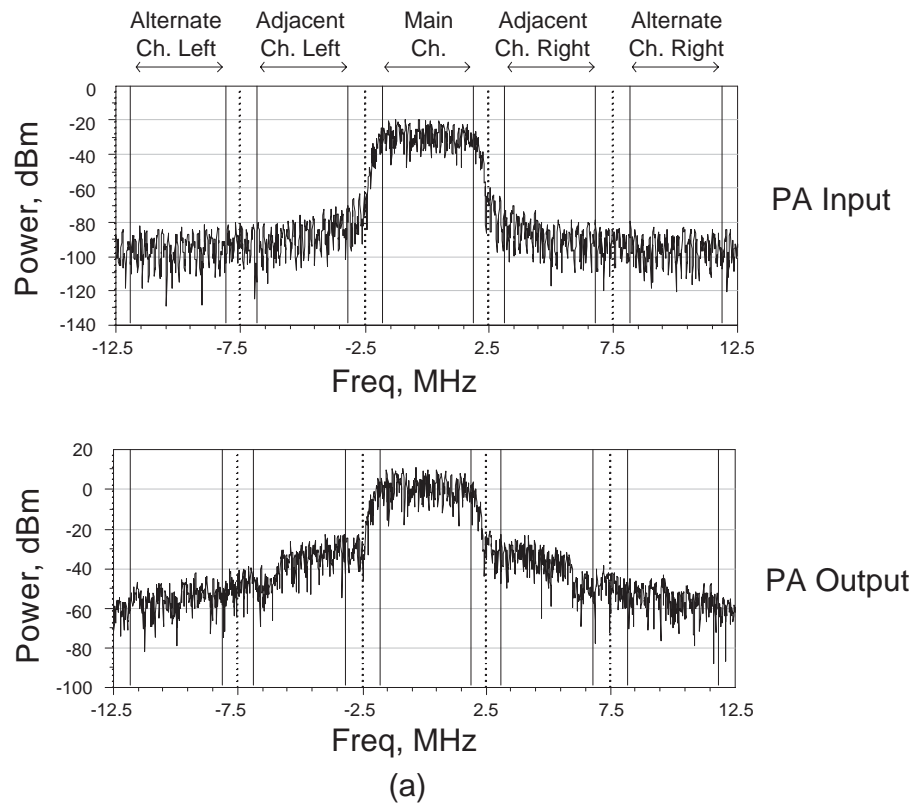


Figure 2.3: Effects of PA nonlinearity on (a) ACPR for a WCDMA signal and (b) EVM [9].

the signal neighborhood in the case of complex modulated signals composed of a lot of spectral components. It is defined as the ratio of the distortion signal power falling in the adjacent channels to the carrier power (main channel power) in dB [9]. In fig. 2.3 (a) PA input and output signals are compared. Under ideal conditions PA output is a shifted version of the input in the vertical direction by an amount equal to PA gain. However, the PA output in fig. 2.3 (a) has some unwanted distortion elements

in the neighbor channels indicating PA nonlinearity. ACPR is a very critical issue in mobile communications. A transmitter must fulfill the specifications and not to disturb dedicated neighbor channels because they are usually used by other transmitters.

EVM can be defined as the distance between the desired and actual signal vectors (error vector), normalized to a fraction of the signal amplitude [9]. In fig. 2.3 (b) the degradation in output signal phasor is shown which corresponds the signal constellation. The actual value of the constellation point can deviate from the ideal one significantly depending on PA nonlinearity. EVM can be defined for each symbol k as

$$EVM(k) = \frac{|E(k)|}{\sqrt{\frac{1}{N} \sum_{k=1}^N |S(k)|^2}} \quad (2.1)$$

where $E(k)$ is the error vector for symbol k , $S(k)$ is the ideal signal vector of the symbol k and N is the number of symbols. Root-mean-square (RMS) value of EVM for a number of symbols is a widely used measure of system linearity and it can be defined as

$$EVM_{RMS} = \frac{\sqrt{\sum_{k=1}^N |E(k)|^2}}{\sqrt{\sum_{k=1}^N |S(k)|^2}} \quad (2.2)$$

EVM is an inband distortion causing high bit error rates during reception of the transmitted data. Therefore EVM specifications must also be fulfilled in order to have proper communication.

2.1.3 Efficiency

Efficiency is another key issue in mobile communications [6, 10], especially for battery operated mobile terminals. It has two widely used definitions, drain (or collector) efficiency and PAE (Power Added Efficiency). Drain efficiency is the ratio of output radio frequency (RF) power to input DC power

$$\eta = P_{outRF}/P_{DC} \quad (2.3)$$

and PAE is the overall efficiency obtained by subtracting input drive power from output RF power and divide it by input DC power [9].

$$PAE = (P_{outRF} - P_{drive})/P_{DC} \quad (2.4)$$

If the gain of a PA is high then its drain efficiency and PAE are close and simply drain efficiency can be used in calculations.

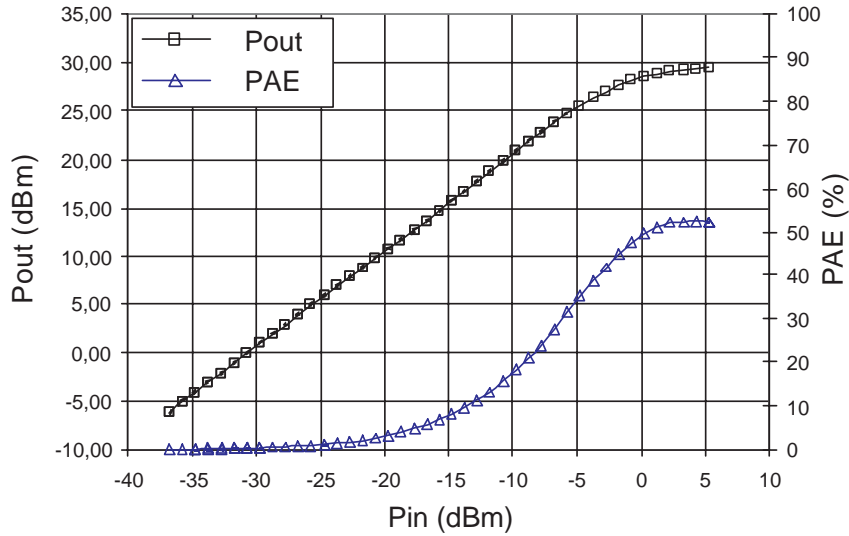


Figure 2.4: Measured output power and efficiency curves of a solid state PA.

Fig. 2.4 shows the measured output power and efficiency characteristics of a commercially available solid state PA. In power amplifiers normally the efficiency increases with increasing output power as shown in the figure. Therefore it is advantageous to operate PAs near to saturation. With PA linearization techniques it is possible to use smaller PAs with lower saturation powers compared to conventional linear PAs, which results in general in higher efficiency operation. Normally PA designers try to obtain the highest efficiency at maximum output power which may be useful in systems delivering always (or most of the time) their maximum output power. However, for new generation mobile communication systems having high output power dynamic ranges as in EDGE and WCDMA, this may not be the optimum way of PA design. In these systems the probability of transmitting maximum output power (P_{max}) can be very low (in the order of 1-2%) and a significantly lower output power value (in general 10-20 dB lower than P_{max}) has the maximum probability of occurrence. Fig. 2.5 shows an estimated function of output power occurrence probability in UMTS. The function can be different in different regions depending on dedicated cell size for each base station, fading due to buildings etc. In such systems PA efficiency must be improved not only at P_{max} but also for lower output powers in order to improve the average efficiency, which determines battery life of a portable system.

From fig. 2.5 it is obvious that P_{max} is required seldom and an output power 15 dB lower than P_{max} occurs most frequently. Therefore the average efficiency of a PA is much more important than its maximum efficiency. Average power efficiency of a PA can be calculated as [11]

$$\eta_{AVG} = \frac{\sum_{k=1}^n \rho_k P_{outRF,k}}{\sum_{k=1}^n \rho_k P_{inDC,k}} \quad (2.5)$$

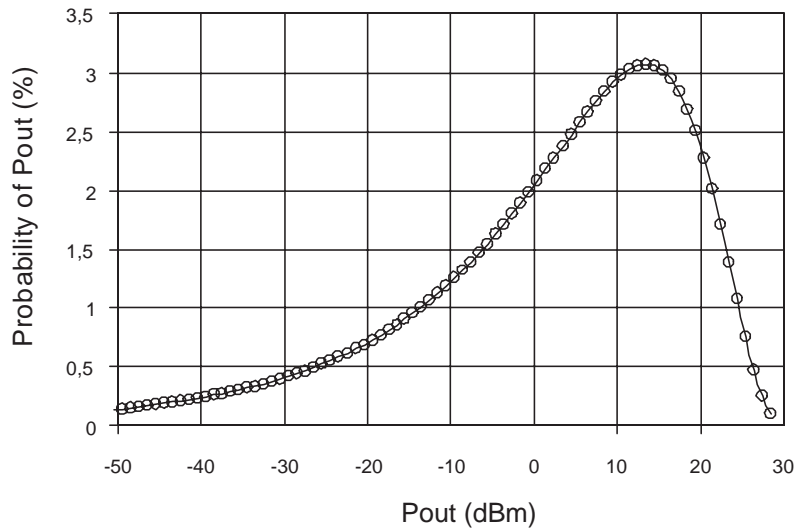


Figure 2.5: Estimated probability of handset PA output power occurrence in UMTS.

where ρ_k is the occurrence probability of k^{th} output power and $P_{outRF,k}$ and $P_{inDC,k}$ are the corresponding output RF and input DC powers.

2.1.4 Back-off

Output back-off (OBO) for a PA is defined as the ratio of saturated output power (P_{sat}) to delivered output power in dB [12]. Peak back-off (PBO) is another term used for systems having varying envelope input signals. It is the ratio of P_{sat} to peak instantaneous power of the output [12]. They can be defined as

$$\text{OBO}[\text{dB}] = 10 \log(P_{sat}/P_{outAV}) \quad (2.6)$$

$$\text{PBO}[\text{dB}] = \text{OBO}[\text{dB}] - \text{PAR}[\text{dB}] \quad (2.7)$$

where PAR is the peak-to-average ratio of the signal. In fig. 2.6 OBO, PBO and PAR are illustrated.

PARs at input and output are equal to each other if the PA operates in linear region. In conventional solid state PAs linearity increases normally with increasing back-off. If back-off is reduced then the PA operates close to saturation and PAR ratio at the output is normally reduced due to compression. This is called AM/AM distortion and its effects in output spectrum are additional distortion signals in the neighbor channels and inband. There is also an increase in phase nonlinearity with decreasing back-off, which is visible in fig. 2.2 (b). This is called as AM/PM distortion and it contributes to PA output spectrum distortion. AM/AM and AM/PM distortion in digital modulation formats are also visible in their constellation and eye diagrams resulting in high BER (Bit Error Rate) and EVM [5]. Although increasing back-off is a very simple method

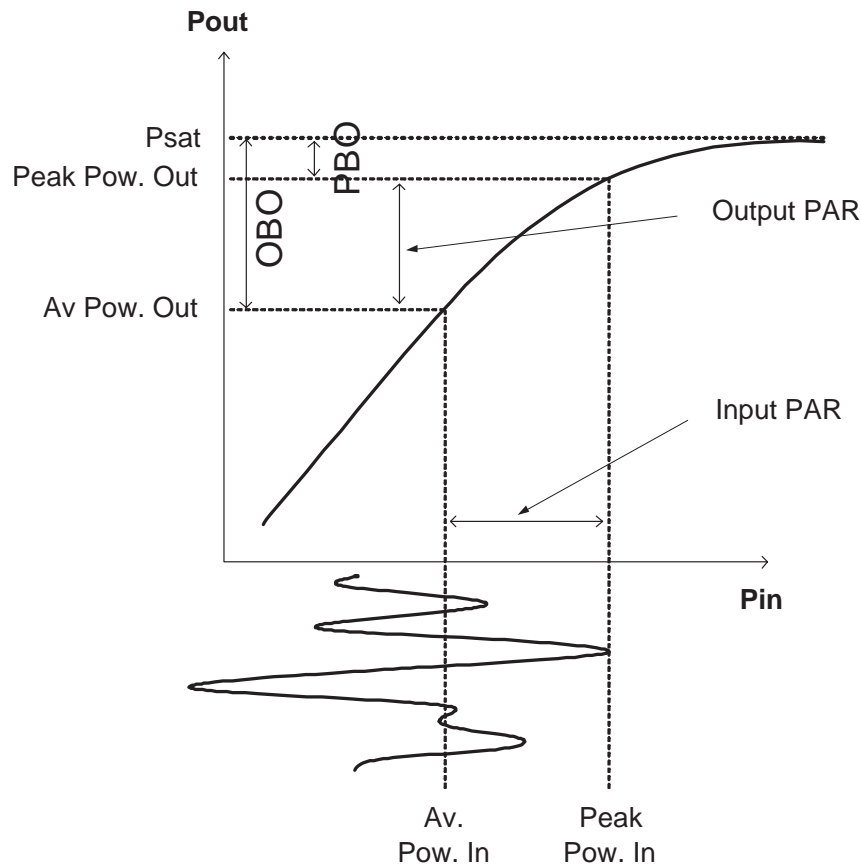


Figure 2.6: Output back-off (OBO) and peak back-off (PBO).

to obtain linear operation, it is not a reasonable solution in linear PA design because efficiency decreases rapidly as shown in fig. 2.4. However, if PA linearization methods are used, then linear operation close to saturation point is possible which gives at the same time high efficiency.

2.1.5 Matching

Matching is a main issue in RF PA design. It is required not only at input and output of the PA, but also between its stages (inter-stage matching). Mismatch in the circuit can cause reduced efficiency and/or output power, increased stresses of the active devices and distortion at the PA output [10]. For a linear, efficient and high power operation matching especially at the output is very important. A compromise between PAE, output power and linearity can be done with optimizing load matching according to load-pull measurements [13, 14].

Fig. 2.7 shows simulated constant PAE and output power contours for a test amplifier and estimated constant ACPR contours with their maximum values at points A, B and C respectively. The figure shows that the PA characteristics are highly dependent on load matching. For different output powers and frequencies the position of these

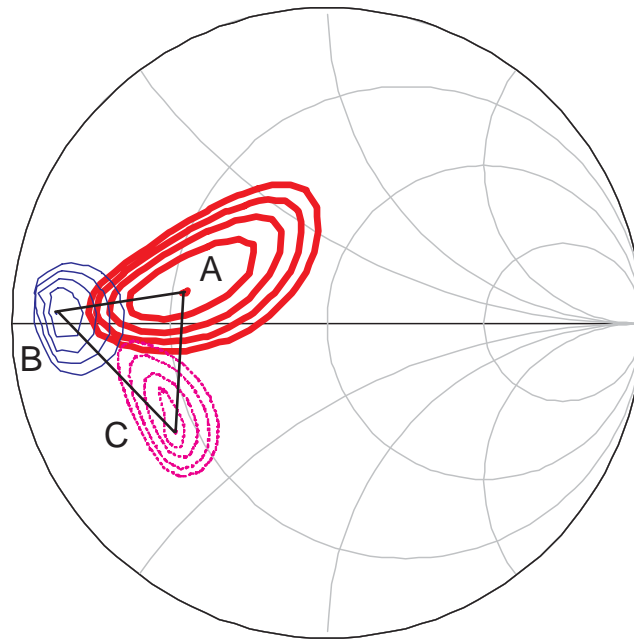


Figure 2.7: Simulated constant PAE (A), output power (B) and estimated constant ACPR (C) contours related to load matching for a test amplifier.

contours can vary significantly. Since it is not much likely that the load values for maximum linearity, efficiency and output power are close to each other, a compromise must be done for output matching. In conventional designs a high linearity match point (near to C in fig. 2.7) may be selected resulting in lower output power and PAE (away from points A and B). However, in the case of DP implementation first the output matching can be optimized for high efficiency and output power and then the PA can be linearized additionally in order to fulfill the system specifications. This makes simultaneous high efficiency, high power and high linearity operation easier to achieve.

2.2 Amplifier classes

There are various types of amplifier classes designed for different applications. The types explained in this part are Class A, B, AB, C, D, E and F. Class A, B and AB can be called as linear mode amplifiers whereas the others are nonlinear. The following sections are an overview of PA classes.

2.2.1 Class A amplifiers

In this class of operation it is possible to preserve the original shape of the input signal. This is because the DC operating point is selected to be in the middle of the linear region avoiding any distortion during signal swing. The amplifier is highly linear but its efficiency is low because a high DC-current is drawn from the supply continuously. A simplified circuit diagram is shown in fig. 2.8.

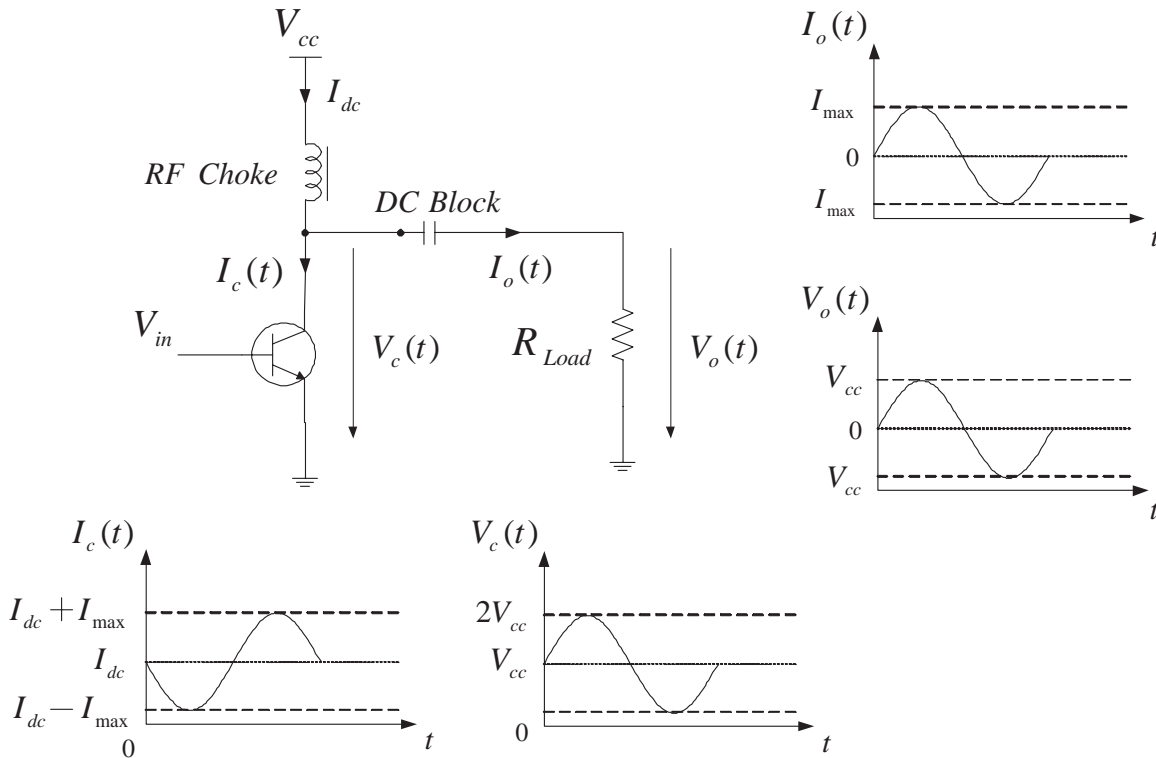


Figure 2.8: Class A power amplifier simplified circuit diagram.

The current and voltage plots in the figure show the maximum achievable swings with this configuration. If we neglect the value of finite saturation voltage, then the collector voltage and current can be written as

$$V_c(t) = V_{cc} + V_{cc} \cos(\omega t) \quad (2.8)$$

$$I_c(t) = I_{dc} + I_{max} \cos(\omega t) \quad (2.9)$$

If I_{max} is equal to I_{dc} , then the maximum swing is obtained.

RF Choke blocks the RF power going into the supply. The output current and voltage have no DC part because of the blocking capacitor. These can be written as

$$V_o(t) = V_{cc} \cos(\omega t) \quad (2.10)$$

$$I_o(t) = I_{max} \cos(\omega t) \quad (2.11)$$

where I_{max} is

$$I_{max} = I_{dc} = V_{cc}/R_{load} \quad (2.12)$$

DC input and RF output powers can be derived as

$$P_{dc} = V_{dc}I_{dc} = V_{cc}^2/R_{load} \quad (2.13)$$

$$P_{rf} = V_{cc}I_{dc}/2 = V_{cc}^2/2R_{load} \quad (2.14)$$

From eqns. 2.13 and 2.14 the maximum efficiency for an ideal Class A PA has been calculated to be

$$\eta = (P_{rf}/P_{dc}) \cdot 100 = 50\% \quad (2.15)$$

However, the maximum practically achievable efficiency is 40-45% [10]. If the output RF power is reduced then the efficiency reduces significantly because the input DC power always stays constant. Output power capability C_p is an important PA figure of merit. It is defined as the maximum output power divided by the peak instantaneous collector voltage times the peak instantaneous collector current and for Class A PAs is given below [10]:

$$C_p = \frac{P_{rf,max}}{(2V_{dc})(2I_{dc})} = 1/8 = 0.125 \quad (2.16)$$

Class A amplifiers are usable as driver stages in power amplifiers due to their high gain and linearity [10]. However using them as output stages in todays mobile communications systems is not reasonable due to their low efficiency.

2.2.2 Class B amplifiers

The DC current drawn from the supply must be lowered, in order to increase the efficiency of an amplifier shown in the previous section. The DC current flowing into an amplifier when its input is set to zero is defined as quiescent current (I_q) and in Class A case it is equal to the constant DC current I_{dc} defined in eqn. 2.12. Fig. 2.9 shows a sinusoidal collector current $I_c(t)$ and its relation to I_q . If I_q is decreased, then $I_c(t)$ becomes negative for a portion of the sinusoid, which means cut-off in reality and no current flows through the transistor. In the other portion where $I_c(t)$ is greater than zero the transistor is conducting.

In order to understand the picture we need another definition called conduction angle derived as

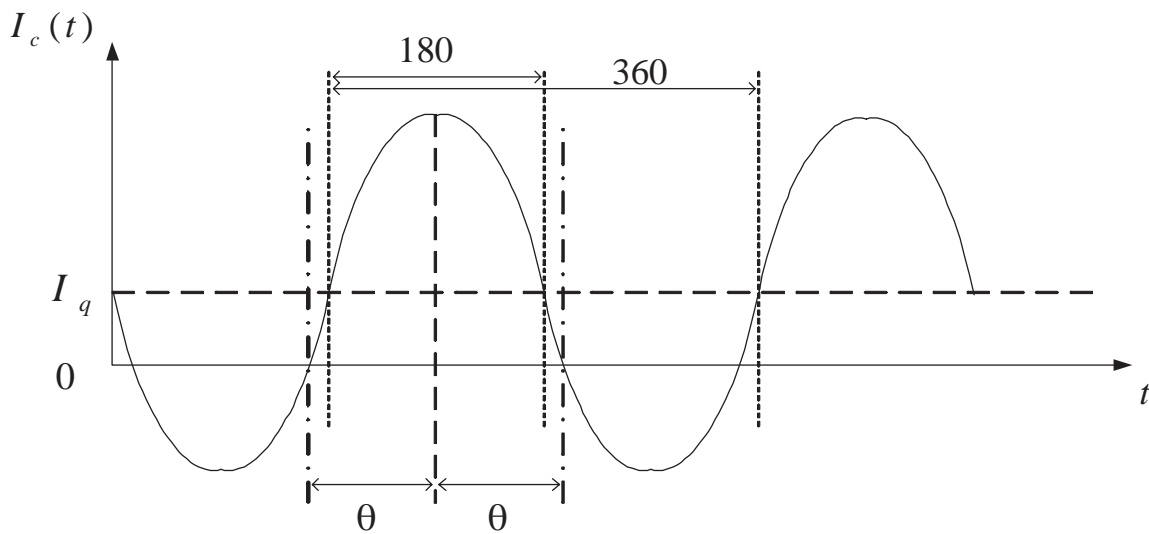


Figure 2.9: The effect of quiescent current on PA conduction angle.

$$\Theta = 2\theta \quad (2.17)$$

Conduction angle is the amount of angle where the transistor is conductive in each full cycle. The differences between Class A, B, AB and C amplifiers are directly related to their conduction angles. Class A has a conduction angle of 360° whereas Class B has 180° meaning I_q of zero [10]. Their implementation in push-pull structures is very useful. In this case two power transistors are used. Current is flowing in each transistor just for a half cycle and it is off in the other half. Using a BALUN (BALanced to UNbalanced) at the output the currents are added up revealing the linearly amplified input signal. This class of operation results in a great improvement in the efficiency ($\eta_{max} = 78.5\%$) compared to Class A and provides still a good level of linearity [5]. A maximum efficiency of 60-70% is realistic for class B PAs [10]. The disadvantage is the usage of two identical transistors in anti phase and requirement for BALUNs at both input and output.

2.2.3 Class AB amplifiers

Although it has been mentioned that linear operation is possible using two Class B amplifiers, it is valid under ideal conditions. In reality there is a source of small signal nonlinearity called crossover distortion [5]. If the conduction angle is exactly 180° then the response of the transistor to the input signals close to zero is nonlinear. Fig. 2.10 shows a normalized trans-conductance curve for a transistor and the resultant nonlinear output current waveform versus time shown in red. This distorted sinusoidal signal requires a higher bias point for linear operation. Therefore normally the conduction angle is set to a value between 180° and 360° (slightly higher than 180°) and the normalized sinusoidal waveform shown with dashed line is obtained. This mode of

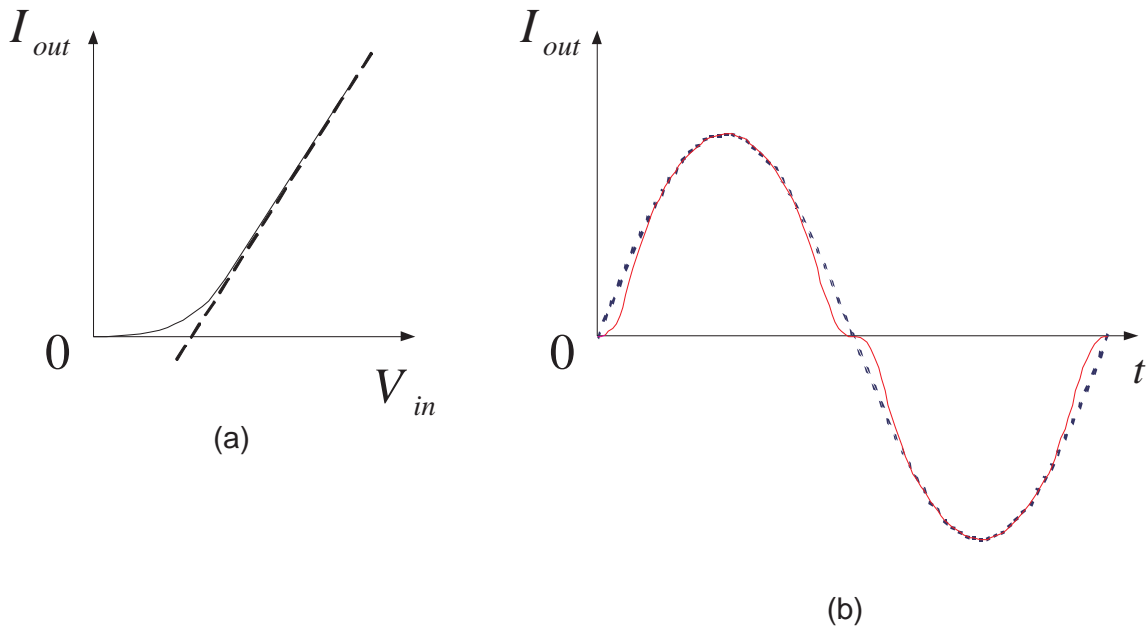


Figure 2.10: Typical (a) transconductance curve of a transistor and (b) its response.

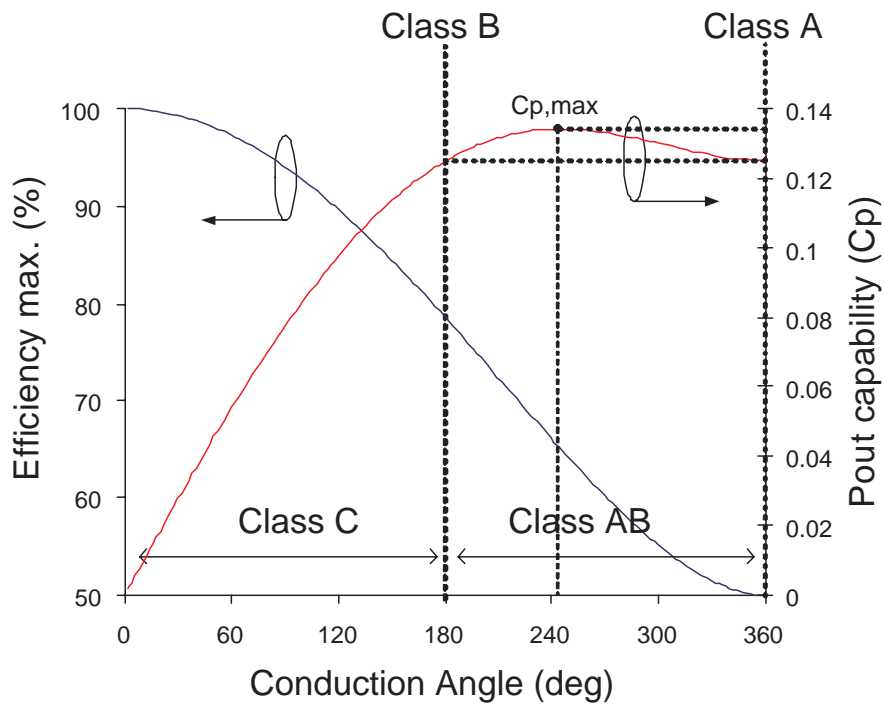


Figure 2.11: Efficiency and the power output capability versus conduction angle.

operation is called as Class AB. The efficiency is reduced compared to Class B but a higher degree of linearity is obtained because of lower crossover distortion [5].

2.2.4 Class C amplifiers

If the conduction angle is smaller than 180° then the amplifier is said to be in Class C mode. In this mode the linearity of the PA is lost. The efficiency is high but the deliverable maximum output power decreases with decreasing conduction angle [10]. Fig. 2.11 gives the relation between the efficiency and the output power capability versus conduction angle. The maximum output power capability of 0.1341 is obtained in Class AB operation when the conduction angle is equal to 245.2° [10]. Output power capability is equal to 0.125 for Class A and B PAs.

2.2.5 Class D amplifiers

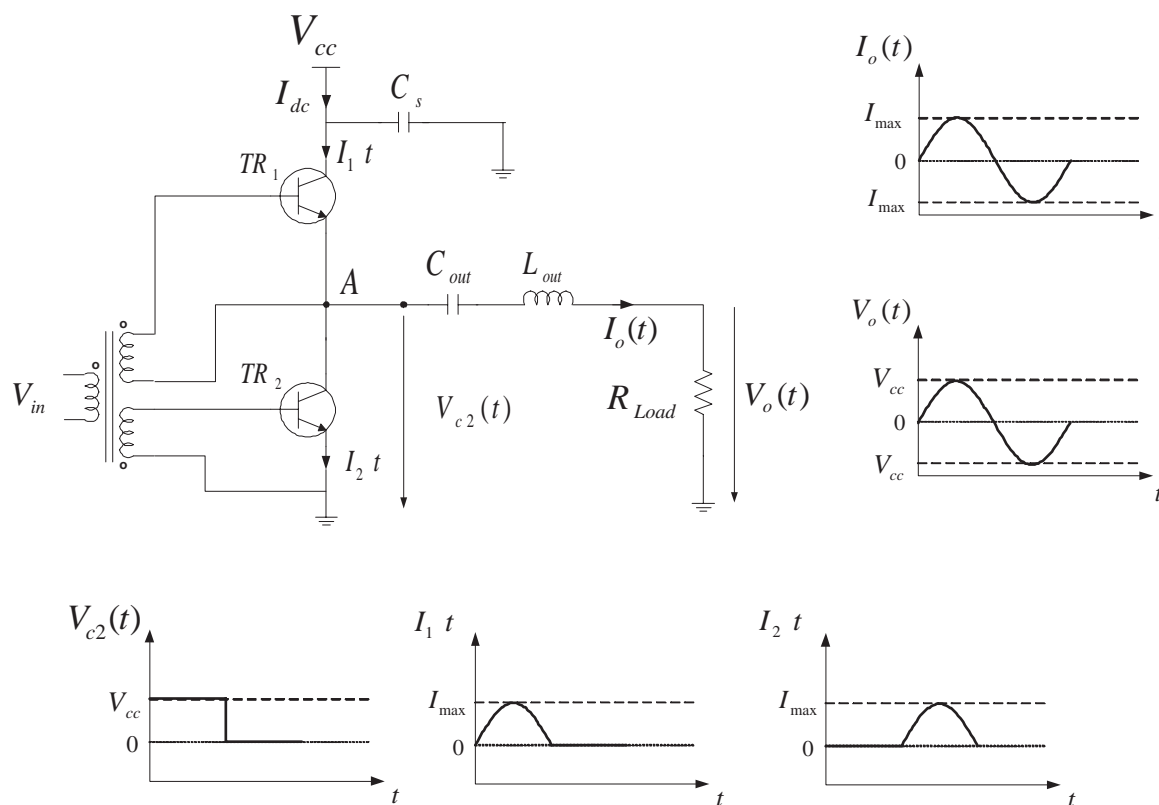


Figure 2.12: Class D complementary voltage switching amplifier [5].

Linearity is lost in switching-mode power amplifiers (Class D, E and F) due to transistor operation just in on and off states. Amplitude modulation at the input can not be preserved at the output. However, phase modulated signals can be handled efficiently. There are some transmitter topologies like EER, which make the usage of switch mode PAs possible in applications requiring linear amplification [6]. With such topologies switch mode power amplifiers are going to gain more importance.

In Class D topology normally two transistors are used in the circuit in a push-pull structure where they are alternatively switched on and off. They can be classified as

complementary voltage, transformer-coupled voltage and transformer-coupled current switching amplifiers [5]. Fig. 2.12 shows a simplified block diagram of complementary voltage switching amplifier and some ideal current and voltage waveforms. The voltage waveform at node A is ideally a square wave. In order to have a sinusoidal voltage at the output, the load circuit contains a resonant circuit tuned to fundamental frequency. The current waveforms of transistors are half sine waves complementing each other. In transformer-coupled voltage and current switching amplifier topologies the main difference is the used transformer at the output of push-pull structure. The collector efficiency in Class D amplifiers is ideally 100%. However, transistors have finite switching speeds and during current flow they stay in their active region for a while. This results in a reduction in efficiency [15]. On the other hand drain and collector capacitances limit the achievable operation frequency.

2.2.6 Class E amplifiers

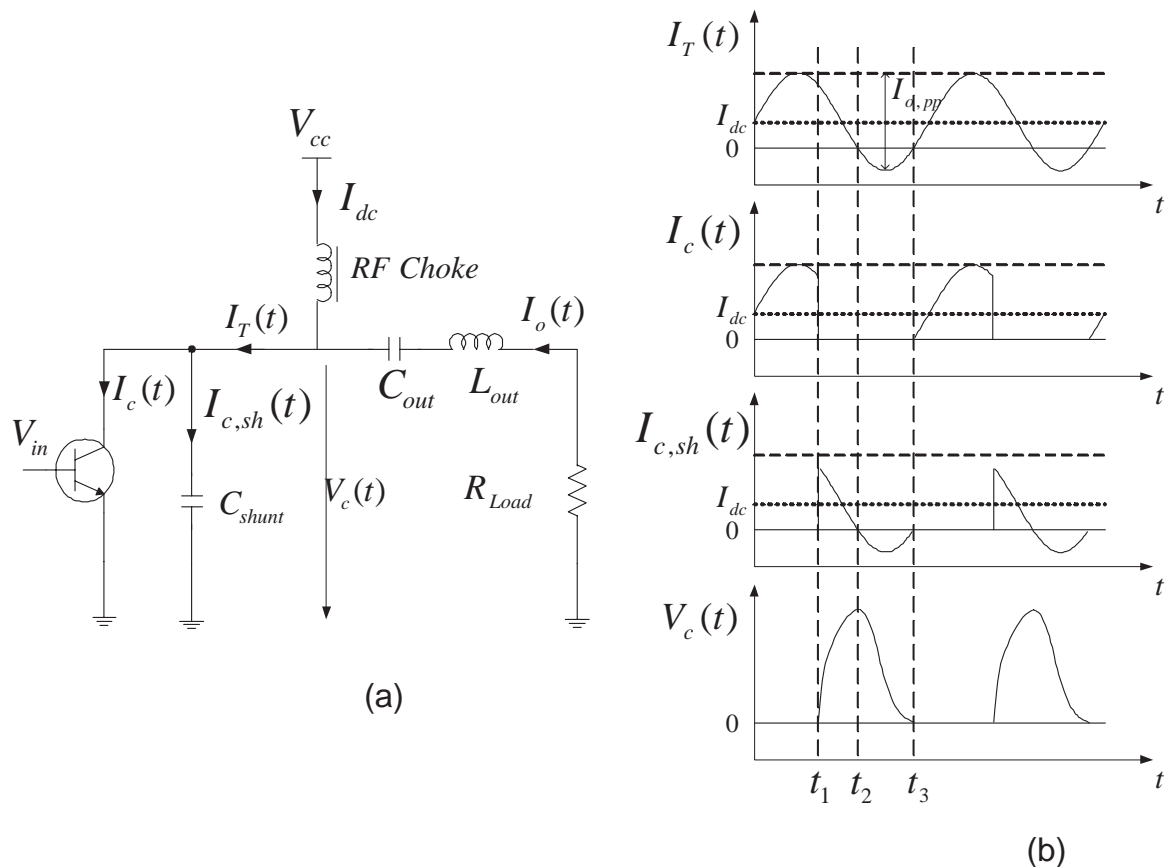


Figure 2.13: Class E PA (a) simplified circuit and (b) current and voltage waveforms [13].

In Class E there is a single transistor operated in switched mode [15] and it has a shunt capacitance at its collector. Fig. 2.13 shows block diagram of a Class E PA with current and voltage waveforms at different points. $I_c(t)$ is the current flowing through

switch transistor, $I_{c,sh}(t)$ is the current of the shunt capacitor C_{shunt} , $I_T(t)$ is the total current flowing through the transistor and C_{shunt} and $V_c(t)$ is the voltage appearing on C_{shunt} .

The aim in using Class E is to decrease transition time between transistor on and off states. This is achieved by reducing the drain voltage to zero just as the transistor turns on (at time $t = t_3$). The slope of the voltage wave should also be zero at this point. The transistor turn off time ($t = t_1$) must be selected accordingly in order to fulfill this condition.

Class E efficiency under ideal conditions is 100% as in Class D but in reality they have better efficiency than Class D due to significant reduction in switching losses. Since the topology works with a shunt capacitance at collector (or drain), the transistor's inherent collector (or drain) capacitance is no longer a source of power loss but becomes an essential part of the circuit [5].

2.2.7 Class F amplifiers

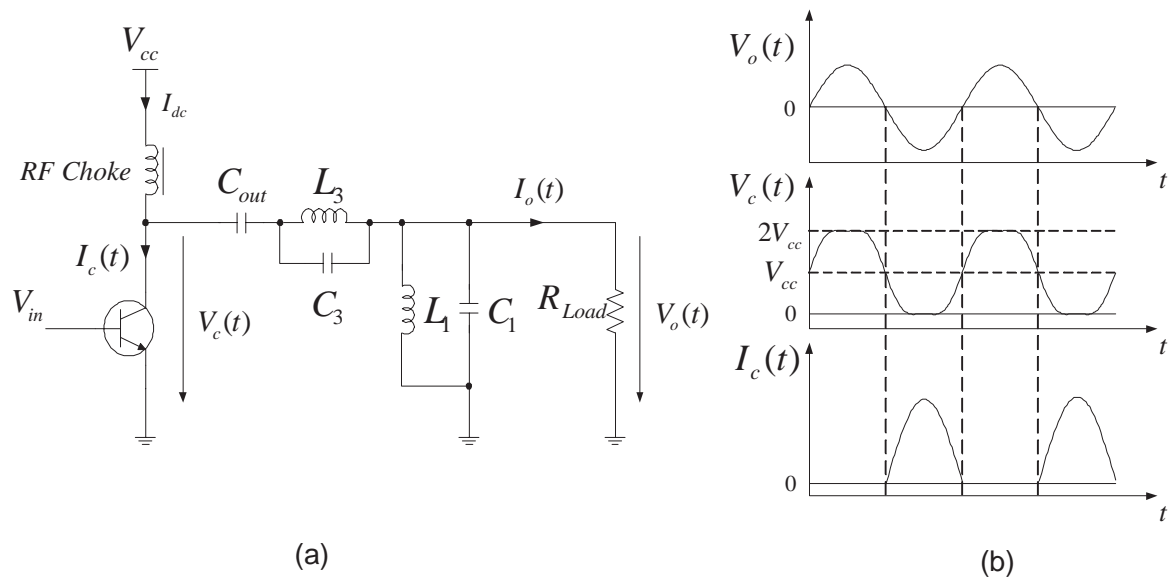


Figure 2.14: Class F PA (a) simplified circuit and (b) current and voltage waveforms [10].

Class F amplifiers are not used only for their high efficiency, but also for high output power [15]. They differ from the other PA classes due to usage of multiple-resonator output filters. Voltage waveforms contain odd harmonics whereas current waveforms contain even harmonics. Fig. 2.14 (a) shows a simplified Class F PA block diagram with added only parallel third harmonic resonator circuit (L_3 and C_3). L_1 and C_1 are selected to resonate on the fundamental frequency. Fig. 2.14 (b) shows output voltage ($V_o(t)$), and collector voltage ($V_c(t)$) and current waveforms ($I_c(t)$). $I_c(t)$ is a half sine whereas $V_c(t)$ is a flattened sine signal [10].

In the ideal case where the number of harmonics is high, the voltage has the shape of a square wave, the current is half sine wave and they are not simultaneously nonzero. This is as in Class D operation and the efficiency is ideally 100%. Several resonators are required at the output in order to get the desired harmonics.

2.3 Amplifier topologies

PAs can be designed in different topologies depending on the application. The basic amplifier topologies are single-ended, differential (push-pull) and balanced PA topologies [13].

2.3.1 Single-ended power amplifiers

This is the simplest topology where there is just one transistor used in the circuit as in Class A topology case. The input signal is applied to the transistors base and its emitter is grounded. Fig. 2.15 shows a simplified general block diagram of a single-ended PA.

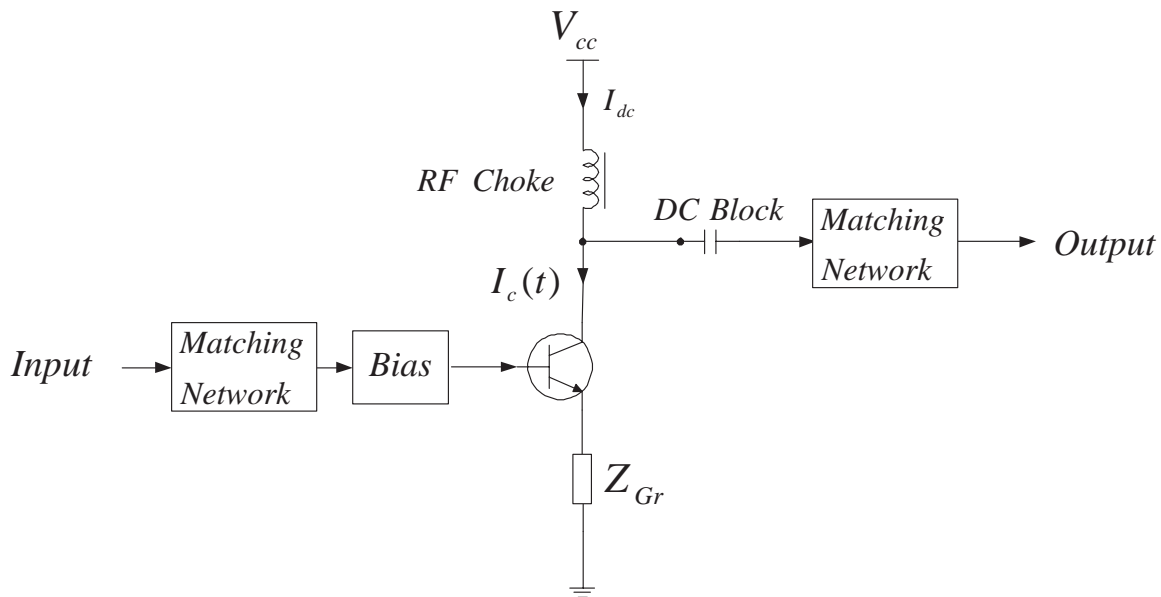


Figure 2.15: Simplified general block diagram of single ended PA topology [16].

The advantage of the topology is its easy input and output matching capability. However, the ground connection (Z_{Gr}) is problematic during implementation in RF because it behaves as an inductor. If the layout of the connection is long, then the inductance will be high and it will influence the operation. Such an inductor can reduce the gain significantly [16] or cause oscillation.

2.3.2 Differential power amplifiers

This is called as push-pull topology. Two identical transistors having 180° shifted input signals are used. Fig. 2.16 shows the general block diagram of the transformer coupled push-pull topology. There are two BALUNs at the input and output of the circuit in order to make the transistors operate 180° out of phase. One very important advantage of the topology is that the RF signal grounding problem is solved because the point where the emitters of the transistors are connected is a virtual ground. There is also no need for DC block capacitors at input and output. Disadvantage is the usage of BALUNs.

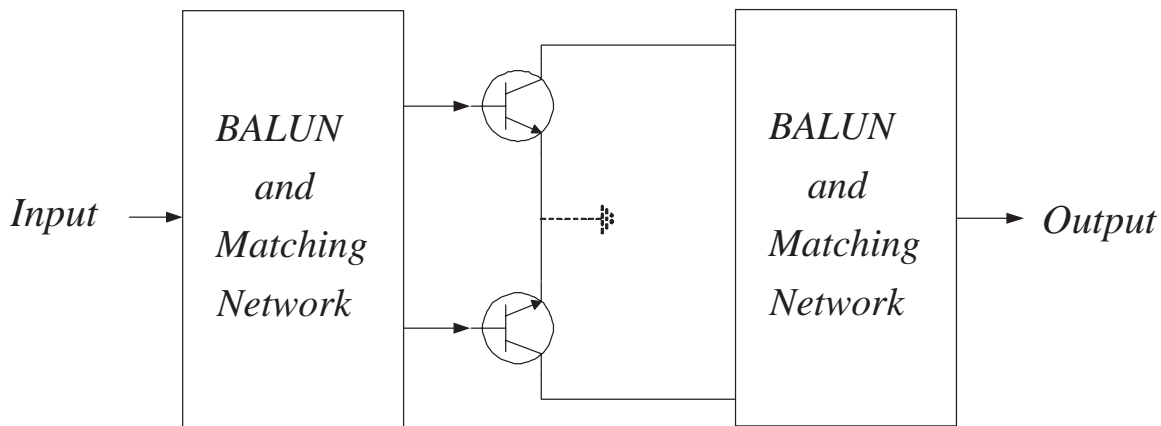


Figure 2.16: Transformer-coupled push-pull power amplifier structure [16].

Differential configuration makes linear operation of Class AB and B amplifiers possible at high frequencies. It is also possible to implement push-pull structures with complementary transistors instead of two identical transistors. Then one transistor is npn whereas the other is pnp type BJT (or n and p type FET). This structure is useful for relatively low frequency applications like in audio frequency systems. It is difficult to use it at high frequencies due to slow RF characteristics of pnp type BJTs (or pFETs) compared to npn (n) type [16].

2.3.3 Balanced power amplifiers

In balanced amplifier topology again two identical transistors are used in parallel. However, this time their inputs have 90° phase difference but not 180° as in differential topology. Fig. 2.17 shows a simplified block diagram of balanced amplifier. Two quadrature 3 dB couplers are used at the input and output in order to obtain 90° shifted inputs and recombine the outputs.

The principal advantage of balanced structures is that any reflections due to mismatch at input and output are passed back through the couplers, diverted to the terminated ports and cancelled [13]. However, there are grounding connections as in single ended PA topology because there is no virtual ground.

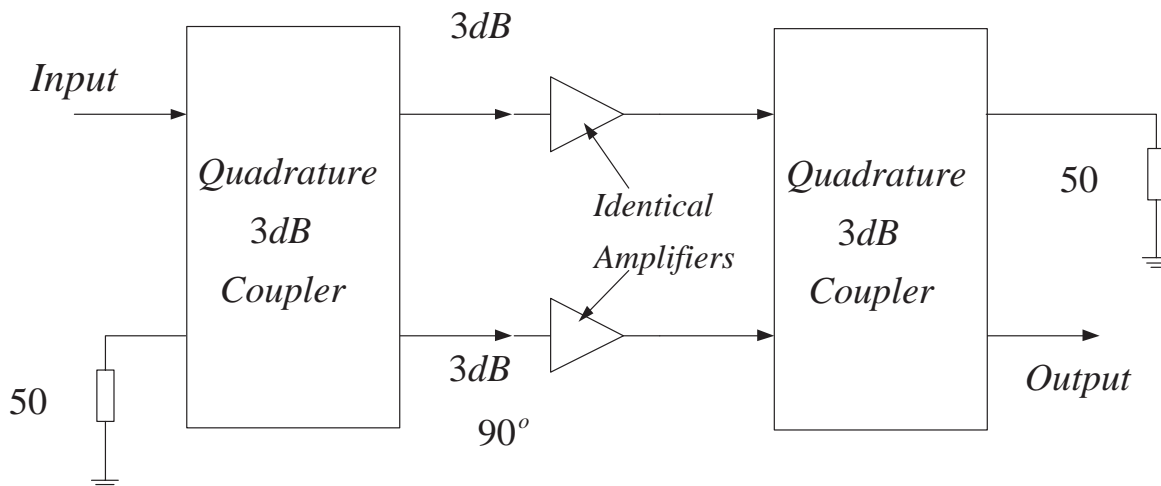


Figure 2.17: Balanced power amplifier configuration [13].

2.4 Investigated power amplifiers

During the studies presented in this thesis various PAs have been investigated. Some investigations were done by simulations with assumed PAs and some were done via measurement of commercially available PAs from RF Micro Devices¹. These PAs have been designed for different terminal applications like CDMA, GSM, EDGE etc. They have been characterized by generating their behavioral models and linearized with MDP accordingly. The results obtained with simulations and performance measurements showed good agreement. The PAs which have been used are listed below.

RF2162, 3V 900 MHz Linear Amplifier, Typical Applications: CDMA/AMPS, JCDMA/TACS and TDMA/AMPS Cellular Handsets.

RF3110, Triple-Band GSM/DCS/PCS Power Amplifier Module, Typical Applications: Dual-Band GSM Handsets, GSM, E-GSM and DCS/PCS Products.

RF3145, Quad-Band GSM/EDGE/GSM850/DCS/PCS Power Amplifier Module, Typical Applications: Dual/Triple/Quad-Band Mode Handsets, GSM850 and GSM900 Products, DCS/PCS Products.

¹7628 Thorndike Road Greensboro, NC 27409, USA

Chapter 3

Mobile communications

Mobile communications is now a part of our daily life. Almost everyone has a mobile phone. Most of the end users are not aware of it but they purchase highly sophisticated systems which have been achieved after a short but very fast evolution period. During this period different systems have been implemented in different countries starting from analog through digital ones. Digital systems have higher information transmission capability, higher security and better communication quality compared to analog systems. Hence they are more dominantly used. However, installing new systems is not an easy task, because of available systems with different frequency allocations in each country or region. It is not always possible to install a system directly in another country. In such cases significant hardware adjustments are necessary. On the other hand new devices must be able to handle the available and new installed systems together in order to communicate with all subscribers. Therefore the trend is to design flexible multi-band multi-mode systems (covering most of the available systems) usable in most countries. In the following parts of this chapter some types of mobile communication systems will be explained which are very important for near future mobile communications. But before proceeding to mobile communication systems, digital modulation formats will be explained briefly.

3.1 Digital modulation formats

Digital modulation formats with large constellations are very important due to their high data transmission rate capability compared to analog modulation. Basically modulation can be divided into two: coherent and non-coherent modulation [17]. In coherent modulation the amplitude or phase of the carrier or both together are modulated giving the possibility of a large constellation. The receiver structures are complicated because the absolute knowledge of the phase (phase lock) and the effect of channel, and complicated synchronization algorithms are required. However, in non-coherent modulations simple receiver structures are used because not the absolute values of symbols but the change between consecutive symbols is important. They are differential schemes and are not popular in high speed communications systems due to their low performance. In this section some widely used coherent modulation schemes are going to be explained

[18, 17].

The constellation of a modulation scheme affects signal BER, PAR and RF spectrum shape. Large constellations have in general worse BER, high PAR and an RF spectrum shape very sensitive to nonlinearities in transmitter, which are tolerated for high spectrum efficiency. There are two main goals for system performance improvement in the design of constellation. First one is to have a constant amplitude for all points and the second one is to have maximum distance between constellation points [17]. Therefore circular constellations are reasonable choices for relatively large number of constellation points.

3.1.1 Amplitude shift keying (ASK)

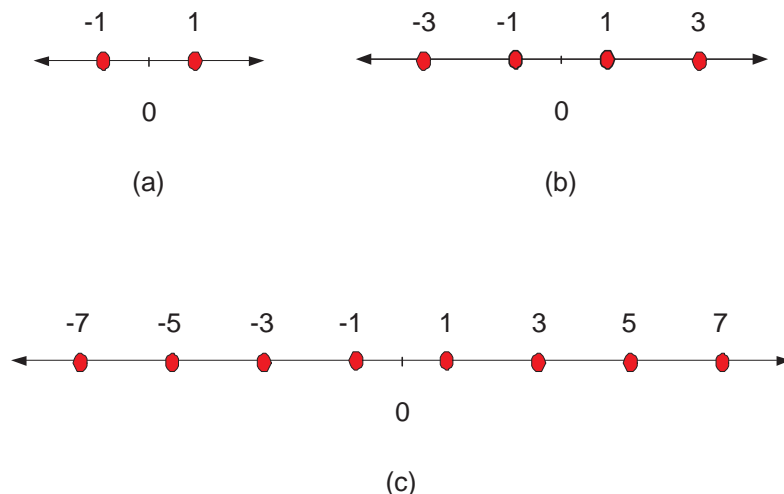


Figure 3.1: Constellation diagrams of (a) 2-ASK, (b) 4-ASK and (c) 8-ASK [17].

In this scheme the modulation is done just with amplitude. Therefore the demodulation can be done simply with a simple envelope demodulation [18]. There are two possible phases with the difference of π . It can also be called M-ary ASK (Amplitude Shift Keying) where M is the number of different points in the constellation diagram. The number of bits coded into one symbol is n, where $M = 2^n$. Fig. 3.1 (a), (b) and (c) show the constellation diagram of ASK modulations with 2, 4 and 8 points in their constellations respectively. In ASK the required amount of increase in the SNR (Signal-to-Noise Ratio) to maintain the same BER when changing to a one step larger constellation (if n is increased by 1) is 6.99 dB from 2- to 4-ASK, 6.23 dB from 4- to 8-ASK and it converges to about 6 dB for further increase, which makes large ASK modulations rarely used [17].

3.1.2 Phase shift keying (PSK)

It is also called M-ary PSK (Phase Shift Keying) where M is the number of different phases in the constellation diagram. Again the number of bits coded into one symbol

is n , where $M = 2^n$. Fig. 3.2 shows some possible constellation diagrams called 2-PSK (binary PSK) which is identical to 2-ASK, 4-PSK (quadrature PSK) and 8-PSK.

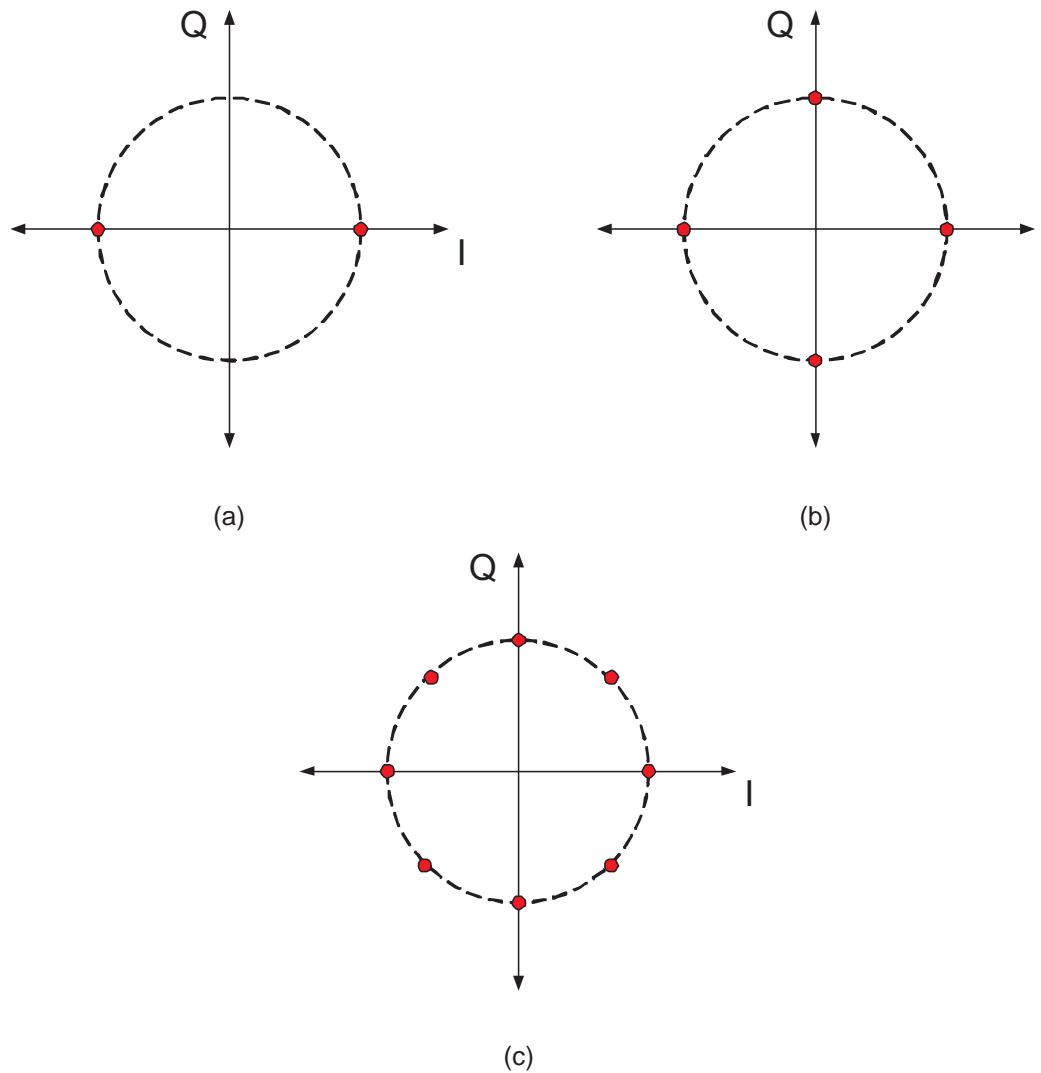


Figure 3.2: Constellation diagrams of (a) BPSK, (b) QPSK and (c) 8-PSK [17].

PSK modulations are linear modulation types because their envelopes are not constant. The reason is the time required for phase jumps from one phase to another, which may result in different phase and amplitude values during transition [18]. This makes them sensitive to nonlinearities in the transmitter path. Their spectral efficiency increases with increasing the number of points in the constellation. The required amount of increase in the SNR to maintain the same BER when changing to a one step larger constellation is better compared to ASK, especially for constellations having low number of points. SNR should be increased only 3 dB from BPSK to QPSK, 5.33 dB from QPSK to 8-PSK and it converges to about 6 dB for further increase as in ASK. Therefore M-ary PSK modulations having larger constellations than 8-PSK are not commonly used [17].

3.1.3 Quadrature amplitude modulation (QAM)

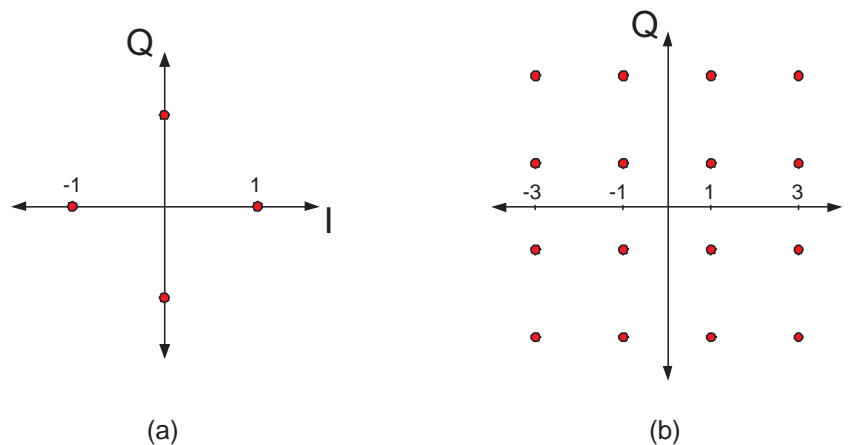


Figure 3.3: Constellation diagrams of (a) 4-QAM and (b) 16-QAM [17].

In QAM (Quadrature Amplitude Modulation) both amplitude and phase of the carrier are modulated. It is also a linear modulation because of its non-constant envelope values. For large constellations BER performance is better than ASK and PSK because it has two dimensional freedom in space to locate the constellation points. However, PAR increases significantly with increasing the number of points in the constellation. The modulation can be called M-ary QAM and the number of bits coded into one symbol is n , where $M = 2^n$. In fig. 3.3 constellation diagrams of 4-QAM (equivalent of QPSK) and 16-QAM are shown. M-ary QAM is especially advantageous if the number of points in the constellation is increased further (e.g. 32 or 64 points), because the required amount of increase in the SNR to maintain the same BER when changing to a one step larger constellation converges to about 3 dB [17].

3.1.4 Gaussian minimum shift keying (GMSK)

GMSK (Gaussian Minimum Shift Keying) is the modulation format used in GSM. It has a constant envelope having continuous phase with no jumps. It is generated by gaussian filtering of an MSK (Minimum Shift Keying) signal which results in a reduction of the signal bandwidth and significant side lobe suppression [18]. As a result a narrow bandwidth signal with sharp cut-off having highly suppressed out of band noise power radiation is obtained.

MSK signal can be assumed as a variation of OQPSK (Offset QPSK) or an FM signal [18]. OQPSK is the special form of QPSK where just 90° phase jumps occur (no 180° phase jumps are allowed). Fig. 3.4 (a) and (b) show the phase trajectories of MSK and GMSK signals respectively. In both cases modulated signal phases are shifted by $\pi/2$ if data is 1 and by $-\pi/2$ if data is 0. However, in GMSK the phase transition is smooth as shown in fig. 3.4 (b).

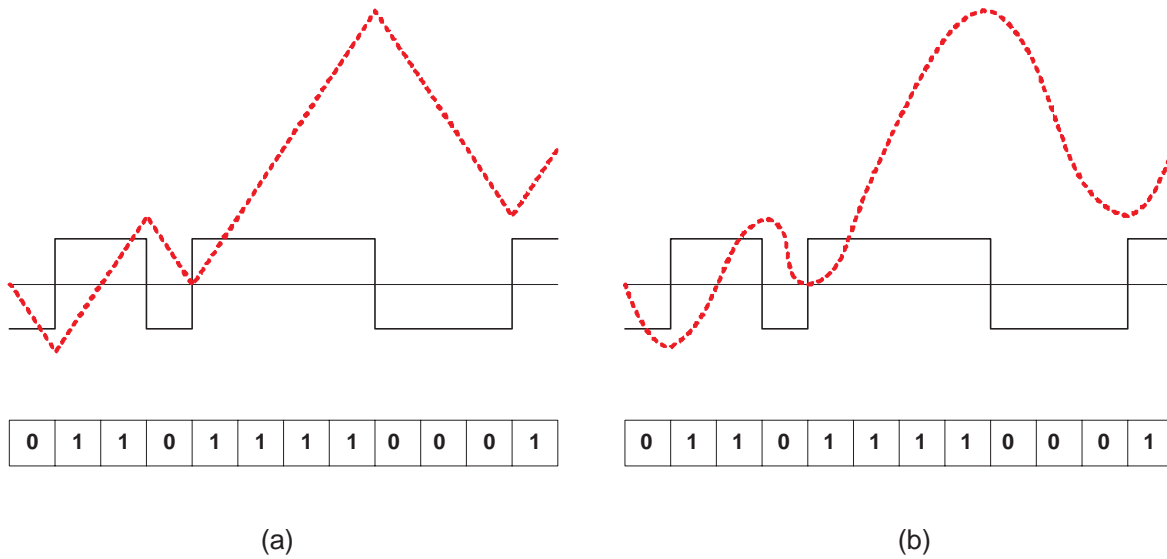


Figure 3.4: Phase trajectories of (a) MSK and (b) GMSK signals for the same data sequence.

3.2 Cellular systems

By early 90s cellular systems became so popular that the capacity of previously used 1st generation (1G) analog systems was not enough to serve all subscribers. In order to keep up with the demand, 2G digital systems were developed (IS-136, IS-95, GSM). Since that time the number of subscribers increased continuously. Some other services are also going to be provided besides voice communication, which require significantly higher data transfer rates. 2G systems seem to be sufficient for voice communication. However, services like internet or video data need higher data transfer capability. Therefore 2.5G and 3G systems (EDGE, CDMA2000, WCDMA) are going to be used which are capable of solving this problem [19, 20]. These systems are called cellular systems because of partitioning the serving area into a number of hexagonal cells as shown in fig. 3.5.

In the simplest case a base station (BS) with an omni-directional antenna is placed in the middle of a cell and provides coverage to mobile terminals in all of the cell area. Size of the cells can be selected to be big especially in rural areas where low number of users may be present. However, size of the cells should be small and their number increase in urban areas in order to serve to large numbers of subscribers. For higher demand additional system capacity improvement techniques are implemented such as using several directional antennas in the base station dedicated for a cell. In order to increase channel separation and reduce interference between neighbor cells, available channels are divided into seven sets and each assigned to a cell (from BS_1 to BS_7) as shown in fig. 3.5 [20]. This structure makes channel reuse possible for the other cell groups composed of seven cells. The same channels can be used in the cells having the same numbers.

In the following sections some cellular systems (GSM, EDGE, WCDMA and CDMA2000) are going to be explained briefly. Their system structure, capacity, advantage and draw-

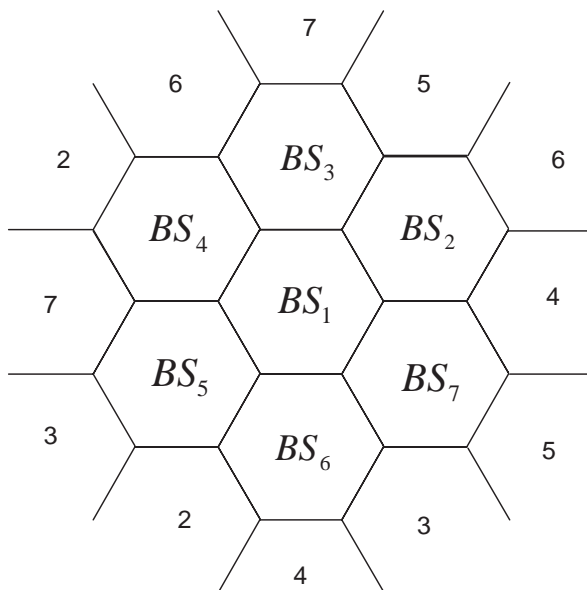


Figure 3.5: Partitioning of a region into equal size cells [20].

backs are discussed. The effects of power amplifier nonlinearities on ACPR and EVM are also considered.

3.2.1 GSM/EDGE

GSM is currently the main cellular system in Europe and one of the most widely used systems in the world. It has been designed to operate around 900 MHz first with the frequency allocation shown in fig. 3.6. The total frequency band is 50 MHz composed of 25 MHz uplink (890-915 MHz) and 25 MHz downlink (935-960 MHz). Uplink is data transfer from mobile station to base station and downlink is from base station to mobile station. If a mobile communication system has different frequency bands for transmit and receive operations, then it is called as FDD (Frequency Division Duplex) system. The bandwidth for each transmit or receive channel is 200 kHz. This means 125 physical channels for each uplink and downlink (actually one channel is not used to avoid interference with other systems in the neighborhood). There are some other frequency bands at 400, 850, 1800 and 1900 MHz dedicated for GSM applications in different countries.

In GSM a channel can be used by more than one user. It is achieved by dividing each frame into 8 slots. Then it is possible to use each slot for a different user and the users send data bursts instead of a continuous transmission. This feature is called TDMA (Time Division Multiple Access). Fig. 3.7 shows a detailed diagram of the channel operation in time. GSM combines TDMA with FDMA (Frequency Division Multiple Access) because each channel operates also at a different frequency. A multiframe is mainly composed of traffic channels (frames) and some control channels called ACCH (Associated Control Channel) as in fig. 3.7. Each frame is divided into 8 slots carrying data and other bits necessary for operation control.

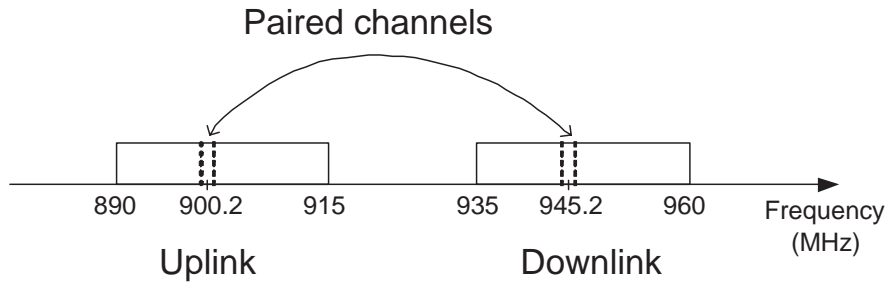


Figure 3.6: Frequency bands for uplink and downlink in GSM900 [20].

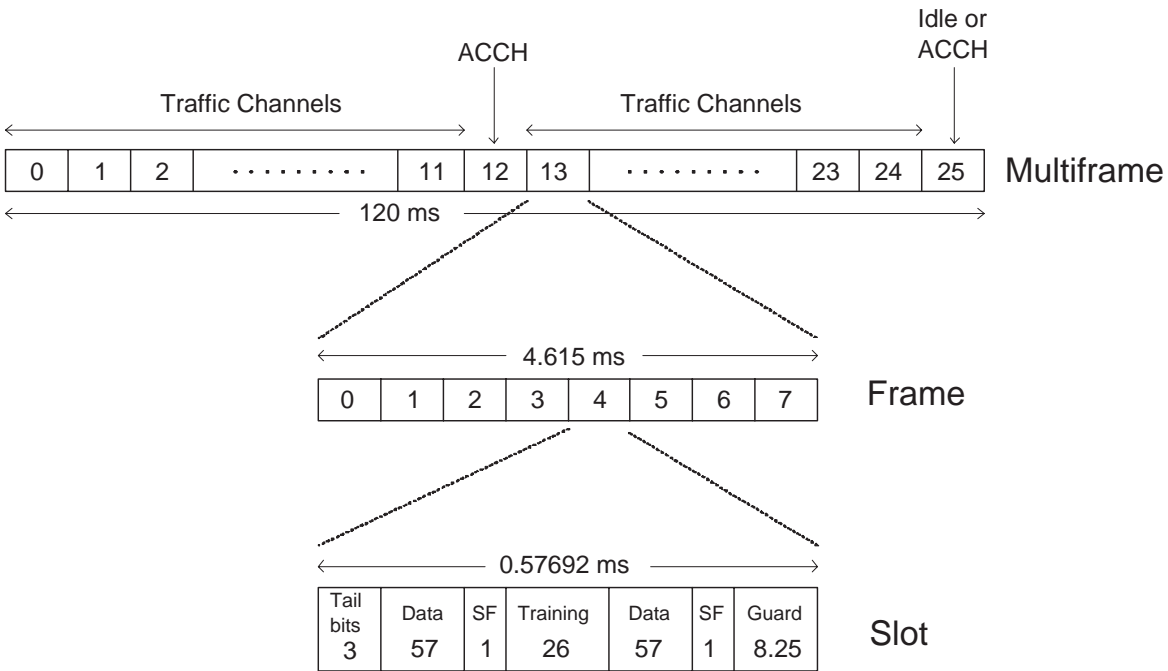


Figure 3.7: TDMA structure of GSM [20].

GPRS (General Packet Radio Service) is a service improving the maximum achievable data rate with packet-switching techniques using the GSM infrastructure. In normal operation of GSM each slot can be used to transfer circuit-switched data rates up to 9.6 kb/s and if 8 slots are used then it can be 76.8 kb/s [20]. Since in GSM the data is transmitted in bursts and the system is often inactive, the channel can stay unused for a considerable time. If the channel is released and captured again during data availability, the system will operate inefficiently due to required call procedures. In GPRS however, each channel can be shared by multiple users and all slots in the frame can be assigned to a user which improves data transfer efficiency considerably. With GPRS data transfer per user can be more than 160 kb/s [20].

In GSM the information is transferred just with phase modulation. The modulation used is GMSK and the envelope of the carrier is constant. In the EDGE however the envelope of the signal is also varying in order to increase the data transfer rate using

the same frequency band. EDGE is actually a 3G system evolved from GSM and it is relatively easy to implement because the available infrastructure of GSM can be used. It is also called 2.5G system indicating that its data transfer capacity (384 kb/s) is not as high as CDMA systems and it is an intermediate step between 2G and 3G. Used modulation type is $3\pi/8$ shifted 8-PSK and each constellation point is defined by three bits. The phase shift of $3\pi/8$ is used to avoid crossing the signal trajectory through the origin which decreases signal dynamic significantly. Signals with lower dynamic are less sensitive to transmitter path nonlinearities. One of the most important features of 8-PSK modulation is that all constellation points are on a circle, which results in low signal PAR. This means the required amount of PA back-off can be reduced resulting in relatively high transmitter efficiency. However, $3\pi/8$ shifted 8-PSK modulation has a varying signal envelope and is very sensitive to transmitter path nonlinearities resulting in worse output RF spectrum and EVM performance. Therefore in EDGE highly linear PAs are required whereas for GSM high efficiency nonlinear PAs can be used.

In GSM/EDGE systems each user must fulfill system specifications [21]. The most important criterias are phase error (GSM), EVM (EDGE) and system output RF spectrum (GSM and EDGE) performances. The RMS phase error in GSM must be less than 5° with a maximum deviation of 20° . EVM_{RMS} must be less than 9% and EVM_{peak} less than 30% in EDGE. The output RF spectrum results from signal modulation and switching transients during operation. Powers at different offset frequencies are measured as defined in [21] relative to the power measured at center frequency. The allowed powers at different offset frequencies for different power classes and bands of GSM are same up to 400 kHz offset. These are -30 dBc at 200 kHz, -33 dBc at 250 kHz and -60 dBc at 400 kHz offsets. At higher offsets performance better than at 400 kHz offset is required. The requirements at offset frequencies greater than 400 kHz become more stringent in power classes having more output power. For EDGE the required output RF spectrum performance is the same as GSM except at 400 kHz, which is set to -54 dBc.

3.2.2 WCDMA/CDMA2000

In CDMA systems the operation is quite different than GSM. The aim of using CDMA systems is to increase data transfer rate. These systems can be operated both in FDD and TDD (Time Division Duplex) modes. If the same channel can be used for uplink and downlink, then the system is in TDD mode.

CDMA systems are also called spread spectrum systems. All users can transmit simultaneously on the whole channel bandwidth. Each user has a unique pseudonoise (PN) code and user data is multiplied with this pulse sequence. In fig. 3.8 one user frequency spreading is shown in a simple way. As it is seen the user data has a narrow bandwidth before multiplication with the spreading code. After multiplication the bandwidth is widened and it is modulated and upconverted. The clock rate of PN code is called as chip rate. PN codes are quite long sequences obtained by shift registers. The receiver detects data from different users by correlating their codes with the received signal [20].

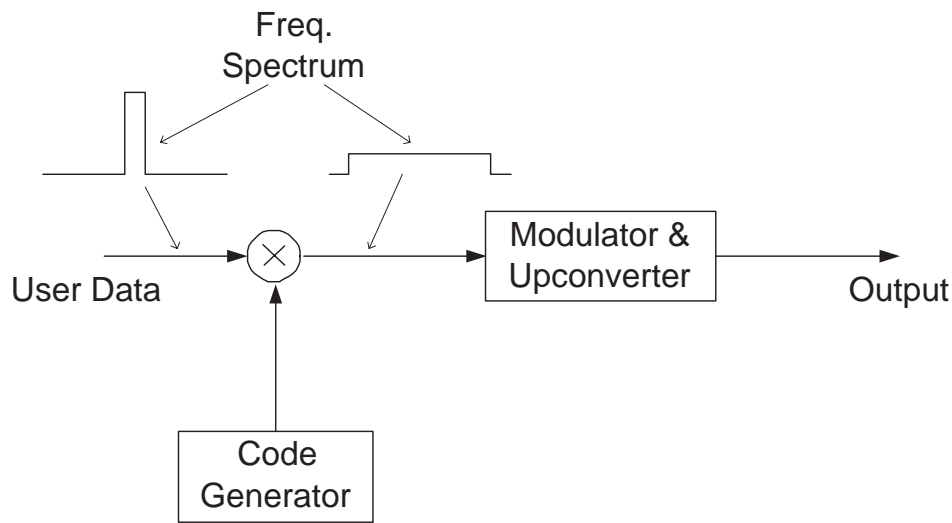


Figure 3.8: Simplified block diagram of direct sequence spread spectrum technique.

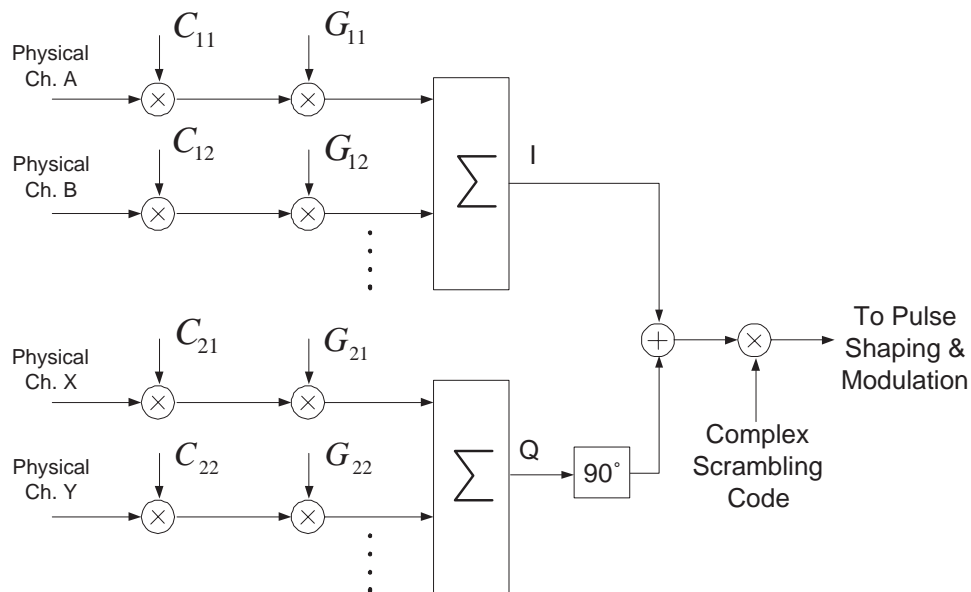


Figure 3.9: Block diagram of UMTS WCDMA in uplink [20].

WCDMA and CDMA2000 systems use DSSS (Direct Sequence Spread Spectrum) technique. User data is spread twice in CDMA2000 and WCDMA systems like UMTS. Fig. 3.9 shows a simplified WCDMA uplink structure in UMTS [20]. The modulation used is QPSK. The first spreading is done with orthogonal codes (C_{ij}), so called channelization and the second one with PN codes, so called scrambling. G_{ij} denotes the gain coefficients for each physical channel. For each data channel an orthogonal channelization code is used which are inherently robust against interference between multiple users. In UMTS WCDMA and CDMA2000 uplink orthogonal Walsh codes having lengths between 4 and 256 chips are used. The scrambling codes are not orthogonal PN codes

and they are used to indicate specific mobile stations. The length of scrambling code can be either 256 (short) or 38400 (long) chips. The orthogonal and scrambling codes have in general a chip rate much higher than the user data rate which results in broadening in spectrum. The ratio of the chip rate to the data rate is called spreading factor (SF).

Scrambling codes are generated using shift registers but channelization codes must be orthogonal and are generated as shown in fig. 3.10 [22]. The length of a code is equal to the number of possible orthogonal codes for a given SF. C_{ij} means the j^{th} orthogonal code for SR of i .

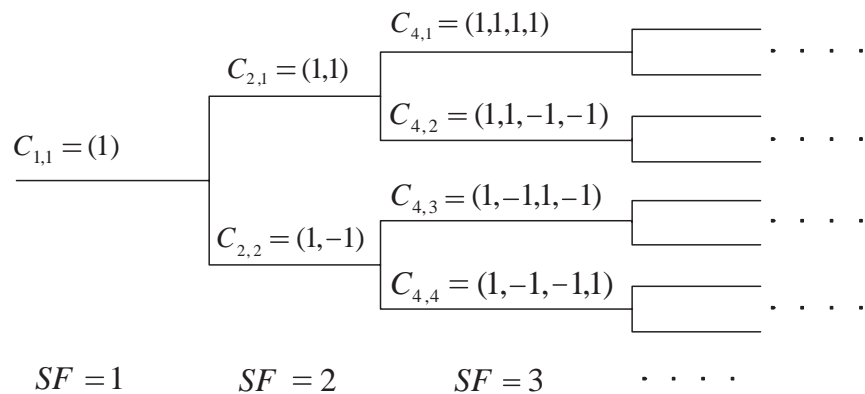


Figure 3.10: Orthogonal channelization codes for different spreading factors [22].

WCDMA and CDMA2000 systems have some similarities but may differ in channel bandwidth, PN code and chip rate. For example UMTS WCDMA has a frequency band of 60 MHz for each of uplink (1920-1980MHz) and downlink (2110-2170MHz) in FDD mode [20]. There are also some additional TDD channels available. The frequency bands are divided in 5 MHz bandwidth channels and the chip rate is 3.84 Mc/s. Channel bandwidth and chip rate can change for other WCDMA applications. In CDMA2000 also comparable data rates are possible. The chip rates of 1.2288 and 3.6864 Mc/s are used for channel bandwidths of 1.25 and 5 MHz respectively.

CDMA systems have varying signal envelopes due to their modulation formats and they are very sensitive to transmitter path nonlinearities. Therefore highly linear PAs are required as in EDGE, which shows the importance of PA linearization methods in new generation systems. ACPR and EVM performances are very important in CDMA systems. System specifications must be fulfilled with sufficient margin. For example ACPR limits for WCDMA in UMTS are -33 dB at 5 MHz (adjacent channel) and -43 dB at 10 MHz (alternate channel) offsets, and the EVM should not exceed 17.5% [23].

Chapter 4

RF transmitters

In a mobile communication system RF transmitter is responsible for modulation, up-conversion, amplification and signal transmission into the air using an antenna. In general inputs of a transmitter are analog baseband signals and its output is a modulated high frequency and high power signal. Output power, linearity, efficiency, circuit complexity and cost are some important criterias in choosing transmitter topologies in wireless applications. In this chapter direct and two step conversion transmitter architectures are explained first. Then various transmitter topologies are described in respect to their benefits and drawbacks for future high efficient terminal transmitter architectures. Nonlinear transmitters as in GSM and different linear transmitter architectures suitable for EDGE, WCDMA, CDMA2000 or Wireless LAN applications are described. Advantages and drawbacks of different linear transmitters such as the conventional linear PA, polar transmitter (PTx), polar loop transmitter (PLTx), envelope follower and power tracking are explained.

4.1 Transmitter architectures

Architecture selection is very important especially in the sense of proper system operation, performance improvement and reduced circuit complexity. Two main architectures are used mostly in RF transmitters: direct and two-step conversion architectures [24, 25, 26, 27].

4.1.1 Direct conversion (homodyne) architecture

In direct conversion transmitters the modulation and upconversion of input baseband signals take place in one step with a modulator as shown in fig. 4.1 in a simplified form. The architecture is also called homodyne. This is a mixer based topology with Cartesian input baseband signals. The modulator is composed of two mixers, one 90° phase shifter and an adder. I and Q are input baseband signals to be modulated. Output of the modulator is applied to the PA and PA output is sent to the antenna through a matching circuit and duplexer (or antenna switch). In some systems modulator output is low-pass filtered to fulfill noise specifications in their receiver bands. This topology

is quite simple and suitable for high degree integration [24]. For high frequency applications in general it is difficult to integrate passive circuit elements with high accuracy. Therefore most of the time discrete passives are implemented in order to have a high performance. The main reason for implementing passive components is requirement of very high quality filters at high frequencies. Homodyne architectures are suitable for high degree integration because they need low number of passive elements.

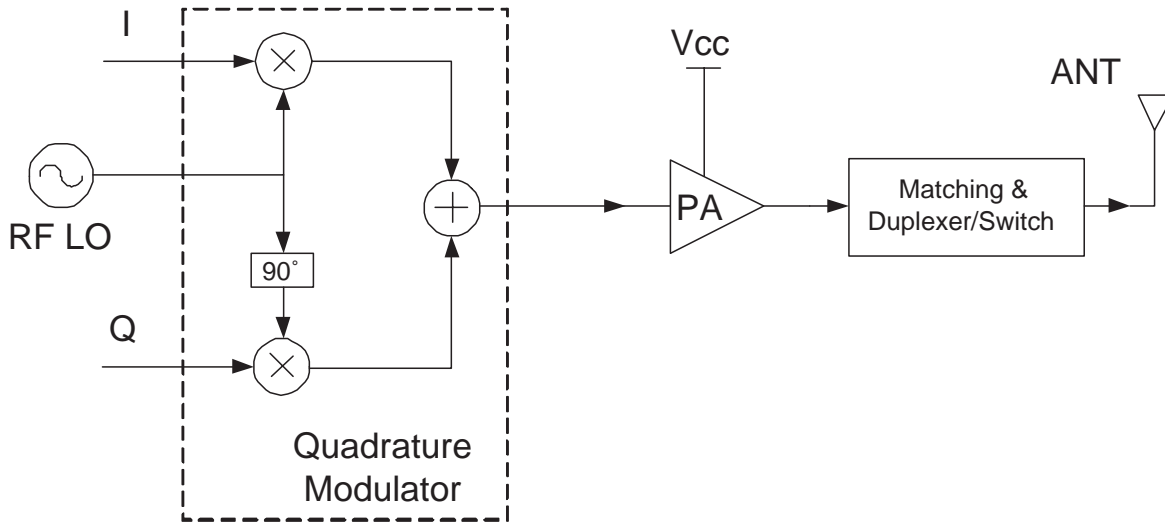


Figure 4.1: Mixer based direct conversion (homodyne) transmitter architecture.

In homodyne transmitters the LO (Local Oscillator) frequency is equal to the carrier frequency at the output. The carrier at PA output has a modulation signal in its vicinity and if there is a coupling to the LO unit, then this will be seen as a kind of noise by the LO loop which may result in locking to a frequency different than the desired carrier. This is called LO pulling and is a very important drawback of direct conversion architecture [24, 25]. If there is not good LO shielding and if PA output power is high, then LO pulling is much more likely to happen. In some systems LO is designed to generate frequencies multiple (in general 2 or 4) of the output carrier and it is divided by 2 or 4 in order to obtain the desired frequency. In this case the second or fourth harmonic power at PA output can cause LO pulling.

A possible solution to the problem is to use offset LO architecture shown in fig. 4.2. In this architecture an additional LO (LO2 with frequency of f_2) is used in order to give an offset to the RF LO (LO1 with frequency of f_1) used in fig. 4.1. The only difference between fig. 4.1 and fig. 4.2 is in generation of the LO signal for quadrature modulation. As a result signals at modulator and PA outputs will have the carrier frequency of $f_1 \pm f_2$, which is far from f_1 and f_2 . However, the mixer used to multiply two LO signals has nonlinearities and if out of band signals are not suppressed by the band-pass filter (BPF) sufficiently, then modulated signal is degraded [24]. Another drawback of the proposed architecture the requirement of an additional LO.

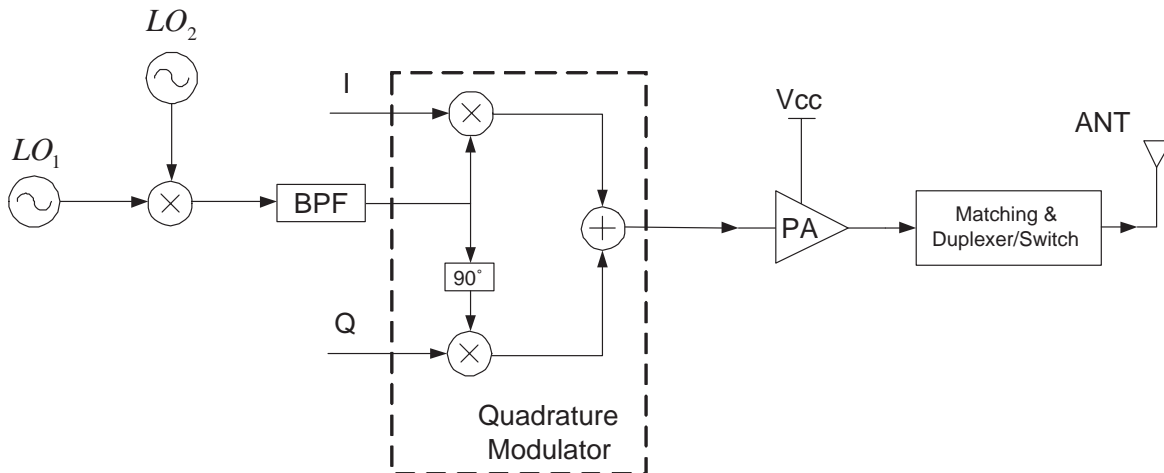


Figure 4.2: Mixer based direct conversion transmitter with offset LO.

4.1.2 Two-step conversion (heterodyne) architecture

Two-step conversion is a widely used transmitter architecture. It is also called heterodyne architecture. Baseband signals I and Q are modulated and upconverted in two steps as shown in fig. 4.3. The carrier frequency at PA output has a frequency different than the two LOs used in quadrature modulation and upconversion steps. Therefore this method is a good solution for LO pulling.

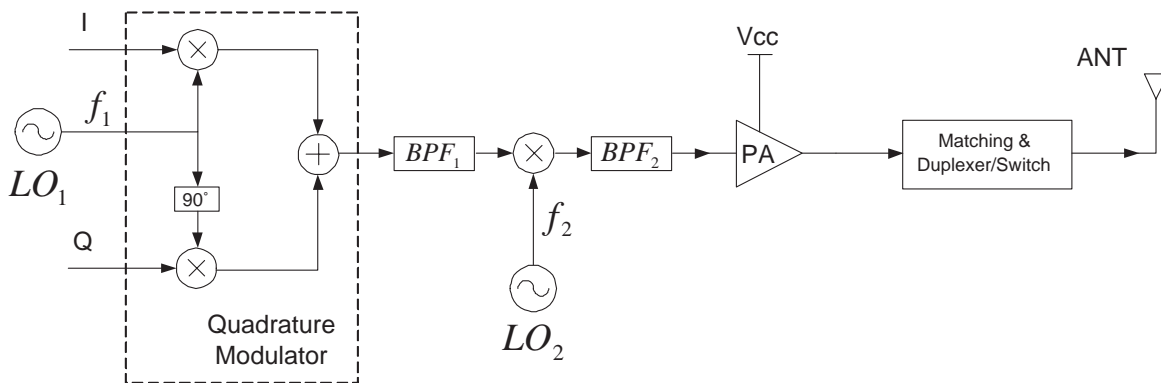


Figure 4.3: Two-step (heterodyne) transmitter architecture.

Baseband signals are first modulated using a quadrature modulator and LO_1 having the frequency of f_1 , which is called as IF (Intermediate Frequency). Then the modulated signal is band-pass filtered and upconverted using a mixer and LO_2 with the frequency of f_2 . Upconverted signal is band pass filtered again and sent to the PA input. As a result the frequency at the PA input and output can be selected to be $f_1 \pm f_2$.

One significant advantage of heterodyne structure is the possibility to filter the modulated signal for a good shape at the output which is easier to do at IF compared to RF. As shown in fig. 4.3 BPF_1 filters out unwanted harmonics at the output of modulator

and BPF_2 filters out the unwanted side band signal at the mixer output (for example at frequency of $f_1 - f_2$). The required amount of BPF_2 suppression is high because both side band signals have equal power and one of them must vanish. Such a filter is relatively difficult to achieve at RF. It is expensive and in general implemented off-chip which reduces system integration level [24].

4.1.3 Modulation loop

Homodyne and heterodyne architectures explained above have high out of band noise power, which can fall in the systems receiver band. Therefore they need in general duplexers after the PA. The modulation loop [26, 27] shown in fig. 4.4 can be a solution for this problem, reducing output noise floor level significantly. This architecture is also called as offset PLL (Phase-Locked Loop) [24] or upconversion loop [25].

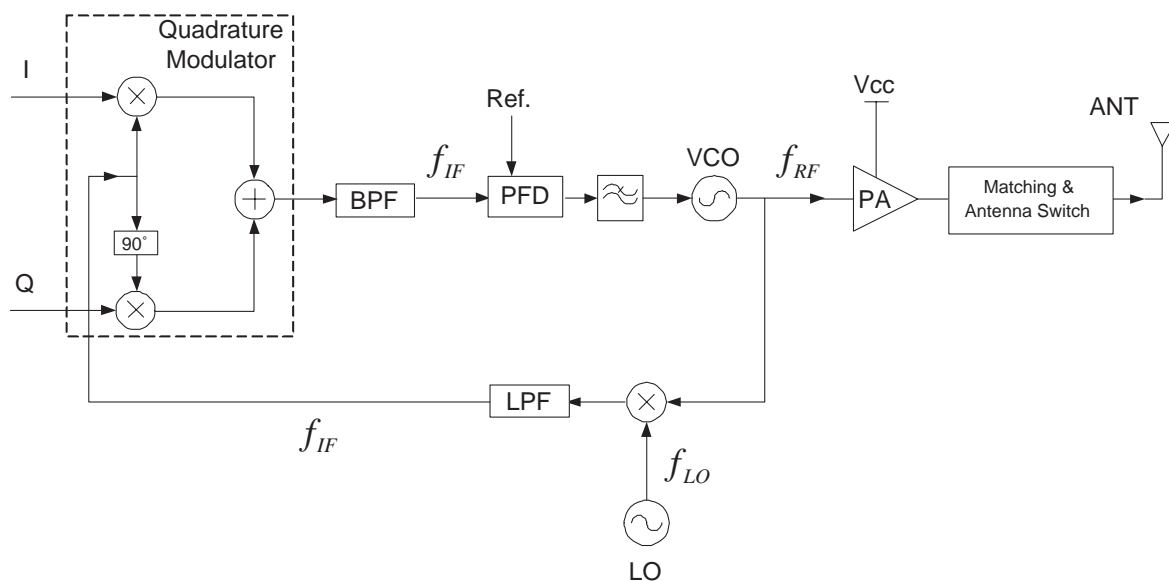


Figure 4.4: Modulation loop usable in nonlinear systems.

The circuit shown in fig. 4.4 is a PLL with a quadrature modulator in its feedback path. Signal at the VCO (Voltage Controlled Oscillator) output is downconverted using an LO and LPF. The resultant IF signal has a frequency of $f_{IF} = f_{RF} - f_{LO}$. The LO frequency can be varied to adjust frequency of the signal at output easily. Baseband I- and Q- signals are sent to the modulator and are modulated at f_{IF} . This signal is bandpass filtered and applied to a PFD (Phase-Frequency Detector) and then to the PLL loop filter in order to modulate the VCO. In general frequency dividers are also implemented between BPF and PFD. The signal at the VCO output is phase modulated with a polarity opposite to the modulation at the quadrature modulator output. This means the VCO must have phase modulation which is cancelled by the quadrature modulator in order to fulfill the requirements of the PLL [27].

In conventional methods the noise floor is the sum of systems VCO noise and noise generated in mixers. However, in modulation loop output noise floor depends effectively

just on VCO noise, which can be very low [24]. The advantage of the system is implementation without duplexer, which is expensive, bulky and causing power loss. The disadvantage of the system is that it is usable for systems having just phase modulation such as GSM.

4.1.4 Polar modulator

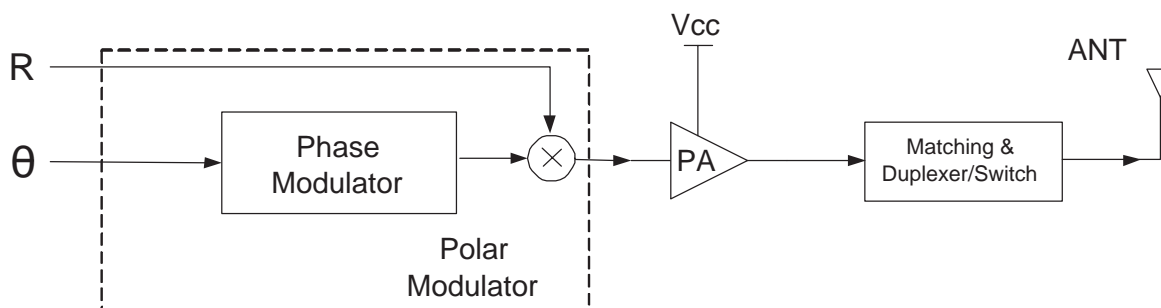


Figure 4.5: Simplified polar modulator system architecture.

A PLL based modulator alone can generate signals with just phase modulation (PM) but not amplitude modulation (AM). To be able to generate signals with AM and PM, another architecture called polar modulator can be used [28]. Fig. 4.5 shows a simplified block diagram of a homodyne polar modulator. In this architecture the baseband signals are not in Cartesian (I&Q) but in polar form (R & θ). R is the magnitude and θ is the phase of the modulation signal. First the phase of the carrier is modulated by a PLL based system like for example a sigma-delta modulator (SDM) and the amplitude modulation is applied later using a multiplier. Since the phase of the VCO is not constant but modulated by the input phase, the frequency spectrum at VCO output has a wide bandwidth and so it has a kind of immunity against LO pulling by the PA.

4.2 Nonlinear transmitter

The phrase "nonlinear transmitter" is used to indicate the difference between RF transmitters requiring no linearity in their PAs as in GSM, and transmitters requiring linear PAs as in EDGE, WCDMA, CDMA2000 and Wireless LAN. Nonlinear PAs are highly efficient but they are mostly used in systems operating with phase modulation like MSK or GMSK. If the envelope of the carrier is also modulated in order to increase spectrum efficiency as in QPSK, 8-PSK or QAM, then linear PAs are required. Fig. 4.6 shows a nonlinear transmitter architecture usable in GSM [29]. The topology in fig. 4.6 and other figures in the following sections are all selected to be direct conversion architectures for simplicity. They can also be realized in two-step conversion architectures.

In fig. 4.6 the carrier is phase modulated first and then sent to a low-pass filter for harmonic suppression. Then the signal is applied to a limiter and amplifier block in

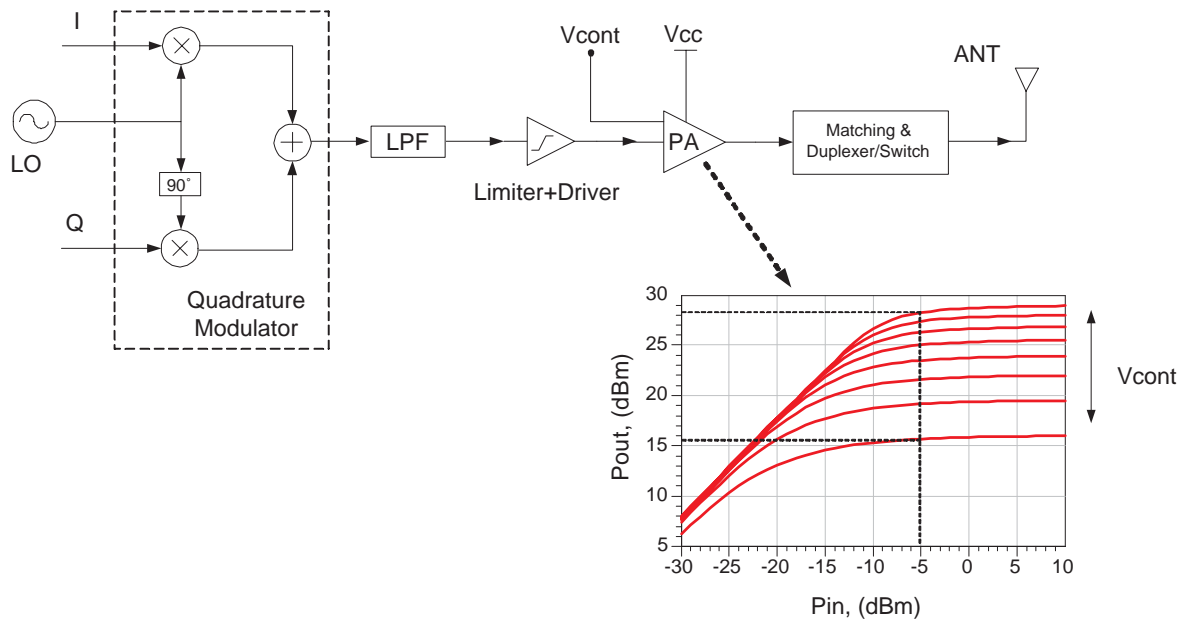


Figure 4.6: Nonlinear transmitter architecture with quadrature modulator.

front of the PA in order to eliminate any unwanted fluctuations in the signal envelope and amplify it so that the PA is kept in saturation with high efficiency. Operating the PA efficiently is a very important feature of nonlinear transmitters in battery operated mobile communication devices. In GSM terminals the PA output power is not controlled by changing the input power, but instead a control voltage (V_{cont}) is directly applied to a control pin for output power adjustment. This control signal is also responsible for power ramping which is required in TDMA systems. Fig. 4.6 shows also possible output vs. input power (AM/AM) characteristics of a PA obtained via simulation of a differential class AB GaAs FET PA. With changing V_{cont} the supply voltage and/or the bias of the PA is changed so that it has different AM/AM characteristics. As an example it is shown that by keeping the input power constant at -5 dBm and changing V_{cont} it is possible to have output powers between 15.5 dBm and 28.5 dBm always in saturation meaning high efficiency.

In fig. 4.6 a quadrature modulator is used. However, the modulation can be realized also with a PLL based modulation loop [27] or a SDM [30] because there is no need to modulate the envelope but just phase. Also the SDM modulator has a better performance in terms of LO pulling. Fig. 4.7 shows the modified block diagram of the nonlinear transmitter architecture with SDM.

4.3 Linear transmitters

Linear transmitters are required in systems which have spectrum efficient modulation types creating fluctuating envelopes at the input of the PA. Such modulation types are essential for high spectrum efficiency. Therefore architectures with linear PAs have

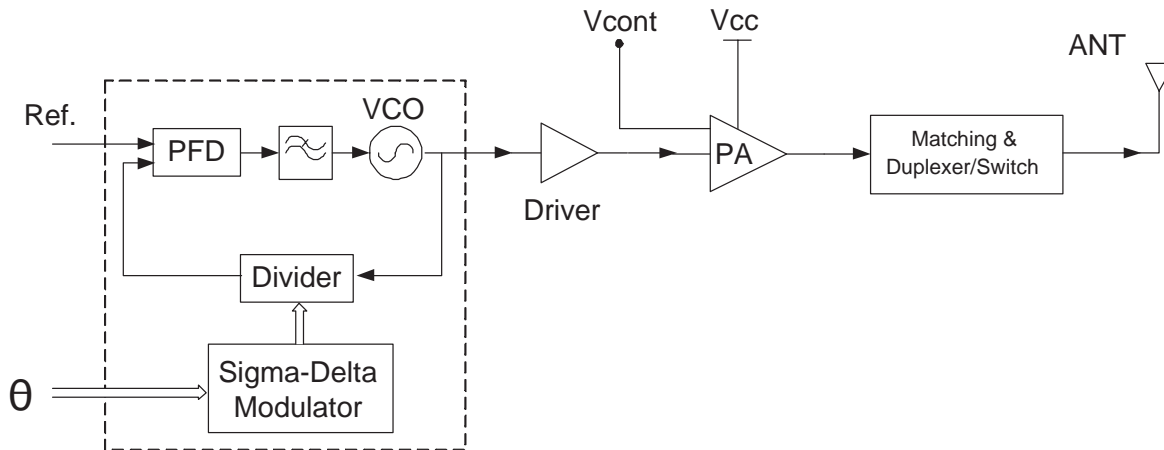


Figure 4.7: Nonlinear transmitter architecture with sigma-delta modulator.

been used for a long time. However, demand on higher system efficiency and multimode-multiband capability forced designers to investigate different linear transmitter topologies using nonlinear but efficient PAs like EER, PLTx etc. This section deals with some important linear transmitter architectures suitable for handset implementations.

4.3.1 Linear transmitter with linear PA

The block diagram of a conventional linear transmitter architecture usable in EDGE [29] is shown in fig. 4.8. In this architecture there is no bandpass filter for harmonic suppression after the modulator as in the nonlinear transmitter (fig. 4.6) because of highly linear operation of the modulator. On the other hand a VGA (Variable Gain Amplifier) is used instead of the limiter and driver block in front of the PA because the PA used in this architecture has a constant gain and the PA output power is adjusted by changing its input power via the VGA. Fig. 4.8 shows also the simulated AM/AM curve of a differential class AB GaAs FET PA. This curve shows how the desired output power to be transmitted is obtained by adjusting the input via the VGA. The PA is operated with some back-off in order to deliver linear output powers. Therefore the PA efficiency is lower compared to nonlinear PAs. The amount of required minimum back-off depends on the application because different systems require different linearity, BER performance etc.

In fig. 4.8 a quadrature modulator is used for amplitude and phase modulation. It can also be realized with a polar modulator as in fig. 4.5 comprising for example a PLL based phase modulator and a mixer joining the amplitude and phase modulations.

4.3.2 Envelope elimination and restoration (EER) / Polar transmitter (PTx)

EER is a well known linear transmitter architecture [31, 32, 33, 34]. It gains in importance with the time because the obtainable efficiency is significantly higher compared

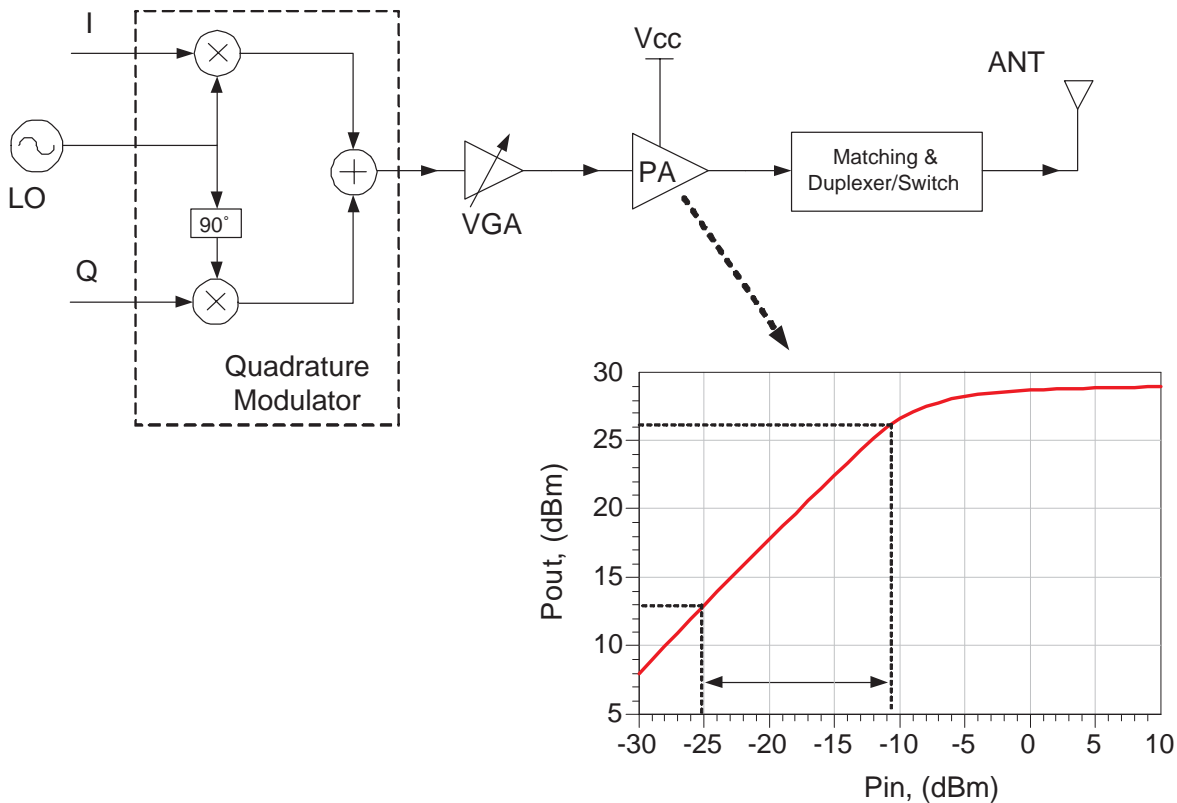


Figure 4.8: Linear transmitter architecture with linear PA.

to architectures with linear PAs. Fig. 4.9 shows a simplified EER block diagram. The amplitude and phase modulated input signal is split into two: one is sent to an envelope detector and the other to a limiter. The hard limited signal containing PM is sent to the PA input and the detected envelope is used to modulate supply voltage of the PA via a switching mode regulator. As a result the amplitude and phase modulated input signal R_{in} is reconstructed at output of the PA with amplification.

There are some modifications possible to do in an EER structure in order to make it simpler. Splitting of the input signal, obtaining its envelope and applying hard limiting can be avoided if the amplitude signal and phase modulated signal are generated in digital signal processing (DSP) unit separately, which is not a big problem for today's advanced mobile communication systems. Then possible degradations in the signal due to these analog operations would be avoided and the system could be called envelope restoration. Fig. 4.10 shows a possible implementation, which is going to be called as polar transmitter (PTx) concept [35, 36, 37]. A SDM is used for generation of phase modulated carrier and the signal envelope is directly converted to analog using a digital-to-analog converter (DAC). The complex baseband signal, which is in general in Cartesian (I&Q) format should be converted to magnitude (R) and phase (θ). While the phase modulated carrier is amplified and sent to the PA input with a power level sufficient to keep it in saturation, the envelope signal is sent to a unit responsible for supply voltage and bias modulation.

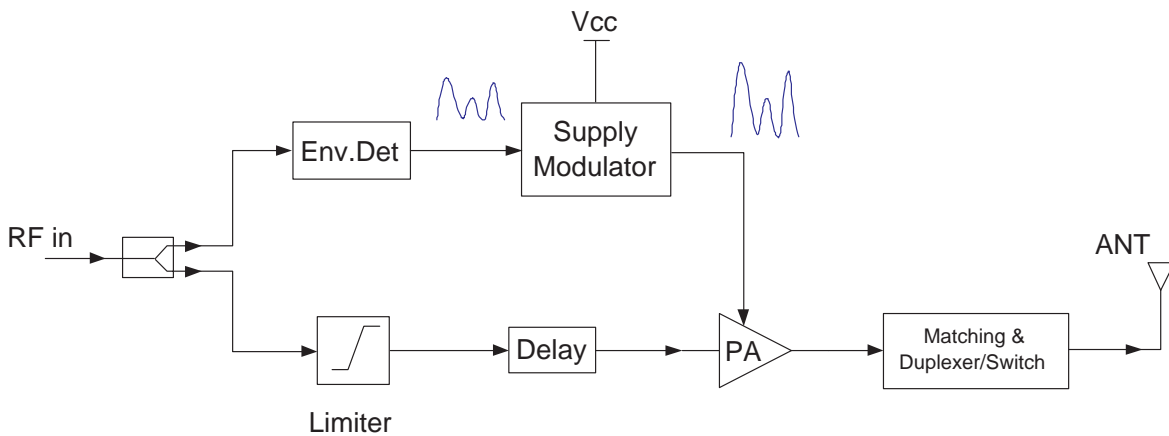


Figure 4.9: Envelope Elimination and Restoration architecture.

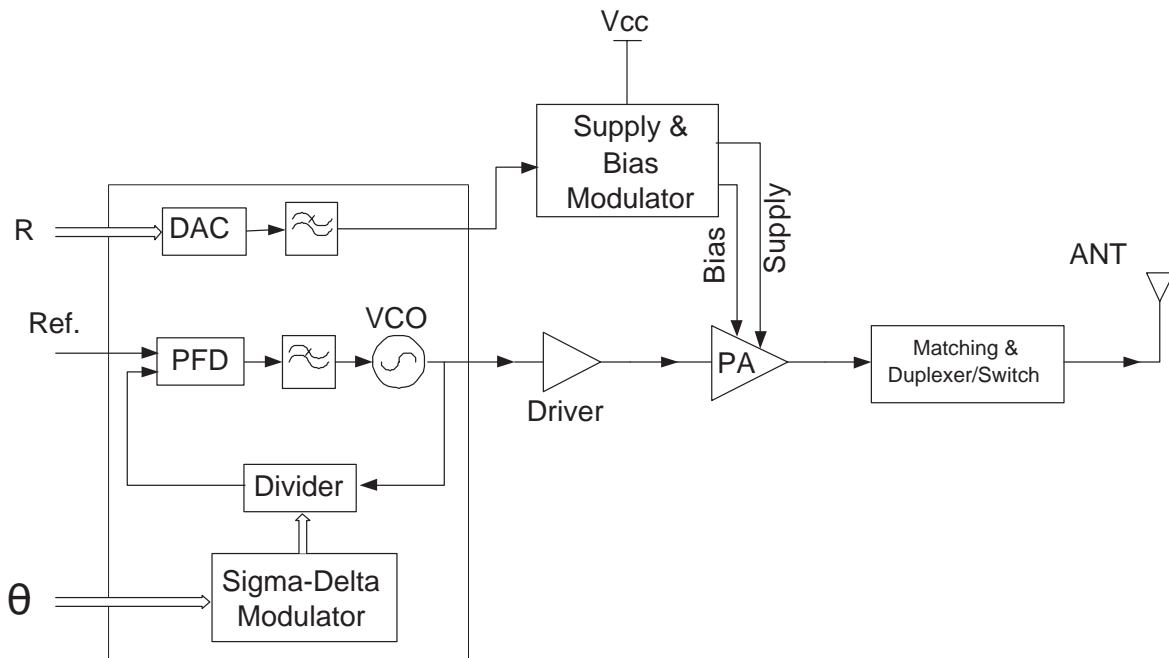


Figure 4.10: Block diagram of polar transmitter concept.

In PTx concept the aim is to improve transmitter efficiency by modulating the PA supply voltage and / or bias. Such a system is suitable for multi-mode system applications and it is supposed to have more robust operation in the case of antenna mismatch. In this concept the PA can be modelled as a three port device: two inputs and one output. The modulated signal containing PM at the PA input and AM at the supply & bias modulator input exists just at the PA output. The advantage of PTx concept is the possible usage of saturated or switch mode PAs having high efficiencies.

One of the most important issues in the PTx concept is to modulate the supply voltage. Modulating phase of the input and the bias can be done easily but supply voltage

modulation is difficult because a high amount of current must be drawn from the supply at the same time. For this purpose either a linear regulator or a switching mode amplitude modulator (DC-DC converter) can be used. DC-DC converters are more efficient compared to linear regulators but they generate more spurious signals falling into modulation bandwidth if the switching frequency is not high enough. Fig. 4.11 shows the block diagrams of a linear regulator and a buck DC-DC converter usable in PTx concept. It is difficult to integrate a DC-DC converter because of the required inductor and capacitor at the output. Passive components must have high quality for low loss and be robust enough in order to be able to handle high currents and voltages. However linear regulators can be integrated more easily. The value and size of passive components in a DC-DC converter change for different modulation bandwidth and switching frequencies. Fast switching power supply modulators use filter components reduced in value and size and their loop bandwidth is high making it possible to use them for wide bandwidth applications [38]. However the efficiency obtainable in a DC-DC converter decays if the switching frequency is increased. Because the transistor transient time, which contributes to losses in the circuit increases and becomes more significant compared to slow switching regulation. In [39] a method is proposed, which reduces switching losses and can handle high bandwidth signals. This is achieved by using multiple slow switching regulators in parallel. High bandwidth can also be problematic in the phase modulation path due to loop filter bandwidth of the PLL. This problem may be solved by using two-point modulation [40]. Although switching regulators are complex and noisy, they are more suitable in battery operated systems compared to linear regulators because they are more efficient [11].

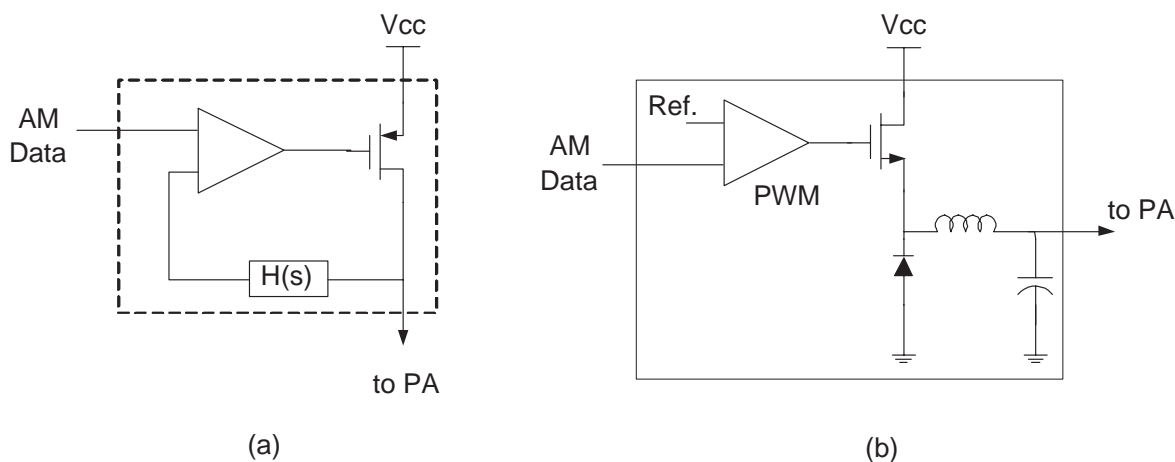


Figure 4.11: Block diagram of (a) linear regulator and (b) buck DC-DC converter.

The bandwidth of the modulation is a limiting effect in both linear regulator and DC-DC converter because the loop bandwidth in both circuits must be much higher than the bandwidth of the incoming AM signal. For example the buck DC-DC converter reported in [11] has been designed to have a closed loop bandwidth four times the input signal bandwidth and a switching frequency of five times the closed loop bandwidth. This means the switching frequency should be at least twenty times the input signal bandwidth. Additionally the bandwidth of the AM signal can also be a couple of times

greater than the bandwidth of the signal at PA output which is amplitude and phase modulated, because in today's mobile communication systems pulse shaping is done in Cartesian coordinates. The baseband I- and Q-signals and so the modulated signal at PA output are shaped and, if they are converted to polar form, this spectral shape will be distorted. This makes the loop bandwidth requirement much tighter because closed loop bandwidth and switching frequency must be increased accordingly.

Time alignment is also an important issue in PTx concept. To be able to obtain a high quality AM and PM modulated signal at the PA output, time delays in amplitude and phase paths must be equal. If not then PA output spectrum exhibits unsymmetry and distortion in its adjacent channels. The system may not fulfil the specifications if the delay mismatch is high. Another problem in PTx concept is the nonlinearity of transfer functions in AM and PM paths. The output power is assumed to be proportional to the square of PA end-stage collector voltage (V_c) which is not valid for very low V_c values. These type of nonlinearities can be corrected by means of predistortion. Dynamic range of the input signal is also important because PAs may not operate properly with very low supply voltages. A possible solution can be avoiding the occurrence of very low instantaneous voltages and zero crossing, which is the case in some modulation types like 8-PSK used in EDGE. However, in some others like QPSK, used in WCDMA, signal trajectory is allowed to pass through the origin, which can be problematic in PTx concept. In [41] a method eliminating zero crossing of modulation signals is proposed which results in degradation in signal spectrum but still fulfills system specifications.

4.3.3 Polar loop transmitter (PLTx)

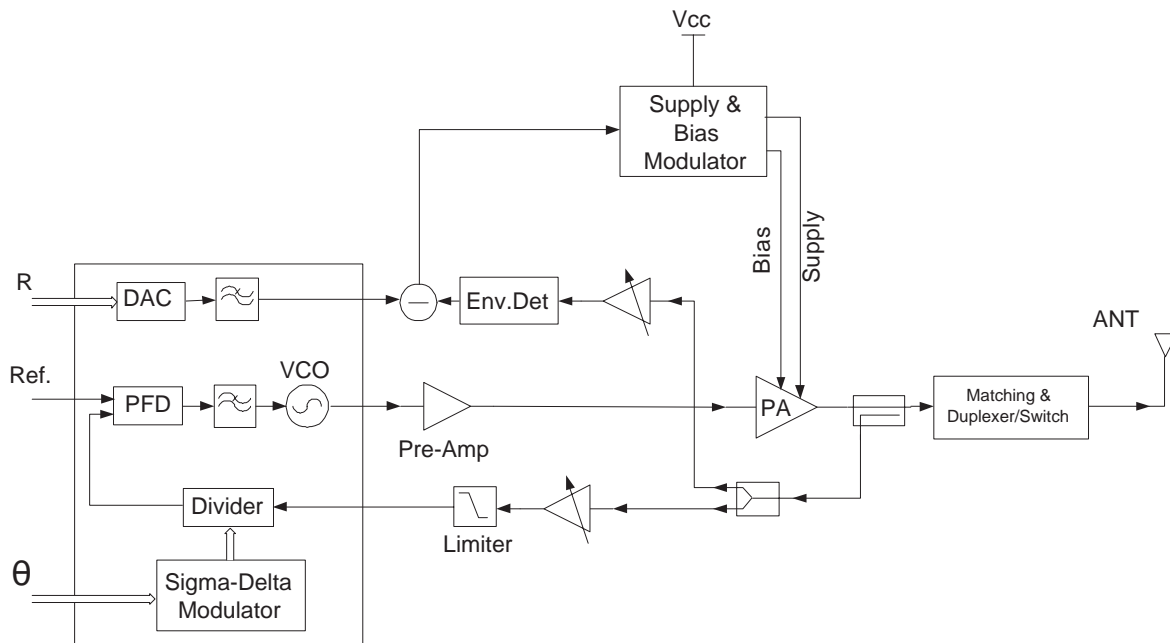


Figure 4.12: Block diagram of polar loop transmitter concept.

PLTx is a closed loop version of PTx. Fig. 4.12 shows a possible system implementation where two feedback loops for amplitude and phase correction are implemented. The reason of feedback is to obtain a good linearity in polar transmitters. It is possible to correct the nonlinearities precisely also under varying operation conditions like temperature and load variations. This means required linearity can be obtained without using predistortion. The main drawbacks of the system are limited modulation signal bandwidth due to loop stability requirements and required additional feedback loops increasing the cost and size. On the other hand for low output powers the effect of noise becomes significant and degrades linearization performance. In [42] a polar loop transmitter topology applicable in EDGE is presented.

4.3.4 Envelope Follower

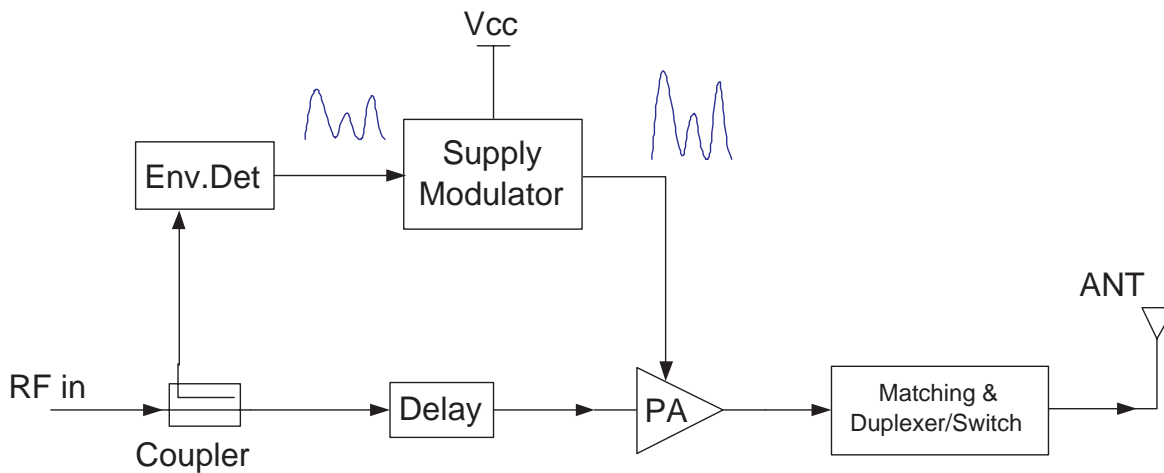


Figure 4.13: Block diagram of envelope follower.

Envelope follower is similar to PTx in the sense that its supply voltage is also modulated. The input of the amplifier, however, is not hard limited and this is the difference between them. This means the PA has a varying envelope input signal and it is not operated in switching mode. Fig. 4.13 shows a possible system implementation. It is not crucial for overall system linearity that supply voltage value exactly replicates the input signal because the PA input is not hard limited, and it contains both AM and PM. However, the supply voltage must have values avoiding clipping [43]. On the other hand the supply modulator must be fast enough for stable system operation.

In such a system both DC bias current and supply voltage can be varied to obtain maximum improvement in system performance. There are nonlinearities in the system mainly due to two sources: amplifier gain and phase characteristics change with changing supply voltage and time delay in DC-DC converter [44]. Fast DC-DC converter and DP can be used together to improve linearity while optimizing efficiency. In [38] an architecture is presented using a boost DC-DC converter as supply modulator. Advantage of a boost converter compared to buck type is that if the input voltage is dropped due

	Advantages	Drawbacks
Conventional linear PA	<ul style="list-style-type: none"> · Wideband signal handling capability 	<ul style="list-style-type: none"> · Low efficiency · Dual mode PA required · Antenna mismatch if no isolator is used
EER/PTx	<ul style="list-style-type: none"> · High average and peak efficiency · Single mode PA in saturation 	<ul style="list-style-type: none"> · Requires fast supply modulator · Predistortion for AM/AM and AM/PM correction · Delay mismatch between AM and PM paths · Dynamic range limitations · Zero crossing problem
PLTx	<ul style="list-style-type: none"> · High average and peak efficiency · Single mode PA in saturation · Adaptive system 	<ul style="list-style-type: none"> · Requires fast supply modulator · Limited modulation bandwidth · Stability problems · Large number of analog components
Envelope follower	<ul style="list-style-type: none"> · High efficiency (lower than EER and PLTx) 	<ul style="list-style-type: none"> · Requires fast supply modulator · Delay mismatch between AM and PM paths
Power tracking	<ul style="list-style-type: none"> · High average efficiency · Slow supply modulator is sufficient · No delay mismatch problem 	<ul style="list-style-type: none"> · Low peak efficiency (better than conventional PA)

Table 4.1: Comparison of different linear transmitter architectures.

to battery depletion, the required high voltage can be still maintained. However, in buck converters the supply voltage can only be less than the battery voltage.

4.3.5 Power Tracking

Power tracking is a simpler architecture compared to the envelope follower because the PAs supply voltage does not need to follow the instantaneous value of the envelope. Supply voltage can be adjusted by using RMS or peak value of the envelope which can be significantly slower. Therefore the required switching frequency is not as high as in the envelope follower. Fig. 4.14 shows a possible system implementation.

In EER and envelope follower peak power efficiency is better than power tracking but overall system efficiency is degraded due to their high transistor switching frequency requirement resulting in high switching losses [11]. Therefore power tracking is a promising technique which can be implemented with low effort especially for systems with wide bandwidth signals. Tab. 4.1 is an overview of different linear transmitter architectures. The main advantages and drawbacks of each system are given. Systems with supply modulation and variation are very attractive due to their high efficiency compared to transmitters with conventional linear PAs. On the other hand they can use single mode PAs for both linear and nonlinear operation which can reduce the PA

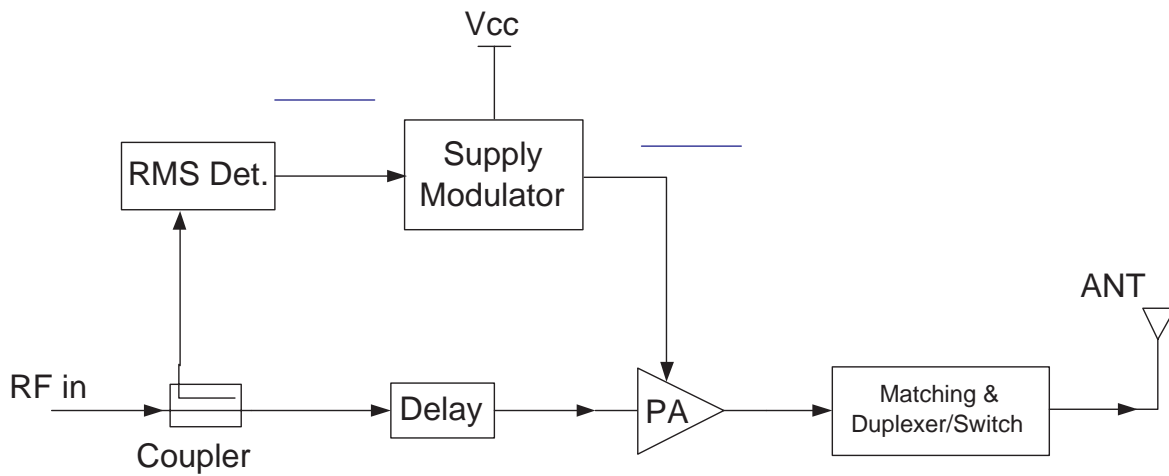


Figure 4.14: Block diagram of power tracking.

cost significantly. The amount of used components in the system is also reduced. However, they need a kind of linearization for proper operation. In PLTx it is an analog feedback loop and in the others it can be predistortion.

Chapter 5

Power amplifier linearization methods

Power amplifier linearization is currently one of the most promising techniques for linearity and efficiency improvement in mobile communication systems. There are numerous techniques which have different levels of complexity, various advantages and limitations [6, 45, 46, 47]. Different linearization methods may fit to different communication systems. For example more sophisticated high performance systems may be used for base station PAs whereas the systems usable in handsets should have low complexity, low cost and high efficiency. Although in general the main reason to implement these systems is to linearize the PA, they improve also the efficiency because a linearized PA can be driven closer to compression (operation with low back-off). In the following sections several PA linearization methods are explained which can be classified mainly as feedback, feedforward and predistortion systems.

5.1 Feedback

Feedback linearization methods are relatively simple compared to feedforward and conventional predistortion. The idea is to force the PA output to follow its input. There are different types of feedback linearization topologies classified mainly as RF feedback and modulation feedback which can be divided again into two: polar and Cartesian feedback. In modulation feedback the modulation components (I&Q or R& θ) of PA input and output are compared whereas in RF feedback the RF signals are compared. Feedback systems can be implemented at RF, IF or baseband frequencies. A major issue in feedback linearization is the stability due to delays in feedback which is critical, especially in systems with discrete components. The group delay increases significantly due to PA matching circuits or filters and couplers in the loop. Especially high order filters like SAWs (Surface Acoustic Wave filter) can not be used due to large group delays in the order of several hundred nanoseconds [46]. In RF power amplifiers it is difficult to have a high loop gain and good stability with RF feedback. Increasing operation frequency in RF feedback or modulation BW in modulation feedback makes stability issues even more critical. Feedback methods are not suitable for wide band

applications in the order of several MHz because the stability and correction capability of a feedback loop is limited by its gain-bandwidth product (GBW). Feedback systems can not distinguish between nonlinearities of PA and other nonlinearities in the forward or feedback paths. Fortunately the forward path nonidealities like nonlinearities, gain and phase mismatches in quadrature modulators can be corrected sufficiently by a close to perfect feedback path. Consequently, the feedback path must be as linear as possible, because it can not be corrected [42, 47].

5.1.1 RF feedback

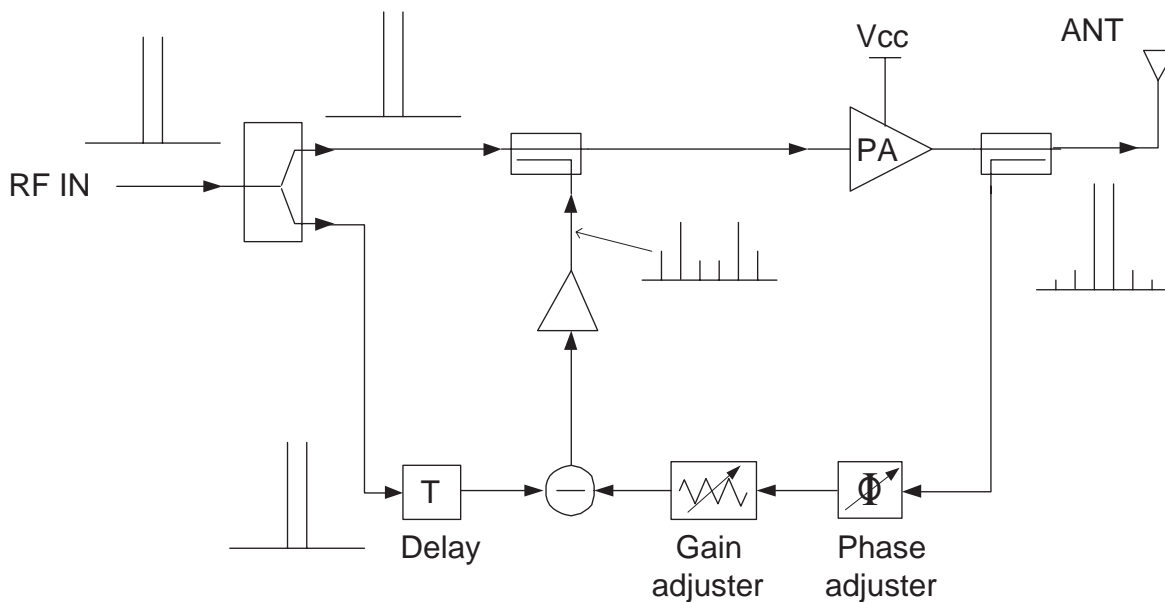


Figure 5.1: RF feedback linearization topology [5].

In this linearization type the RF output is subtracted directly from the input without demodulation or down conversion. Various topologies are possible in RF feedback [5]. They are mainly used to linearize an individual stage rather than a transmitter whereas modulation feedback techniques can be applied to complete transmitter systems. Gain stabilization is an important application of RF feedback. There are some RF feedback topologies applied to systems containing complete transmitters. However, the delay in the loop has to be small to ensure the stability, which may be achieved with MMIC (Monolithic Microwave Integrated Circuit) devices rather than discrete elements. Fig. 5.1 is an example of such an RF feedback topology called distortion feedback [5]. The input signal is divided into two parts. One part is compared with the distorted PA output signal to obtain an error signal canceling the error generated by the PA. This error signal is added to the second part of the input signal and sent to the PA input. The system looks like a predistortion system but uses real time feedback.

5.1.2 Polar loop

In polar loop linearization AM/AM and AM/PM nonlinearities are corrected by two individual loops as shown in fig. 5.2. The feedback is done in general at IF but RF implementation is also possible. In [42] a polar loop concept is presented having low complexity and being applicable to EDGE. In the previous chapter PLTx has been introduced which is an efficiency enhancement method, rather than linearity improvement method but it has also a good degree of linearity.

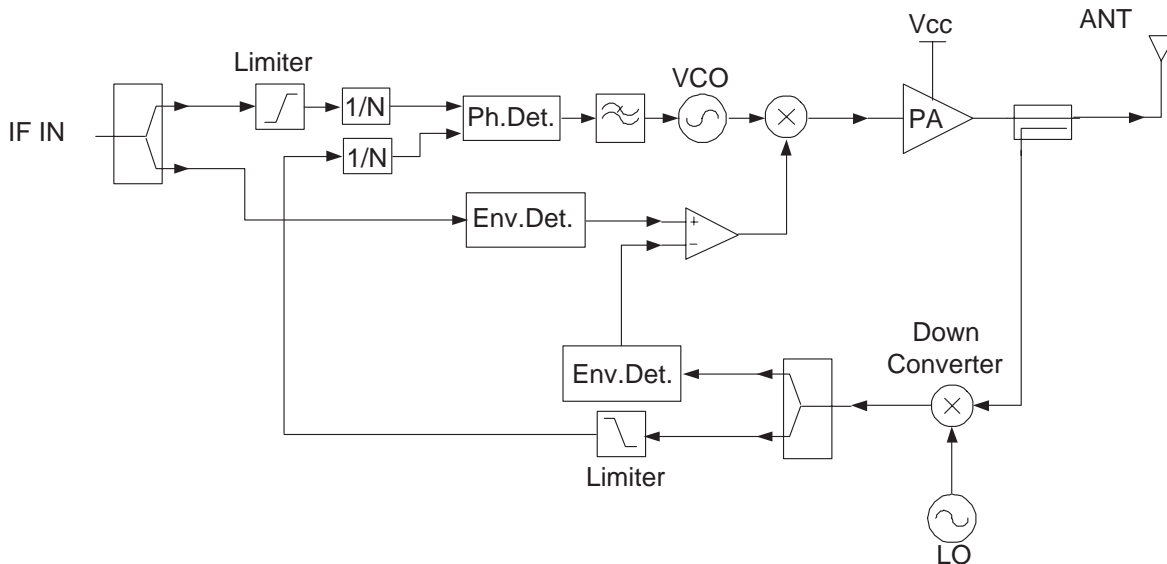


Figure 5.2: Polar loop linearization topology.

The topology shown in fig. 5.2 is different from PLTx in the sense that the amplitude loop does not modulate the PA supply voltage or bias, but modulates the envelope of the PA input signal. The input is assumed to be an envelope and phase modulated IF signal. It is first split into two parts. Envelope of the first one is detected in order to obtain AM data and the second one is sent to a limiter to obtain just the phase modulated carrier. A portion of the PA output is taken using a coupler and it is down converted. This signal is also split into two parts. Again one part is envelope detected to obtain AM data and the other is sent to a limiter to obtain the phase modulated carrier, both including PA nonlinearities. The two phase modulated signals from input and feedback are sent to frequency dividers and a PLL in order to force phase modulation to cancel the AM/PM nonlinearity of the PA. Also, the envelope detected input and feedback signals are sent to a differential amplifier to obtain an error signal canceling the AM/AM nonlinearity. VCO and differential amplifier output signals are sent to a mixer in order to obtain an amplitude and phase modulated PA input. In addition to fig. 5.2 there are various implementation possibilities. For example in some cases the required amount of linearization is low and it is sufficient to correct just AM/AM nonlinearities with envelope feedback. Another difference can be related to the phase loop where a phase shifter controlled by the phase error between input and feedback signals can be used instead of the PLL. The topology shown in fig. 5.2

can be realized at RF instead of IF with the result of reduced circuit complexity.

As a rule of thumb the correction loop bandwidth in a feedback system should be at least 5 times higher than the signal bandwidth in order to achieve a stable operation [42]. If a modulated signal with pulse shaping done in Cartesian coordinates is separated into its magnitude and phase components, then these have considerably higher bandwidths than the original signal. This additional increase in the bandwidth makes the stability issue in polar loop linearization more critical because the loop bandwidth should be accordingly higher for a proper operation. If we assume that the possible linearization bandwidth at cellular frequencies is typically less than 1 MHz with polar loop [48] (this is the bandwidth of magnitude or phase signal), then the maximum bandwidth of the signal to be corrected is much lower than 1 MHz, which is not sufficient for CDMA or WCDMA systems. Another disadvantage of the polar loop is locking problems of the PLL in the phase loop due to small instantaneous powers and abrupt phase jumps [45, 47].

5.1.3 Cartesian loop

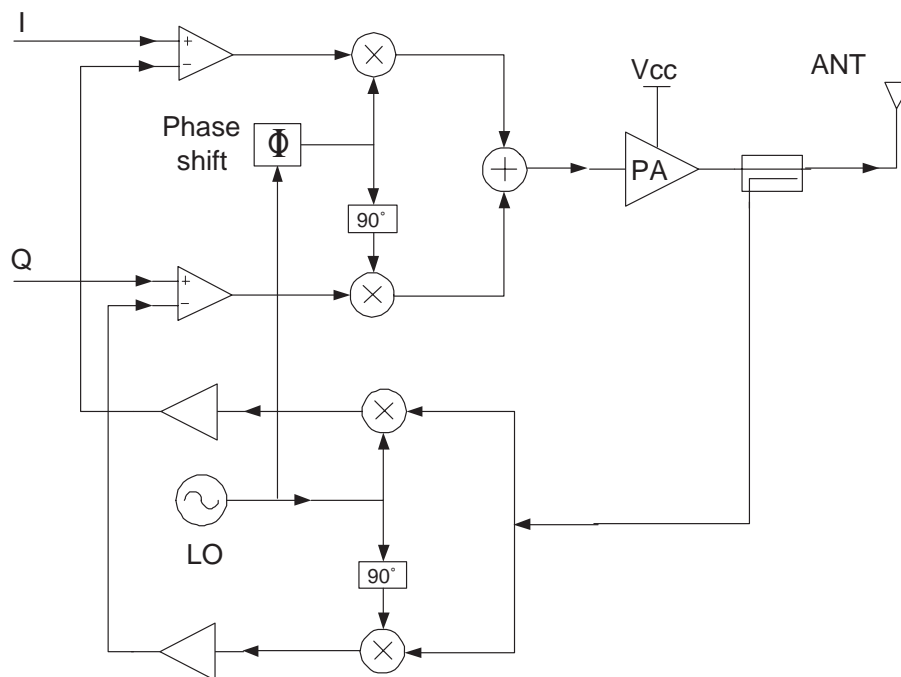


Figure 5.3: Cartesian loop linearization block diagram.

The problem of bandwidth widening in polar loop can be solved by Cartesian loop linearization technique. Fig. 5.3 shows a general block diagram. In Cartesian feedback I- and Q-signals are used to correct amplifier nonlinearities instead of R and θ as in polar loop. I and Q have similar spectral properties as RF signal whereas R and θ have much larger bandwidths [6, 46, 47]. In fig. 5.3 a demodulator is used in the feedback path in order to obtain distorted Cartesian modulation components from PA output.

Demodulated and scaled I- and Q-signals are subtracted from the input I- and Q-signals to obtain the PA input baseband signals resulting in linear operation.

The circuit in fig. 5.3 is implemented in RF because IF Cartesian loop is undesirable due to the additional delay added to feedback loop. Compared to polar loop, Cartesian loop is easier to implement, because in general digital circuits generate the baseband signals in I&Q form. Cartesian loop has been already implemented in narrow band systems [46]. For narrow band signals achievable degree of linearity is high. For wide band systems, however, it is not suitable due to high loop delays resulting in stability problems. A phase adjuster is necessary for LO signal in Cartesian loop in order to maintain the relationship between the input and feedback signals [6, 47, 49]. Since LO phase shift depends on temperature, power level and process variations which make the stability issue difficult [50], a control loop for phase shift may be necessary in order to maintain the synchronization in the system.

5.2 Feedforward

The feedforward method allows high linearization performance and is currently used in base stations of mobile communications systems. The idea is to extract the distortion at the PA output, amplify it and add it to the PA output in opposite phase in order to cancel the distortion. Out of all linearization methods, only feedforward systems provide a very good distortion reduction over a wide bandwidth. The drawback of these systems is the low power efficiency due to high power requirement of the error amplifier operated in class A mode and losses due to couplers and delay lines in the system.

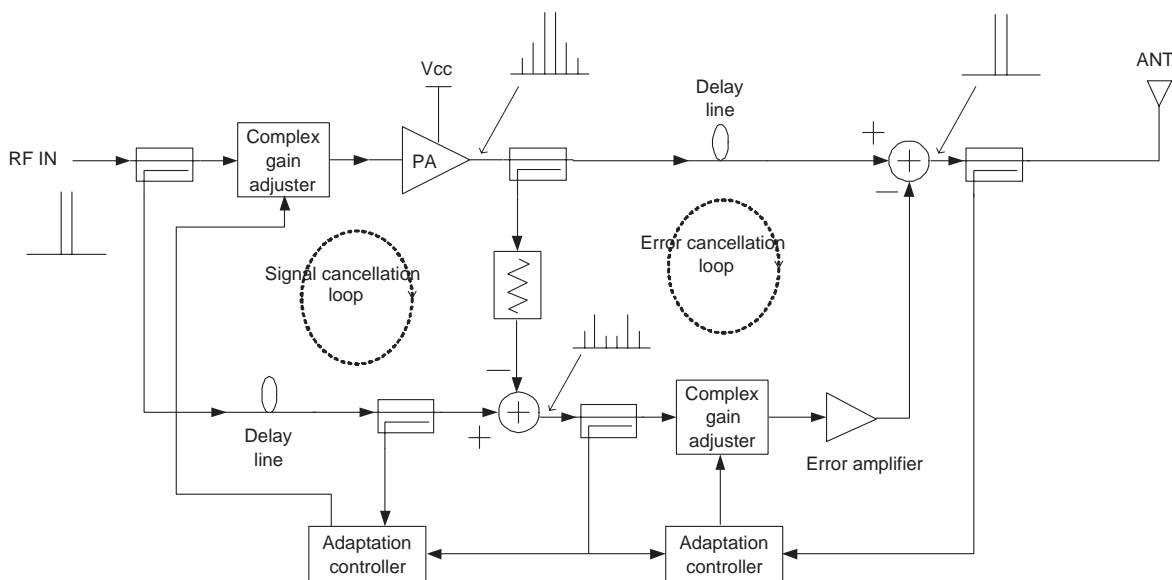


Figure 5.4: Feedforward linearization block diagram [51].

Fig. 5.4 shows the basic block diagram of feedforward comprising a PA and a high number of external components. The system is composed of two main parts: signal

cancellation and error cancellation loops. The signal cancellation loop works as follows. First, a portion of the PA input signal is taken using a coupler, which is used as reference signal in the loop. A portion of the PA output is also taken and its power is reduced to the level of the reference signal from input by using an attenuator. The subtraction of these two signals gives the error signal generated at the PA output which is going to be used to cancel the PA distortion at the system output. A delay line is implemented in the reference signal path in order to compensate time delay differences between these two paths. Since feedforward is based on subtraction and addition of almost equal signals, it must have a precisely controlled adaptation compensating the possible changes of the system due to changing environmental or operating conditions. Therefore the adaptation controller of the signal cancellation loop adjusts the complex gain adjuster in front of the PA in order to obtain just the error signal at the output of the loop. The controller uses the reference and error signals to do this adjustment.

The error cancellation loop works in a way similar to the signal cancellation loop. The error signal obtained from the signal cancellation loop is phase shifted using a complex gain adjuster in front of the error amplifier. It is amplified by the error amplifier and added to the delayed PA output. Also in error cancellation loop a precise control of the complex gain adjuster is required. This is achieved by a second controller using the error signal from the signal cancellation loop and the resultant system output. A second delay line is used at the PA output in order to eliminate time mismatch between upper and lower paths in the error cancellation loop and achieve a proper error cancellation at the output of the final combiner. For relatively narrow band signals delay lines are good enough solutions to adjust the phases such that the reference and error signals are sufficiently cancelled in the loops. However, for very wide bandwidth signals this is difficult to achieve. A possible solution is presented in [52] using a phase equalizer to obtain a better phase match at each frequency in the band of interest.

Adaptive feedforward linearization is able to handle wide bandwidths with continuous adjustment for component drifts and power level changes. The adaptation is done by using pilot signals or gradient methods. In [53] two examples with these techniques are presented comparing their performance. A DSP controlled feedforward system having an adaptation with gradient signals is presented in [54], and in [55] detailed derivations of gradient method are given.

The main strength of feedforward is its high level of intermodulation reduction capability for wideband signals with unconditional stability [56]. It has no stability problem because all signals in the system flow in the same direction meaning no feedback loops causing conditional stability. Distortion due to memory effects can also be compensated with feedforward because these effects are also included in the error signal and this is subtracted from the PA output [51]. The main issues to be considered in feedforward are improving system efficiency and reducing complexity. [56] proposes a method immigrating a part of the analog signal processing into the digital domain, which reduces the power requirement of the error amplifier meaning better efficiency and eliminates the output delay line. However, feedforward needs some more improvement in terms of efficiency in order to become usable in battery operated handsets.

5.3 Predistortion

The idea behind predistortion is to expand the input signal prior a PA in such a way that the nonlinearities due to the PA are compensated. It is realized by implementing a nonlinear block in front of the nonlinear PA generating input signal level dependent distortion elements opposite of the distortion caused by the PA. As a result the cascade of these nonlinear blocks has a linear response.

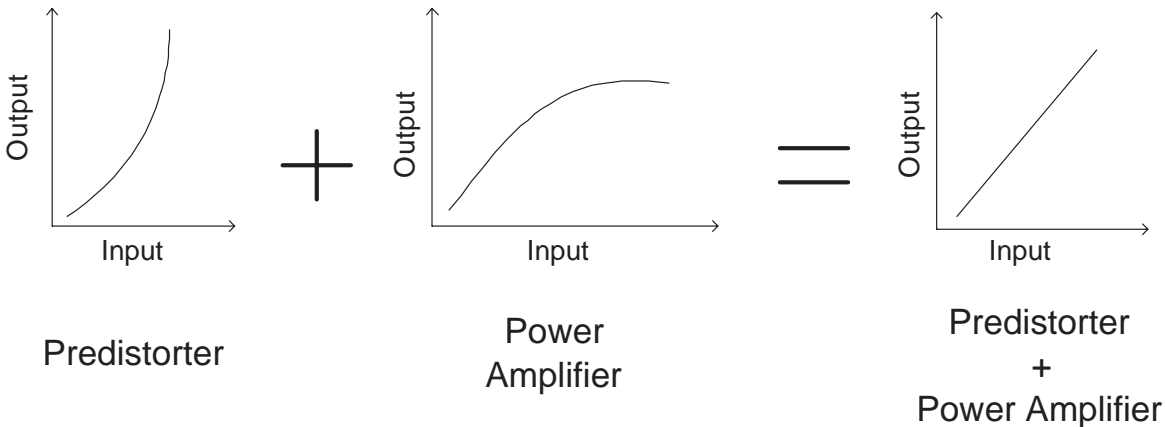


Figure 5.5: Simplified operation of predistortion.

Fig. 5.5 illustrates predistorter operation in a simplified way. The figure shows AM/AM correction done by the predistorter. In general the similar correction is also done for phase (AM/PM) by adding a phase to the input signal opposite of the phase shift due to the PA.

Predistortion can be realized in two different ways, analog or digital implementation. Analog predistortion is realized by creating the required AM/AM and AM/PM nonlinearities canceling the effects of PA using analog components. It can be implemented at RF, IF or baseband. In the digital predistortion case however the system is realized with digital components and it is implemented usually at baseband.

In predistortion systems first the PA characteristics must be obtained in order to calculate the required inverse nonlinearity compensating the PA nonlinearity. For a good system performance precise AM/AM and AM/PM characteristics are required. Although in some cases they can be assumed not to depend on frequency (static case), actually they do. In the case of static AM/AM and AM/PM characterization the PA output is assumed to depend just on the momentary input signal. However, in general the output depends on the momentary and previous input signal values. These previous values can change depending on signal bandwidth. This means the PA behaves in different ways if modulation signals with different bandwidths (for example two tone signals with same power but different tone spacings) are applied to it. This phenomena is called memory effect. In this thesis digital predistortion systems will be divided into two: systems taking memory effects into account and systems neglecting it such as MDP. Memoryless predistorters are much simpler compared to predistorters

with memory and if memory effects in a PA are not strong, then memoryless predistortion is a reasonable solution with high performance. However, the amount of linearity improvement is limited if the PA exhibits strong memory effects.

5.3.1 Analog predistortion

The advantages of analog predistortion are its relatively simple circuitry, low cost, low power consumption, wideband signal handling capability and integrity. However, these systems can have in general just a moderate linearization performance and they introduce insertion loss. Moreover if they are implemented adaptively, then system complexity may increase significantly. There are various ways to implement analog predistortion. It can be a simple circuit composed of diodes or transistors as in RF predistorters, or it can be composed of multipliers to realize polynomial nonlinearities. The system can be adaptive or fixed depending on environmental conditions and system specifications. However, a reliable system must have a kind of adaptation adjusting the predistorter according to the environmental conditions especially in today's mobile communication systems, which may operate under extreme conditions and still must fulfill the specifications. High linearity systems based on RF predistortion are extremely difficult to achieve and are not widely available [45]. A typical ACPR improvement of about 10 dB is possible [6]. In [57] a simple predistorter based on a diode circuit is presented which improves ACPR performance by about 5 dB. In analog predistortion the gain and phase flatness of the predistorter and of the PA limit the operating bandwidth, and the memory effects in both of them limit the linearization performance [6].

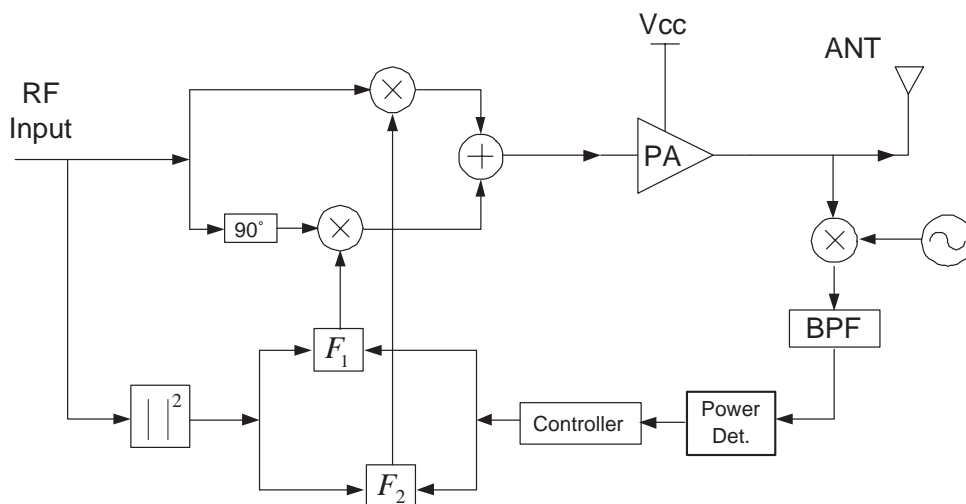


Figure 5.6: Block diagram of an adaptive RF predistorter [58].

RF predistortion operates just in front of the PA at high frequency. Fig. 5.6 shows the block diagram of a possible implementation [58]. The predistortion is done using a circuit changing the PA input signal according to polynomial functions. These polynomials are implemented using analog circuits and their coefficients are supplied and

changed by a digital control circuit. The system has an adaptation based on adjacent channel emission. The measured power in adjacent channels of PA output and squared magnitude of the system input signal are used in order to calculate the required polynomial multiplicands F_1 and F_2 . After multiplying the input signal with F_1 and F_2 , the signal is predistorted in a way that PA output linearity is improved.

The predistorter shown in fig. 5.6 is implemented at RF, but IF implementation is also possible. IF predistortion is a reasonable way for linearization because then it is possible to use the system for more than one frequency by using local oscillators for desired up- and downconversions. In the presented system the feedback path utilizes signal downconversion to simplify the design of the high selectivity BPF which is supposed to give a signal related to the adjacent channel power emission at the PA output. In [59] an IF predistorter is presented which is similar to the explained RF predistorter. The downconverter in its feedback and upconverter in its forward paths do the required frequency conversions.

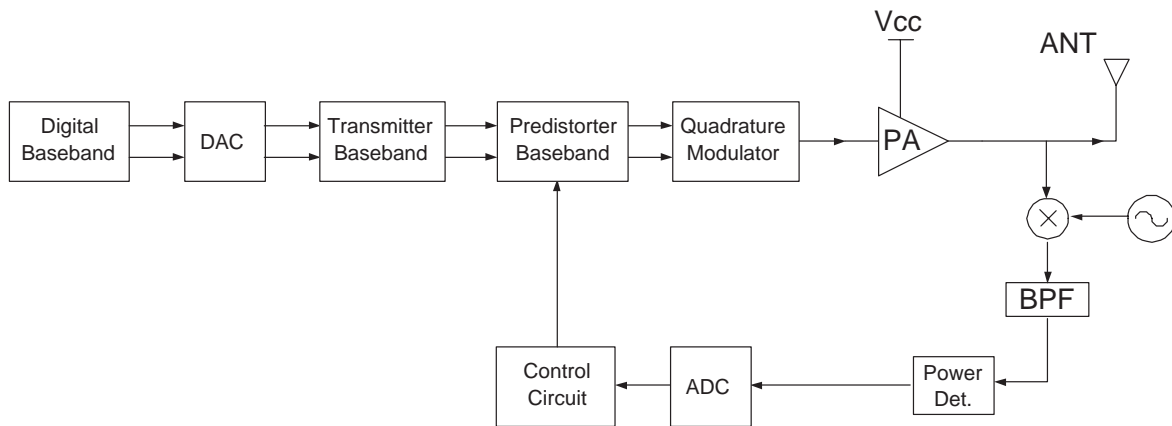


Figure 5.7: Block diagram of an adaptive baseband predistorter.

Fig. 5.7 shows a possible implementation of adaptive baseband analog predistortion. The control circuit in the feedback path is similar to the presented RF predistorter. A portion of the output signal is downconverted, the power in the adjacent channel is detected and the required polynomial coefficients are calculated. Actually different coefficient sets can be stored in a LUT and the required coefficients can be read from this table during operation. The adaptation may be used for coefficient update in this LUT. The predistortion takes place in the block named as "*Predistorter Baseband*" in fig. 5.7. The circuit inside this block responsible for polynomial predistortion at baseband is shown in fig. 5.8. Two 5th order polynomial predistortion signals F_i and F_q are generated and these are multiplied with the input baseband signals I_{in} and Q_{in} using a complex multiplier. The coefficients c_i , c_q , c_{3i} , c_{3q} , c_{5i} and c_{5q} are either read from a LUT or taken from the "*Control Circuit*" in fig. 5.7. In [60] and [61] similar predistorters are presented, which can be implemented both in IF and baseband.

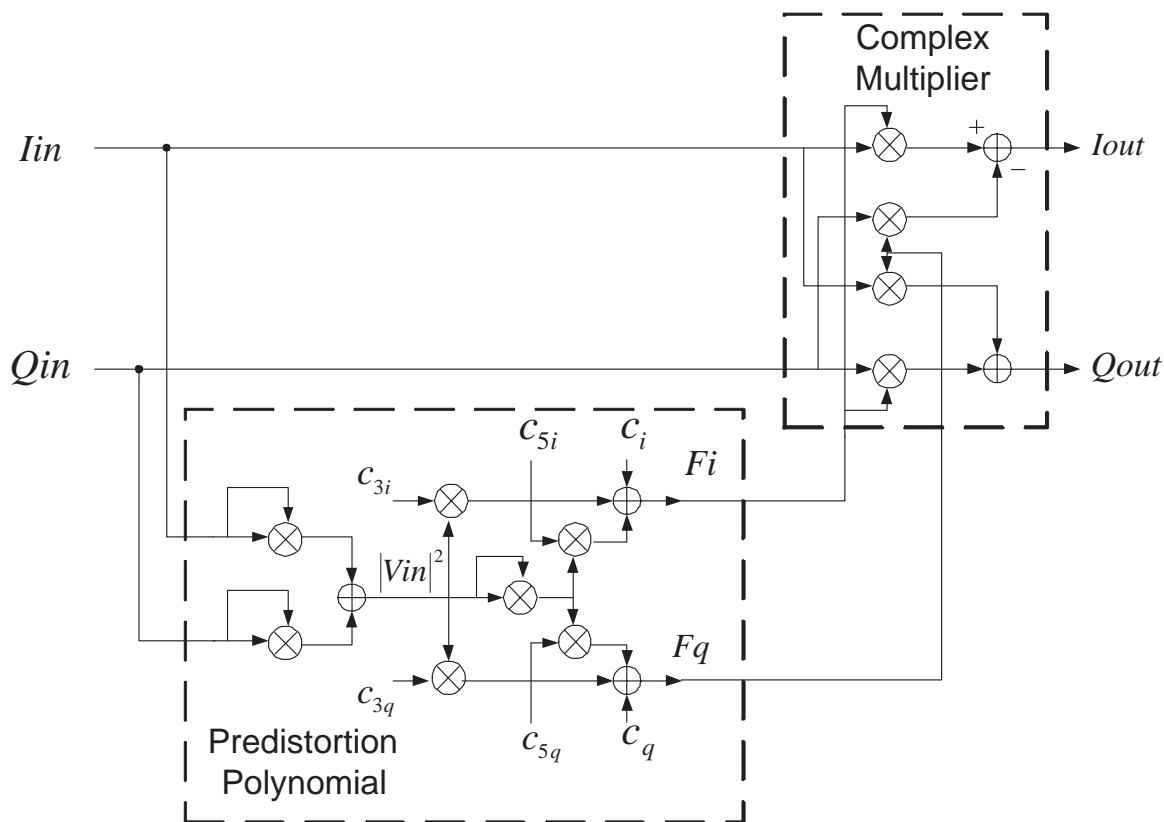


Figure 5.8: The structure of a 5th order predistortion polynomial and the complex multiplier for baseband predistorter.

5.3.2 Digital predistortion

DP is usually implemented in digital baseband but it is also possible to do it at IF. The theory behind is the same as in analog predistortion. This method is in general used for base stations in mobile communication systems in order to improve linearity, which is very important in systems with wide bandwidths. A significant improvement can be achieved for class B and AB amplifiers in applications requiring high linearity. DP is simple compared to feedforward linearization widely used in base stations. It is unconditionally stable and a precise linearisation is possible. Since the implementation is done with digital components, the system is more robust and flexible compared to analog circuits. The method is robust against drifts in PA characteristics due to component variations, temperature, aging, if it is implemented adaptively. This is at the expense of increased complexity due to significant amount of added hardware and software.

The main drawback of DP is its limited bandwidth. Since all data samples must be modified continuously, a high amount of mathematical operations in digital domain is required. If the sample frequency or bandwidth of the modulation signal increases, then the required clock frequency and the amount of operations also increase. Higher clock frequency or higher amount of operations means higher power consumption. However, there is a continuous improvement in digital IC technology. Power consumption de-

creases as the integration level increases. Therefore DP seems to be one of the most promising linearization techniques for future applications.

We can divide adaptive DP into two parts: the forward and feedback paths. Fig. 5.9 shows a simplified block diagram of the system. The forward path is actually a transmitter chain with an additional block where predistortion is applied. The feedback path however is composed of additional components required to update the predistorter in order to track PA characteristics changes and ensure a reliable operation. Complexity level of the feedback path can change for different applications. It can be like a complete receiver or be in a simpler form compromising system performance and complexity. The contents of "Analog Feedback Circuitry" block in fig. 5.9 can be a demodulator and the required baseband circuitry, or an envelope and a phase detector, or a circuit detecting the power in the adjacent channels. For all these cases different adaptation circuits are required in order to update the predistorter block.

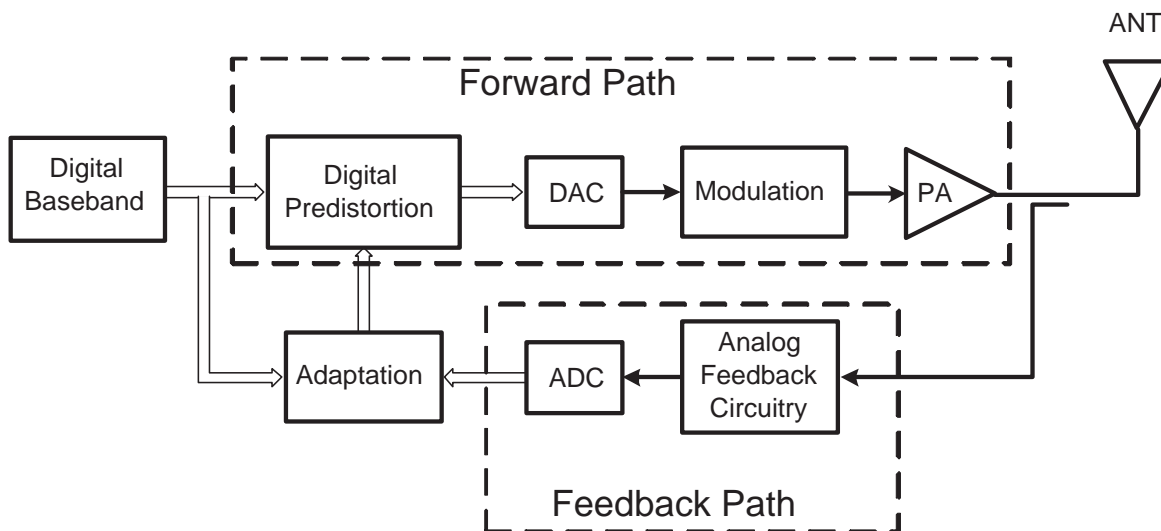


Figure 5.9: Simplified block diagram of adaptive digital predistortion.

The predistorter in the forward path must operate continuously whereas the feedback path can be used just when it is required or it can be programmed to operate with a given duty cycle. Therefore the forward path is very critical, and the maximum operation bandwidth is limited by the clock frequency and the amount of required operations [62]. The amount of mathematical operations in the adaptation unit is in general quite high compared to the predistorter in the forward path but since the adaptation unit does not need to operate continuously, power consumption can be kept reasonably low.

In some systems like TDMA, where transmission and reception are not done simultaneously, the additional feedback path may be avoided by using the available receiver path for adaptation. However, if there is simultaneous transmission and reception as in CDMA and WCDMA systems, then the receiver path can not be used and additional components for adaptation path are required.

In the next sections DP is explained in detail with special focus on MDP. In tab.

	Advantages	Drawbacks
Feedback	<ul style="list-style-type: none"> · Adaptation to environmental conditions 	<ul style="list-style-type: none"> · Useful for narrowband systems · Stability problems
Feedforward	<ul style="list-style-type: none"> · High degree of linearization · Wideband signal handling capability 	<ul style="list-style-type: none"> · High complexity · Large size · Low efficiency
Analog predistortion	<ul style="list-style-type: none"> · Wideband signal handling capability · Moderate power consumption 	<ul style="list-style-type: none"> · Usable for weakly nonlinear PAs · Moderate linearization · High complexity if conventional adaptation is used
Digital predistortion	<ul style="list-style-type: none"> · High degree of linearization · High flexibility · High reliability · High integrability · No stability problem · Progress in digital ICs 	<ul style="list-style-type: none"> · Limited bandwidth · High power consumption and clock frequencies for wideband systems · High complexity if conventional adaptation is used

Table 5.1: Comparison of different PA linearization methods.

5.1 the main advantages and drawbacks of feedback, feedforward, analog and digital predistortion systems are summarized. Advantages of DP make it the favourite method applicable in terminal applications.

5.4 Memoryless digital predistortion (MDP)

There are mainly two different MDP types: the LUT based predistorter [12, 63, 64] and the polynomial predistorter [58, 65, 66]. In LUT based DP, predistortion coefficients for all input values are stored in a LUT and the incoming signal is multiplied sample by sample with these coefficients. In polynomial predistorter case, however, the characteristics of the PA and the predistorter are described by polynomial functions. The polynomial coefficients of the predistorter are adjusted to fit the PA and to result in a linear system. Theoretically, LUT based predistorter can linearize a PA very precisely, whereas performance with polynomial predistorter depends on the order of polynomial. For example in the case of the adjacent and the alternate channel emission suppression at least a 5th order polynomial predistorter is required because such a predistorter will be able to reduce the 3rd and 5th order IMD products at the PA output [58].

Adaptations of these two predistorter types are different. In the LUT based one the update of coefficients is normally done by comparing I- and Q-values of the demodulated PA output with the originally generated ones. In this case the feedback path is a receiver circuit requiring a demodulator, which means high circuit complexity. If the PA input signal is polar modulated then the envelope and phase of the PA output are detected and compared with the original ones. However, in polynomial predistorters the adaptation is done in general by measuring the adjacent channel power or EVM at PA output and minimizing them with direct search or gradient methods. In [67]

different adaptation algorithms for LUT based and polynomial predistorters are given. Adaptation algorithms for polynomial predistorter are computationally more intensive compared to algorithms for LUT based predistorters. However, their analog circuit complexity in the feedback path is lower.

5.4.1 Look-up table (LUT) based predistortion

LUT based predistorter is simpler compared to polynomial one in the critical forward path. A magnitude or squared-magnitude calculation of a complex signal in the addressing unit and a complex multiplication unit are required whereas in polynomial predistorter significantly more multiplication and addition operations may be required depending on the order of polynomial. Fig. 5.10 shows a LUT based adaptive DP system. It can be assumed to be the detailed version of the system shown in fig. 5.9 and is going to be explained later in more detail. The predistorter is composed of an addressing unit, a LUT, a delay unit and a complex multiplier.

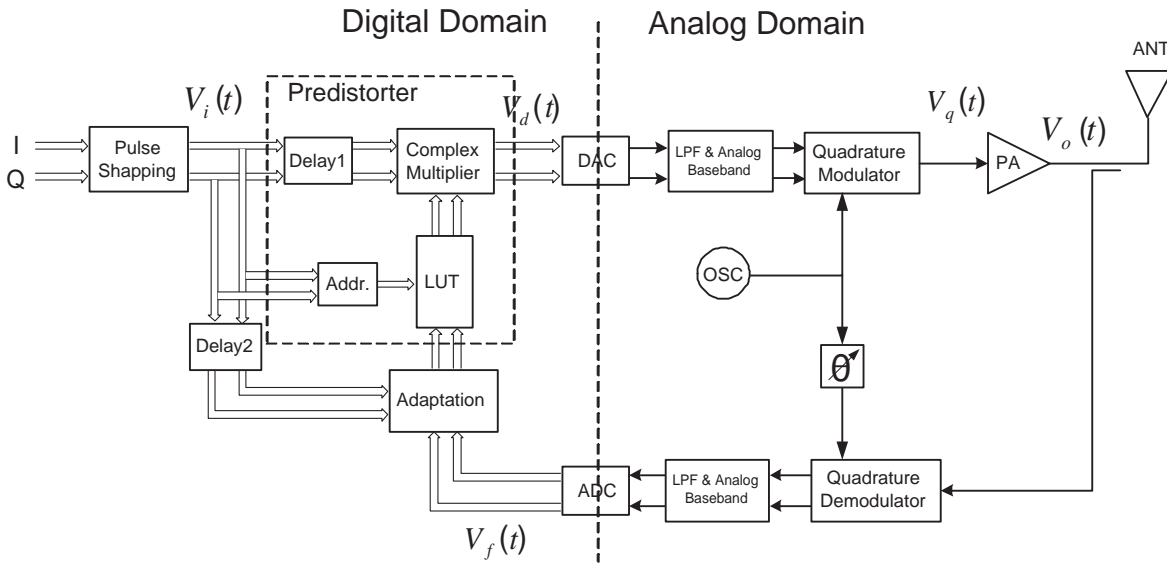


Figure 5.10: Block diagram of the LUT based adaptive digital predistortion.

Nagata [68] has proposed a LUT based adaptive DP having a big LUT size because of addressing by both input I- and Q-signals. This is a two dimensional LUT (mapping predistorter). If I- and Q-branches have k quantization levels, then the size of the LUT is k^2 . However, the amplifier nonlinearity does not depend on the input signal phase but just its amplitude if it is assumed to be memoryless [12], which gives the possibility to reduce the size of the LUT to k . In this case the addressing unit calculates the amplitude of the input signal and LUT addressing is done accordingly. This is called gain based predistorter [12]. Instead of the magnitude, magnitude square of the input can also be used which is proportional to the signal power.

In the following the LUT based adaptive digital predistorter will be explained in detail. PA characterization, LUT coefficient calculation, system operation and its adaptation

will be handled separately.

Measurement of AM/AM and AM/PM characteristics

In a predistortion system, if the measured AM/AM and AM/PM characteristics are not precise, the calculated LUT coefficients will not match the PA and performance of the linearization will be degraded. The easiest way of measuring AM/AM and AM/PM characteristics of a PA is using single tone excitation as shown in fig. 5.11. However, with this method just a static characterization is possible because the input signal envelope is constant, which means a constant instantaneous power during the excitation.

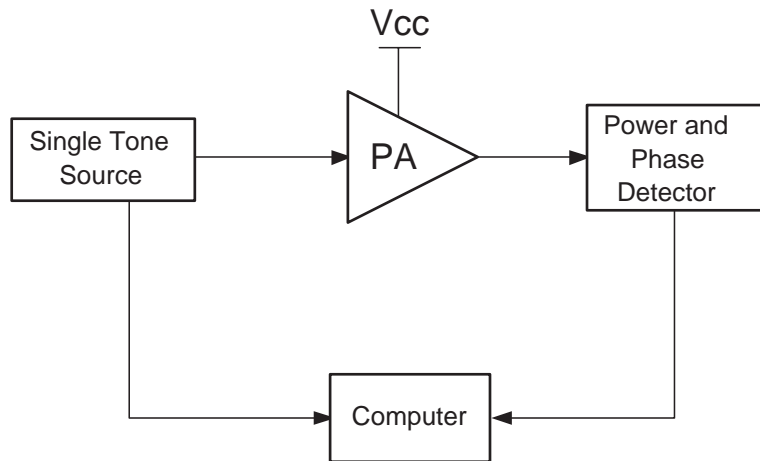


Figure 5.11: Static AM/AM & AM/PM measurement setup.

In single tone measurements the obtained characteristics are based on average power measurements. However, in memoryless predistortion systems the incoming signals are modified according to their instantaneous power or magnitude. Therefore a PA characterization based on instantaneous power measurement should give better results compared to the static characterization.

In [69] a PA characterization method with multi tone excitation is proposed which gives a dynamic AM/AM and AM/PM characterization due to its varying input signal envelope. It has been observed that there is a significant difference between the characteristics obtained with average and instantaneous power measurements [69]. The instantaneous power measurement may exhibit hysteresis loops in the gain and phase characteristics depending on the input power which is a measure of memory effects. If the obtained data is fitted to a polynomial function, then this PA characteristics can be used in memoryless DP systems like static AM/AM and AM/PM characteristics and it is supposed to give better results compared to static characterization because it reflects the behaviour of the PA during operation with modulated input signals. This dynamic characterization method is explained in chapter 6 in detail.

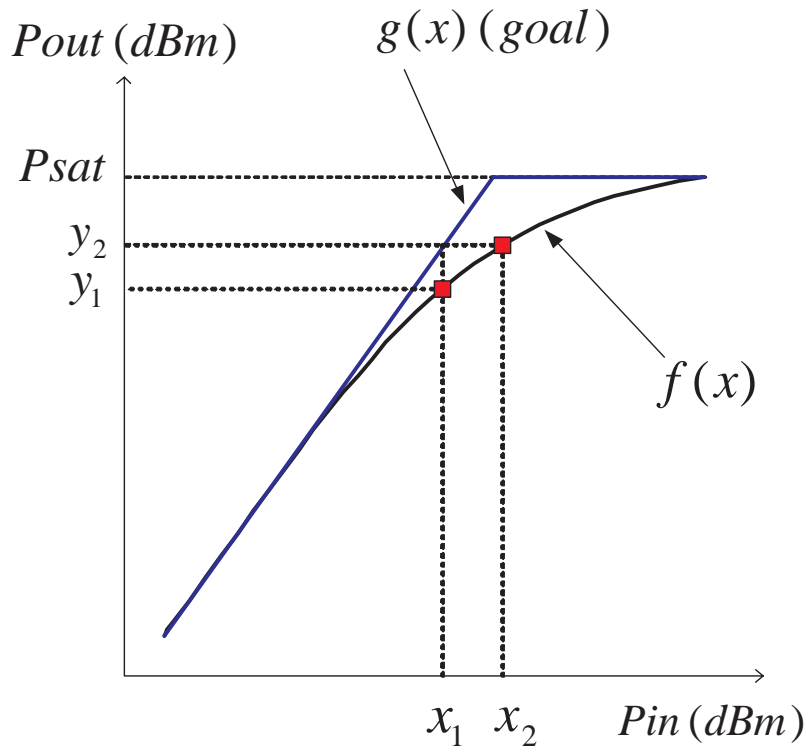


Figure 5.12: AM/AM characteristics before and after linearization.

Calculation of LUT coefficients

The next step after obtaining PA characteristics is LUT coefficient calculation. In a memoryless PA the output depends just on the momentary input value which makes LUT coefficient calculation very simple compared to systems with memory and it results in a small size LUT. The process is the same after obtaining AM/AM and AM/PM characteristics either with static or dynamic characterization. Fig. 5.12 shows a possible nonlinear AM/AM characteristics given as $f(x)$ and the target linear AM/AM as $g(x)$. Two points y_1 and y_2 have been selected from the figure such that

$$y_1 = f(x_1) \quad (5.1)$$

$$y_2 = f(x_2) \quad (5.2)$$

where x_i and y_i are magnitude or squared magnitude of the PA input and output respectively.

$$y_2 = g(x_1) \quad (5.3)$$

is the desired function having a linear response. If we define the coefficient c_{x_1} as

$$c_{x_1} = x_2/x_1 \quad (5.4)$$

multiply it with x_1 and apply to the function f , then it is possible to obtain the linear function g as shown in the equation below.

$$y_2 = f(x_2) = f(c_{x_1}x_1) = g(x_1) \quad (5.5)$$

This means for each x_i value a coefficient c_{x_i} must be calculated and stored in a LUT in order to cover the complete input signal range and linearize the PA accordingly. The size of LUT depends on quantization levels of the input signal. c_{x_i} is magnitude of the complex coefficient stored in the LUT for x_i , which is responsible for AM/AM correction. The phase of each coefficient should also be calculated and stored in the LUT using nonlinear AM/PM characteristics of the PA in order to correct also AM/PM nonlinearities.

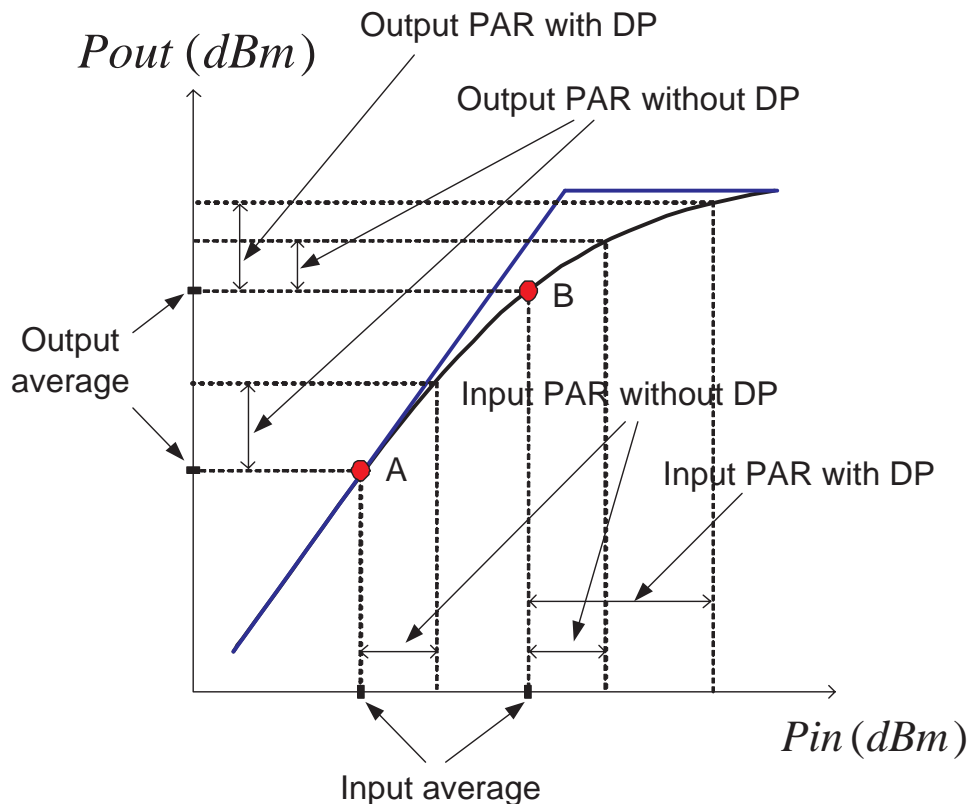


Figure 5.13: Improvement in deliverable linear output power with digital predistortion.

As it is seen from in fig. 5.12 a predistorter can correct distortion up to the full saturation level of the PA where any further increase of the input does not increase the output [64]. Fig. 5.13 shows possible improvement in the deliverable maximum linear output power with DP. A is a point where the PA has a highly linear response without DP. This is achieved due to its high back-off. In a linear system there is no compression and input and output PARs are equal. If the input is increased such that the PA

operates at point B, then a compression reducing the output PAR occurs which must be corrected using DP. As it is seen from fig. 5.13 for point B the input signal must be expanded significantly in order to obtain the same PAR at the output as in a linear system.

Calculating the phase of LUT coefficients is a relatively easy process compared to amplitude calculation. They can be obtained by subtracting the input dependent phase values from a constant target phase ph_t as shown in fig. 5.14. This is an extension of the fig. 5.12 with nonlinear and target AM/PM characteristics of the PA. Phase of the output is ph_1 for input of x_1 and ph_2 for x_2 . However, the phase of LUT coefficient should be stored for x_1 is not $(ph_t - ph_1)$ but $(ph_t - ph_2)$ because if the input is x_1 , then it is multiplied with the magnitude coefficient c_{x_1} and as a result the input becomes x_2 . This means the instantaneous phase is shifted from ph_1 to ph_2 and a phase shift equal to $(ph_t - ph_2)$ is required in order to obtain a constant phase at the output for this input value.

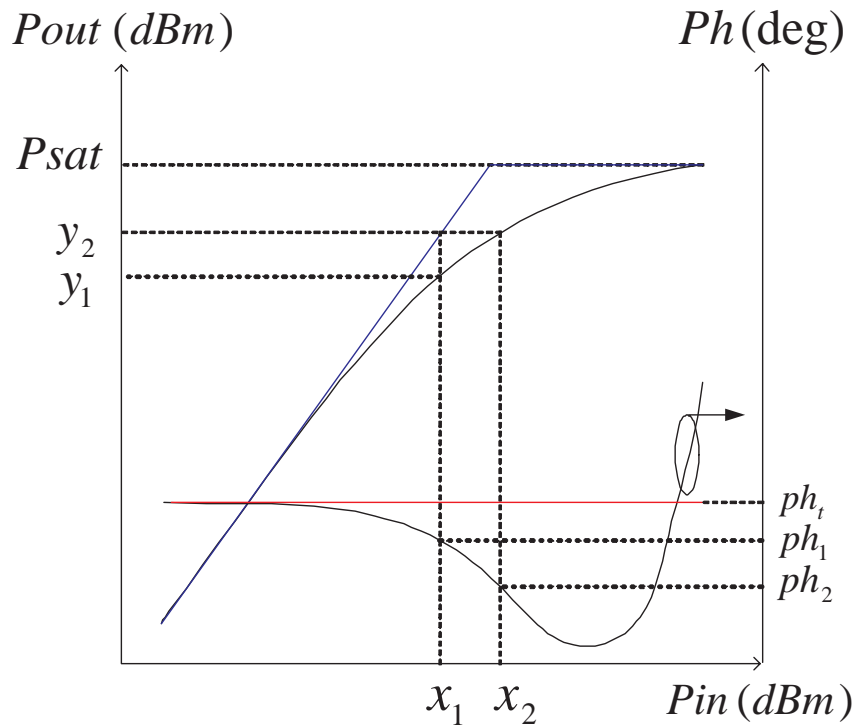


Figure 5.14: Static AM/AM and AM/PM characteristics before and after linearization.

The calculation of LUT coefficients must be done according to the preferred addressing. Two mostly used types are magnitude and power addressing. In [63] the difference between these two is explained. Power addressing is the easiest one and it requires squaring the signals in I- and Q-branches and adding them up in the addressing block. The result is squared magnitude of the complex input signal which corresponds to its power. Since the LUT coefficients are calculated for input signal values equispaced in power, there is a high coefficient density (low spacing between coefficients) near to saturation, which means good linearization for low back-off operation. However, if the PA

has also nonlinearities in the high back-off region as in class B, then the correction may not be sufficient in this region. Magnitude addressing gives in general a better IMD suppression due to its uniform coefficient distribution equispaced in voltage for both high and low back-off. However, for magnitude addressing a square-root calculation unit is required in addition to the operations in power addressing method which may be a computationally intensive block [70]. One other possibility is using optimum addressing. In this case the coefficients are dense in the regions where the PA nonlinearity is high and less dense in low nonlinearity regions [71]. This means the coefficients are closely spaced in highly nonlinear regions in order to increase the performance. According to [71], the IMD performance of the magnitude addressing is better than the power addressing by about 10 dB but the best IMD performance is obtained with the optimum addressing which is 1-4 dB better than the magnitude addressing. However, optimum addressing is cumbersome and it depends on the amplifier, modulation signal and back-off during the operation. Therefore the amplitude addressing is a good overall compromise in terms of its performance, modulation format and PA type independency and simplicity. These issues are important especially for applications in battery operated small size handsets which should have a simple structure.

System operation

Fig. 5.10 is a detailed block diagram of a conventional LUT based MDP system. It is composed of a predistortion circuit (an address calculation unit, a LUT, a complex multiplier), an adaptation circuit, DACs, ADCs, a transmitter chain (filters and baseband amplifiers, quadrature modulator, high power amplifier) and the additional feedback path for adaptation of LUT coefficients (coupler, quadrature demodulator, filters, baseband amplifiers). Pulse shaped digital I- and Q-signals are taken and each I- and Q-sample is modified according to a LUT table containing the coefficients generating inverse of the PA characteristics. The LUT is composed of two arrays containing real and imaginary parts of the complex predistortion coefficients. These coefficients are in Cartesian form and obtained by polar to Cartesian conversion of the magnitude and phase coefficients. $V_i(t)$ is the complex input signal to the predistorter used also for addressing. The address is obtained by magnitude calculation and quantization of $V_i(t)$ and it is sent to the LUT. The coefficient stored for each input sample is sent to the complex multiplier and multiplied with the corresponding sample. There is a delay element in front of the multiplier in order to compensate the delay in address calculation unit and LUT. The predistorted signal at the output of the multiplier is denoted as $V_d(t)$. It is analog converted, filtered, processed at baseband, sent to the modulator and then to the PA. The outputs of the modulator and the PA are denoted as $V_q(t)$ and $V_o(t)$ respectively.

The predistorter must adapt itself according to variations in the amplifier characteristics for a reliable operation. This means the LUT needs to be updated periodically or just if it is required to keep the following equation valid.

$$V_o(t) = KV_i(t) \quad (5.6)$$

K is small signal gain of the amplifier, which is selected to be the target gain for all input powers up to saturation. In order to update the LUT coefficients, a portion of the amplifier output is taken by a directional coupler and it is demodulated. The demodulator may use the available local oscillator used for quadrature modulation. I- and Q-signals at the demodulator output are filtered, baseband processed and converted to digital form using ADCs. This complex baseband signal is denoted by $V_f(t)$. The adaptation circuit compares the feedback signal $V_f(t)$ with the source signal $V_i(t)$ and the difference between these two signals, $V_{\text{error}}(t)$ guides the adaptation of the LUT coefficients.

In the following basic derivation of a predistortion system is given. Magnitude addressing has been used in this example. For simplicity time dependence of the variables are not shown. Magnitudes of the complex baseband signals at the input and, predistorter and modulator outputs shown in fig. 5.10 are defined as

$$x_i = |V_i| \quad (5.7)$$

$$x_d = |V_d| \quad (5.8)$$

$$x_q = |V_q| \quad (5.9)$$

If a unity gain is assumed in the analog baseband and modulator chain, then

$$V_q = V_d \quad (5.10)$$

and so

$$x_q = x_d \quad (5.11)$$

which will simplify our derivations. PA has an input voltage dependent complex gain denoted by $G(x)$ and its output can be defined as

$$V_o = V_q G(x_q) = V_d G(x_d) \quad (5.12)$$

The predistorter also has an input voltage dependent complex gain, denoted by $F(x)$. Its output is

$$V_d = V_i F(x_i) \quad (5.13)$$

The system transfer function is

$$K = V_o/V_i \quad (5.14)$$

and using eqns. 5.7, 5.8, 5.12 and 5.13

$$K = F(x_i)G(x_i|F(x_i)|) \quad (5.15)$$

The predistorter phase equation for a constant phase response is

$$\Phi_F(x_i) = -\Phi_G(x_d) = -\Phi_G(x_i|F(x_i)|) \quad (5.16)$$

where Φ_F and Φ_G are input magnitude dependent phase shifts in the predistorter and the PA. The predistorter gives a phase rotation that is the negative of the PA phase rotation.

Output of the PA can be rewritten as

$$V_o(t) = KV_i(t) + V_{o_{error}}(t) \quad (5.17)$$

where $V_{o_{error}}$ is an error function giving the PA output deviation from the desired linear output. If we define the amount of coupling as C , then the following equations can be derived from eqn. 5.17.

$$V_f(t) = CV_o(t) = CKV_i(t) + CV_{o_{error}}(t) \quad (5.18)$$

$$\Rightarrow V_{f_{error}}(t) = V_f(t) - CKV_i(t) = CV_{o_{error}}(t) \quad (5.19)$$

The adaptation algorithm modifies the LUT coefficients in order to minimize the error signal $V_{f_{error}}(t)$ given in eqn. 5.19.

Adaptation

The adaptation circuit in fig. 5.10 has $V_f(t)$ and the delayed $V_i(t)$ as input and it minimizes $V_{o_{error}}(t)$. Two widely used adaptation methods in LUT based predistorters are linear and secant methods. In both methods each LUT coefficient is updated when the input signal value corresponding to this coefficient occurs. The conversion speed of a coefficient depends on the number of adaptation iterations, and thus on how often the signal trajectory passes through this value.

Linear adaptation for a DP system with squared-magnitude addressing is explained in [72] in detail. In the following derivations for magnitude addressing will be shown. It is based on successive substitutions. Using eqn. 5.15 the following iterative equation can be written,

$$F(x_i, j+1) = \frac{K}{G[x_i|F(x_i, j)|]} \quad (5.20)$$

where $F(x_i, j)$ is the LUT coefficient stored for the quantized input x_i after j^{th} iteration.

Under ideal conditions in modulator and demodulator and unity gain assumption in both transmitter and feedback chains, eqn. 5.20 can be modified as given below by substitution of eqns. 5.12, 5.13 and 5.17.

$$F(x_i, j + 1) = F(x_i, j) \frac{KV_i(j)}{V_o(j)} = F(x_i, j) \left[1 - \frac{V_{oerror}(j)}{V_o(j)} \right] \quad (5.21)$$

In order to avoid divergence in the case of high errors at the output, eqn. 5.21 can be further modified as follows

$$F(x_i, j + 1) = F(x_i, j) \left[1 - s \frac{V_{oerror}(j)}{V_o(j)} \right] \quad (5.22)$$

where $s \ll 1$ is a small positive number. This new formula gives a better convergence with an increase in the convergence time. Since not $V_o(t)$ but $V_f(t)$ is available for the adaptation unit, the final form of the adaptation equation can be derived from eqn. 5.22 as given below.

$$F(x_i, j + 1) = F(x_i, j) \left[1 - s \frac{V_{ferror}(j)}{V_f(j)} \right] \quad (5.23)$$

The secant method is also an iterative adaptation as in the linear case [12]. If the error signal calculated in the adaptation unit from eqn. 5.19 can be defined as,

$$e_f = V_{ferror} = V_f - CKV_i \quad (5.24)$$

then LUT coefficient adaptation with secant method works according to the following equation.

$$F(n, j + 1) = \frac{F(n, j - 1) e_f(F(n, j)) - F(n, j) e_f(F(n, j - 1))}{e_f(F(n, j)) - e_f(F(n, j - 1))} \quad (5.25)$$

$F(n, j)$ is value of the complex coefficient stored in n^{th} position of the LUT after j^{th} iteration.

The secant method has a faster convergence than the linear one, however, the computational burden to processor is much higher. On the other hand it needs no phase shifter in the feedback path [12]. Both linear and secant methods have convergence problems near to saturation because of drastic increase in nonlinearity. Achieving 0 dB peak back-off is almost impossible and maximum instantaneous output power can be about 95% of the saturated output power meaning 0.2 dB back-off [12].

There are also other adaptation algorithms available with different complexity levels [73, 74, 75]. Selection of an adaptation algorithm depends on the required accuracy and affordable amount of mathematical calculations. For handset applications achieving a sufficient performance with low computational burden and less amount of additional components is a very important issue due to their limited power and size. Since the calculations in adaptation are not continuously done and secant method needs no phase shifter it is reasonable to use it in handset applications.

5.4.2 Polynomial predistorter

The second possible DP method is the polynomial type. In this system each digital data sample is processed in the predistorter not according to a LUT but to a polynomial function. This polynomial function can be 3rd, 5th order or more depending on the desired degree of linearization in adjacent and alternate channels. Fig. 5.15 shows a possible implementation based on the adjacent channel power minimization [58, 66]. Predistorter polynomial is fit to the opposite of PA characteristics and is controlled by an optimizer or adapter. The adaptation unit adjusts the polynomial coefficients, which should be in complex form in order to correct both gain and phase nonlinearities. Also in polynomial predistorters the forward path must be continuous as in LUT based one and therefore is critical. The coefficients can be stored in a small LUT and optimization can be done with a duty cycle or activated just if it is required. The difference compared to the LUT based predistorter would be highly reduced size of the LUT. For example it would have only 4, 6 and 8 positions for 3rd, 5th and 7th order polynomial predistorters respectively.

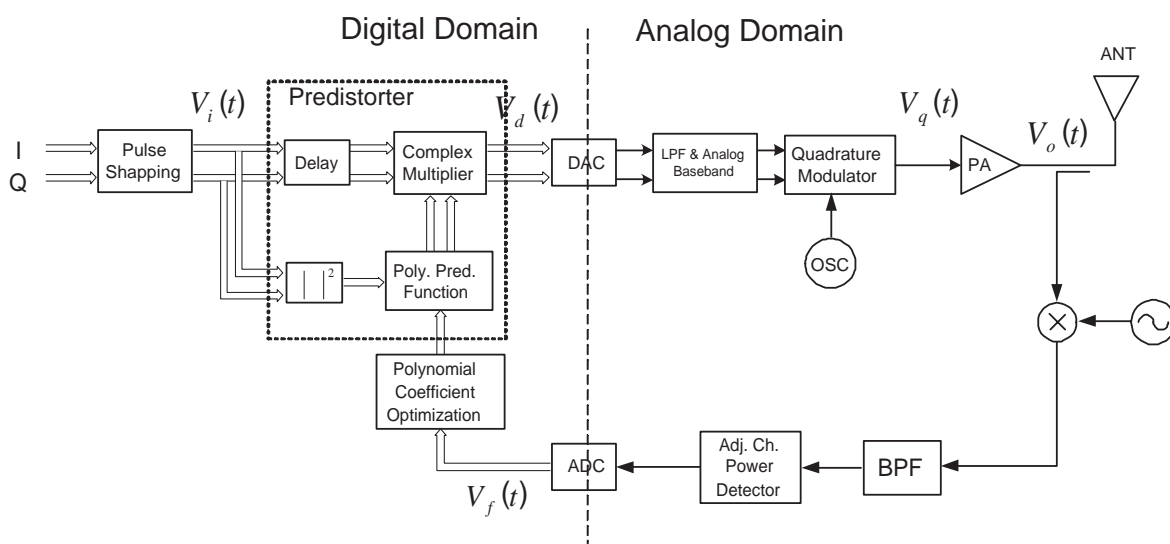


Figure 5.15: Block diagram of polynomial adaptive digital predistortion based on adjacent channel power minimization.

System operation

Fig. 5.15 shows the block diagram of polynomial MDP in detail. It is composed of a predistortion circuit (a squared magnitude calculation unit, a polynomial predistortion function calculator, a complex multiplier, a delay element), an optimization circuit for polynomial coefficients, DACs, ADCs, a transmitter chain as given in LUT based predistorter and a feedback path for calculation of adjacent channel power emission (coupler, down-converter, bandpass filter, power detector). The critical forward path is similar to the one in LUT based predistorter. The difference is in the predistorter which has a polynomial predistorter function unit instead of a LUT. The amount

of mathematical operations in this unit can be quite high depending on the order of predistorter. This in turn limits the bandwidth of the modulation signal to be linearized because of limited system clock frequency.

As shown in fig. 5.15 the pulse shaped digital I- and Q-data is taken and each sample pair is modified in the predistorter unit. The complex voltages $V_i(t)$, $V_d(t)$, $V_q(t)$ and $V_o(t)$ are as defined before in the LUT based predistorter case. Just the feedback signal $V_f(t)$ is no more a complex voltage but a scalar value proportional to the unwanted adjacent channel power emission.

In the following the derivation of a polynomial predistortion system is given which is done according to magnitude square of the input. The squared magnitudes at different points in fig. 5.15 are defined as

$$a_i = |V_i|^2 \quad (5.26)$$

$$a_d = |V_d|^2 \quad (5.27)$$

$$a_q = |V_q|^2 \quad (5.28)$$

If unity gain assumption is done for the analog baseband and modulator chain as before, then

$$a_q = a_d \quad (5.29)$$

As an example the PA will be assumed to have a fifth order nonlinearity. We can define power series function of it as

$$G(a_q(t)) = G(a_d(t)) = \beta_1 + \beta_3 a_d(t) + \beta_5 a_d^2(t) \quad (5.30)$$

where β_1 , β_3 and β_5 are complex coefficients. Output of the PA is

$$V_o(t) = V_d(t)G(a_d) \quad (5.31)$$

From eqns. 5.27, 5.30 and 5.31,

$$V_o(t) = \beta_1 V_d(t) + \beta_3 V_d^3(t) + \beta_5 V_d^5(t) \quad (5.32)$$

As it can be seen from eqn. 5.31 the PA nonlinearity is 5th order and there are just odd nonzero polynomial coefficients. Even order nonlinearities are assumed to be zero for simplicity because the inband distortion is due to the odd order nonlinearities and they must be compensated by means of predistortion having the same order. The corresponding predistorter function can be defined as

$$F(a_i(t)) = \alpha_1 + \alpha_3 a_i(t) + \alpha_5 a_i^2(t) \quad (5.33)$$

with complex coefficients of α_1 , α_3 and α_5 . Polynomial predistortion function unit takes the squared magnitude as input and calculates F for each sample as shown in

fig. 5.15. Complex multiplication of the input samples with the corresponding F give the predistorted samples.

Assuming K as the target gain obtained by combination of the predistorter and PA, an equation similar to eqn. 5.15 can be obtained as given below

$$K(a_i(t)) = F(a_i(t))G(a_i(t)|F(a_i(t))|^2) \quad (5.34)$$

K can not be constant due to the nature of polynomial predistorters . If K is defined as a 5th order polynomial function as given below

$$K(a_i(t)) = \gamma_1 + \gamma_3 a_i(t) + \gamma_5 a_i^2(t) \quad (5.35)$$

and derivation are done, then the following equations are obtained [58].

$$\gamma_1 = \alpha_1\beta_1 \quad (5.36)$$

$$\gamma_3 = \alpha_3\beta_1 + \alpha_1\beta_3|\alpha_1|^2 \quad (5.37)$$

$$\gamma_5 = \alpha_5\beta_1 + \alpha_3\beta_3|\alpha_1|^2 + \alpha_1\beta_5|\alpha_1|^4 + 2\alpha_1\beta_3Re\{\alpha_1\alpha_3^*\} \quad (5.38)$$

By optimizing the predistorter coefficients α_1 , α_3 and α_5 , the 3rd and 5th order terms of K (γ_3 and γ_5) should be minimized. As a result a quasi linear PA output $V_o(t)$ can be obtained.

Adaptation

There are different ways of optimizing polynomial predistorter coefficients. For example it can be based on minimization of adjacent channel emission as shown in fig. 5.15 or minimization of EVM at the PA output [76]. After selecting the system structure, the adaptation algorithm should be selected. There are mainly two groups of methods applied in polynomial predistortion systems: direct search methods and gradient methods. Direct search methods are robust and have low computational load compared to gradient methods but they can not converge as fast as gradient methods. A simple example for direct search method is as follows. Assume that $F(x)$ is a function of $x = (x_1, x_2, \dots, x_n)$ in an n -dimensional space. Starting from x^i , $F(x)$ is evaluated in all coordinates till a point x^{i+1} is found where

$$F(x^{i+1}) < F(x^i) \quad (5.39)$$

then the direction of approximate gradient d^i is as given below

$$d^i = x^{i+1} - x^i \quad (5.40)$$

where i is the number of iteration. Then the next point x^{i+2} in this coordinate is given by

$$x^{i+2} = x^{i+1} + d^i \quad (5.41)$$

The function minimum is found with continuing the same procedure [58].

In gradient methods, however, the direction of descent is observed by taking derivative of the function at each step which gives the steepest descent and results in a faster convergence.

5.4.3 Effects of system imperfections

As it can be seen from fig. 5.10, adaptive DP system has some other components beside PA, like modulator, demodulator, filters, analog baseband circuitry etc. Imperfections in these components have in general a negative effect on the system performance. For example modulators and demodulators can have unwanted amplitude and phase imbalance and DC offset, which are not easy to eliminate completely just by careful predistorter design. In [72] and [77] effects of such imperfections on predistortion systems are investigated and correction circuits are proposed. Modulator imperfections can result in spectral regrowth in adjacent channels and increase in the EVM. Fig. 5.16 shows possible effects of gain and phase imbalance and DC offset on signal constellation for a 8-PSK system. Constellation points are no more on a circle because there is a constellation asymmetry. The gain imbalance distorts the constellation symmetry and causes an ellipse-shaped constellation, the phase error rotates the constellation and the DC offset can contain two perpendicular components in I- and Q-paths resulting in a origin shift [78].

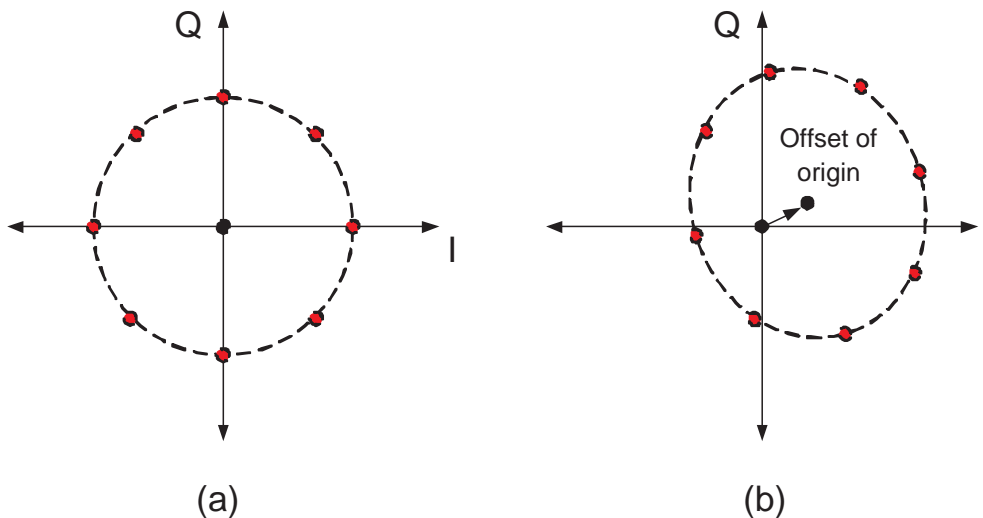


Figure 5.16: 8-PSK constellation (a) without and (b) with modulator gain and phase imbalance and DC offset.

In fig. 5.17 the block diagram of a simple quadrature modulator correction circuit is shown [63]. This circuit must be placed between the complex multiplier and DACs in fig. 5.10. I_d and Q_d denote the predistorted digital I- and Q-signals, and I_c and Q_c denote signals after quadrature modulator correction. g_c and p_c are coefficients for gain and phase imbalance correction, and I_{dc} and Q_{dc} are coefficients for DC offset compensation.

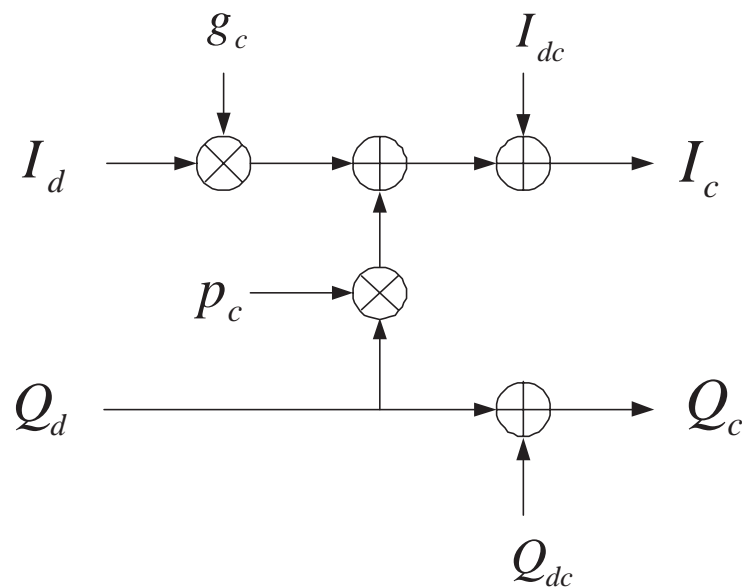


Figure 5.17: Correction circuit for quadrature modulator gain and phase imbalance and DC offset [63].

Demodulator linearity is also very important in adaptive DP. Any imperfection in the feedback path can result in deviations in LUT coefficients from desired values even after adaptation. Some interesting results are presented in [79] showing that mainly the DC offsets in demodulators worsen ACI performance of adaptive predistorters whereas gain and phase imbalances have less effect on it. However, BER performance is degraded by all three errors significantly. Since a demodulator is just the inverse of a modulator, a circuit inverse of fig. 5.17 can be inserted between ADCs and adaptation unit in order to correct demodulator errors in fig. 5.10.

There are some other deterioration sources in the system shown in fig. 5.10. The effects of reconstruction filters after DACs and anti-aliasing filters after the demodulator are very important. There should be no additional error in the transmitter chain between the predistorter and the PA in order to have a good cancellation performance with DP. Reconstruction filters are low pass filters implemented after DACs (in the block "LPF & Analog Baseband" in fig. 5.10 and fig. 5.15) in order to cancel image signals after analog conversion. A predistorted signal can have a bandwidth in general a couple of times wider than the signal without predistortion and this signal must reach the PA without significant distortion. If the cut-off frequency of a reconstruction filter is kept low in a DP system, then the linearizer performance degrades significantly because the

added distortion elements which are opposite of the PA nonlinearity will be cancelled out. Therefore the reconstruction filter bandwidth must be increased in order to let the predistorted signals pass through. However, a sufficiently high image suppression is required at the same time. These new filter requirements can be fulfilled in two different ways: by either increasing the system oversampling ratio and using a low order filter, or by leaving the oversampling ratio as it is and using a higher order filter [80]. Increasing the oversampling ratio decreases the achievable modulation bandwidth due to limited clock frequencies and increases the power consumption in the digital circuitry due to higher number of samples and operations. Therefore it should be kept as low as possible. On the other hand high order filters require additional components and if they are discrete elements, system size and cost can increase significantly. Therefore a compromise is required for an optimum system. Moreover, phase response and ripple of these filters are also important parameters in terms of achievable performance. In [80] it has been shown that low-ripple Chebyshev filters give the lowest order filter for a good performance.

Anti-aliasing filters are low pass filters implemented after demodulators in order to suppress the noise out of the modulation signal band. In general low order filters are used and have an effect on the convergence speed and achievable linearity in adaptive predistorters. The cut off frequency must be lowered for a high noise suppression, however, this result in a decrease in the convergence speed [81]. Increasing the cut off frequency improves the performance up to an optimum value. Further increase has no effects on ACI performance because there are other limiting effects like LUT size. Butterworth type filters have been found to be good candidates for low order anti-aliasing filters required in feedback paths [81]. The value of filter ripple is also an important parameter in the case of Chebyshev type filter implementation. Low ripple has in general a better ACI performance.

Error in the feedback delay is another important issue in adaptive digital predistorters. If there is a delay mismatch between the delayed input and the feedback signals going into the adaptation unit, then the LUT coefficients will be adapted erroneously and this effect will be seen as noise at the PA output. Even if the system is perfectly linear at start up, the LUT coefficients will be changed to incorrect values and the performance will be degraded. In [82] a method of calculating ACI degradation depending on delay errors in the feedback path of an adaptive digital predistorter is presented.

Feedback delay can be compensated in the digital circuitry by using discrete valued delay elements. However, since the step size which is equal to the clock period ($T_{Clock} = 1/f_{Clock}$) of the ADC is fixed, there is a possible delay mismatch which can not be corrected easily. The maximum value of this delay is $T_{Clock}/2$. This is due to the sampling of the incoming feedback signal not exactly at the same instant where the delayed input values are available for adaptation as a reference. Fig. 5.18 shows the worst case scenario of a sine wave where the feedback signal is sampled with the maximum delay mismatch of $T_{Clock}/2$. In this example system clock rate is equal to ADC clock rate. The maximum magnitude error is shown in fig. 5.18 which causes erroneous adaptation of the system. There are different possibilities to solve this problem. For example the ADCs with higher sampling frequency can be used in order to decrease the maximum value of possible delay mismatch. Other solutions could be adding ad-

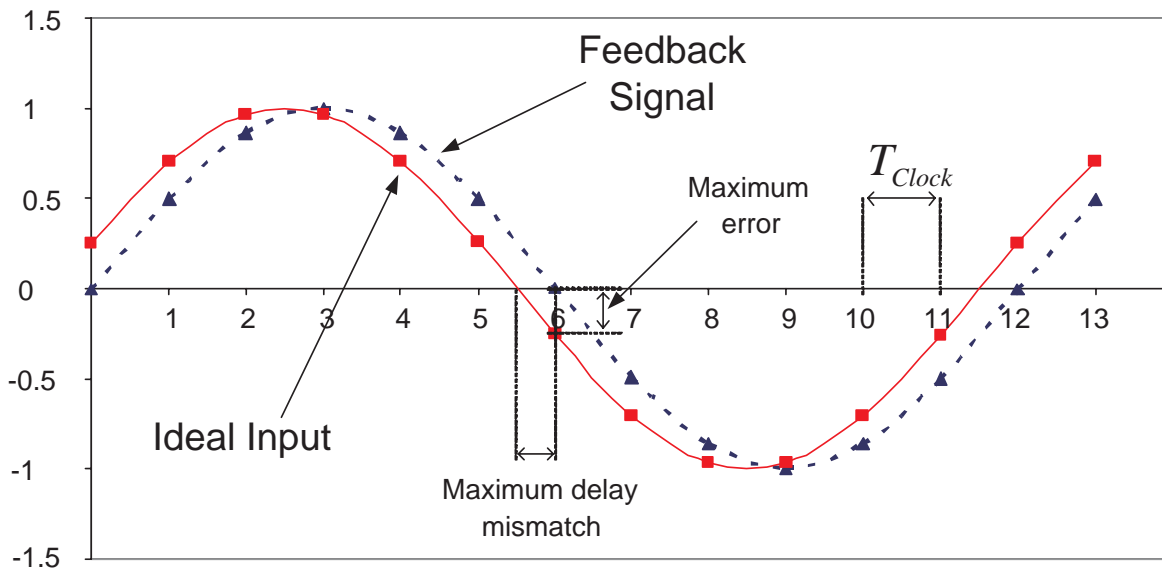


Figure 5.18: Delay mismatch due to ADC sampling frequency.

justable delay elements in the feedback path or using sample interpolation. Sample interpolation seems to be a reasonable solution because of the flexibility and accuracy in digital circuits. Simple interpolation algorithms should not be very complicated and power consuming.

5.5 Predistortion of PAs with memory

In previous sections some analog and digital predistortion systems have been presented which were designed to correct PA nonlinearities having static AM/AM and AM/PM characteristics (memoryless PA). These methods may also be applied to PAs with quasi-static AM/AM and AM/PM characteristics. However, not all PAs have necessarily such characteristics. Especially high power amplifiers used for base station transmitters in mobile communications have dynamic AM/AM and AM/PM characteristics, which may depend on modulation signal bandwidth, matching and bias circuits of the PA and environmental conditions like temperature variations. These types of effects are called as memory effects because the PA response does not depend just on the momentary value of the input but also on the previous values of it. Therefore some sophisticated predistorter structures are required in order to correct nonlinearities of the PAs with memory.

Memory effects can be divided in two effects: electrical and thermal. Electrical memory effects are mainly due to the frequency dependence of impedances in the circuit. The major part of memory is produced by envelope impedances at frequencies from DC to the maximum modulation frequency [83]. One way of reducing memory effects is to design bias networks carefully. Thermal memory effects, on the other hand, are due to changes in the junction temperature of a device. Change in the temperature

results in changes in PA characteristics, especially gain, which can be imagined as an additional temperature dependent modulation. Electrical memory effects are significant for modulation signals having high bandwidth. However, thermal memory effects are long time constant effects becoming significant at low modulation frequencies. An easy way of observing memory effects in a PA is to check its output spectrum which exhibits an asymmetry in case of memory. If these effects are strong, then the predistorter must consider them because otherwise the linearity improvement is limited.

The first step to build a predistortion system with memory is to characterize the PA precisely. Then the predistorter with opposite PA characteristics is designed. The characteristics of a PA with memory can be defined by Volterra series [84] or simplified systems like Wiener model based ones [85, 86]. Volterra series model is computationally intensive and time consuming especially if the PA is highly nonlinear. Therefore simpler methods are investigated in order to reduce system complexity with reasonable performance. There are different setups for PA characterization but the most widely used methods for memory effects measurements are two tone based setups, where tone spacing is changed and its effects are measured [87, 83, 88, 89, 90]. There are also some other characterization methods proposed recently which use baseband modulation data at the PA output for its characterization [91, 92, 93, 69, 94]. These are relatively fast and quite accurate characterization techniques which can be used especially in system level simulations.

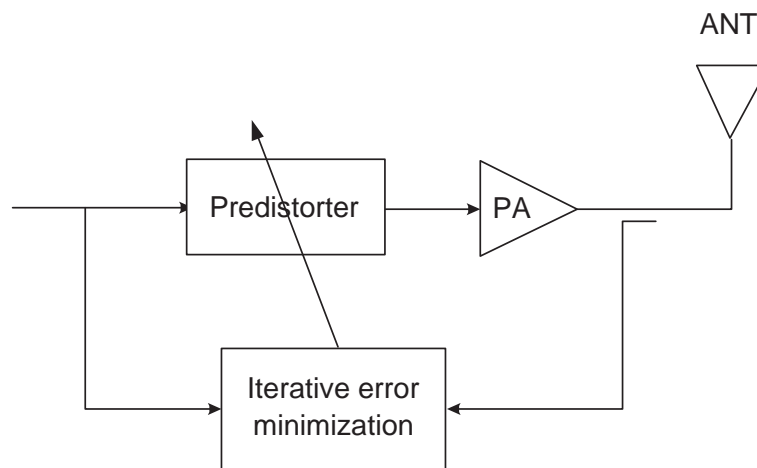


Figure 5.19: General predistortion structure with memory.

A simplified architecture for predistortion systems with memory is shown in fig. 5.19. Parameters of the predistorter in front of the PA are adjusted adaptively in order to minimize the difference between the actual and target PA characteristics. Since the PAs have nonlinear functions, the predistorter function can not be derived explicitly from the ideal input and distorted output signals. Therefore iterative optimization methods minimizing the error between these two signals are required. The complexity and performance of the predistorter depends on the selected characterization method because the predistorter is basically the inverse of these PA characteristics.

The output of a nonlinear system with memory can be defined with Volterra series [84]

as

$$\begin{aligned}
 y(t) &= \int_{-\infty}^{\infty} h_1(\tau_1)x(t - \tau_1)d\tau_1 \\
 &+ \int_{-\infty}^{\infty} \int_{-\infty}^{\infty} h_2(\tau_1, \tau_2)x(t - \tau_1)x(t - \tau_2)d\tau_1d\tau_2 + \cdots \\
 &+ \int_{-\infty}^{\infty} \cdots \int_{-\infty}^{\infty} h_n(\tau_1, \tau_2, \dots, \tau_n)x(t - \tau_1)x(t - \tau_2) \cdots x(t - \tau_n)d\tau_1d\tau_2 \cdots d\tau_n
 \end{aligned}
 \tag{5.42}$$

which can be rewritten as

$$y(t) = H_1(x(t)) + H_2(x(t)) + \cdots + H_n(x(t)) \tag{5.43}$$

The first term in eqn. 5.42 describes the linear response and the others are for nonlinear effects of the system. $h_n(\tau_1, \tau_2, \dots, \tau_n)$ is an n dimensional impulse response called Volterra kernel. $H_n(x(t))$ in eqn. 5.43 is called n^{th} order Volterra operator. The system is considered as combination of operators with different orders. A PA model can be fitted to the equations above by calculating Volterra kernels using measurement data. The main drawback of the model is its increased complexity with increasing system memory and nonlinearity.

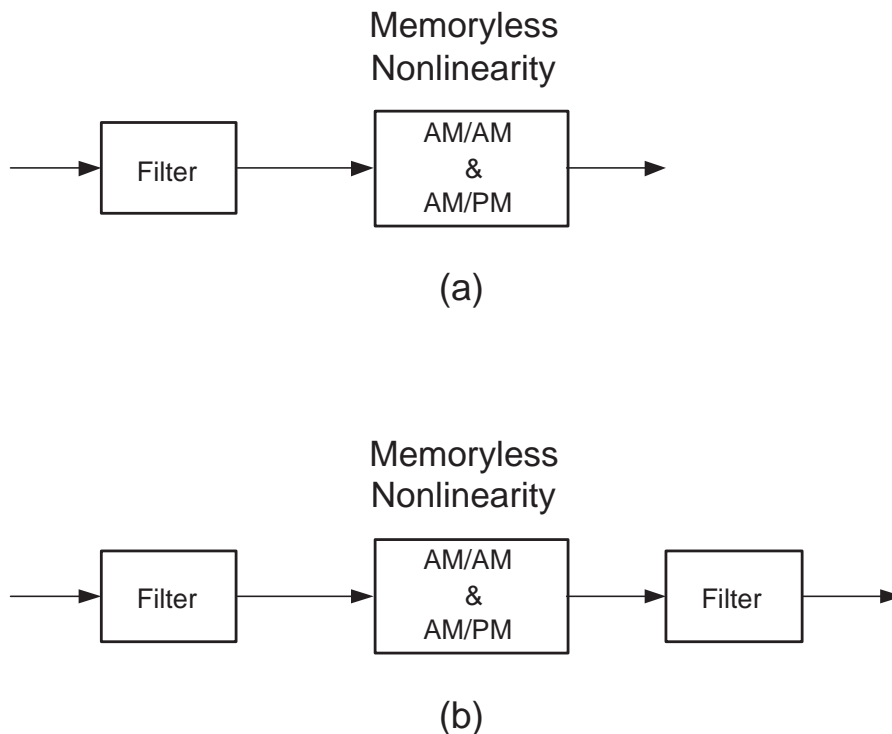


Figure 5.20: (a) Two box and (b) three box models used to characterize a PA with memory.

The idea in Wiener model is to separate the memory and nonlinear behavior of the PA. The basic Wiener model is composed of a filter and a memoryless nonlinear block as

shown in fig. 5.20 (a). It is also called two box model. The model can be improved by adding another filter at the end of chain as shown in fig. 5.20 (b) and it is called three box model. Memory effects are entirely defined in the filters whereas the nonlinearities are defined in the memoryless nonlinearity block [85]. These models have significantly lower complexity, but their accuracy is low compared to Volterra model. In [86] a parallel Wiener model is used to characterize PAs with memory in order to improve performance and keep the complexity acceptable. It compensates the drawbacks of the complicated Volterra model and two and three box models.

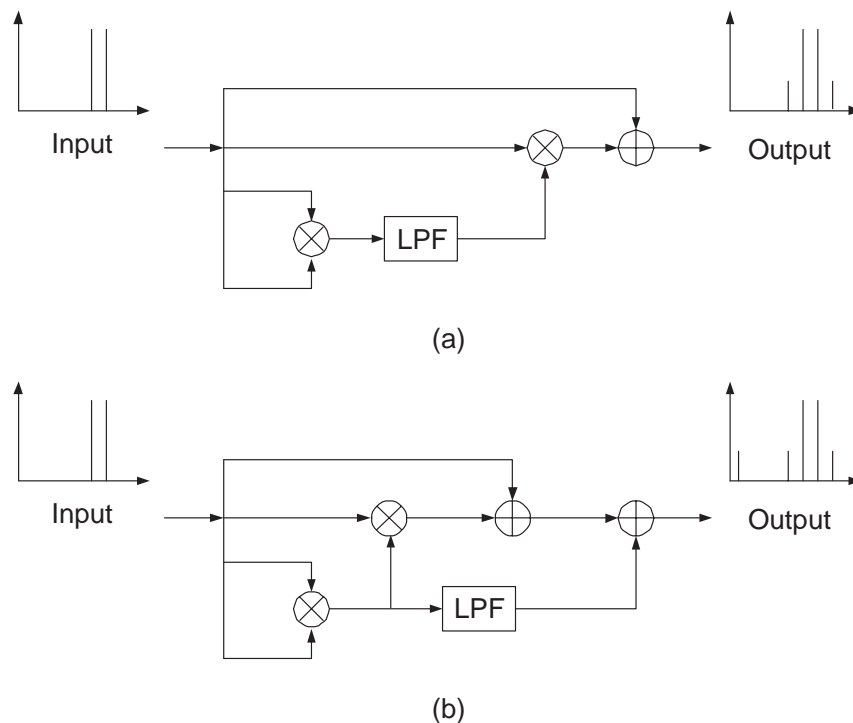


Figure 5.21: Predistorted input signal generation in (a) envelope filtering and (b) envelope injection techniques [95].

There are also some other predistortion structures which are relatively simple but take memory effects into account. In [95] two different methods called envelope filtering and envelope injection are proposed. Predistorted signal generation in these two methods are shown in fig. 5.21 (a) and (b) respectively. Envelope filtering is realized by lowpass filtering the squared input signal of a third order RF predistorter. Thus the input signal is modified depending on the frequency of its spectral components, which can be seen as intentionally added memory effects. For maximum predistorter performance the memory effects due to envelope filtering should be opposite of the PA memory. Therefore the goal is to design a lowpass filter modifying the amplitude and phase of IMD sidebands such that the predistorted signal and PA output sidebands have equal amplitudes and 180° phase shift. In envelope injection the system is a third order RF predistorter with additional injection of the baseband portion of the squared input signal. Both methods exhibit improved predistorter performance in the case of using PAs with memory.

Chapter 6

Memoryless digital predistortion for terminals

By now, general information about power amplifiers, mobile communications and transmitter structures has been given and analysis of some linearization methods have been done. It is obvious that designing PAs with high linearity and high efficiency at the same time is a very critical issue. In conventional adaptive DP systems used in base stations, the focus is achieving very high linearity. However, in terminals the linearity is not as critical an issue as in base stations because of the relatively low output power and single carrier operation. Therefore in terminals it is also possible to implement simple predistortion systems with moderate improvement like analog predistortion with 3rd or 5th order intermodulation distortion compensation whereas in base stations sophisticated DP systems are applied in order to take the memory effects into account and thus achieve a high degree of linearity. In this chapter we will concentrate ourselves on implementation of DP in terminals, specifically on MDP in order to solve this problem.

Although DP is a PA linearization method, our aim is to use it for transmitter power efficiency improvement. Since a linearized PA can be driven near to compression, it can be operated more efficiently. Considering high power consumption of the PA in a transmitter, improvement in its efficiency means significant improvement in the system efficiency. Even more system efficiency improvement can be achieved if the PA is designed for high efficiency and its linearity is improved with DP in order to fulfil system specifications. Such a strategy will increase freedom in PA design and thus make highly efficient systems possible. In this way the efficiency not only at maximum but also at lower output powers can be improved which means high average efficiency. Such optimized systems are essential for future multi-mode, multi-band systems in order to exploit overall system performance improvement possibilities to the utmost. There are some other methods having more headroom in efficiency improvement like PTx concept comprising a DC-DC converter. However, this is a completely different topology than the conventional one and it is complicated and cumbersome [37, 39], whereas MDP can be implemented in a conventional linear transmitter without substantial modifications. On the other hand PTx concept has in general highly nonlinear characteristics requiring linearization. The best candidate is again DP due to its high performance and flexibility.

MDP has a high linearization performance if the PA has low memory and therefore can be assumed to be memoryless. This may be the case for terminal PAs [96] due to their relatively low output power and modulation bandwidth. If we consider that handsets are small and battery operated, then MDP is a reasonable method for PA linearization due to its simple implementation, low size, low cost and low power consumption. It is reliable and flexible because of implementation with digital circuitry. Moreover it benefits from continuous development of digital ICs, which improves the power efficiency and speed, meaning wide bandwidth signal handling capability.

In the following sections different aspects of MDP for terminal applications in mobile communications are investigated. First of all a suitable PA characterization method is proposed. Next the performance of MDP in EDGE and WCDMA is presented and the required system modifications are explained. Then possible improvement in system efficiency is estimated if DP is used with a DC-DC converter in WCDMA. Also effects of supply voltage changes on DP performance are discussed. A novel LUT addressing method usable in Cartesian predistorters is proposed, which should decrease the required clock frequency and power consumption in digital circuitry. Then advantages and drawbacks of open- and closed-loop DP implementations in mobile communications terminals are discussed. Finally the application of MDP in PTx concept has been investigated, which is gaining more importance in next generation systems. For this purpose a PA characterization method using three port measurement data is proposed and achieved system performance with linearization is presented.

6.1 Power amplifier characterization

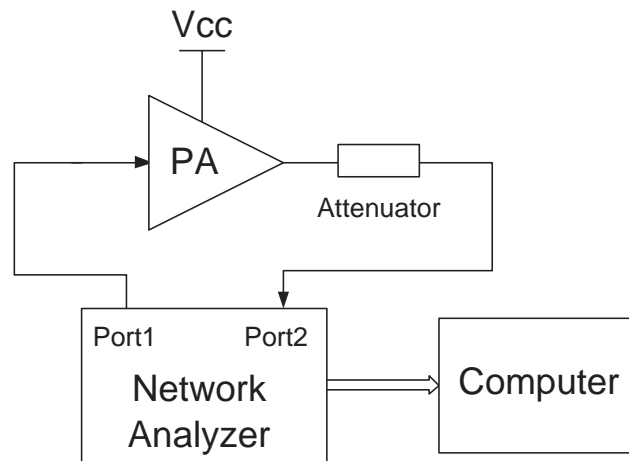


Figure 6.1: Static AM/AM & AM/PM measurement setup using network analyzer.

The first step of linearization by means of DP is a precise characterization of the amplifier to be linearized. Although there are different methods for PA characterization, we have concentrated ourselves just on two methods due to their relative simplicity. As mentioned in chapter 5, the fast and easy way of measuring AM/AM and AM/PM

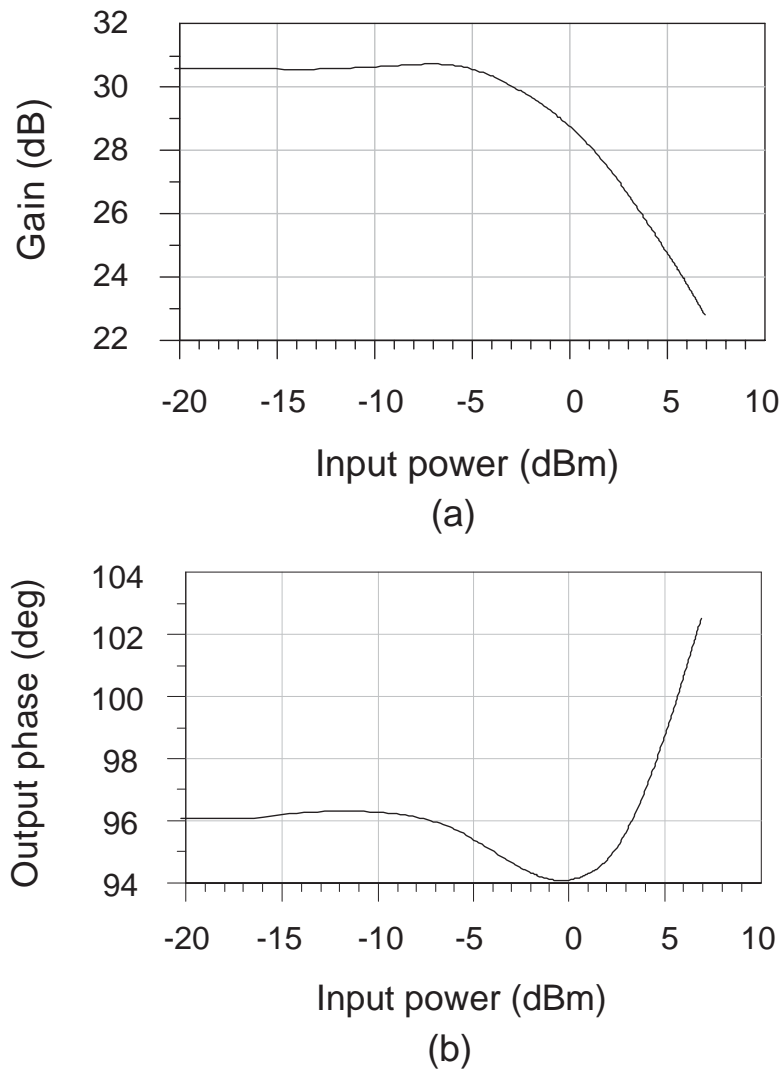


Figure 6.2: Measured (a) gain and (b) phase characteristics of RF2162 using static measurement setup.

nonlinearities is using single tone excitation. Fig. 6.1 shows a simple setup using a network analyzer which gives a static characterization independent of modulation signal bandwidth. In order to characterize AM/AM and AM/PM nonlinearities of a PA, a power sweep of a single tone input is carried out using a network analyzer. An attenuator is placed at the PA output in order to protect the network analyzer. PA input-output power and phase values are transferred to the computer using Labview measurement software. The obtained raw data is used in order to generate a file based behavioural two port PA model usable in system simulations.

The Software used for simulations is ADS (Advanced Design System) from Agilent Technologies. This software has a simple file based behavioural model for amplifiers (AmplifierP2D) which contains measured or simulated large signal S-parameters. The obtained behavioural models can be used in system level simulations being fast and sufficiently accurate. In fig. 6.2 (a) and (b) measured gain and phase characteristics

of RF2162 operating at 850 MHz are given. In these figures the behaviour of the PA in compression is clearly visible with input 1 dB compression point at about -2 dBm. There is also increasing phase deviation near to compression point.

The next step is to calculate the LUT coefficients. Matlab has been used for this purpose. First the PA is simulated and its input-output signal magnitude and phase values for each discrete magnitude value are sent to Matlab. Next the PA characteristics is fitted to a high order complex polynomial function and then the complex coefficients, which give effectively the inverse of the PA characteristics, are calculated for each discrete input magnitude value. As an example fig. 6.3 shows real and imaginary parts of the calculated complex coefficients for a LUT having 250 coefficients. 250 coefficients means the input signal has been quantized uniformly, where the maximum instantaneous input signal has the value of 250. This is at the same time the address of LUT position where the complex coefficient for this input is stored. In fig. 6.3 the inverse triangles in red are real and the squares in blue are imaginary parts of the complex LUT coefficients for 250 discrete input values.

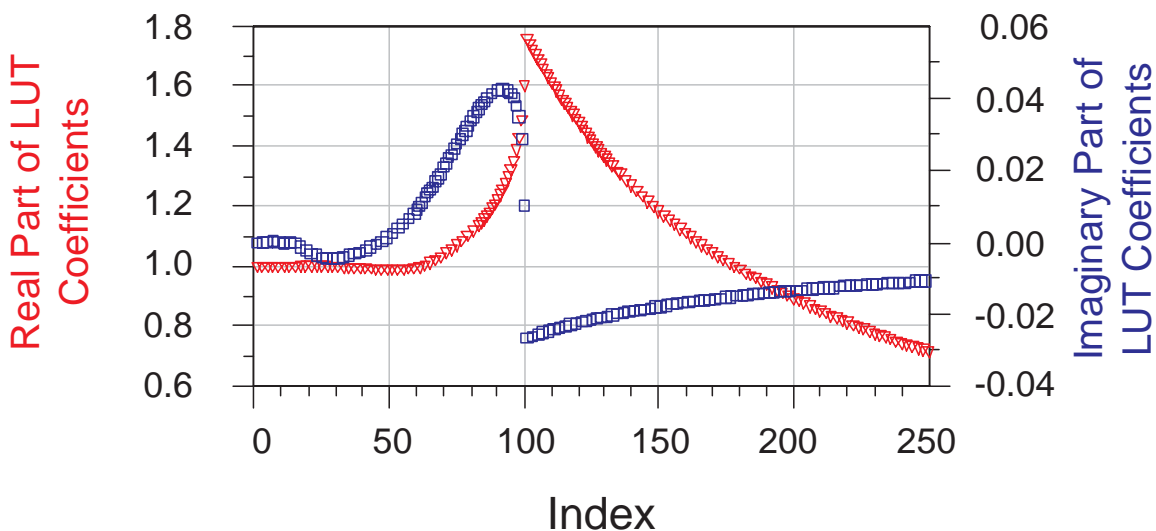


Figure 6.3: Calculated real and imaginary parts of the complex LUT coefficients for quantized input values.

Fig. 6.4, fig. 6.5 (a) and (b) show the output power, gain and output phase versus input power characteristics of RF2162 before and after linearization. The linearized characteristics are all shown in blue. In fig. 6.4 the change in the compression characteristics after linearization is clearly visible. The output power increases linearly up to the maximum achievable output power and does not increase with further increase in the input power. It has characteristics like a limiter clipping input powers greater than -1 dBm. These effects are visible also from the gain characteristics in fig. 6.5 (a). The gain is constant up to an input power of -1 dBm and then it decreases with the amount equal to the increase in the input power fulfilling constant output power condition as shown in the fig. 6.4. Phase of the PA output is constant after linearization which is shown in fig. 6.5 (b).

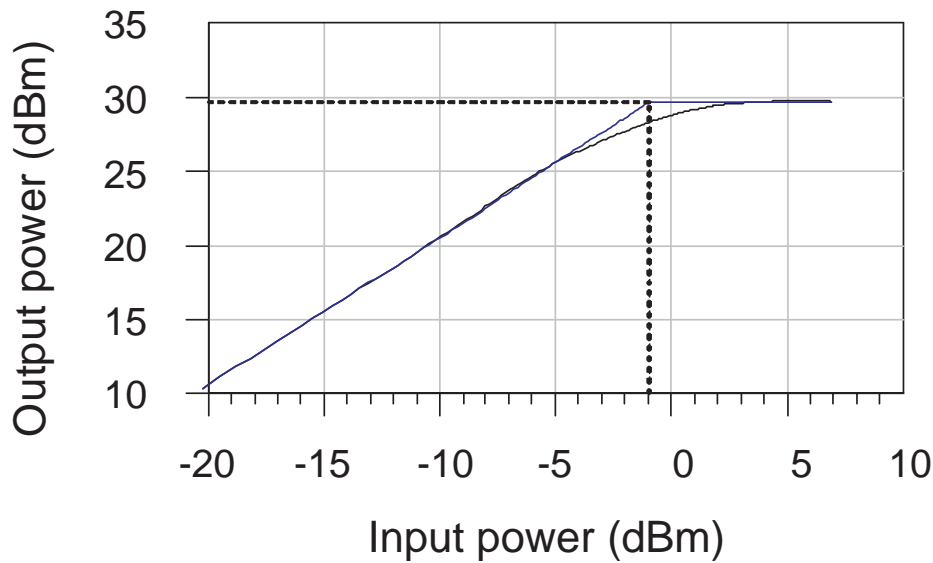


Figure 6.4: Output power characteristics of RF2162 before (black) and after (blue) linearization.

In a digital predistorter each input sample (Cartesian or polar) in baseband is multiplied with a coefficient depending on sample magnitude, which is proportional to instantaneous power of the input at this sample. This means the input signal is modified according to its envelope. However, in the static AM/AM and AM/PM measurement method explained above the obtained PA characteristics are based on average or RMS power measurements. This means the behaviour of the PA with DP may be different from the measured PA characteristics. There are some PA characterization methods based on multi tone excitation, which are supposed to deliver more enhanced PA models usable in predistortion systems with memory [83, 90, 88] but they are complicated. What we need is a relatively simple method delivering sufficiently accurate PA models usable in system simulations for terminals. If we consider that the major part of the memory is produced by envelope impedances [83], then the method proposed in [69] seems to be very attractive. This will be called instantaneous power measurement method throughout the thesis.

Fig. 6.6 shows the test bed for PA characterization proposed by Boumaiza [69]. Portions of the multi-tone input (RF_1) and output (RF_2) are taken, attenuated and downconverted using a double channel downconverter simultaneously. The two intermediate frequency signals (IF_1 and IF_2) are sent to the double channel vector signal analyzer and the delay between them is compensated. The computer captures the complex modulated IF signals and does further processing in order to obtain the baseband waveforms revealing the effects of PA gain and phase nonlinearity on input signal envelope and phase. In our measurements however (fig. 6.7), we have implemented the instantaneous power measurement method with some modifications making the setup simpler. We eliminated the double channel downconverter and used a high speed sampling digital oscilloscope instead of double channel vector signal analyzer. There is also no need for an LO signal for down conversion.

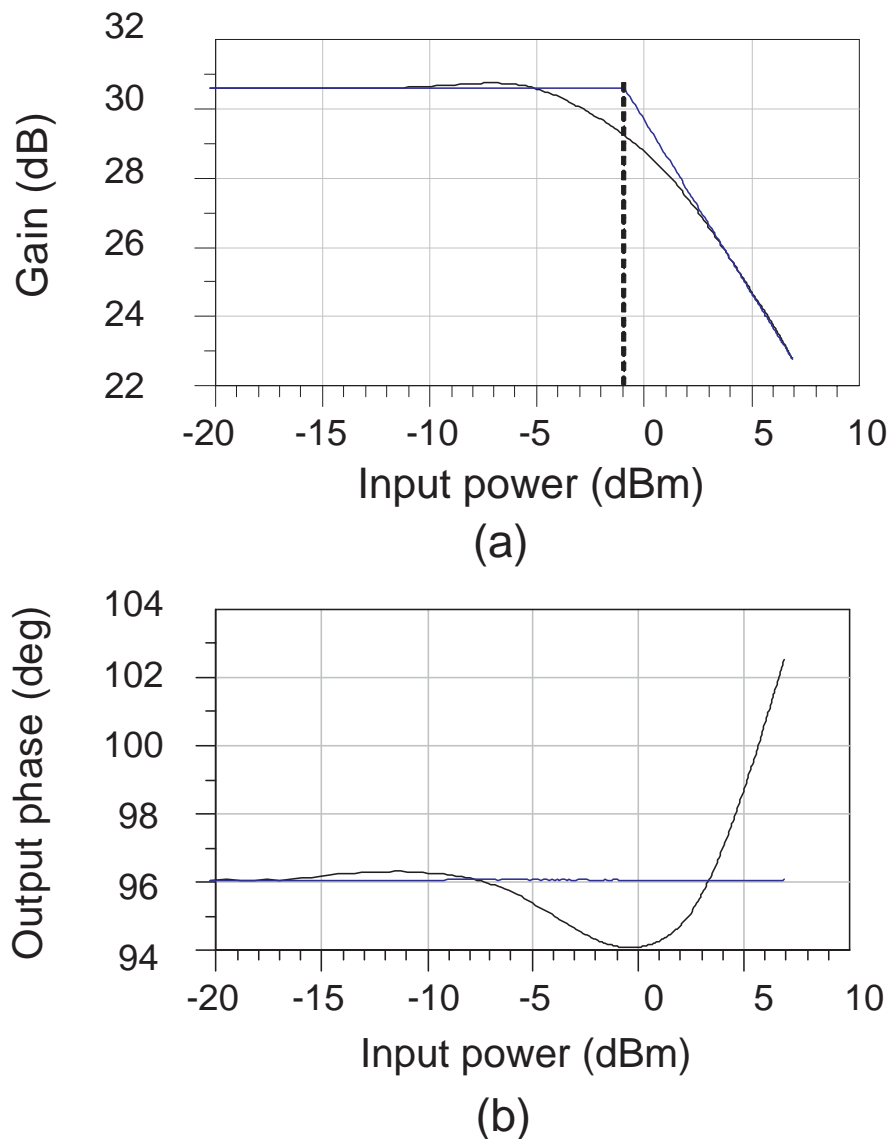


Figure 6.5: (a) Gain and (b) output phase characteristics of RF2162 before (black) and after (blue) linearization.

As shown in fig. 6.7 a two-tone signal is applied to the PA input and to channel 1 of the oscilloscope. At the same time the PA output signal is applied to channel 2 of the oscilloscope. Input and output waveforms are stored simultaneously and transferred to the computer for further processing. This data is used to obtain the baseband signal waveforms at the PA input and output in order to get gain and phase characteristics as in [69]. Downconversion, filtering, demodulation and all other necessary processing took place inside the computer. Thus possible measurement imperfections and imbalance in two measurement paths due to downconverters and analogue image rejection filters are avoided. This makes our setup simpler and PA characterization more accurate compared to [69]. The drawbacks of the simplified instantaneous power measurement setup are its low dynamic range and relatively high noise. However, in conventional PA

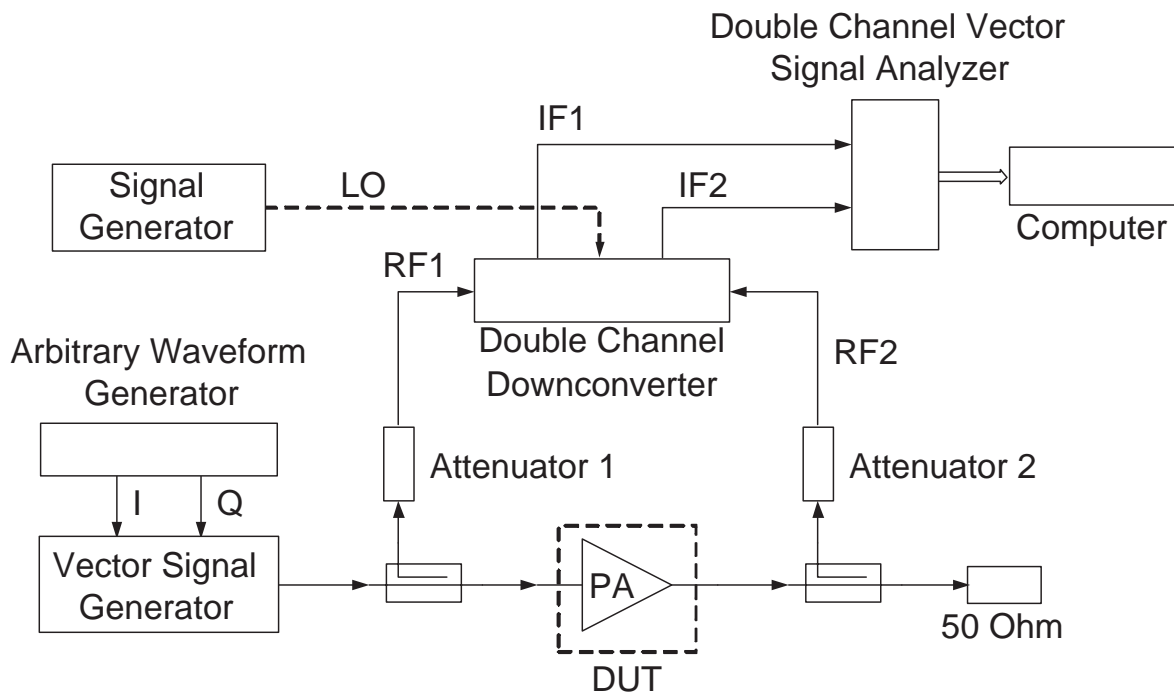


Figure 6.6: Instantaneous power measurement setup for PA AM/AM and AM/PM characterization [69].

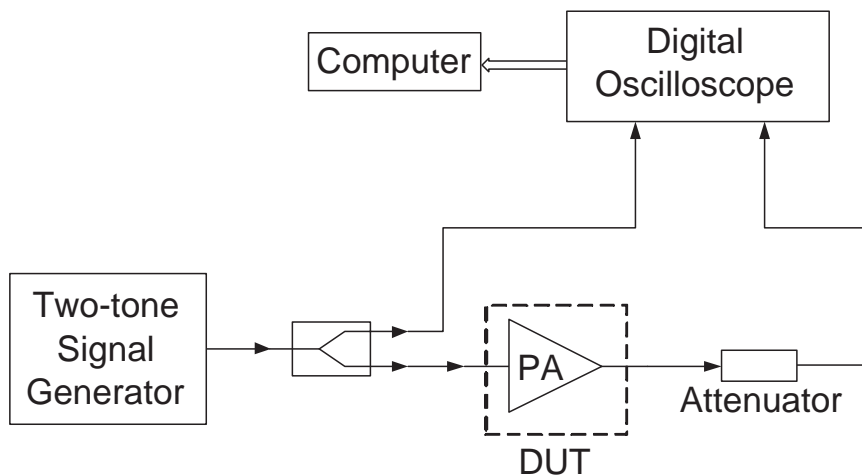


Figure 6.7: Simplified instantaneous power measurement setup for PA AM/AM and AM/PM characterization.

linearization methods linearization is required mostly at high output powers exhibiting high nonlinearity and the method is sufficiently accurate at high power levels with low noise.

In the following details on the characterization of RF3110 at 900 MHz are given. Since the purpose of this PA characterization was to use the obtained behavioural model

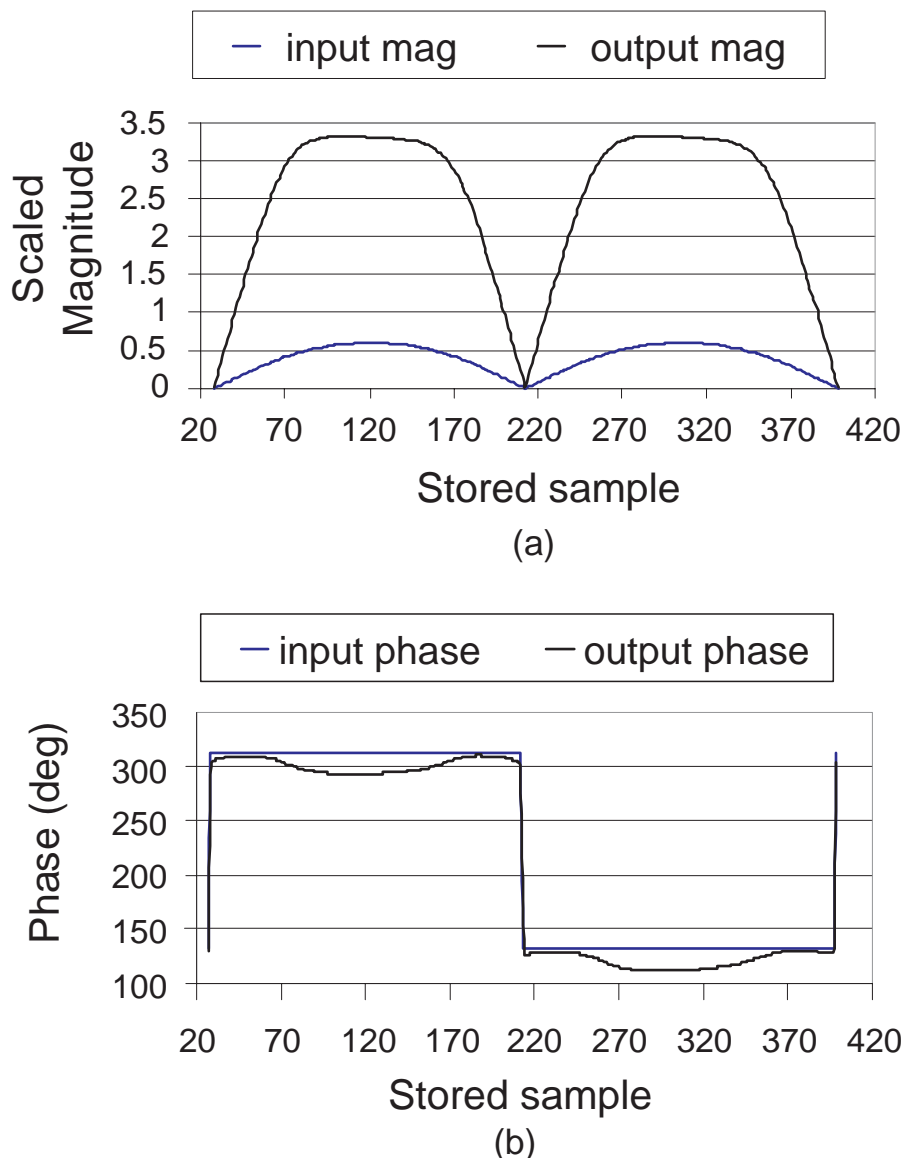


Figure 6.8: PA input and output two tone signal (a) envelope and (b) phase curves.

in EDGE and see the performance of DP, the characterization has been done with a two-tone input signal having 270 kHz tone spacing. PAR of a two-tone signal is 3 dB, which is close to PAR of the EDGE signal (~ 3.2 dB) and covers the complete input signal range from zero to peak value. Since AM/AM and AM/PM distortion in a PA varies due to the applied input power but not the phase [12], such a simple signal having just amplitude modulation has been used. The PA characteristics have been investigated at high output power levels intentionally in order to see the compression characteristics. Fig. 6.8 (a) and (b) show the stored, downconverted, low-pass filtered and delay compensated PA input and output signals magnitude and phase curves respectively. The values seen on y-axis of fig. 6.8 (a) are scaled for demonstration purposes. The compression at PA output is obvious from this time domain signal which exhibits strong AM/AM distortion for high input instantaneous power values. From

fig. 6.8 (b) AM/PM distortion is also obviously seen at high instantaneous powers if the deviation in the output phase curve at the stored sample index values of 120 and 310 are considered. At these sample instances maximum instantaneous input power occurs as shown in fig. 6.8 (a).

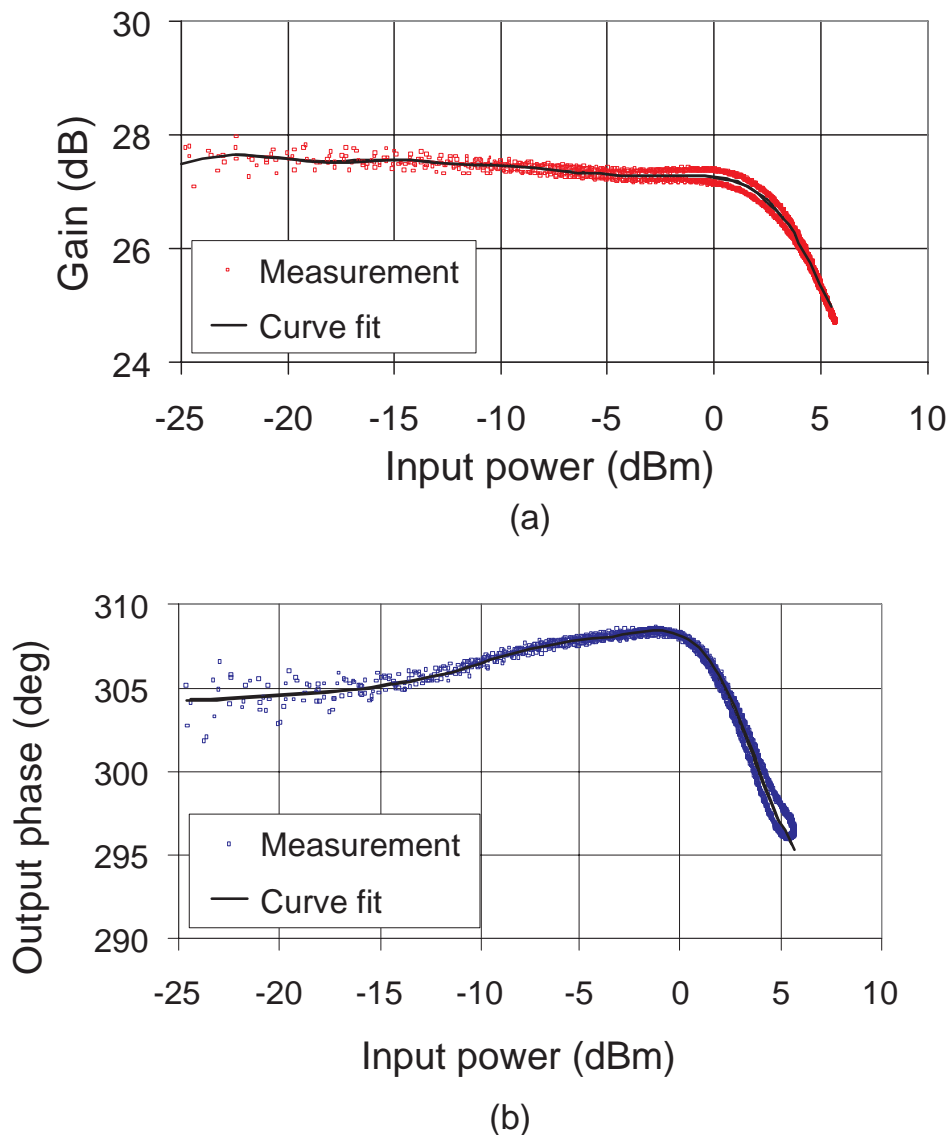


Figure 6.9: Measured (a) gain and (b) phase characteristics of RF3110 using simplified instantaneous power measurement setup.

The gain characteristics of the PA is obtained by dividing the output signal magnitude by the input signal magnitude shown in fig. 6.8 (a) and the phase characteristics by subtracting the input phase from the output phase shown in fig. 6.8 (b) for each stored sample. If the gain and output phase shift values for all index points are used then the gain and phase characteristics shown in fig. 6.9 (a) and (b) are obtained. There are small hysteresis loops visible in the gain and phase characteristics at high input power values, which is a measure of memory effects. A high order polynomial function

has been fitted to those data revealing an approximate dynamic PA characteristics which can be significantly different than the characteristics obtained with average power measurement setup [69]. This approximate dynamic PA characteristics are used in order to generate LUT coefficients as explained previously for average power measurement case.

The characterization of RF3110 is done using a two-tone signal but this behavioural model is used to calculate the LUT coefficients in order to linearize the PA with an EDGE input signal. Therefore one can think that a possible mismatch can occur during EDGE linearization performance measurements. There are two main reasons for possible mismatch: one is the difference between PARs and the other is the effect of PA memory. Since PARs of the two tone and EDGE signals are close to each other, it is assumed that the deviation due to PAR is negligible. EDGE signal is composed of a lot of spectral components in a specified bandwidth and if there were strong memory effects, then the deviation between two-tone and EDGE signal characterizations would be significant. However, handset PA memory effects are in general low [96] and we simply neglect them because we try to find a method giving good results with very low effort. Two-tone signal characterization shows that there are memory effects for a frequency spacing of 270 kHz but they are very low. Therefore the static PA characteristics obtained by polynomial fit is close to the real dynamic characteristics and the instantaneous power measurement method is the optimum way compromising the model accuracy and required effort for terminal PA characterization.

6.2 Application of MDP in EDGE

This part of the thesis describes a LUT based MDP system usable for EDGE handset transmitters and presents the performance of it. Minimum system requirements in terms of the LUT size and the wordlength of the data and LUT coefficients are calculated. The effects of antenna mismatch and required system changes in terminal transmitters for DP implementation are also discussed. The proposed system is capable of improving average efficiency and performance in terms of the leakage power at offset frequencies and error vector magnitude. It is simple compared to basestation implementations comprising power amplifier memory compensation and can be easily implemented in handsets in order to improve the overall system performance. Thus a single amplifier fulfilling GSM and EDGE specifications can replace currently used dual mode GSM/EDGE PAs.

In [97] the performance of a DP system in a GSM/EDGE base station PA has been demonstrated. In handsets the current trend is to implement simple predistortion systems with moderate improvement like analog predistortion with 3rd or 5th order intermodulation distortion compensation. However, in EDGE the requirement for leakage power at 200 kHz offset is not critical compared to 400 and 600 kHz offsets [97]. Therefore a system capable of compensating high order nonlinearities like DP is required. If the power consumption of the digital signal processing in DP can be kept low compared to the efficiency improvement due to linearization, then DP can be implemented also in handsets.

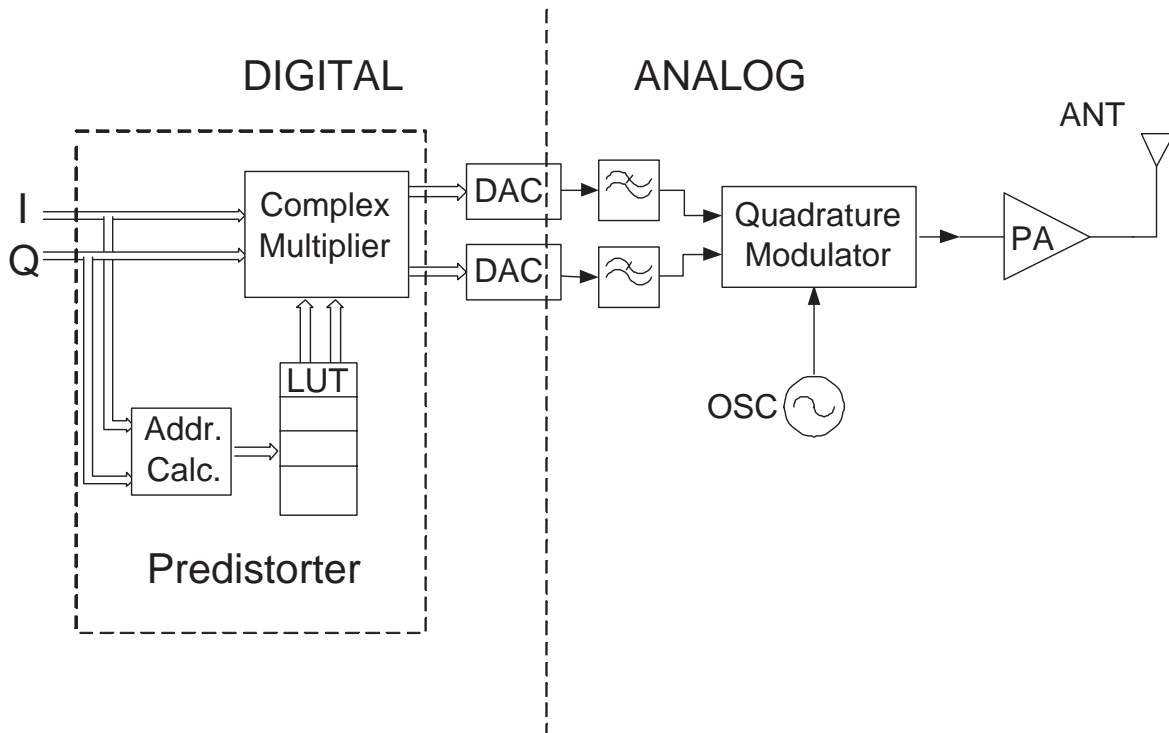


Figure 6.10: Memoryless digital predistortion block diagram for systems with quadrature modulator.

The topology of DP should also be simple for handset implementation. The structure of DP depends on the transmitter path architecture. In today's mobile communication systems usually baseband signals in Cartesian form are used where a quadrature modulator upconverts the baseband signals to IF or directly to RF. Fig. 6.10 shows an appropriate DP structure for direct conversion. It is a so-called gain-based predistorter [12]. On the other hand, recent developments show that polar modulators gain more interest. A simple transmitter architecture with a polar modulator and DP is shown in fig. 6.11. In the following, those two architectures are compared in respect to their complexities. In the case of quadrature modulation, the signal samples in the digital domain are multiplied one by one with LUT coefficients selected by the input signal addressing. Predistorted digital signals are converted to analog signals using DACs. They are low-pass filtered and sent to the quadrature modulator. It is assumed that the modulator between the predistorter and PA is ideal. The directly modulated predistorted signal is sent to the PA and then to the antenna. In the case of polar modulation (fig. 6.11) again the signal samples in the digital domain are modified one by one as in the quadrature modulator case. A SDM is used to modulate the carrier phase, and this phase-modulated signal is multiplied with the amplitude signal. The resultant signal is applied to the PA and then sent to the antenna. Magnitude addressing would be especially advantageous if a polar modulator is used instead of a quadrature modulator. Since the amplitude data is already available in the polar architecture, there is no need to have an address calculation block ("Addr. Calc.") in the system shown in fig. 6.10 with a quadrature modulator. The predistorter is also simpler and needs only a multiplier and

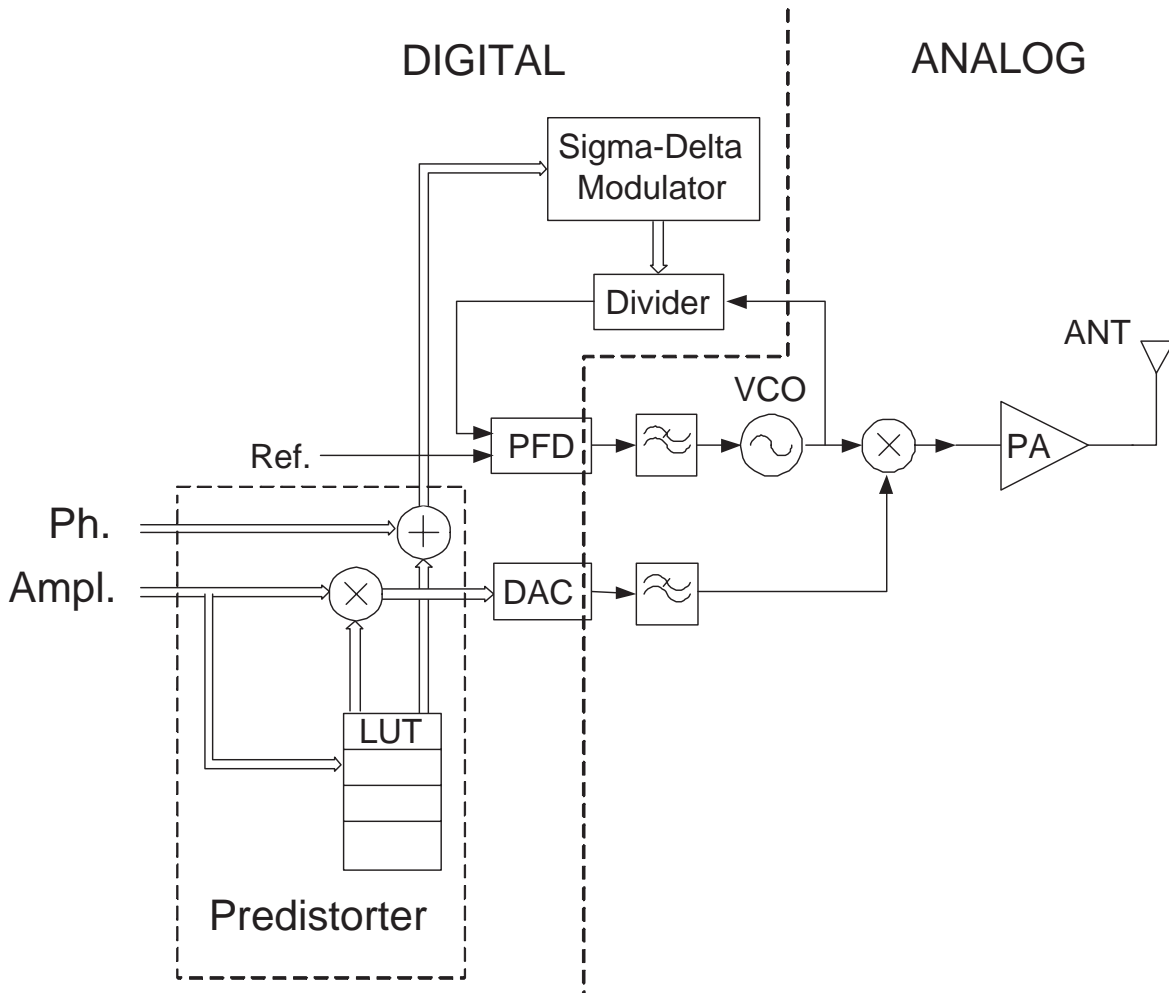


Figure 6.11: Memoryless digital predistortion block diagram for systems with polar modulator.

an adder to perform DP. In contrast to that in a quadrature modulator case a complex multiplier composed of 4 multipliers, one adder and one subtractor is needed. However, with a clever design the digital computational burden in quadrature modulation can also be reduced significantly. One of the possibilities is to use CORDIC (COordinate Rotation Digital Computer) algorithm for phase predistortion, which is implemented in most of digital baseband ASICs for frequency correction. Such a predistorter will need two additional scalar multipliers in I and Q branches for amplitude modulation instead of a complex multiplier.

6.2.1 System performance

AM/AM and AM/PM characteristics of a GSM PA (RF3110) have been obtained by the instantaneous power measurement technique in order to linearize it for EDGE application. LUT coefficients calculation has been done in Matlab and system simulations in ADS. Fig. 6.12 shows DP performance measurement setup. The input predistorted

EDGE signal has been obtained by means of simulations for each measured output power level. Those data have been downloaded to a signal generator with arbitrary waveform generator and used as an input signal for the PA. A precision signal generator has been used as a modulator that is assumed to be ideal. The resultant output is analyzed by a vector signal analyzer.

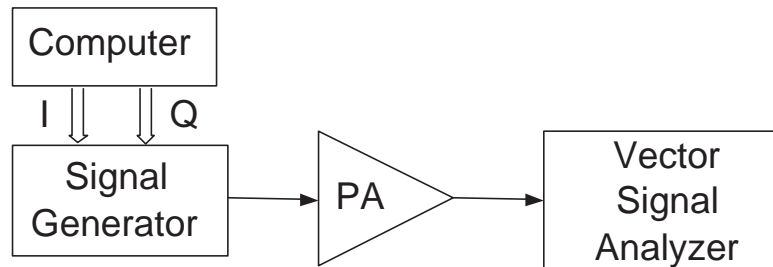


Figure 6.12: Block diagram of digital predistortion measurement setup.

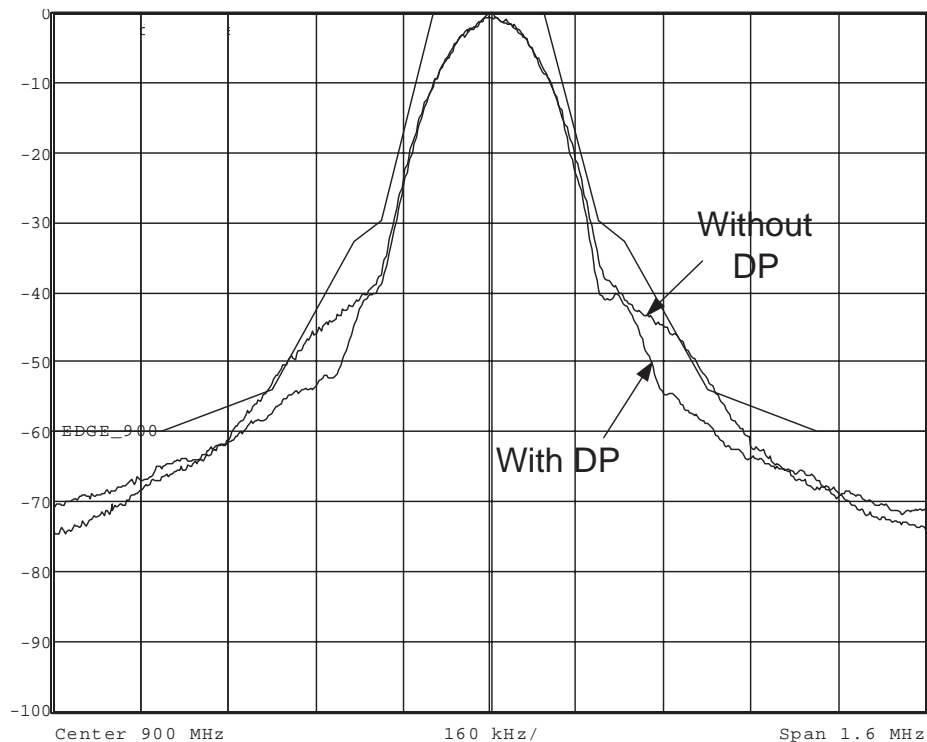
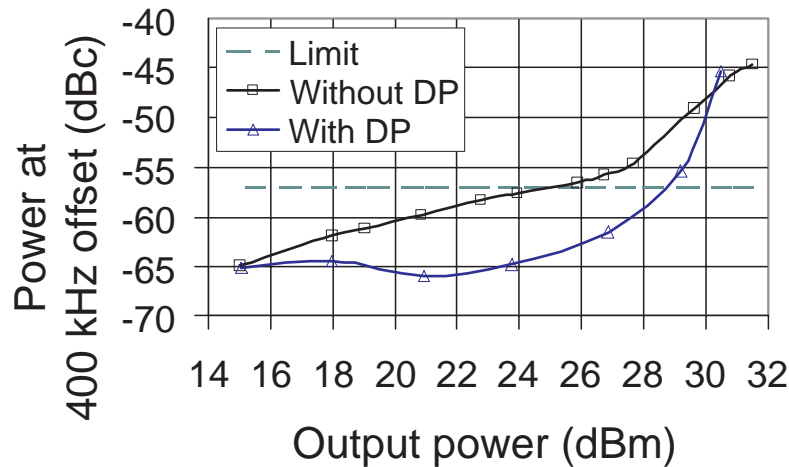
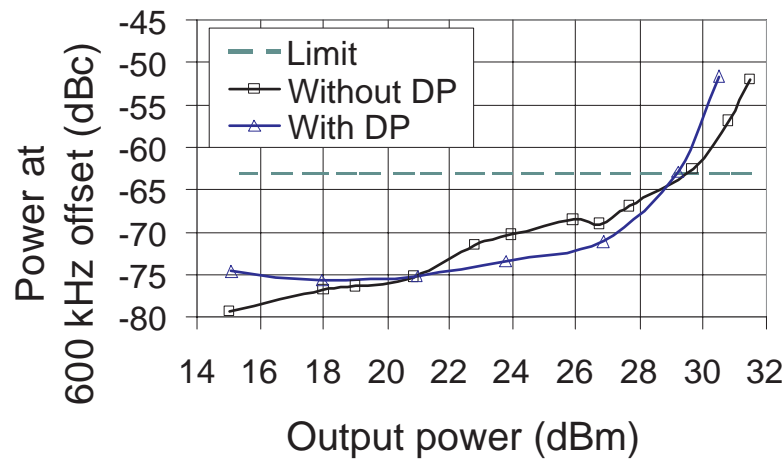


Figure 6.13: RF3110 EDGE output spectrum with and without predistortion at 28.5 dBm output power.

The measurement setup is such that the measurement results are representative for quadrature as well as polar modulator architectures. The reason is that the predistorted



(a)



(b)

Figure 6.14: Measured output powers at (a) 400 and (b) 600 kHz offsets with and without digital predistortion.

signals are generated under ideal conditions eliminating analog imperfections in front of the PA which would normally be different for those two architectures. Fig. 6.13 shows the PA output spectrum with and without DP for 28.5 dBm output power. Without DP the spectrum mask is not fulfilled, whereas with DP 3 dB margin is obtained showing the usefulness of the concept. A significant improvement in leakage power at offsets and EVM have been observed using DP. Power at 400 and 600 kHz offset frequencies versus output power and EVM versus output power are shown in fig. 6.14 (a), (b) and fig. 6.15 respectively. Power at 200 kHz offset is not shown because it is not critical compared to 400 and 600 kHz. The specification limits [21] including 3 dB spectrum mask margin are also shown in fig. 6.14 (a) and (b) for comparison. As it can easily be seen from these figures, DP improves the output RF spectrum at 400 kHz significantly and at 600 kHz slightly. There is also improvement in EVM_{RMS} values as shown in fig.

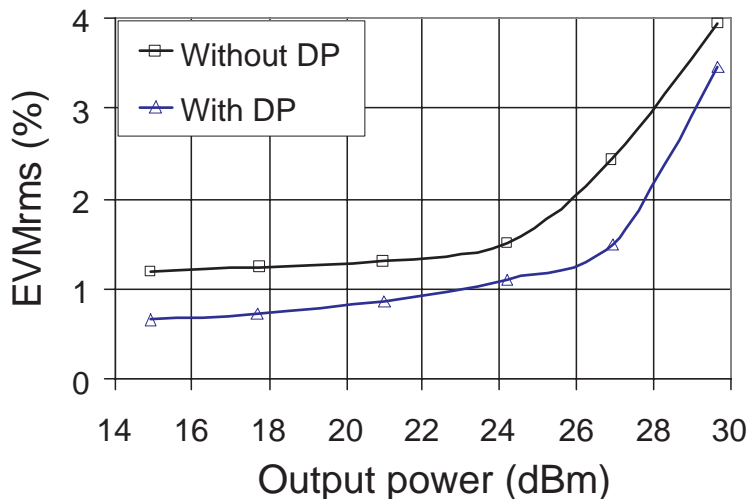


Figure 6.15: Measured EVM_{RMS} with and without digital predistortion.

6.15. EVM_{RMS} should not exceed 9% according to specifications [21], which is fulfilled even without DP.

By applying DP the maximum output power is increased from 25 dBm to 28.5 dBm and PA efficiency from 15.2% to 23.4% while fulfilling the spectrum mask with 3 dB margin. EVM_{RMS} has also been reduced from 3.4% to 2.6% at 28.5 dBm output power. At maximum linear output power of 28.5 dBm PAE of the PA (RF3110) plus DP is 23% (estimated power consumption of DP is 50 mW), which is close to commercial PAs designed for EDGE. However, for lower output powers the proposed system is significantly better because the quiescent current for the GSM PA has been measured to be 180 mA whereas it is 480 mA for an EDGE PA (RF3145) from same manufacturer. Measured performance of RF3110 with and without DP is also given in tab. 6.1 for comparison. Since handsets in EDGE are not supposed to transmit always at maximum output power, the system efficiency depends not only on PA efficiency at maximum output power, but also on efficiencies at lower output powers. Measured PAs are not state of the art but measurement results show that the proposed system is advantageous especially during operation with high back-off. This results from the fact that constant envelope PAs can be more easily designed for lower quiescent currents compared to dual mode linear PAs where more design trade-offs have to be taken into account. The efficiency can be further improved with a careful design of PAs. For example the PA used has been designed to give maximum GSM output power of 35 dBm with high efficiency which is not optimum for EDGE.

DP is not required for all output power values according to the measurement results in fig. 6.14 (a) and (b). It is required just for output power values above 25 dBm where the PA by itself does not fulfill linearity requirements. DP can be switched off during lower output power transmission in order to save power meaning improved system efficiency.

The measurement and simulation results agree well at high output powers where DP is beneficial. For decreasing power levels the agreement gets worse. At 400 kHz offset the maximum difference comes up to about 5 dB and at 600 kHz up to 10 dB. The

	With DP	Without DP
Maximum linear P_{out}	28.5 dBm	25 dBm
Efficiency at maximum linear P_{out}	23%	15.2%
EVM_{RMS} at 28.5 dBm P_{out}	2.6%	3.4%

Table 6.1: Measured performance of RF3110 with and without DP.

reasons for deviations are assumed to be measurement, simulation errors and memory effects. However, there is still a significant improvement in system performance due to the benefit at high output powers.

6.2.2 Quantization analysis

In [63] a detailed quantization analysis for digital baseband predistortion is presented. The relation between ACI (Adjacent Channel Interference) and wordlength at different parts of the system has been calculated and it has been stated that with a careful design the efficiency of the system can be highly improved. We are going to define the minimum requirements of a DP system in EDGE mobile stations in terms of LUT size and wordlength by means of simulations done in ADS. For this purpose DP simulations have been done for 6 different LUTs having 2560, 1280, 640, 320, 160 and 80 coefficients and their performances have been compared in fig. 6.16 (a) and (b). The figures show the improvement in the leakage powers at 400 and 600 kHz offsets and spectrum mask limits including 3 dB margin. The measurement results without DP are also shown in the same figures. Simulation results are shown just for these two frequencies because they are the most critical issues in terms of linearity in EDGE. The wordlength in DP has been selected to be 14 bits. As can be seen from fig. 6.16 (a) and (b), with decreasing LUT size the offset power at PA output can still be in the specified region and be improved compared to the output without linearization. However, there is a trend in leakage power to increase with respect to carrier with decreasing output power for small LUTs. For large LUTs this effect is negligible and leakage power ratio stays almost constant for small output powers. The reason for worse performance at low powers is the decrease in the number of LUT coefficients used to multiply with the input signal. Fig. 6.16 (a) and (b) show that the performances of LUTs having 640, 1280 and 2560 coefficients are very similar. This means a LUT having 640 coefficients can be used for a good DP performance in the case that a wordlength of 14 bits is used.

Simulations show that the noise floor at PA output increases with decreasing LUT size. However, effect of the wordlength on noise floor has been observed to be much more important. In the following simulations the LUT size has been kept constant and the system wordlength changed in order to see its effect on DP performance. The LUT having 2560 coefficients has been used for simulations in order to see degradation just due to the wordlength but not due to the LUT size. Fig. 6.17 shows the simulation results with wordlengths of 11, 12, 13 and 14 bits at 1.8 MHz frequency offset. It is visible that the noise floor decreases about 6 dB for each additional bit, agreeing with the relation between SNR and wordlength [63]. The wordlength is not critical for 200

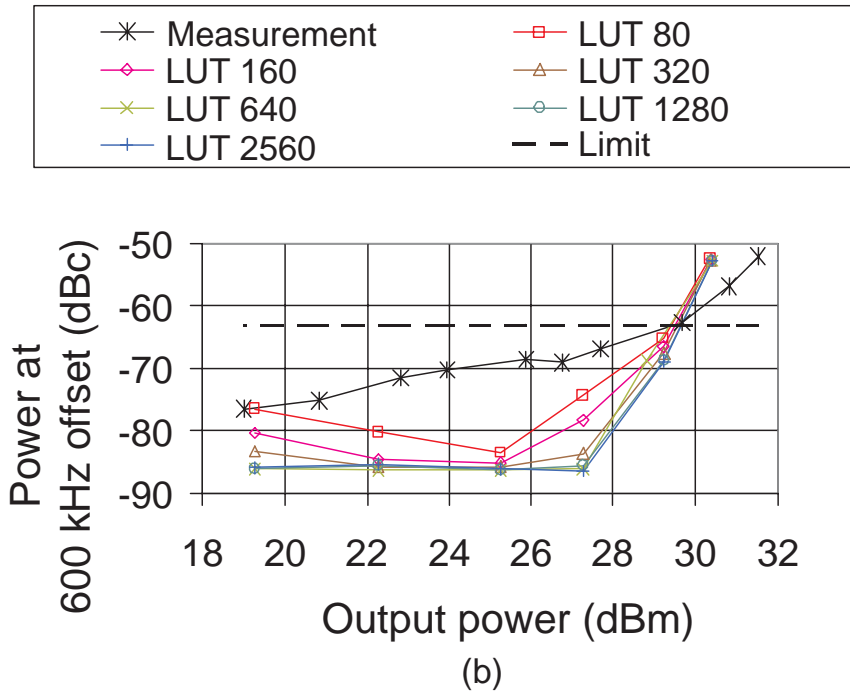
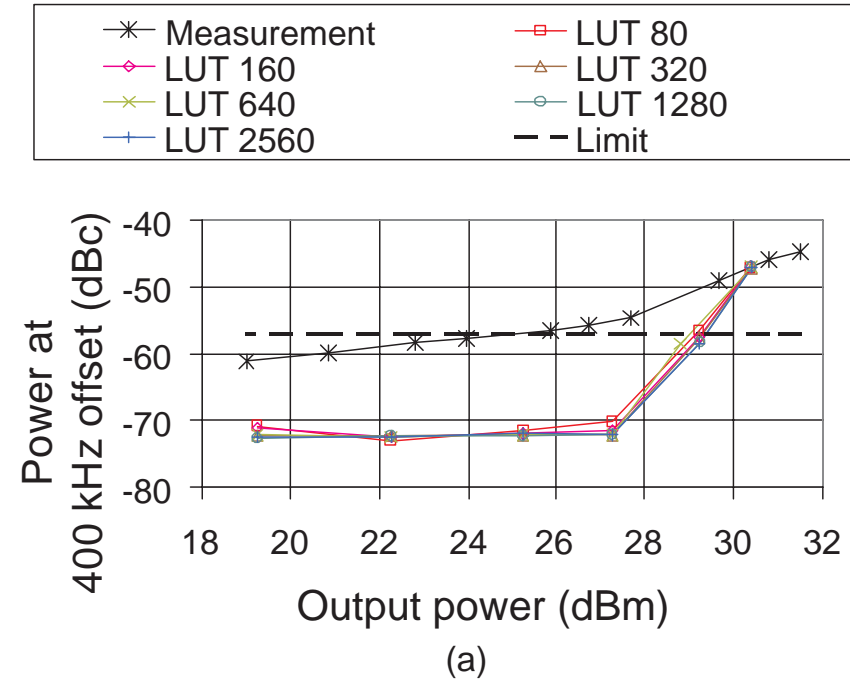


Figure 6.16: Simulated output powers at (a) 400 and (b) 600 kHz offsets with different LUT sizes.

and 400 kHz offsets but its effect becomes obvious for higher frequency offsets. We assume that if output power spectrum fulfills the spectrum mask at 1.8 MHz then the power at lower frequency offsets should also be below the spectrum mask. The noise floor increases with reducing the wordlength and the simulations showed that the power

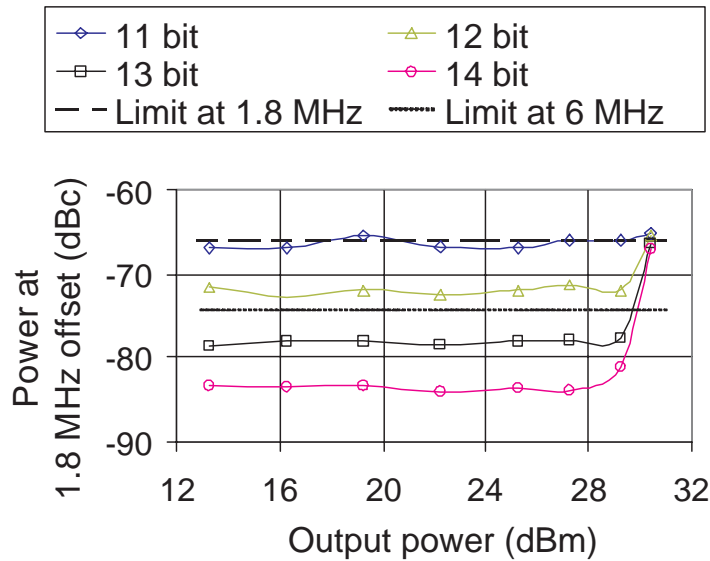


Figure 6.17: Simulated output powers at 1.8 MHz offset with different wordlengths.

at frequencies higher than 1.8 MHz is almost equal to the power at 1.8 MHz if DP is used. The maximum allowed power is -63 dBc at frequency offsets greater than 1.8 MHz [21]. If a MDP system as shown in fig. 6.10 is implemented and a reconstruction filter with a bandwidth smaller or equal to 1.8 MHz is used then the wordlength of 11 may be enough resulting in a noise power of about -67 dBc according to fig. 6.17. Depending on DP implementation in the system a greater wordlength may be necessary because today's mobile communication systems are not as simple as shown in fig. 6.10. There are some additional blocks in digital domain like frequency, DC offset and IQ imbalance correction and interpolation units. The wordlengths required for these operations are relatively high (12-13 bit) in order to avoid large rounding errors. Therefore the wordlength of DP may be increased up to 13 bit for proper system operation if it is implemented between such blocks.

There is a mismatch between output leakage power measurements and simulations, because simulation results in fig. 6.16 (a) and (b) only show the effects of LUT size due to ideally selected environmental conditions. A LUT size of about 500 coefficients seems to be acceptable since there is no significant improvement in the performance of DP by increasing LUT size further. If a lower LUT size is used, then the linearization performance is expected to be worse especially at lower output powers which may be acceptable for some applications.

6.2.3 Effects of antenna mismatch

Very good DP system performance has been shown under optimum PA output match conditions. In the following the impact of antenna mismatch is investigated. Since mobile phones can be moved continuously and the environment of an antenna can change, and therefore the antenna impedance seen by the system can change continuously. This results in changes of VSWR (Voltage Standing Wave Ratio) at the PA output.

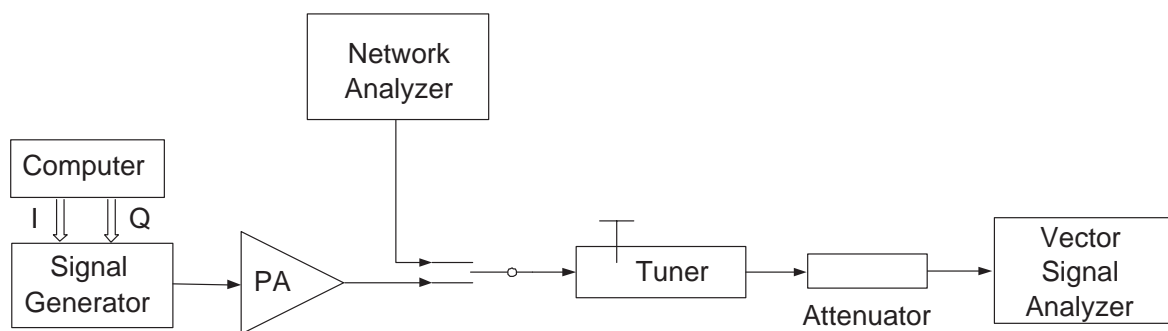


Figure 6.18: Measurement setup for antenna mismatch.

We have used the measurement setup shown in fig. 6.18 in order to see the effects of antenna mismatch on the performance of MDP. The measurements have been done with and without linearization cases. A signal generator having an integrated arbitrary waveform generator has been used for downloading and regeneration of the PA input signals generated in ADS. The network analyzer used in the setup is for adjusting the tuner precisely for different VSWR values and phases of the load. The output of the tuner has been connected to an attenuator and then to a vector signal analyzer for output RF spectrum and EVM measurements. The attenuator is for protection of the vector signal analyzer.

Fig. 6.19 (a) and (b) describe the influence of antenna mismatch at maximum output power of 28.5 dBm with and without DP for VSWR of 3 and phase angles of load between zero and 360 deg. Fig. 6.19 (a) shows leakage power values at 200, 400 and 600 kHz offsets as a function of the load phase. The system performance under worst case conditions with DP is at 200 kHz superior (~ 3 dB), at 400 kHz comparable and at 600 kHz inferior (~ 3 dB) to the performance without DP. On the other hand fig. 6.19 (b) describes EVM_{RMS} as function of the load phase. The performance without DP under worst case conditions is 11.2% however with DP only 9.7%. These results indicate that the load mismatch performances in both cases are about the same order. To take full advantage of DP system also under mismatch conditions additional measures are required such as using an isolator or using adaptive DP.

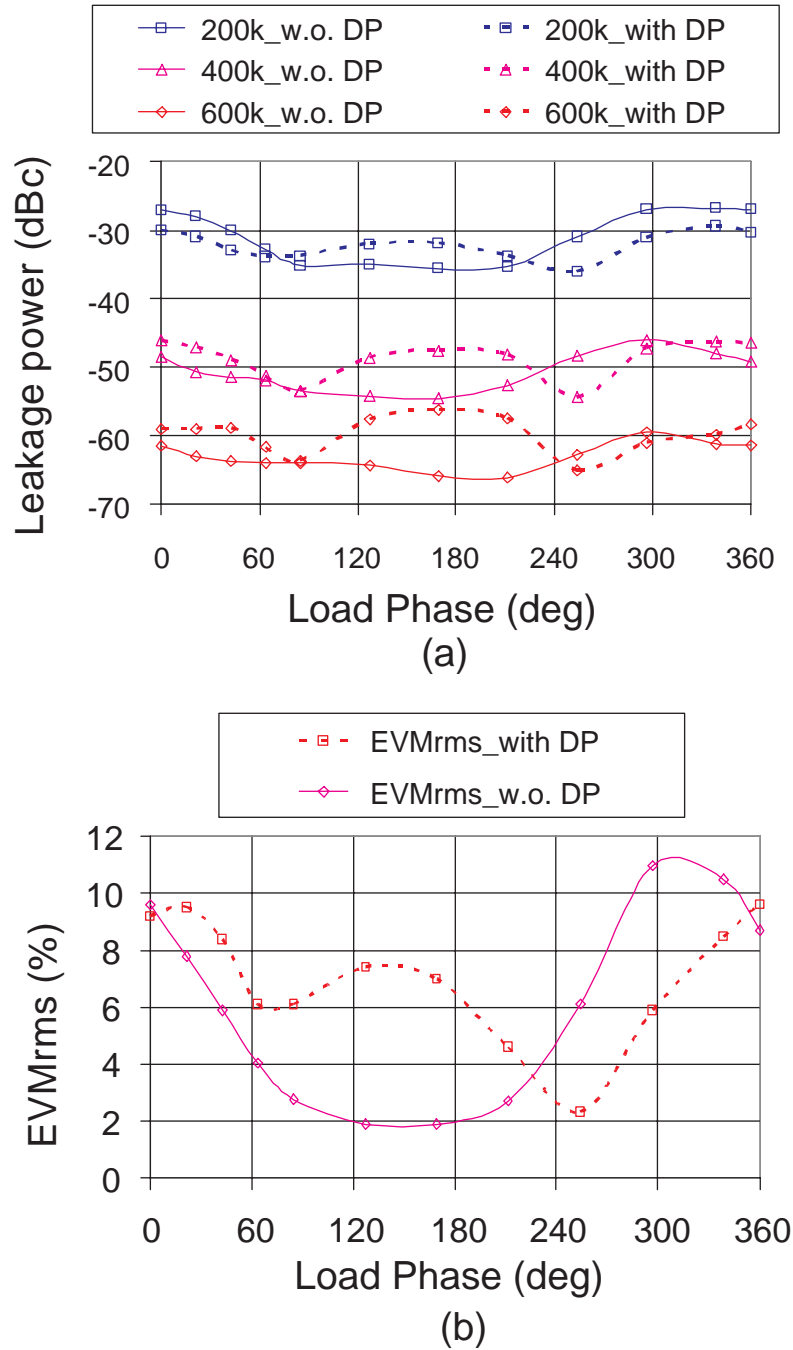


Figure 6.19: Variation of (a) leakage power for 200, 400 and 600 kHz frequency offsets and (b) EVM at the output with and without predistortion as a function of load phase (P_{out} is 28.5 dBm and VSWR is 3) .

6.2.4 Required system modifications

Some modifications in terminal transmitters should be done in order to implement DP. The first point to be discussed is the wordlength of DACs in figs.6.10 and 6.11. Since PAR of the predistorted I- and Q-signals (fig. 6.10) will be higher than the signals

without predistortion (this is valid also for the predistorted magnitude signal in polar modulator case), increasing the wordlength can be helpful to keep quantization noise low. Fig. 6.20 (a) and (b) show the real part and magnitude of an EDGE input signal respectively with and without predistortion. Increase in the peak values after predistortion is obvious in the figures. Each input sample is modified by the corresponding complex LUT coefficient according to magnitude addressing.

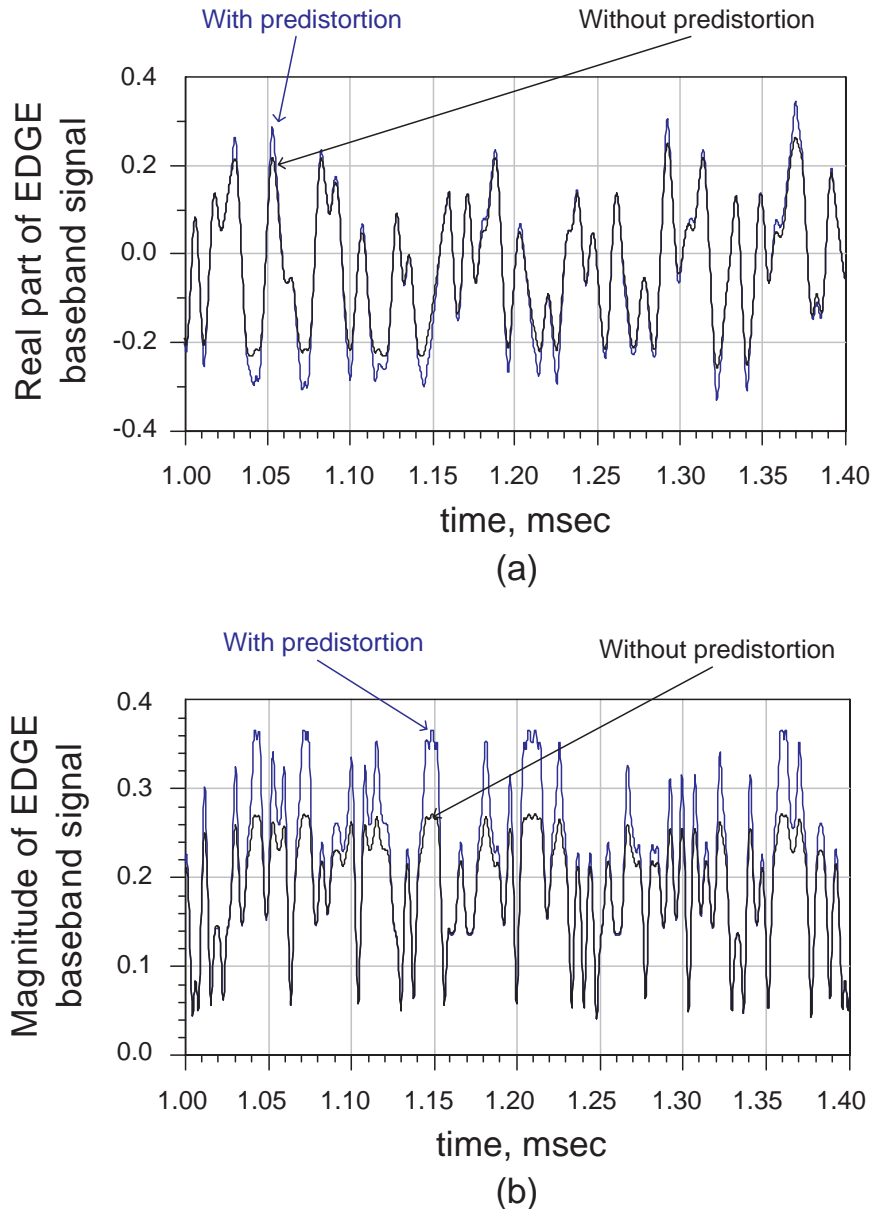


Figure 6.20: Increase in signal peak-to-average ratio of the (a) real part and (b) magnitude of an EDGE baseband signal after predistortion.

Signal to quantization noise power ratio can be defined as [63]

$$SNR = 6.02n + 4.77 - 20\log(k) \quad (6.1)$$

where n is the number of bits (wordlength) and k is peak to RMS amplitude of the signal. If the signal is not a scalar but a complex one, then SNR decreases by 3.01 dB as given below.

$$SNR_{comp} = 6.02n + 1.76 - 20\log(k) \quad (6.2)$$

From eqns. 6.1 and 6.2 it is seen that an increase in k will result in lower SNR. By experience we know that the maximum value of LUT coefficients can be about 2 or more (fig. 6.3). It changes depending on compression characteristics of the PA. In the case that PA delivers maximum linear output power with predistortion, the peak value of the signal is multiplied with the maximum LUT coefficient. The coefficient used for RMS value of the input signal is much lower being close to 1. If we assume that the RMS value of the signal does not change significantly after predistortion, then magnitude of the maximum LUT coefficient will be the factor of increase in peak to RMS ratio in signal magnitude. If we denote this factor as p , then for a predistorted complex signal the eqn. 6.2 can be rewritten as

$$SNR_{comp,pred} = 6.02n + 1.76 - 20\log(k \cdot p) \quad (6.3)$$

In this way a rough estimation of the effects of predistortion on SNR can be calculated. For example if p is equal to 2, 4, 8, ..., then the decrease in SNR will be 6.02, 12.04, 18.06, ... dB respectively. This means for each doubling of p , SNR is decreased such that the number of bits is one less, which can be called the effective number of bits n_{eff} . It is equal to $(n - 1)$, $(n - 2)$, $(n - 3)$, ... for p of 2, 4, 8, ... and SNR after predistortion can be calculated as

$$SNR_{comp,pred} = 6.02n_{eff} + 1.76 - 20\log(k) \quad (6.4)$$

If predistortion is applied and the same SNR is desired to have as without DP, then n must be increased depending on p . If p is equal to 2, 4, 8, ... then n should be increased by 1, 2, 3, ... respectively.

There should also be some modifications in the reconstruction filters following the DACs, as already mentioned in chapter 5. In transmitters with a quadrature modulator (fig. 6.10) the bandwidth of the reconstruction filters after DACs must be increased because the predistorted signals have wider bandwidths than the signals without predistortion. The predistorted baseband signal must pass through the reconstruction filter without losing the spectral components out of the band because these are the components, which are supposed to cancel out the distortion elements at the PA output. As an example fig. 6.21 (a) shows the simulated spectrum widening of the real part of a baseband EDGE signal after predistortion. Black colored graphic in the figure is the pulse shaped real part of the EDGE signal whereas the blue colored one is the signal after predistortion. Since in the simulations no reconstruction filters are used, the noise power at high offset frequencies is high but it is normally suppressed by reconstruction filters. Bandwidth of the reconstruction filter for a predistorted signal should be equal to the bandwidth in which leakage power suppression is required. This means in EDGE if the unwanted leakage powers at 400 and 600 kHz offsets are going to be

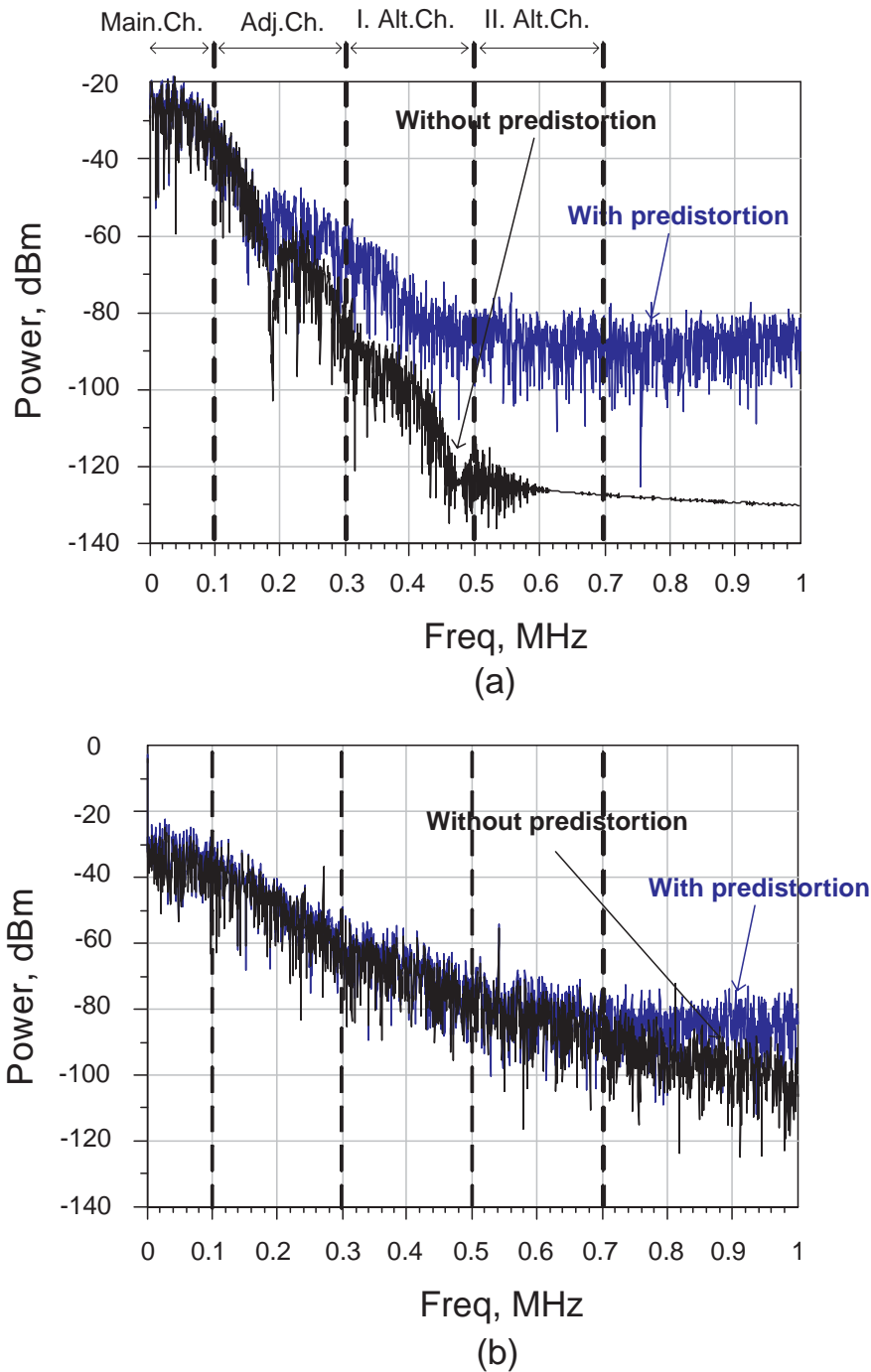


Figure 6.21: Spectrum of the (a) real part and (b) magnitude of an EDGE baseband signal with and without predistortion.

suppressed, then the minimum filter bandwidth must be 700 kHz as shown in fig. 6.21 (a). Simulations showed that in the case of transmitters with a polar modulator, however, bandwidth of the reconstruction filter does not need to be increased because it is already wide enough. Fig. 6.21 (b) shows the spectrum of baseband input magnitude in a polar modulator case with (blue colored) and without (black colored) DP. Since

pulse shaping of the digital data is done when it is in Cartesian form, modifications like predistortion in Cartesian form result in a widening in spectrum. However, if an undistorted pulse shaped input signal is converted to polar form, then the spectrum of both magnitude and phase signals are much wider than pulse shaped I- and Q-signals. For magnitude signal this can be seen in fig. 6.21 (b). According to the figure there is no significant spectrum widening in EDGE amplitude signal if it is predistorted.

The third modification may be in the transmitter chain portion between the reconstruction filters and the PA, which can be composed of analog baseband amplification and correction circuits, modulator and preamplifier. This path should be linear enough, have no significant IQ imbalance and thus be able to handle the predistorted signals without significant distortion, which have higher PAR.

6.3 Application of MDP in WCDMA

Performance of MDP in WCDMA handsets will be discussed in this part. Since the used modulation scheme is QPSK, linear amplification is necessary in order to obtain sufficiently high ACPR and EVM values. WCDMA systems are based on continuous transmission and reception, therefore system efficiency improvement is a very important issue especially in terminals. The method applied requires minimum change in the conventional transmitter path configuration whilst considerable PAE improvement can be achieved because a smaller PA, which fulfills system specifications with DP, can be used instead of a linear PA having a larger output stage.

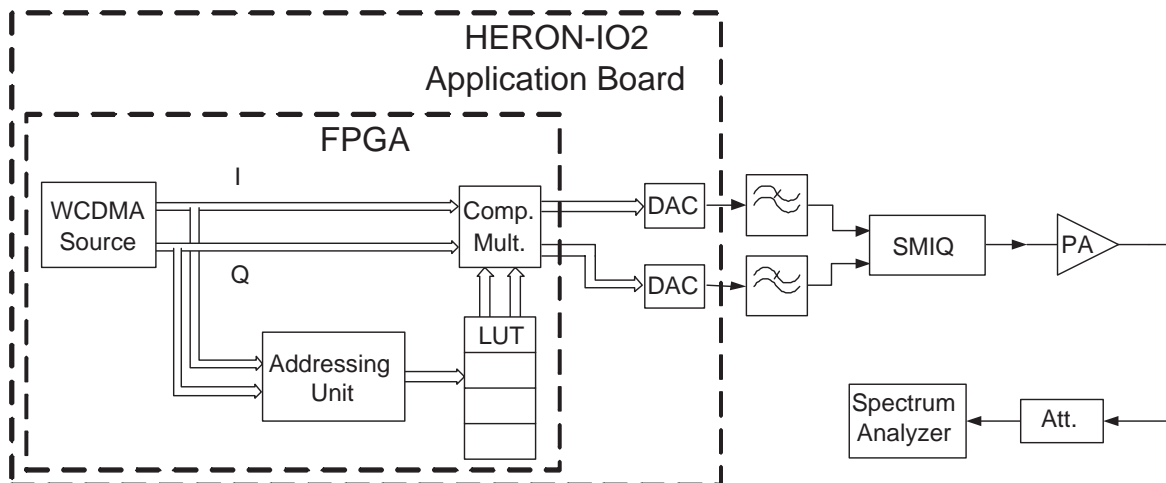


Figure 6.22: Measurement setup of MDP implementation in WCDMA.

An FPGA (Field Programmable Gate Array) has been used in order to implement MDP. The block diagram of implemented system is shown in fig. 6.22. FPGAs are programmable devices like microprocessors and they are very fast. It is reasonable to use them if simple mathematical operations are going to be done as in the critical

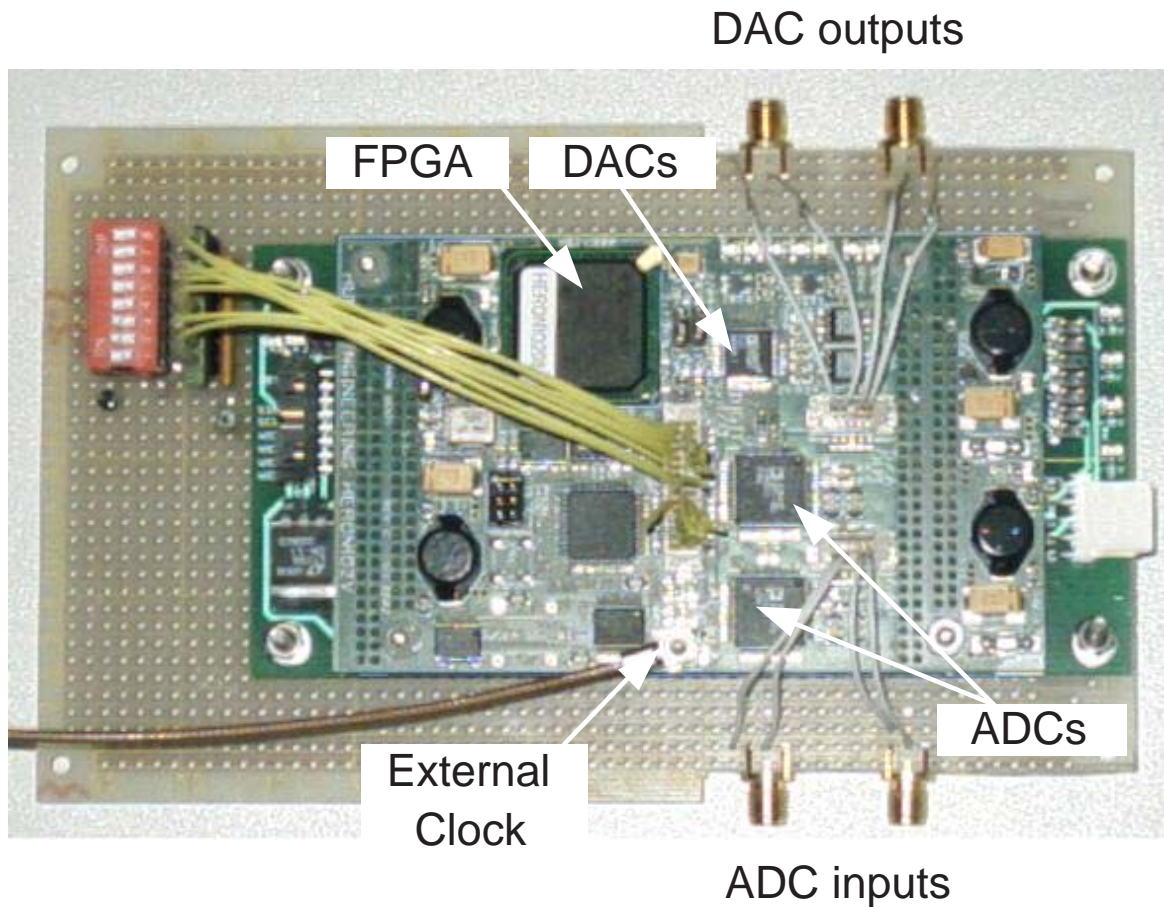


Figure 6.23: Picture of the used FPGA (HERON-IO2) application board.

forward path of DP. A complete application board (HERON-IO2¹) having an FPGA module with two ADCs and two DACs has been used for digital processing of I- and Q-signals and converting them to analog for DP performance measurements. Fig. 6.23 shows a picture of HERON-IO2. The predistorted signals follow the transmitter path composed of reconstruction filters, a quadrature modulator and a PA as shown in fig. 6.22. A signal generator (SMIQ) from Rohde & Schwarz has been used instead of the quadrature modulator and VGA in order to develop a principal understanding of the system characteristics. The PA used is RF2162 at 850 MHz.

The predistorter is composed of an address calculation unit, a LUT and a complex multiplier. Power addressing has been used due to its simple implementation in an FPGA. The square of the input complex baseband signal is calculated for addressing which is proportional to its power. The LUT contains 256 complex coefficients. The input signal is a WCDMA like signal with 3.84 MHz bandwidth and peak to average ratio of 4.7 dB. It is generated in ADS and downloaded to the FPGA. The system wordlength is 10-bit and predistorted I- and Q-signals are sent to 12 bit DACs after predistortion. However, the effective number of bits is 11 (from eqns. 6.1 and 6.2)

¹Hunt Engineering, Chestnut Court, Burton Row, Brent Knoll, Somerset, TA9 4BP, UK

because the maximum LUT coefficient value p is about 2.

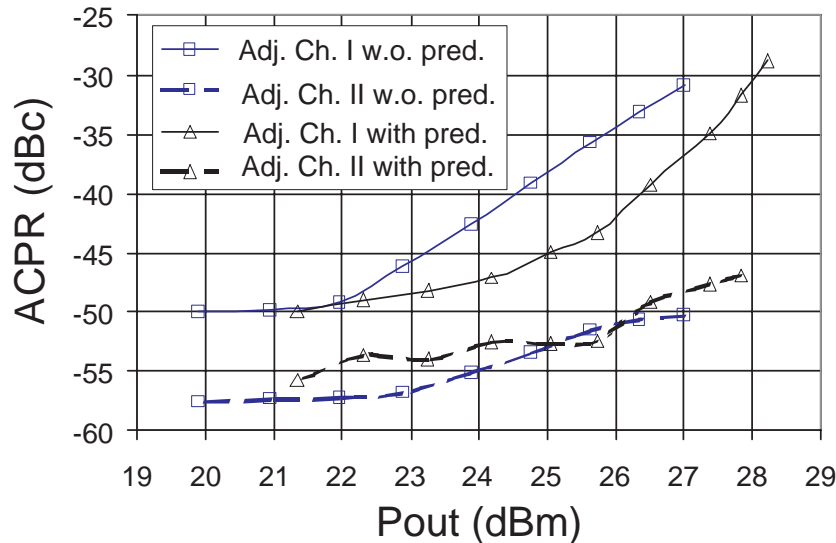


Figure 6.24: ACPR I and II measurements with and without MDP.

In order to use the complete dynamic range of the DACs, the peak-to-peak values of input I- and Q-signals from WCDMA source are kept constant and the PA input power is adjusted by SMIQ which is used as a VGA. Fig. 6.24 shows the measured adjacent and alternate channel power ratios (ACPR I and II) with and without DP. There is a significant linearity improvement in ACPR I but no improvement in ACPR II. The amplifier gives about 2 dB more linear output power if DP is implemented. If we assume ACPR of -40 dBc for the first and -50 dBc for the second channel as the linearity condition with 7 dB margin, then DP is not required below 24.5 dBm output power as it can be seen from fig. 6.24. It is therefore suggested to use DP only if higher linear output powers are required. For a WCDMA handset the probability of transmitting the highest output powers is low (in the order of 1-2%). This means the DSP will be used for MDP infrequently and hence the average power consumption is low. The additional power consumption in digital circuitry during DP has been estimated to be less than 100 mW. By implementing MDP this additional power is consumed in digital circuitry but on the other hand a PA delivering 2 dB less linear output power can be used which is more efficient. Moreover if the size of a PA output stage is reduced, then its cost is reduced significantly. Fig. 6.25 (a) shows the estimated efficiency enhancement with a linearized PA. Solid lines are the measured output power and efficiency curves of the amplifier which delivers 26.5 dBm output power fulfilling the linearity conditions (-40 dBc for ACPR I and -50 dBc ACPR II) with DP. The dashed lines are the output power and efficiency curves of an estimated amplifier delivering 26.5 dBm output power fulfilling the linearity condition without DP. Thus the amplifiers with and without DP are assumed to show similar power and linearity performance for the specified linearity condition. Comparison shows that there is an efficiency improvement from 32% to 39% at maximum linear output power of 26,5 dBm and from 2.4% to 3% at 10 dBm if the DP is used. The improvement at 26.5 dBm results in a power saving

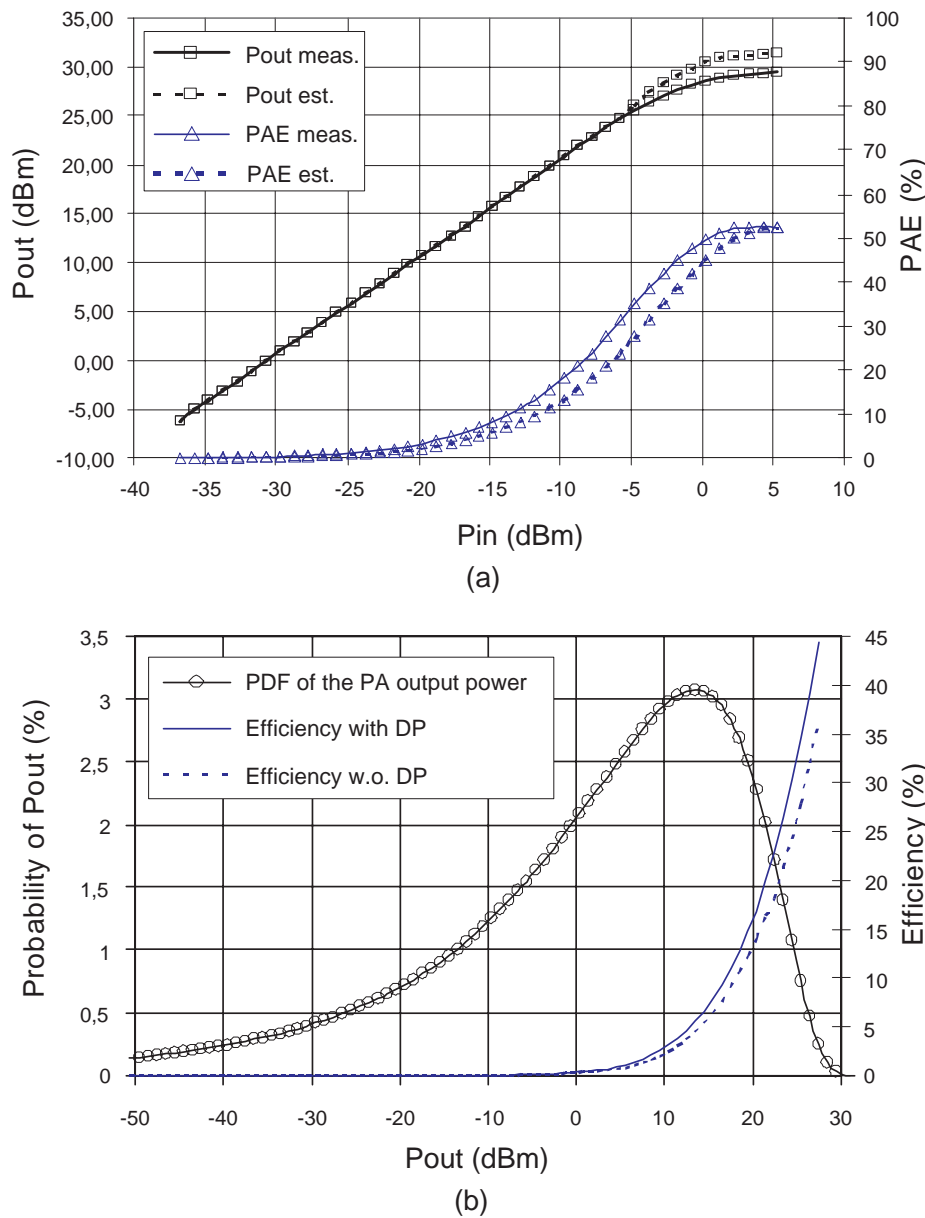


Figure 6.25: (a) Measured output power and efficiency vs. input power curves of RF2162 and the curves of an estimated PA having same performance without DP, and (b) estimated probability of output power occurrence in UMTS terminals and PA efficiency with and without MDP vs. output power curves.

of 250 mW, which compensates more than the power consumption of the processor. Due to the smaller power stage usable in combination with the DP considerably higher efficiencies can be obtained over typically used lower output power ranges. This is a very useful improvement for WCDMA systems having high output power dynamic range. For example in UMTS terminals output powers from -50 dBm to 24 dBm (power class 3 [23]) are required which depend on the position of the user with respect to the base station, the number of users in the channel etc. The maximum output power can

	With DP	Without DP
Efficiency at 26.5 dBm P_{out}	39%	32%
Efficiency at 10 dBm P_{out}	3%	2.4%
Average efficiency	7.6%	6.23%

Table 6.2: Comparison of PA efficiency with and without DP in WCDMA which delivers the same maximum linear output power.

increase up to 33 dBm depending on the power class. An estimated probability function of UMTS terminal output power is given in fig. 6.25 (b). According to this figure the output power having maximum occurrence probability is about 12 dBm which is 12 dB lower than the maximum output power. Therefore it is very important to improve the efficiency not only for high output powers but also for the average output power. Fig. 6.25 (b) shows also estimated improvement in the efficiency at different output powers with DP. The average efficiency regarding the output power probability function with and without DP has been calculated and an increase from 6.23% to 7.6% has been observed which means an improvement of more than 20%. Achievable efficiency improvement with DP is also given in tab. 6.2.

In a mobile communication terminal, PA supply voltage drops occur with discharging battery. In order to see the effects of such drops the performance of MDP has also been measured by changing the DC supply voltage by +/-100 mV from the nominal value. Measured ACPR I and II are close to the values in nominal case with a maximum degradation of 2 dB. During measurements possible performance degradations due to nonlinearities in the modulator and preamplifier have not been considered because instead of them a signal generator has been used for modulation and pre-amplification. Some simulations have been done in order to investigate the effects of these components on the predistortion. First a behavioral saturation model for these stages has been developed using measurement data of a UMTS direct conversion transceiver from Infineon Technologies. This model has been used for a system simulation with an input signal composed of the control and a data channel (DPCCH+DPDCH) having a peak to average ratio of 3.7 dB. It has been observed that the maximum ACPR degradation due to the nonlinearities in the modulator and the preamplifier at the PA output are 0.3 dB for the first adjacent and 0.9 dB for the alternate channels. This is an acceptable degradation meaning that this transceiver can be used in a MDP system without any change in its specifications.

6.4 MDP for PAs with DC-DC converters

The investigations for EDGE and WCDMA systems show that MDP can be used as an efficiency improvement method in terminals. It is also possible to implement MDP together with a DC-DC converter to achieve higher efficiencies [44]. In order to see possible PA efficiency improvement with combination of DP and DC-DC converters, some simulations and measurements have been done. The PA used for measurements is an Infineon SiGe Wireless LAN PA operated at 1950 MHz with a WCDMA input.

No DC-DC converter has been used, instead, the value of supply voltage has been adjusted manually in order to measure ACPR and efficiency values at different supply voltages. The setup used is as in fig. 6.10 with a 3.84 MHz chip rate UMTS input signal composed of the DPCCH and a DPDCH. The aim is to compare efficiencies of the PA alone, PA with DC-DC converter and PA with DC-DC converter and DP. Fig. 6.26 shows measured efficiency results for these three cases.

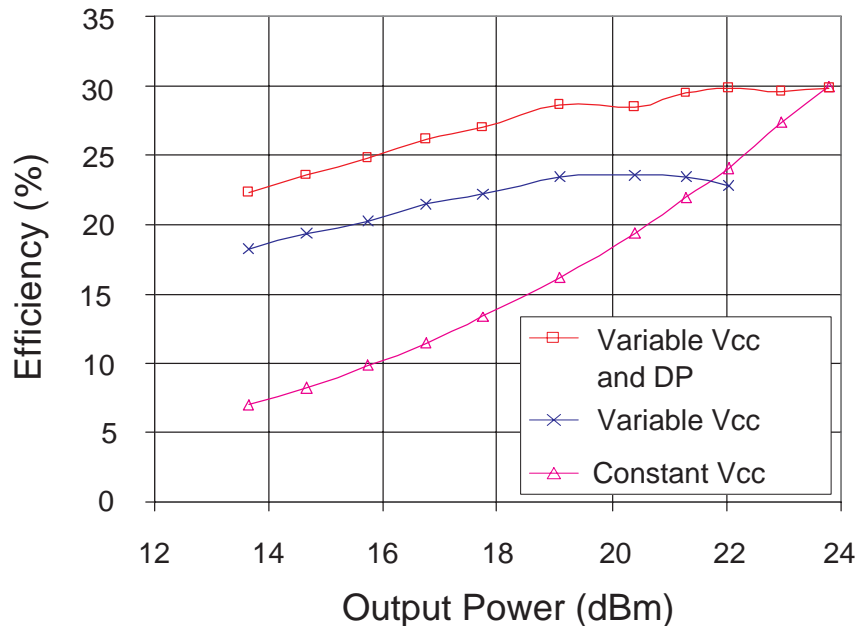


Figure 6.26: Measured efficiency vs. output power curves with constant supply voltage, with variable supply voltage and estimated efficiency with combination of DP and variable supply voltage.

ACPR performance and efficiency of the PA without predistortion has been measured initially with a constant supply voltage of 3.5 Volt. Then the supply voltage has been adjusted to verify its effects on efficiency. This has been done in the following way: supply voltage has been decreased in order to increase efficiency and get the same output powers as measured before. The same output powers have been obtained also with lower supply voltages, although there was a degradation in ACPR performance. If ACPR I of -40 dBc is assumed to be enough to fulfill UMTS specifications, then supply voltage can be decreased until this limit value is reached, then efficiency at this point can be measured. These test results show a significant improvement in the efficiency as shown in fig. 6.26. The next step is to show possible efficiency improvement with variable supply voltage and DP. It has been observed that it is possible to suppress ACPR I by more than 10 dB at high PA outputs by means of DP. If we assume that this is also possible for other supply voltage values, then we can measure approximately how much efficiency can be gained with both linearization and variable biasing. This time the supply voltage has been reduced until ACPR I of -30 dBc (10 dB worse than the case without predistortion) has been reached and the efficiency has been measured. These results are also presented in fig. 6.26. It is clearly visible that DP can improve the

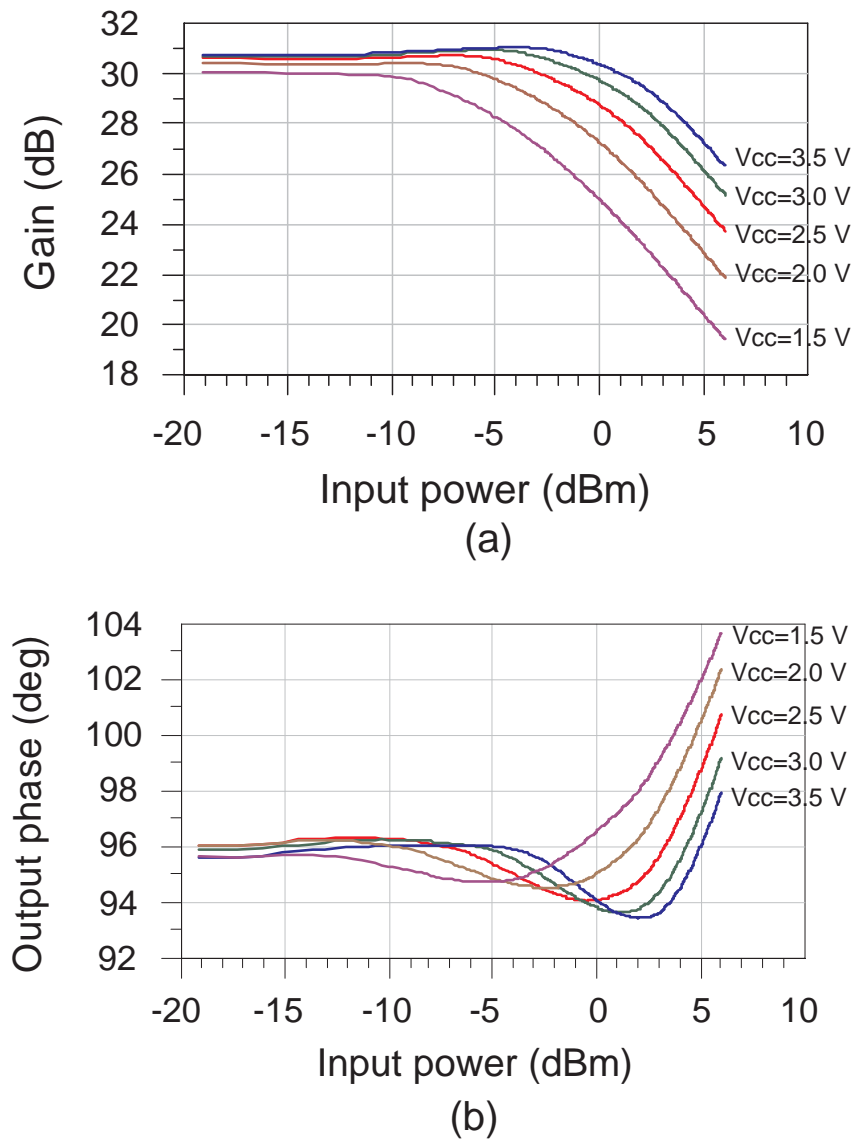


Figure 6.27: Measured (a) gain and (b) phase characteristics of RF2162 for V_{cc} of 1.5, 2.0, 2.5, 3.0 and 3.5 V.

system efficiency significantly if it is implemented together with a DC-DC converter. However, there is one point to be considered in order to have a good linearization performance. In such an application LUT coefficients may be different for different supply voltage values because the PA characteristics can change significantly with changing supply voltage (V_{cc}). For example fig. 6.27 (a) and (b) show the measured gain and phase characteristics variations of RF2162 for V_{cc} of 1.5, 2.0, 2.5, 3.0 and 3.5 V. There is no big change in small signal gain and phase shift when changing the supply voltage. However, for higher output powers there are significant changes in both gain and phase characteristics. This means the LUT coefficients calculated for a V_{cc} value may not match this PA well if V_{cc} is changed as in the case of DC-DC converters.

In order to see the effects of varying V_{cc} on linearization, the following test has been

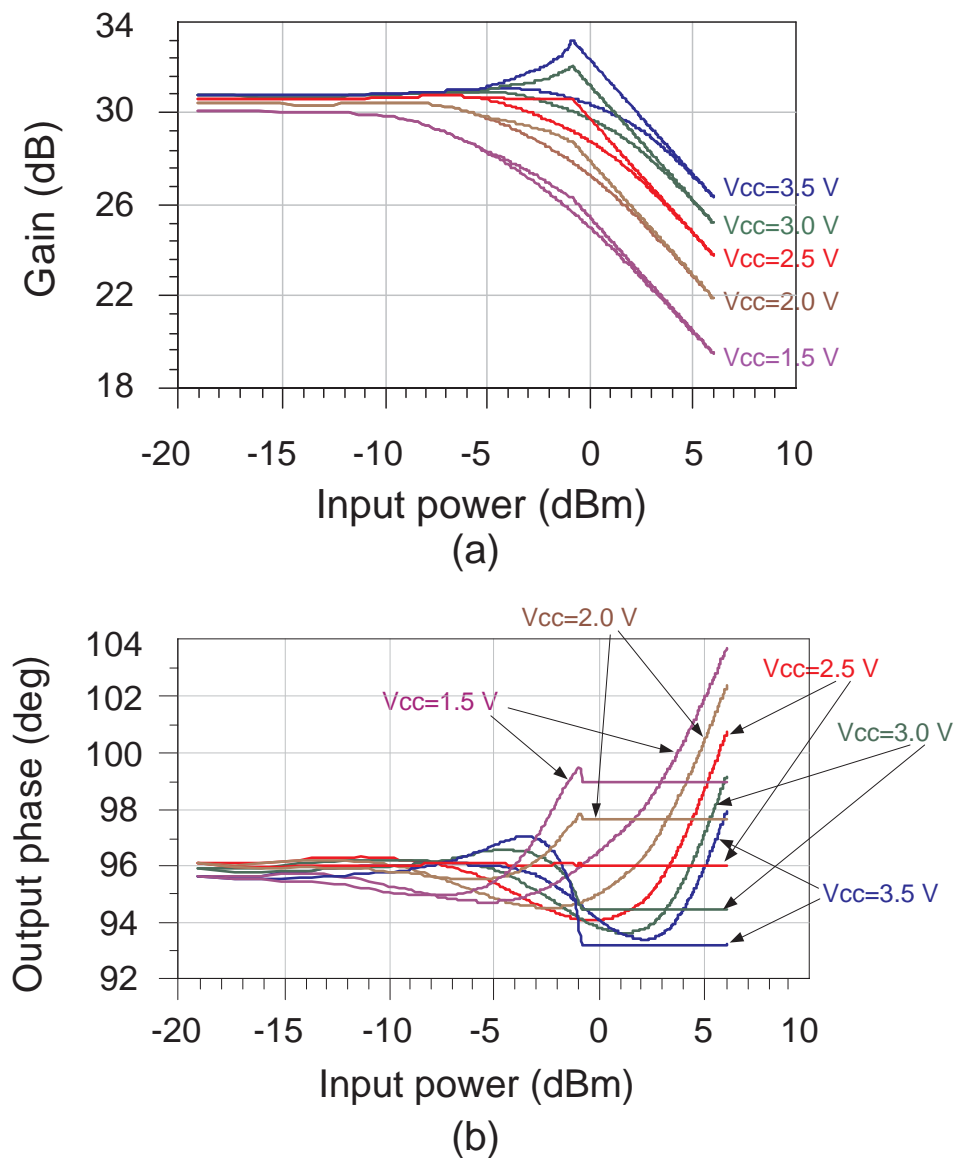


Figure 6.28: RF2162 (a) gain and (b) phase characteristics for V_{cc} of 1.5, 2.0, 2.5, 3.0 and 3.5 V before and after linearization using LUT coefficients calculated for V_{cc} of 2.5 V.

done. The complex LUT coefficients of RF2162 for V_{cc} of 2.5 V have been calculated and these coefficients have been used to linearize the PA with five different V_{cc} values (1.5, 2.0, 2.5, 3.0 and 3.5 V). Fig. 6.28 (a) and (b) show the gain and phase characteristics with and without DP. As it is expected these coefficients match the PA perfectly when V_{cc} is 2.5 V, which can be seen from the red colored constant gain and phase characteristics in fig. 6.28 (a) and (b). However, if V_{cc} is changed, then there is a degradation in linearity proportional to the change in V_{cc} . For example if V_{cc} is increased to 3.0 or 3.5 V, then a significant expansion and if it is decreased to 2.0 or 1.5 V, then a compression in the gain close to saturation is observed with linearization. There is also deviation in the phase characteristics of the linearized PA output near to

compression if V_{cc} is changed. This problem can be solved by using different LUTs for each discrete supply voltage value.

6.5 Symbol addressing

MDP requires some additional digital circuitry capable of fast real time signal processing. The required clock frequency depends on bandwidth of the modulation signal, oversampling ratio (OSR) and complexity of predistorter. If DP is going to be implemented in handsets, it must be simple and low power consuming. In the following a new addressing method called symbol addressing is proposed for LUT based digital predistorters applicable to transmitters with quadrature modulation, which makes addressing very fast and reduces power consumption in digital circuitry.

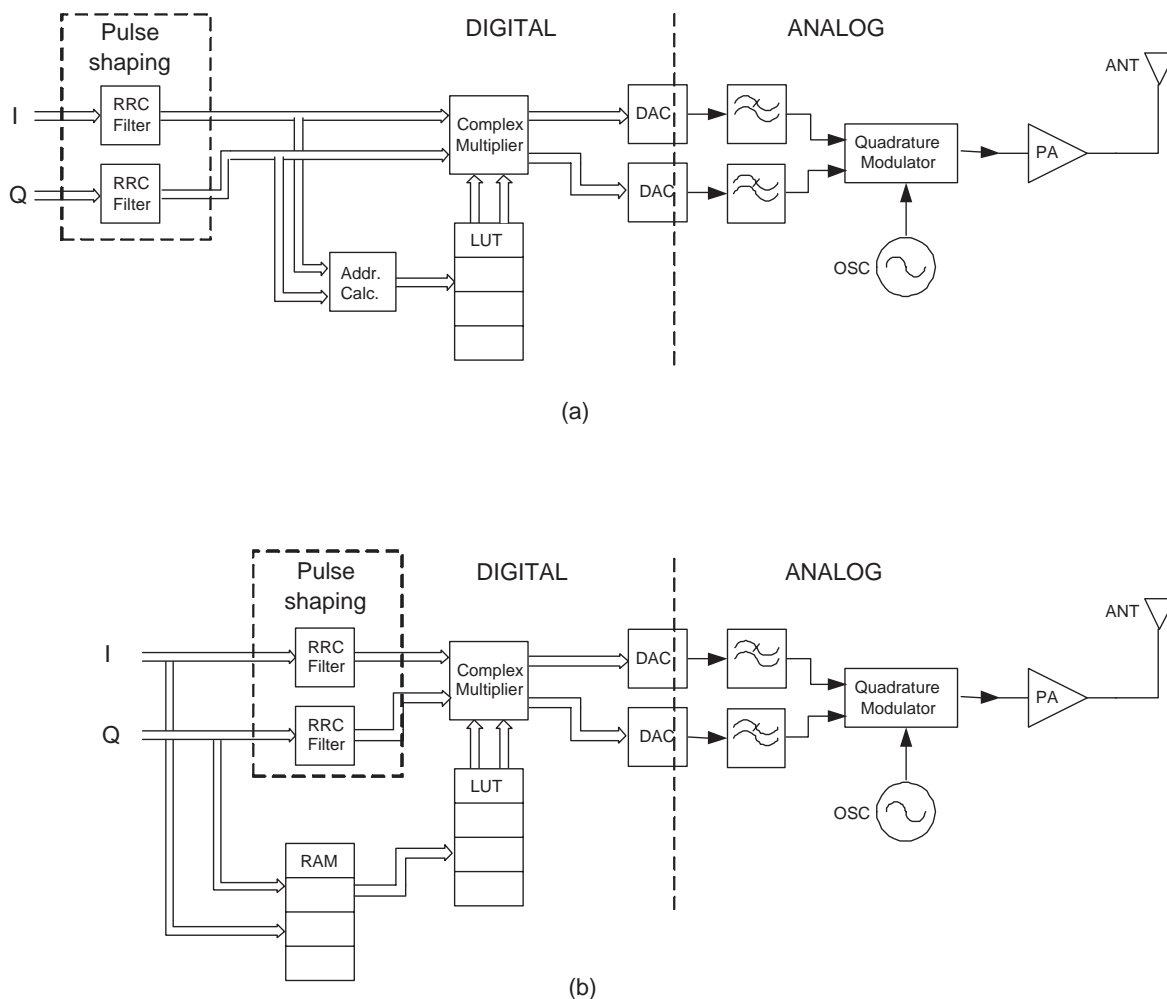


Figure 6.29: Block diagrams of (a) conventional MDP and (b) MDP with symbol addressing.

Fig. 6.29 (a) shows the conventional model for the forward path of LUT based DP. The forward path is critical due to requirement of high speed real time processing.

The required operations in forward path are LUT address calculation and complex multiplication of baseband signal samples with corresponding LUT coefficients for each sample after pulse shaping. The measurements and simulations have been done using WCDMA signals. Therefore RRC (Root Raised Cosine) filters have been used for pulse shaping.

Complex multiplication of baseband signals in Cartesian format seems to be inevitable if both AM/AM and AM/PM distortions are going to be compensated. The calculation of LUT address on the other hand can be done in different ways. In conventional DP magnitude and power addressing are the most commonly used two simple methods. However, both of them require mathematical operations. Andreani [62] shows an example how to calculate the maximum allowed bandwidth of modulation signal to be predistorted for a given clock frequency. It depends on OSR and the required amount of operations in the predistorter for each sample. If the amount of operations for each sample can be reduced during predistortion, then DP can be implemented with lower clock frequencies or signals with higher modulation bandwidth can be predistorted in real time. This means a significant power efficiency improvement in digital circuitry and implementation with lower clock frequencies, which makes it more simple. Symbol addressing reduces the amount of mathematical operations required for each sample significantly. It is done by using raw digital I and Q data (will be called symbols) before pulse shaping as shown in fig. 6.29 (b).

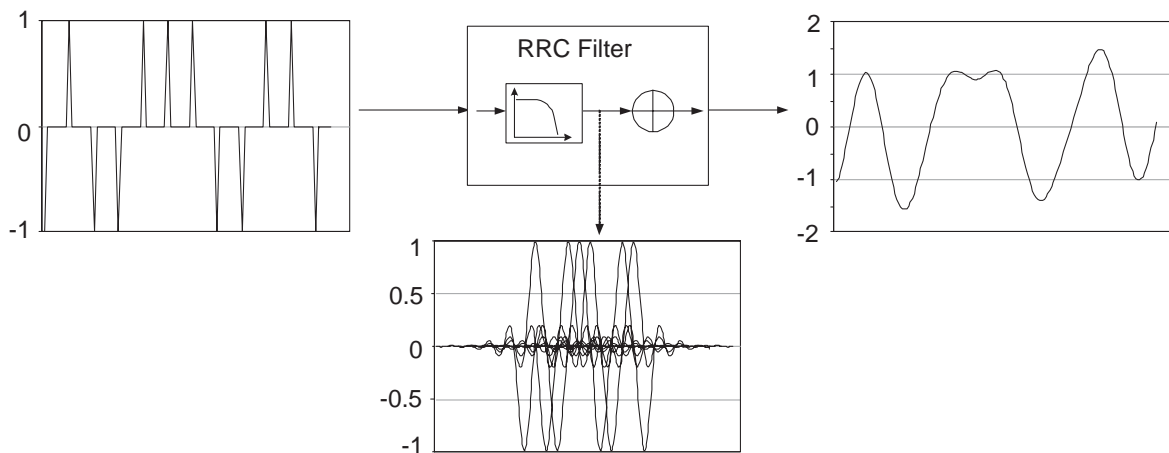


Figure 6.30: Pulse shaping with root raised cosine filter.

In mobile communications baseband signals are pulse shaped in order to minimize bandwidth of the modulation signal and reduce power leakage into adjacent channels. These are low-pass filters and are mostly implemented in the digital domain. These filters have raw digital data symbol streams as input and they generate the corresponding discrete baseband signal samples (one symbol contains a number of samples equal to OSR) ready for digital-to-analog conversion. Shape of the filter output signal depends on the filter length and filter coefficients as shown in fig. 6.30. Impulse responses of the input symbols are generated and summed up in order to get the resultant output. If the input symbol stream and filter characteristics are known, then it is possible to

calculate the value of each sample at the filter output. The idea in symbol addressing is to calculate the magnitude of each complex filter output sample using parallel I- and Q-signal samples and store them in a LUT which can be addressed by the filter input data symbol sequence easily. This means we store all possible amplitudes of the input signal, which in turn will be used as address of the LUT containing complex predistortion coefficients. The LUT containing input signal magnitude will be called RAM (Random Access Memory) in order to avoid confusion with the LUT containing complex predistortion coefficients. The question is how big must be the size of the RAM for a good performance. The number of positions in the RAM is equal to the number of possible amplitude values, which depends on the number of consecutive data symbols used for RAM addressing, OSR, the number of the points in the constellation diagram and their symmetry. The formula derived for RAM size calculation is

$$M = (r/2)(n_I^x/2)(n_Q^x/2 + 1), \quad n_I = n_Q \quad (6.5)$$

$$M = r(n_I^x/2)(n_Q^x/2), \quad n_I \neq n_Q \quad (6.6)$$

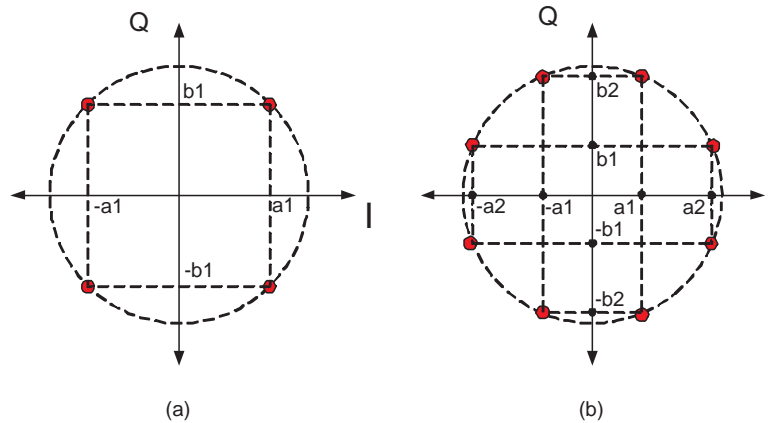


Figure 6.31: Constellation diagrams of (a) QPSK and (b) 8-PSK.

where M is the RAM size, n_I and n_Q are the number of different values possible for I and Q symbols in the constellation, x is the number of symbols in each branch used for RAM addressing and r is the OSR. In fig. 6.31 (a) and (b) constellation diagrams for QPSK and 8-PSK are shown respectively as an example in order to clarify the determination of n_I and n_Q . In QPSK case both are equal to two because they can take discrete values $-a_1, a_1$ and $-b_1, b_1$ respectively. Then eqn. 6.5 can be used to calculate the required RAM size. However, 8-PSK constellation is a little bit different. Actually each of n_I and n_Q can have four different values ($-a_2, -a_1, a_1, a_2$ and $-b_2, -b_1, b_1, b_2$ respectively). However, there are some points which are not allowed to appear in the constellation like $(-a_2, b_2)$, $(-a_1, b_1)$ etc as shown in fig. 6.31. Fortunately, this feature reduces the system complexity and RAM size of symbol addressing in 8-PSK. If n_I is assumed to take four different values, then n_Q can take only two because the

	With magnitude addressing	With symbol addressing
Maximum linear P_{out}	26.5 dBm	26.5 dBm
Improvement in ACPR I	12 dB	8 dB
Improvement in ACPR II	3 dB	3 dB

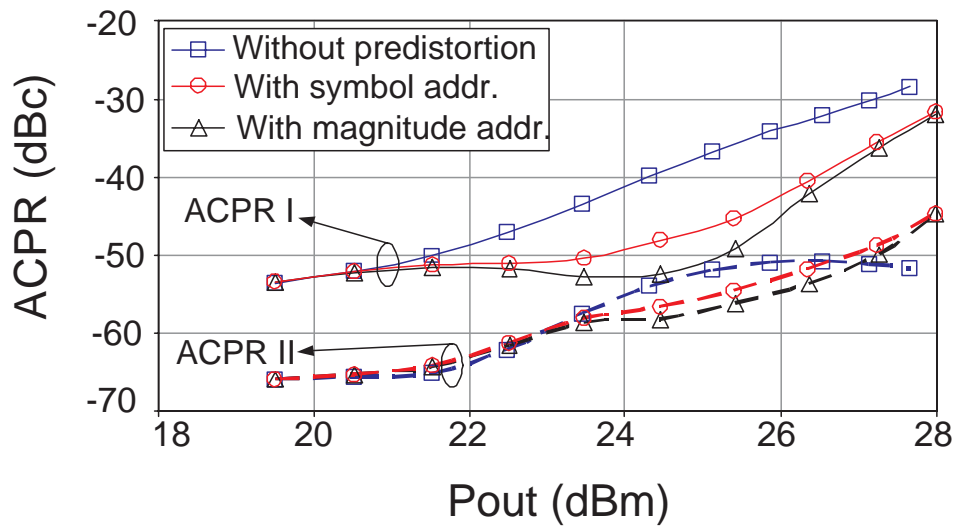
Table 6.3: Measured performance with magnitude and symbol addressing for a QPSK signal.

others are not allowed and vice versa. As a result n_I is not equal to n_Q and eqn. 6.6 can be used to calculate the required RAM size.

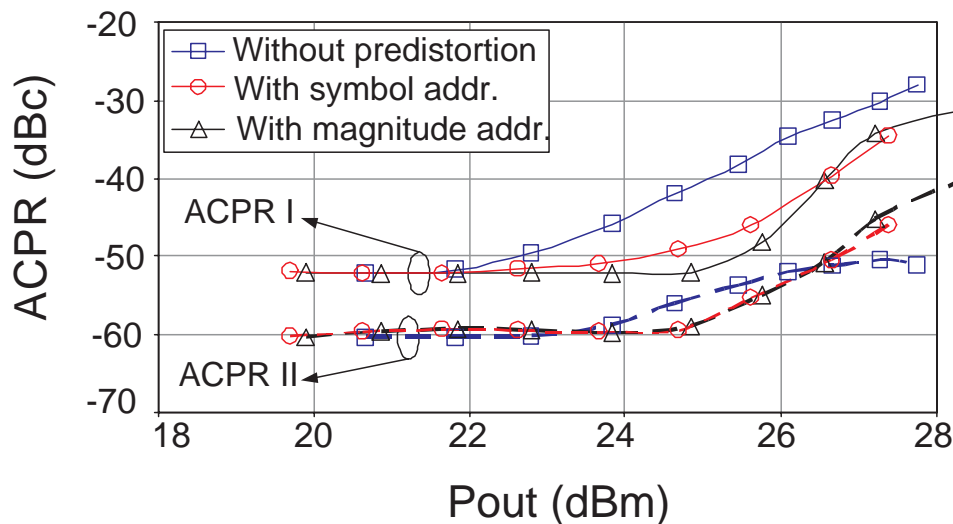
A QPSK signal having four points in its constellation diagram has been simulated and measured. In this particular case equation eqn. 6.5 has been used to calculate the RAM size which is about 4k words. The used filter is a symmetrical RRC filter with a roll-off factor of 0.22 and the length of 16. The OSR is 8 and for RAM addressing 6 consecutive data symbols in I and Q branches have been used. Simulations done with 4 and 6 consecutive data symbols showed that 6 symbols are optimal for low RAM size and good performance. Contents of the RAM are calculated and stored once and there is no need for update. If sample interpolation is used as it is the case in modern communication systems, then OSR can be reduced, which leads to reduction of RAM size. For example if OSR is halved, then the RAM size will also be halved, which can be easily seen from eqn. 6.5. In the QPSK case increasing the number of consecutive addressing symbols x by 2 would result in a RAM which is 16 times greater but the performance would be improved only slightly. RAM size increases very rapidly also with increasing the number of points in constellation diagram. For example if an eight (QPSK or 8-PSK) and sixteen (16-QAM) points constellations are used instead of four point QPSK, then the RAM sizes would be 512k and 16M words according to eqns. 6.6 and eqn. 6.5 respectively. Therefore a good optimization of system constellation, OSR and number of addressing symbols are necessary in order to achieve a good performance with a small RAM.

Symbol addressing can be very useful especially for wideband systems with relatively simple modulation formats like QPSK and 8-PSK. LUT addressing is very fast, because it must be done just one time in one symbol duration and is basically just reading the position in RAM without any calculations. In conventional magnitude addressing the address is calculated for each sample [62], which means 8 times in one symbol duration for this particular case, and the mathematical operations of two times squaring, one adding and one square root calculation are required for each I and Q sample pairs. Taking the square root can be done faster with some table based implementations [70] but the computational burden in the magnitude addressing is still too high compared to the proposed symbol addressing, where no calculations are required. As a result a wideband system can be predistorted with significantly low system clock frequency compared to conventional predistortion systems. However, since the characteristics of pulse shaping filters and data constellation must be known to be able to address the LUT, symbol addressing works for a particular modulation format. For multi-standard, multi-mode systems different RAMs are required for each mode.

Fig. 6.32 (a) and (b) compare ACPR simulation and measurement results obtained for



(a)



(b)

Figure 6.32: ACPR (a) simulation and (b) measurement results obtained with QPSK modulated signal for three cases: without predistortion, predistortion with symbol addressing and predistortion with magnitude addressing.

a gain based predistorter with magnitude and symbol addressing. Modulation signal is a pseudo random WCDMA signal with PAR of 5.25 dB. It is QPSK modulated having four constellation points. The used RRC filter has a roll-off factor of 0.22 and length of 16 and the PA used is RF2162. The results obtained in simulations and measurements are close to each other. The improvement in ACPR I and II after linearization are for magnitude addressing about 12 dB and 3 dB, and for symbol addressing about 8 dB and 3 dB respectively. In respect to ACPR I performance symbol addressing

is 4 dB worse compared to the magnitude addressing. The deviation is due to the error in the calculated approximate magnitude values stored in the RAM. ACPR II obtained in the measurements for output powers lower than 23 dBm is not as good as in the simulations. The reason is the noise contribution of the used spectrum analyzer. The performance of the symbol addressing is good especially if it is implemented for efficiency improvement in handsets. As we mentioned earlier, DP is going to be used just if otherwise the specifications are not fulfilled. If -40 and -50 dBc are assumed to be the limits for ACPR I and II, at which points DP is activated, then according to measurement results in fig. 6.32 (b), both magnitude and symbol addressing will let DP be activated almost at the same time. This means improvement in the maximum achievable linear output power with symbol addressing is almost same as magnitude addressing which is about 26.5 dBm. Tab. 6.3 gives a comparison of performances with magnitude and symbol addressing.

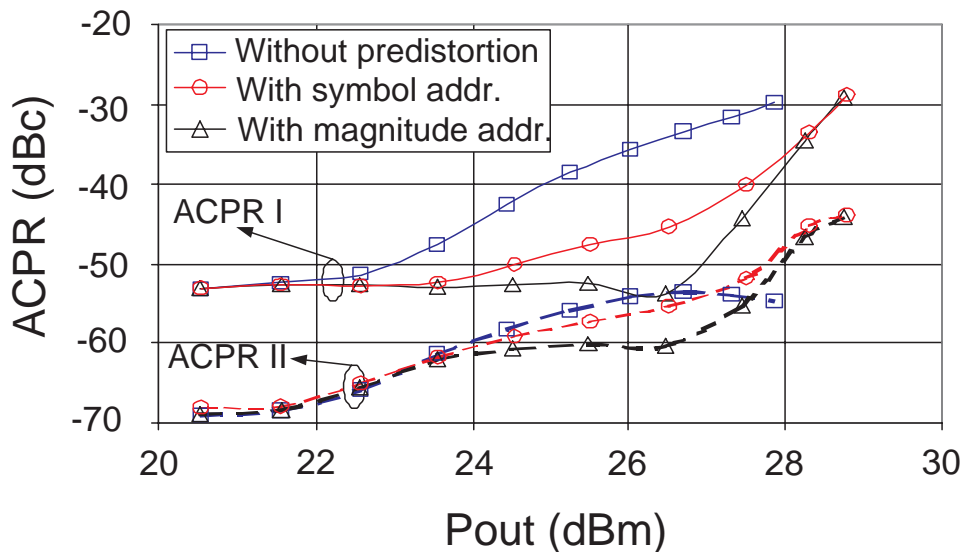


Figure 6.33: ACPR simulation results obtained with eight point QPSK signal for three cases: without predistortion, predistortion with symbol addressing and predistortion with magnitude addressing.

Simulations have been done also for eight point QPSK. Fig. 6.33 shows the simulation results obtained again for a gain based predistorter with magnitude addressing and symbol addressing in order to compare them. Since the simulation and measurement results for four point QPSK (fig. 6.32 (a) and (b)) are close to each other, the simulation results obtained for eight point QPSK are assumed to be reliable. The modulation signal PAR is 3.4 dB. The same RRC filter with the roll-off factor of 0.22 and length of 16 has been used to linearize RF2162. The improvement in ACPR I and II after linearization are for magnitude addressing about 20 dB and 6 dB, and for symbol addressing about 11 dB and 2 dB respectively. ACPR I performance of symbol addressing is 9 dB worse compared to the magnitude addressing. However, the maximum achievable linear output power with symbol addressing (27.5 dBm) is close to the magnitude addressing case (27.75 dBm), which means symbol addressing is a viable method also for eight

point QPSK and 8-PSK modulation. Compared to four point QPSK the achievable linear output power with the same PA has been observed to be higher in eight point QPSK because the PAR of the test signal is lower.

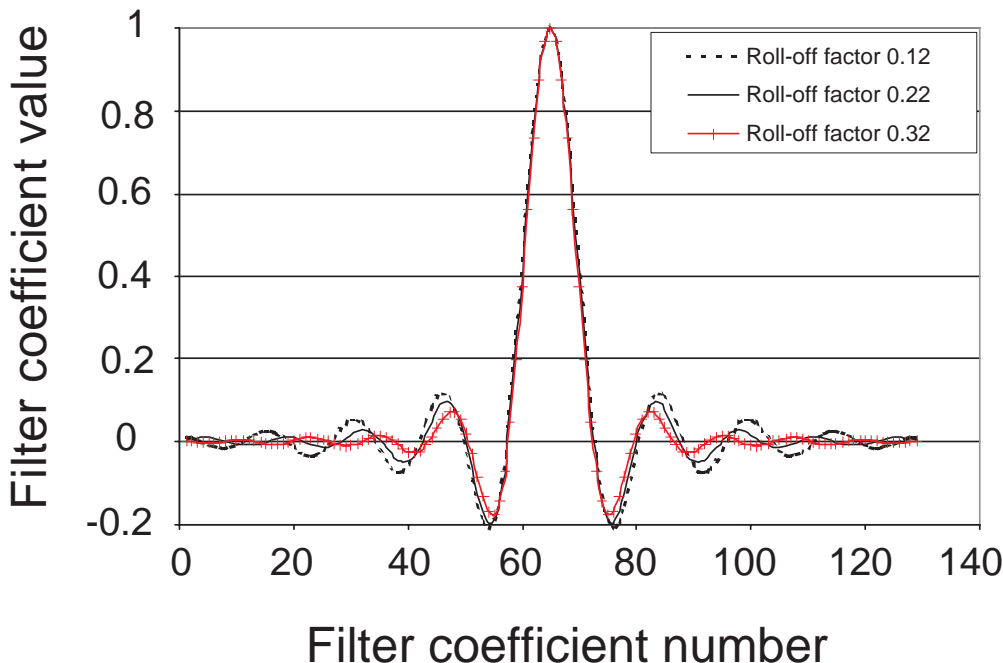


Figure 6.34: Normalized RRC filter coefficients with different roll-off factors.

In simulations and measurements 6 consecutive I- and Q-symbols have been used for RAM addressing in order to keep RAM size small. Values of I- and Q-signal samples at the RRC filter outputs depend on 16 consecutive symbols due to the length of the filter, but only 6 symbols having the maximum effect on sample magnitudes have been used to calculate approximate magnitudes stored in the RAM. This means the calculated magnitudes stored in the RAM have an error. This error depends also on the roll-off factor of the used RRC filters because the weight of filter coefficients falling in the range of the used 6 consecutive symbols can change with it. In fig. 6.34 normalized symmetrical RRC filter coefficients for three different roll-off factors (0.12, 0.22 and 0.32) are shown. Filters with high roll-off factors are desirable for symbol addressing because the weight of filter coefficients in the far side lobes, which are not considered during the calculation of magnitudes in the RAM, are decreased with increasing roll-off factor. If the roll-off factor of the RRC filters is decreased, then the quantization error in magnitude calculation will increase and more degradation is expected in the ACPR performance with symbol addressing.

6.6 MDP implemented as open- and closed-loop

In a MDP system LUT coefficients can match PA characteristics very well if a proper PA measurement has been done. However, it is not sure that the PA behaviour will

stay as it was during the measurement. There may be some deviations in AM/AM and AM/PM characteristics of the PA and then LUT coefficients will not be able to correct the distortion completely. If DP is implemented, then LUT coefficients must match the PA well and the system must have a good performance under various conditions like sample variations, aging, changing temperature or supply voltage value. There are mainly two possible implementations: open-loop, where critical forward path is implemented, and closed-loop that has also an additional feedback path for adaptation. In the following these two methods are investigated in terms of their applicability to terminals.

6.6.1 Open-loop

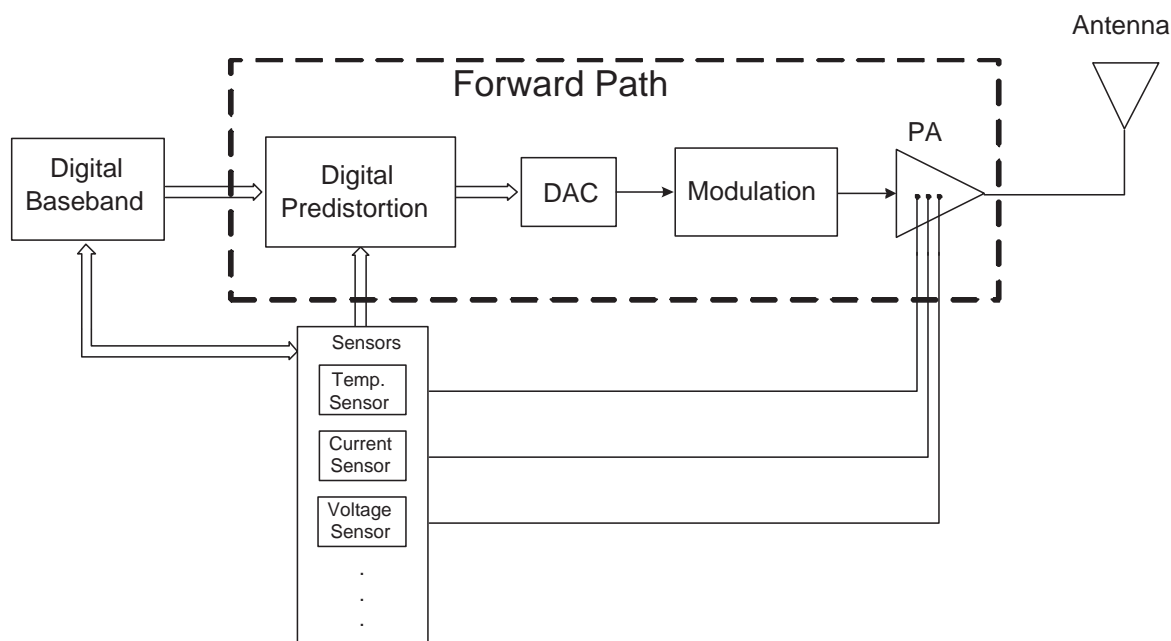


Figure 6.35: Block diagram of open-loop digital predistortion.

The reason for open-loop MDP implementation is to have a simple system requiring minimum additional components. It can be realized with additional hardware capable of logic and simple mathematical operations like additions and multiplications. Such a system does not necessarily require significant support from system DSP, which means also no additional computational burden for the processor. However, a closed-loop implementation requires a processor capable of complicated mathematical operations as well as an additional feedback path. Therefore either system processor must support the predistorter during the adaptation, which means additional computational burden, or an additional ASIC is required meaning increased system complexity, size and cost. Therefore if a reliable operation and high yield in production can be achieved with an open-loop implementation, then it is the best candidate for terminal applications. Predistorters in base station applications, however, use in general additional ASICs in

order to have a proper operation with PAs exhibiting high memory effects and achieve a high degree of linearization.

In the open-loop case a possible way is to calibrate each system by measuring its AM/AM and AM/PM characteristics individually, which is highly complicated. However, if the PA characteristics are reproducible having low deviations with process or assembly variations, then there is a good chance that simple calibration procedures similar to those already used today may be sufficient. Effects of temperature and supply voltage and current variations can be taken into account by implementing additional or using available sensors in the system. Simplified block diagram of such a system is shown in fig. 6.35. The forward path is as given in fig. 5.9 and instead of a feedback path, sensors measuring temperature, supply voltage, current etc are used in order to adjust the predistorter such that best performance is obtained under various operating conditions. On the one hand additional feedback path composed of analog and digital components is avoided but on the other hand large LUTs may be required because the system will contain multiple small LUTs with complex coefficients each matching PA characteristics under different environmental and operating conditions. Also simple interpolation functions may be used in order to increase system performance by generating new LUTs from the available ones which match the PA better.

6.6.2 Closed-loop

Closed-loop MDP is attractive due to its reliable operation. Effects of all operating condition variations are corrected automatically, requiring no special calibration process during fabrication. The drawback is the requirement of an additional feedback path and signal processing increasing the system complexity, size and cost as stated before. However, in some systems it is possible to reduce closed-loop implementation complexity by using some components which are already available in the system. For example TDMA systems like EDGE seem to be suitable for such an implementation because transmission and reception do not take place simultaneously and the receiver path can be used as a feedback path for adaptation of predistorter during transmission. Moreover in future multi-mode systems probably more than one receiver path will be used. Then it may be possible to use one of the receiver paths as a feedback path for a short time without disturbing system operation. Then low complexity closed-loop implementation will also be possible for systems like WCDMA with simultaneous transmission and reception.

In fig. 6.36 adaptive DP is implemented in a mobile communications terminal using an additional feedback path. Predistorted I- and Q-signals are sent through the transmitter path where analog conversion, modulation, upconversion and amplification take place. The PA output signal is sent to the block called antenna connection unit, which can be a duplexer or a simple antenna switch, and then to the antenna. During receiver operation, however, the modulated signal comes from the antenna, is bandpass filtered, amplified using an LNA (Low Noise Amplifier), demodulated and converted to digital for further evaluation. The additional feedback path, however, takes the signal from PA output via a directional coupler. This signal is demodulated and resultant I- and Q-signals converted to digital. Input I- and Q-signals are compared with feedback

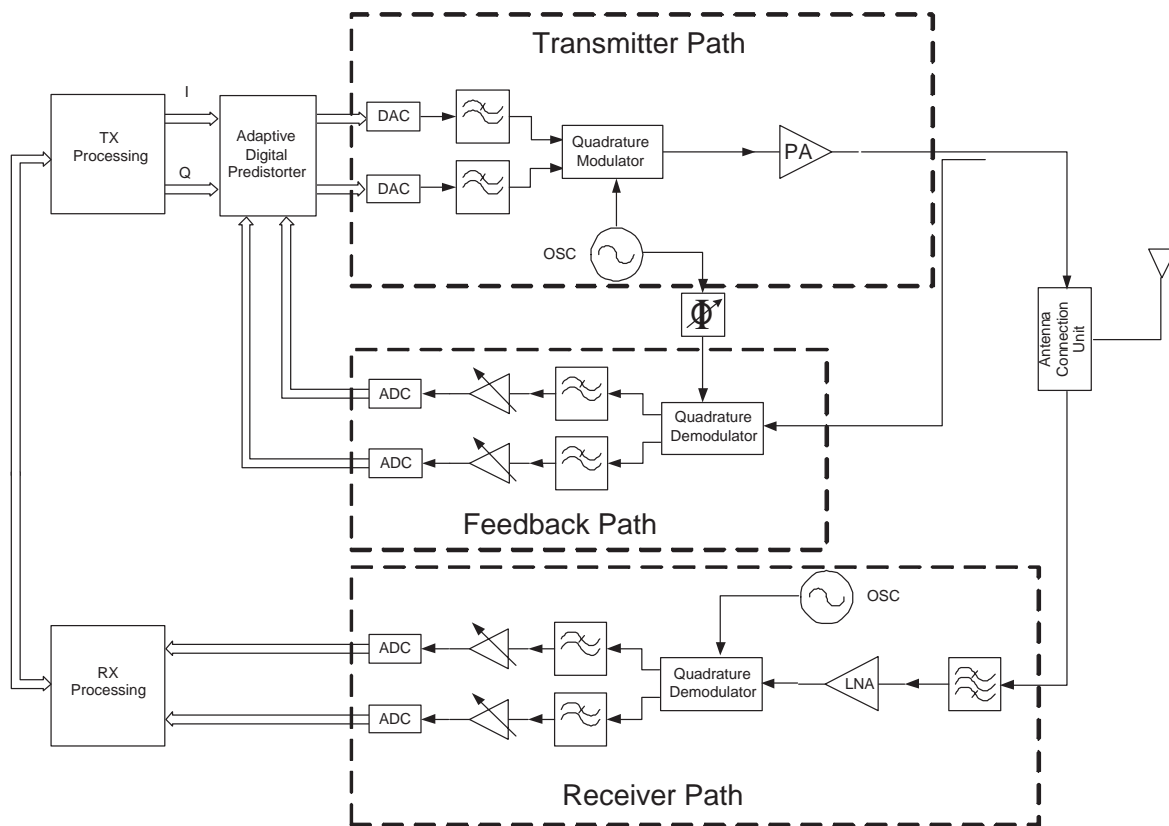


Figure 6.36: Block diagram of closed-loop digital predistortion system implemented in terminals with additional feedback path.

signals point by point and LUT coefficient corresponding to each point is updated accordingly. Adaptation will be done mainly when the PA has a high output power because then the compression characteristics of the PA can be obtained. Therefore it is very important that the feedback path is highly linear avoiding additional distortion due to saturation of the components. For example the system shown in fig. 6.36 should have a highly linear demodulator. Another important point to be considered in designing the feedback path is the bandwidth of the filters after the demodulator. In adaptive DP systems PA output is used as a control signal for adaptation. Since the signal at the PA output can be highly distorted having distortion power in its neighbor channels, the bandwidth of these filters must be wide enough during feedback operation in order to avoid disturbing the control signal. If an additional feedback path is implemented in addition to the receiver path as in fig. 6.36, then additional pinning between the digital baseband chip and the analog transceiver chip will be required. However, if there is a digital interface between digital baseband and analog transceiver, then the problem is solved due to flexibility and high speed of digital interface.

In a TDMA system additional demodulator, anti-aliasing filters, baseband amplifiers and ADCs may be avoided by using the available receiver path for adaptation. As a matter of fact interfaces between digital baseband and analog transceiver chips for transmission and reception must be separate or there is a digital interface. Then system

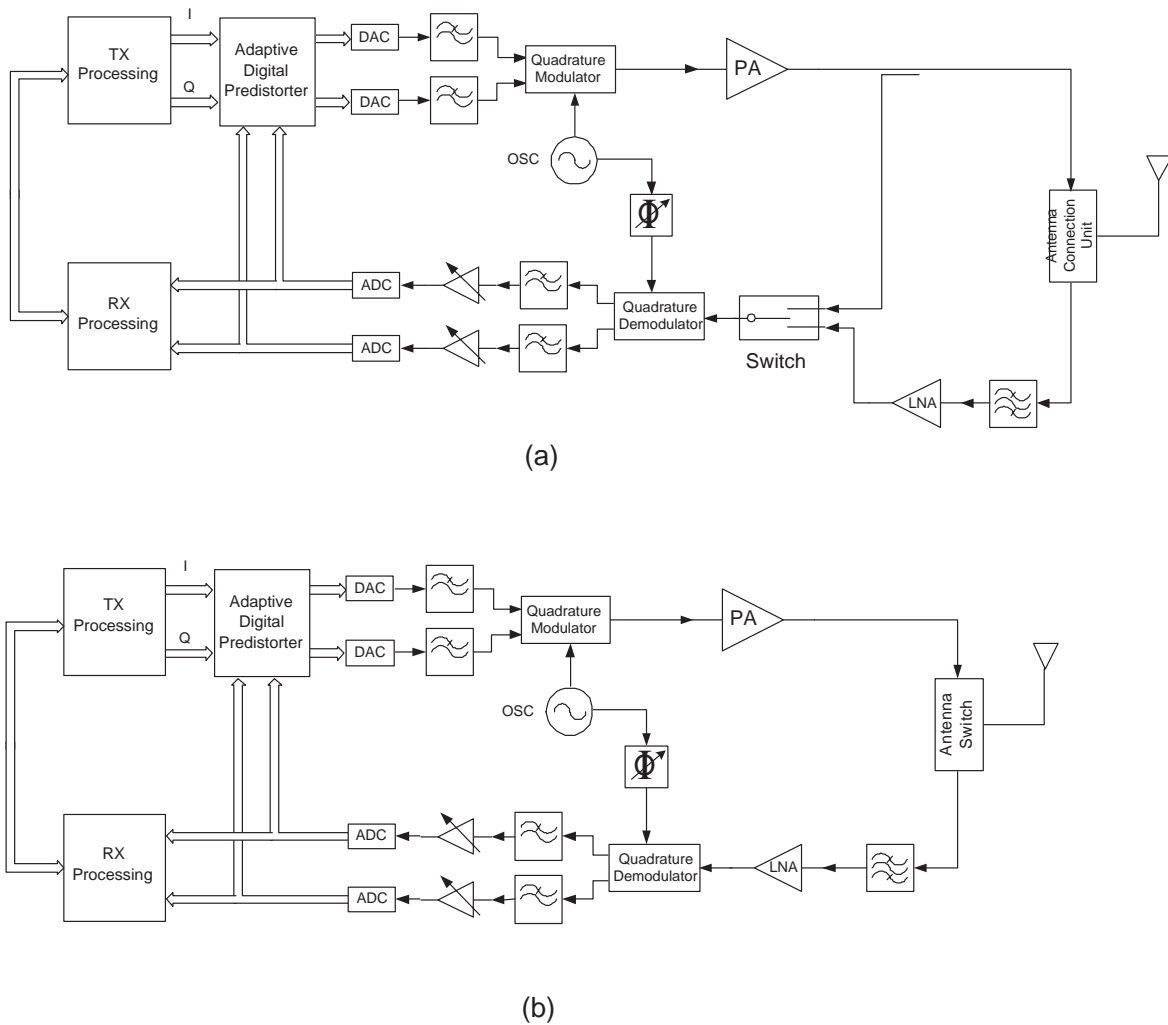


Figure 6.37: Block diagram of closed-loop digital predistortion implemented in a TDMA based system (a) with an additional coupler and a switch unit and (b) without additional components in the feedback path.

block diagram can be as shown in fig. 6.37 (a). An additional coupler at PA output and a switch in front of demodulator will be enough for implementing a feedback path for adaptive DP. The switch will connect the demodulator to the PA output during transmission and to the LNA output during reception. After the demodulator, lowpass filters and baseband processing the output of ADCs will be sent either to the adaptive DP unit or receiver processing unit respectively. The demodulator must have a wide operation bandwidth covering transmit and receive frequency bands and the lowpass filters after it must have wider bandwidth than required for receiver operation in order to avoid additional distortion in feedback path. This can be done by implementing 3-5 times wider band filters parallel to the available ones and switch between them during feedback and receiver operations.

It may be even possible to use the complete receiver path for adaptation without additional components as shown in fig. 6.37 (b). This can be achieved by using transmitter

leakage signal into the receiver path which should be about 20-25 dB lower than the transmitted signal due to the isolation of the antenna switch. There may be also an additional loss of about 15-20 dB at transmit frequency band due to bandpass filter in front of the LNA used in the receiver path. This means during transmission a portion of PA output (35-45 dB) is coupled to the receiver path which is actually an unwanted signal and it is used to update the LUT in predistorter unit as explained previously. Of course the LNA and demodulator should also be able to operate in transmitter frequency band properly and their inputs must be kept low enough in order to operate them in their linear region. One additional advantage of this architecture is that the directional coupler at PA output is not required meaning no additional insertion loss in the transmitter path.

6.7 Application of MDP in polar transmitter concept

New generation mobile communication systems require high linearity and efficiency at the same time. On the other hand complexity and power consumption of products in this area increases rapidly because of the demand for multi-mode operation in order to cover a high number of services and thus be able to serve more subscribers. It is possible to fulfill system specifications with conventional linear PAs but in general the achievable efficiency is low. Moreover the number of components will increase considerably for multi-mode operation. This makes systems more complex, expensive and bulky. A possible solution in transmitters is using PTx explained in chapter 4, which is a method similar to EER and makes multimode operation possible with relatively high efficiency and low number of components. According to our measurement based calculations, a comparison of linear transmitters and PTx revealed that PTx can improve system efficiency by 30-70% using a PA with integrated linear regulator. Achievable improvement with DC-DC converter is about 150%. This improvement is due to the fact that either saturated or switch mode PAs are used in PTx [32, 31, 37]. However, system linearity of PTx needs to be improved. It needs a kind of predistortion in order to linearize the transfer function of the separate amplitude and phase paths. The non-linearity in AM/AM and AM/PM characteristics is high for both low and high output powers whereas conventional linear transmitters exhibit high nonlinearity mainly at high output powers. DP is a promising linearization technique also applicable to PTx due to its flexibility and high degree of performance.

In this part of the work a PA characterization setup and the application of LUT based MDP in PTx for EDGE using a commercially available GSM PA is presented. It has been shown that AM/AM and AM/PM nonlinearities can be compensated significantly fulfilling EDGE requirements.

6.7.1 PA characterization

In order to apply MDP in PTx, PA must be characterized first. Since PA has two input and one output ports in PTx concept, it is no more a two port component but a three

port one. Therefore a new behavioral three port PA model is required for simulations. To overcome this problem three port measurement results have been used to generate an equivalent two port PA model in ADS. It is a simple file based behavioral model, which has been used previously in linearization of linear PAs. The required data for this two port model are input and output powers, and input power dependent gain and phase shifts obtained with three port measurement setup shown in fig. 6.38.

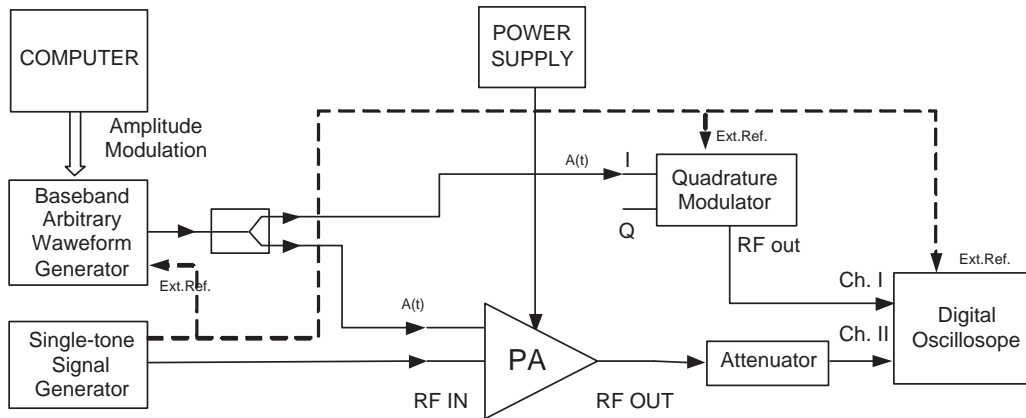


Figure 6.38: PA characterization setup for polar transmitter concept.

The PA used in the setup has an integrated linear regulator with an external control pin. The idea is to apply an AM signal ($A(t)$) to this control pin, modulate PA output and measure the resultant AM/AM and AM/PM nonlinearities at the PA output. PA input is a single carrier signal with relatively high power in order to keep the PA in saturation. A single-tone signal is used because AM/AM and AM/PM nonlinearities do not depend on the value of input signal phase (RF IN) but just on the value of AM signal applied to the linear regulator control pin. A single-tone signal is reasonable to choose because of its constant phase. Any phase fluctuations at PA output are due to AM/PM nonlinearity of the PA. $A(t)$ has been generated and downloaded to a baseband arbitrary waveform generator as shown in fig. 6.38. This signal has been applied to the linear regulator control pin as well as to a modulator in order to create an undistorted signal, which should represent the PA output in case that it is ideally linear. The reason for creating this ideal signal is to have a signal behaving as the PA input as if the PA is a two port component. Signals generated at modulator and PA outputs have been stored simultaneously using a high sampling digital oscilloscope in order to characterize the PA with an instantaneous power measurement technique explained in the power amplifier characterization section of this chapter. Signal at Ch.I (channel I) of digital oscilloscope has the same carrier frequency as the PA output. The envelope of it corresponds to $A(t)$ and its phase is constant whereas the signal at Ch.II is the PA output with envelope compression and phase shift depending on $A(t)$. Single tone signal generator, arbitrary waveform generator, quadrature modulator and oscilloscope must be synchronized otherwise there would be a gradually changing phase shift between Ch I and Ch II data and this would result in erroneous determination of AM/PM characteristics. After generating the two port PA model, PTx has been simulated like a transmitter with linear PA in order to see the system performance

with and without DP.

The PA used for characterization measurements is RF3145 operated in GSM mode. This PA has an input port for power ramping (V_{ramp}), which controls an integrated linear regulator. Characterization measurements have been done with an EDGE signal in order to obtain the best characteristics match for EDGE operation. The loop bandwidth of the integrated linear regulator is assumed to be large enough for EDGE envelope signal.

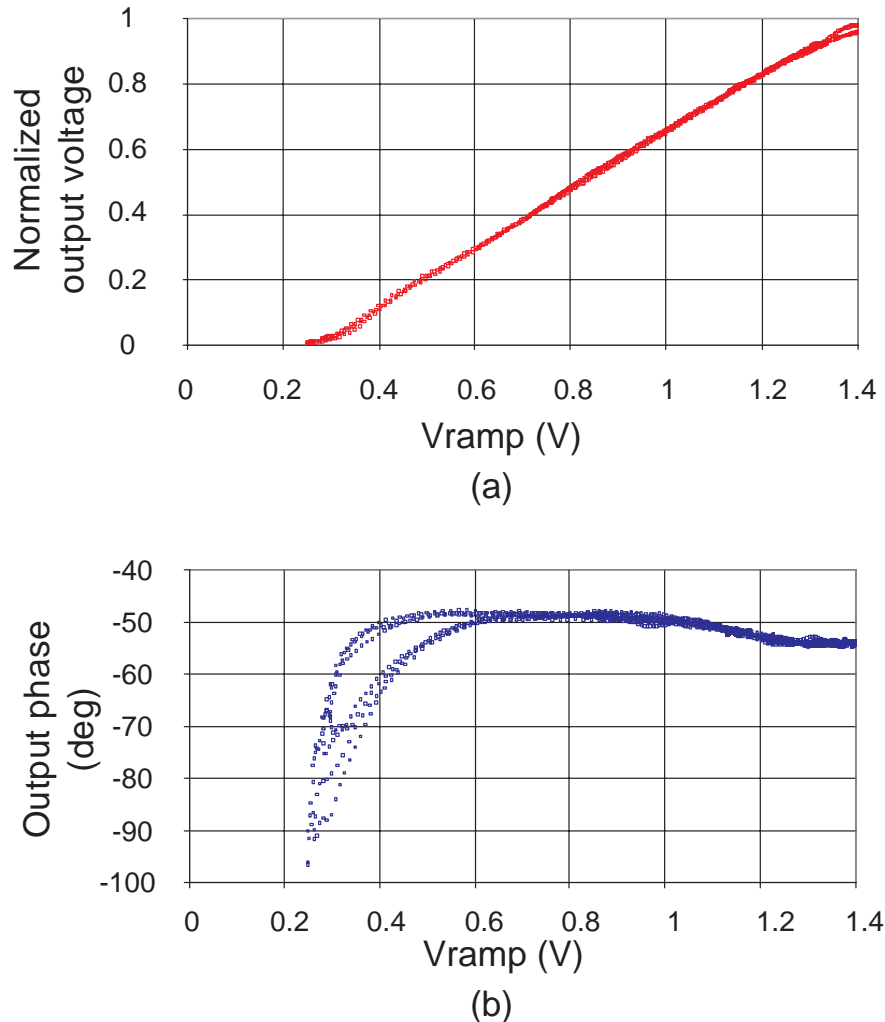


Figure 6.39: (a) Normalized output voltage and (b) output phase characteristics of RF3145 in polar transmitter concept.

Fig. 6.39 (a) and (b) show the obtained normalized output voltage and output phase curves of RF3145 with respect to the input signal magnitude applied to V_{ramp} . Increasing the output voltage and phase nonlinearity with decreasing V_{ramp} is clearly visible. There is also a kind of hysteresis in the phase characteristic for low V_{ramp} , which may be caused by memory effects. There is also noise in the phase characteristics visible at very low values of V_{ramp} . The output voltage approaches to zero if V_{ramp} is about 0.25 V. This means for V_{ramp} voltages lower than this value clipping will occur. The

phase deviation is also very high at this point. This is bad news because mobile communication systems may have high dynamic ranges, which is about 40 dB in EDGE. This problem can be solved by adding a constant DC offset of 0.25 V to V_{ramp} which will shift the characteristics shown in fig. 6.39 (a) to the left and let the curve pass through the origin. In ideal case output voltage should increase linearly with V_{ramp} and phase should be constant, which are supposed to be obtained with linearization. In the following the performance of MDP is investigated.

6.7.2 System performance

Fig. 6.40 shows the measurement setup. The PA is RF3145 in operated in GSM900 mode which has been characterized in the previous section. LUT coefficients have been calculated using the measured characteristics in fig. 6.39 (a) and (b). Used AM and PM signals with and without DP have been generated in ADS separately. AM signal is easy to regenerate by using a baseband arbitrary waveform generator. PM signal has been generated in Cartesian form and sent to another arbitrary waveform generator and then to a quadrature modulator. The PA input power is selected to be 6 dBm in order to keep it in saturation. It has been operated with a duty cycle of 20% to avoid high temperatures. The setup has been adjusted such that the delay mismatch between AM and PM paths is less than 20 ns. This is achieved by changing the delay of the trigger signal from arbitrary waveform generator 1 step by step. Step time is the clock period and is about 40 ns because a clock frequency of 26 MHz has been selected. This results in a maximum delay mismatch equal to the half of clock period.

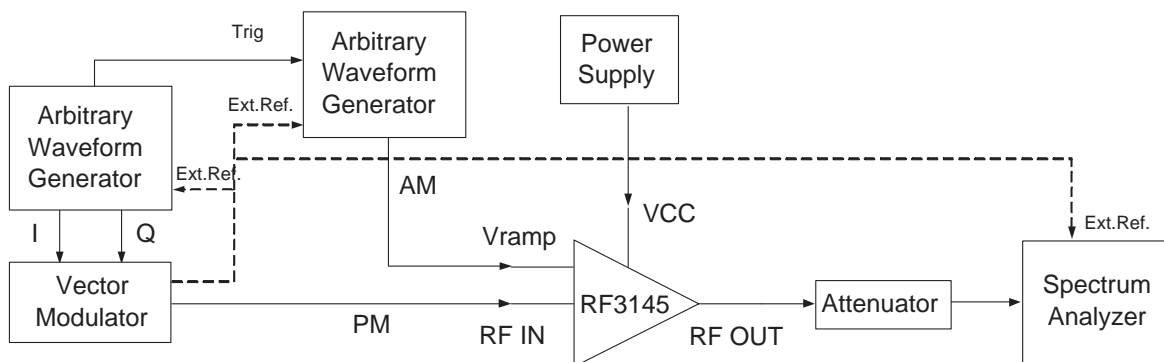


Figure 6.40: Measurement setup for polar transmitter concept with and without predistortion.

Measurements have been done first without DP by setting the constant DC offset to 0.25 V at V_{ramp} . For 29.5 dBm PA output power leakage power values of -33.5, -49 and -57 dBc have been obtained at 200, 400 and 600 kHz offsets respectively meaning that EDGE spectrum is not fulfilled at 400 and 600 kHz offsets without DP. For lower output powers the performance is even worse. However, if linearization is applied, then for 29.5 dBm output power leakage powers of -34, -56 and -62 dBc have been obtained at 200, 400 and 600 kHz offsets respectively. This means EDGE specifications are fulfilled with 4 dB margin at 200 kHz, and 2 dB at 400 and 600 kHz offsets. Fig. 6.41 shows the

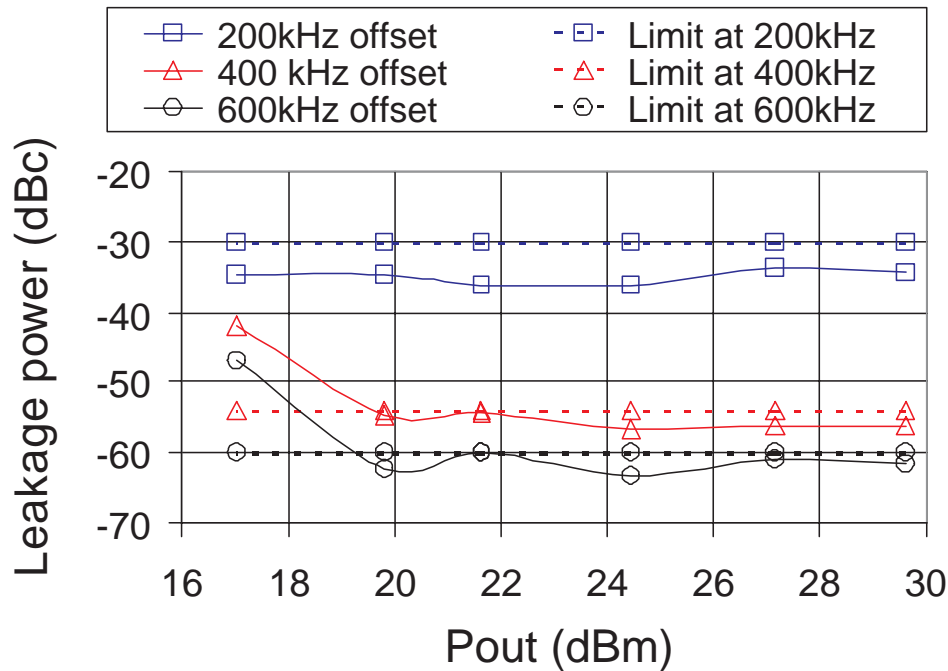


Figure 6.41: Measured leakage power values at 200, 400 and 600 kHz frequency offsets for different output powers with linearization.

measured power values at offset frequencies with linearization. The leakage powers are lower than the limits for output powers from 29.5 down to 20 dBm. However, there is a rapid increase at 400 and 600 kHz for output powers lower than 20 dBm. The reason may be that the PA characteristics obtained for linearization does not match well to real behavior of the PA for low V_{ramp} values. A possible solution is to characterize the PA for lower V_{ramp} values separately. Another possibility is to adjust also the PA bias [37] which was not possible on the RF3145 board. In such a case an increase in the LUT size is expected because PA characteristics change with changing bias conditions and therefore different LUTs are required.

In order to operate a PA in PTx, the DC offset of V_{ramp} should be adjusted depending on PA characteristics. The measurements show that setting DC offset of the V_{ramp} input is not critical if linearization is not applied. However, with linearization even small shifts in DC offset can result in high degradations because a significant mismatch can occur between PA characteristics and the calculated LUT coefficients.

Chapter 7

Conclusions

The usage of spectrum efficient modulation schemes in new generation mobile communication systems is indispensable. However, they require high linearity in their transmitter paths for proper operation due to their non-constant signal envelopes. The main contributor of the nonlinearity in a transmitter is the PA. Therefore PA linearization techniques are very important and are going to be widely used in new generation systems. MDP is one of the most attractive linearization methods for terminal applications due to its relative simplicity, good performance, low size and low cost. In this thesis the performance of LUT based MDP in handset applications is investigated.

The summary of the obtained results is:

- Static and dynamic PA AM/AM and AM/PM characterization methods are compared and an accurate and simple dynamic PA characterization method is proposed. The number of required analog components in the conventional measurement setup is reduced. Behavioral models based on large signal S-parameters usable in system simulations are generated [1, 2]. The resultant behavioral characteristics match to real PAs which in turn results in good linearization performance.
- Different aspects of MDP for EDGE and WCDMA terminal applications are investigated. A nonlinear GSM PA is linearized and tested for EDGE. The maximum deliverable linear output power is increased by 3.5 dB (from 25 dBm to 28.5 dBm) which results in maximum linear output power efficiency improvement from 15% to 23% [2]. The obtained efficiency of 23% at the maximum linear output power of 28.5 dBm is comparable to commercial EDGE PAs but efficiency values at back-offs are superior. Application of MDP in WCDMA using an FPGA for digital signal processing shows that the method is capable of increasing the maximum achievable linear PA output power by 2 dB and the average system efficiency by 20% compared to the available linear PA [3]. Possible efficiency improvement with a DC-DC converter and minimum system requirements on wordlength and LUT size are investigated.
- A novel LUT addressing method called symbol addressing is proposed and tested successfully for terminal applications [4]. It is capable of reducing the required

system clock frequency and the number of mathematical operations and thus the power consumption in digital circuitry. The method is modulation format dependent and the required memory size increases with modulation complexity and linearization accuracy. Measurement and simulations with WCDMA signals show significant ACPR improvement. With a QPSK signal having four points in its constellation improvement of 8 dB for the first and 3 dB for the second adjacent channels have been obtained. With increasing the number of points to eight the obtained improvement is 11 dB for the first and 2 dB for the second adjacent channels. For four point QPSK the required memory size is 4k and for eight point QPSK (or 8-PSK) is 512k words.

- It is verified that LUT based MDP is able to improve linearity of the highly efficient transmitter architecture EER in EDGE handsets. For measurements a commercially available GSM PA is used. A measurement setup for PA characterization is proposed. The PA is operated in saturation for high efficiency. EDGE specifications are fulfilled for 20 to 29.5 dBm output power levels by modulating only the supply voltage which was not possible without DP.

An optimum system operation is not necessarily based on good performance of all used components, but a good joint performance. Therefore the strategy of designing a highly efficient but nonlinear PA and then linearizing it using MDP can improve system performance significantly. For example designing highly efficient and linear wideband PAs is a very difficult task but it is necessary for future multi-mode and multi-band systems. The performance, reliability and flexibility of MDP make it very attractive for such systems. Due to its flexibility MDP can be switched off during low output power transmission where the specifications are fulfilled without MDP and switched on for high output powers or operation in frequency bands where the specifications are not fulfilled without predistortion. Moreover methods based on digital implementation benefit from continuous development of digital ICs which improves the speed and power efficiency. Although DP is known to be a high power consuming and complicated linearization method affordable in base station applications where extremely high linearity is required, the studies show that with a careful system design and optimization DP is also applicable in handsets resulting in significant linearity and efficiency improvement.

7.1 Future work

Understanding the limitations of MDP for different systems and adaptation for reliable operation are important issues to be investigated further. The environmental conditions like sample variations, aging, changing temperature and supply voltage etc can degrade system performance significantly. Implementing adaptive systems is the best solution for mass production. However, the conventional adaptation methods requiring a receiver path may not be always possible to implement due to additional complexity, cost and size. Therefore some simple adaptation methods applicable in terminal applications are required, which may compromise system complexity and performance. Another interesting issue is to investigate the applicability of MDP to nonlinear CMOS PAs which are gaining importance due to their low cost and high integration capability.

PTx is very attractive due to its high efficiency and multi-mode system handling capability with low number of circuit components. Designing a reliable PTx system for multi-mode systems is a great challenge. There are various problems to be faced with in order to achieve this. An efficient supply voltage modulator with high bandwidth signal handling capability is required for amplitude modulation. Delay mismatch between amplitude and phase paths and zero crossing problems are other important issues to be considered. A big step toward PTx implementation is to have a precision PA characterization and performance verification setup in order to understand its limitations and behavior under different conditions.

Bibliography

- [1] N. Ceylan, J.-E. Mueller, R. Weigel, "Optimization of EDGE terminal power amplifiers using memoryless digital predistortion," in *Proc. of the Radio Frequency Integrated Circuits Symposium*, Jun. 2004, pp. 373–376.
- [2] N. Ceylan, J.-E. Mueller, R. Weigel, "Optimization of EDGE terminal power amplifiers using memoryless digital predistortion," *IEEE Transactions on Microwave Theory and Techniques*, vol. 53, pp. 515–522, Feb. 2005.
- [3] N. Ceylan, J.-E. Mueller, T. Pittorino, R. Weigel, "Mobile phone power amplifier linearity and efficiency enhancement using digital predistortion," in *Proc. of the 33rd European Microwave Conference*, Oct. 2003, vol. 1, pp. 269–272.
- [4] N. Ceylan, J.-E. Mueller, R. Weigel, "A new addressing method for look-up table based digital predistortion linearizers," in *Proc. of the International Symposium on Signals, Systems, and Electronics*, Aug. 2004.
- [5] P. B. Kenington, *High-linearity RF amplifier design*, Artech House, Boston, London, 2000.
- [6] F. H. Raab, P. Asbeck, S. Cripps, P. B. Kenington, Z. B. Popovic, N. Potheary, J. F. Sevic, N. O. Sokal, "Power amplifiers and transmitters for RF and microwave," *IEEE Transactions on Microwave Theory and Techniques*, vol. 50, pp. 814–826, Mar. 2002.
- [7] G. L. Madonna, M. Pfof, R. Schultheis and J.-E. Mueller, "Investigations of linearity characteristics for large-emitter area GaAs HBT power stages," in *GAAS Conference*, Sep. 2001, pp. 219–222.
- [8] T. Iwai, S. Ohara, H. Yamada, Y. Yamaguchi, K. Imanishi and K. Joshin, "High efficiency and high linearity InGaP/GaAs HBT power amplifiers: Matching techniques of source and load impedance to improve phase distortion and linearity," *IEEE Transactions on Electronic Devices*, vol. 45, pp. 1196–1200, Jun. 1998.
- [9] F. H. Raab, P. Asbeck, S. Cripps, P. B. Kenington, Z. B. Popovic, N. Potheary, J. F. Sevic, N. O. Sokal, "RF and microwave power amplifier and transmitter technologies-part1," *High Frequency Electronics*, pp. 22–36, May 2003.
- [10] M. Albulet, *RF power amplifiers*, Noble Publishing, Atlanta, GA, 2001.

- [11] B. Sahu, and G. A. Rincon-Mora, "A high-efficiency linear RF power amplifier with a power-tracking dynamically adaptive buck-boost supply," *IEEE Transactions on Microwave Theory and Techniques*, vol. 52, pp. 112–120, Jan. 2004.
- [12] J. K. Cavers, "Amplifier linearization using a digital predistorter with fast adaptation and low memory requirements," *IEEE Transactions on Vehicular Technology*, vol. 39, pp. 374–382, Nov. 1990.
- [13] S. C. Cripps, *RF power amplifiers for wireless communications*, Artech House, Norwood, MA 02062, 1999.
- [14] K. Alvarino, H. Bui, S. Coryell, S. Egolf, H. Jiang, C. Lazinbat, E. T. Spears, D. Spooner and D. A. Teeter, "Next-generation CDMA2000 1X power amplifier modules," *Applied Microwave & Wireless*, vol. 14, pp. 74–84, May 2002.
- [15] F. H. Raab, P. Asbeck, S. Cripps, P. B. Kenington, Z. B. Popovic, N. Pothecary, J. F. Sevic, N. O. Sokal, "RF and microwave power amplifier and transmitter technologies-part2," *High Frequency Electronics*, pp. 22–36, Jul. 2003.
- [16] W. Bakalski, *Integrated microwave power amplifiers*, Ph.D. thesis, Technical University of Vienna, Nov. 2003.
- [17] J. Heiskala, J. Terry, *OFDM Wireless LANs: A Theoretical and Practical Guide*, Sams Publishing, Indianapolis, Indiana, 46290 USA, 2002.
- [18] R. Maeusl, J. Goebel, *Analoge und digitale Modulationsverfahren*, Huethig Verlag, Heidelberg, Germany, 2002.
- [19] T. Halonen, J. Romero, J. Melero, *GSM, GPRS and EDGE performance: Evolution towards 3G/UMTS*, John Wiley & Sons Ltd., West Sussex, England, 2nd edition, 2003.
- [20] M. R. Karim, M. Sarraf, *W-CDMA and CDMA2000 for 3G mobile networks*, McGraw-Hill, New York, 2002.
- [21] 3GPP organizational partners (ARIB, CWTS, ETSI, TI, TTA, TTC), "3rd generation partnership project; Technical specification group GSM/EDGE radio access network; Radio transmission and reception - 3GPP TS 45.005 V6.2.0," Apr. 2003.
- [22] T. Ojanpera, S. D. Gray, "An overview of CDMA2000, WCDMA and EDGE," *Mobile Communications Handbook*, CRC Press LLC, 1999.
- [23] 3GPP organizational partners (ARIB, ATIS, CCSA, ETSI, TTA, TTC), "3rd generation partnership project; Technical specification group radio access network; User equipment (UE) radio transmission and reception (FDD) - 3GPP TS 25.101 V5.11.0," Jun. 2004.
- [24] B. Razavi, "RF transmitter architectures and circuits," in *Proc. of the Custom Integrated Circuits Conference*, May 1999, pp. 197–204.

- [25] P. C. Davis, "Merits and requirements of a few RF architectures," in *Proc. of the 1999 Bipolar/BiCMOS Circuits and Technology Meeting*, Sep. 1999, pp. 62–66.
- [26] A. Bellaouar, "RF transmitter architectures for integrated wireless transceivers," in *11th International Conference on Microelectronics*, Nov. 1999.
- [27] S. Heinen, S. Herzinger, "Transmitter concepts, integration and design trade-offs," *Circuits and Systems for Wireless Communications, Kluwer Academic Publications*, pp. 141–155, Dec. 1999.
- [28] M. Elliott, T. Montalvo, F. Murden, B. Jeffries, J. Strange, S. Atkinson, A. Hill, S. Nandipaku, J. Harrebeck, "A polar modulator transmitter for EDGE," in *Proc. of the International Solid-State Circuits Conference*, Feb. 2004, pp. 190–191.
- [29] Infineon Technologies, "PMB 6258, GSM/EDGE 850/900/1800/1900 voice and data multi-band/multi-mode transceiver," Tech. Rep., Infineon Technologies AG, Balanstrasse 73, D-81541 Munich, 2003.
- [30] M. Tiebout, "Design and optimization of RFCMOS-circuits for integrated PLLs and synthesizers," *Analog Circuit Design, Kluwer Academic Publishers*, pp. 325–337, 2000.
- [31] F. H. Raab, "Intermodulation distortion in Kahn-technique transmitters," *IEEE Transactions on Microwave Theory and Techniques*, vol. 44, pp. 2273–2278, Dec. 1996.
- [32] F.H. Raab, B.E. Sigmon, R.G. Myers and R.M. Jackson, "L-band transmitter using Kahn EER technique," *IEEE Transactions on Microwave Theory and Techniques*, vol. 46, pp. 2220–2225, Dec. 1998.
- [33] M.D. Weiss, F.H. Raab, and Z. Popovic, "Linearity of X-band class-F power amplifiers in high-efficiency transmitters," *IEEE Transactions on Microwave Theory and Techniques*, vol. 49, pp. 1174–1179, Jun. 2001.
- [34] D. K. Su, and W. J. McFarland, "An IC for linearizing RF power amplifiers using envelope elimination and restoration," *IEEE Journal of Solid-State Circuits*, vol. 33, pp. 2252–2258, Dec. 1998.
- [35] E. McCune, W. Sander, "EDGE transmitter alternative using nonlinear polar modulation," in *Proc. of the International Symposium on Circuits and Systems*, May 2003, pp. 594–597.
- [36] E. W. McCune, "GSM/CDMA multimode terminals using polar modulated transmitters," in *Proc. of the 12th Wireless Personal Communications Symposium*, Jun. 2003, pp. 119–127.
- [37] W. B. Sander, S. V. Schell, B. L. Sander, "Polar modulator for multi-mode cell phones," in *Custom Integrated Circuits Conference*, Sep. 2003, pp. 439–445.

- [38] G. Hanington, P.-F. Chen, P. M. Asbeck, and L. E. Larson, "High-efficiency power amplifier using dynamic power-supply voltage for CDMA applications," *IEEE Transactions on Microwave Theory and Techniques*, vol. 47, pp. 1471–1476, Aug. 1999.
- [39] P. Nagle, P. Burton, E. Heaney and F. McGrath, "A wide-band linear amplitude modulator for polar transmitters based on the concept of interleaving delta modulation," *IEEE Journal of Solid-State Circuits*, vol. 37, pp. 1748–1756, Dec. 2002.
- [40] K.-C. Peng, J.-K. Jau, and T.-S. Horng, "A novel EER transmitter using two-point delta-sigma modulation scheme for WLAN and 3G applications," in *MTT-S International Microwave Symposium Digest*, Jun. 2002, pp. 1651–1654.
- [41] R. Booth, S. Schell, T. Biedka and C.-P. Liang, "Reduction of average-to-minimum power ratio in communications signals," May 2003, International publication no. WO 03/036894 A2.
- [42] T.J. Fergus, "EDGE modulation - How linearization improves amplifier performance," *RF Design*, pp. 18–30, Oct. 2002.
- [43] P. Asbeck, G. Hanington, P. F. Chen, and L. Larson, "Efficiency and linearity improvement in power amplifiers for wireless communications," in *20th GaAs Integrated Circuits Symposium Digest*, Nov. 1998, pp. 15–18.
- [44] M. Ranjan, K. H. Koo, G. Hanington, C. Fallesen and P. Asbeck, "Microwave power amplifiers with digitally-controlled power supply voltage for high Efficiency and high linearity," in *MTT-S International Microwave Symposium Digest*, Jun. 2000, pp. 493–496.
- [45] P. B. Kenington, "Linearized RF amplifier and transmitter techniques," Tech. Rep., Wireless Systems International Ltd., Clifton Heights, Triangle West, Bristol BS8 1EJ, UK, 1998.
- [46] L. Sundstroem, "Linear transmitter architectures," *Analog Circuit Design, Kluwer Academic Publishers*, pp. 303–323, 2002.
- [47] S. Mann, M. Beach, P. Warr, J. McGeehan, "Increasing talk-time with efficient linear PAs," in *IEE Seminar on TETRA Market and Technology Developments*, Feb. 2000.
- [48] D. W. Bennett, J. R. MacLeod and J. P. McGeehan, "Broadband high dynamic-range RF transmitter technology for flexible multi-standard radios," in *Proc. of ACTS Mobile Commun. Summit 98*, Jun. 1998, pp. 127–132.
- [49] M. A. Briffa, M. Faulkner, "Stability analysis of cartesian feedback linearization for amplifiers with weak nonlinearities," *IEE Proceedings in Communications*, vol. 143, pp. 212–218, Aug. 1996.
- [50] B. Razavi, *RF microelectronics*, Prentice Hall, Upper Saddle River, NJ 07458, 1998.

- [51] S. P. Stapleton, "Adaptive feedforward linearization for RF power amplifiers," *Microwave Journal*, pp. 136–144, Oct. 1999.
- [52] Y. K. G. Hau, V. Postoyalko and J. R. Richardson, "Compensation of amplifier nonlinear phase response to improve wideband distortion cancellation of feedforward amplifiers," *Electronic Letters*, vol. 33, pp. 500–501, Mar. 1997.
- [53] G. Zhao, F. M. Ghannouchi, F. Beaugard and A. B. Kouki, "Digital implementations of adaptive feedforward amplifier linearization techniques," in *International Microwave Symposium Digest*, Jun. 1996, vol. 2, pp. 543–546.
- [54] S. J. Grant, J. K. Cavers, P. A. Goud, "A DSP controlled adaptive feedforward amplifier linearizer," in *Proc. of International Conference of Universal Personal Communications*, Sep. 1996, pp. 788–792.
- [55] J. K. Cavers, "Adaptation behavior of a feedforward amplifier linearizer," *IEEE Transactions on Vehicular Technology*, vol. 44, pp. 31–39, Feb. 1995.
- [56] E. G. Jeckeln, F. M. Ghannouchi, M. Sawan and F. Beaugard, "Efficient baseband/RF feedforward linearizer through a mirror power amplifier using software-defined radio and quadrature digital up-conversion," in *MTT-S International Microwave Symposium Digest*, Jun. 2001, pp. 789–792.
- [57] K. Yamauchi, K. Mori, M. Nakayama, Y. Itoh, Y. Mitsui, and O. Ishida, "A novel series diode linearizer for mobile radio power amplifiers," in *MTT-S International Microwave Symposium Digest*, Jun. 1996, pp. 831–834.
- [58] S. P. Stapleton, F. C. Costescu, "An adaptive predistorter for a power amplifier based on adjacent channel emission," *IEEE Transactions on Vehicular Technology*, vol. 41, pp. 49–56, Feb. 1992.
- [59] M. Ghaderi, S. Kumar and D. E. Dodds, "Fast adaptive polynomial I and Q predistorter with global optimization," *IEE Proc.-Commun.*, vol. 143, pp. 78–86, Apr. 1996.
- [60] E. Westesson, L. Sundstroem, "A complex polynomial predistorter chip in CMOS for baseband or IF linearization of RF power amplifiers," in *Proc. of the 1999 IEEE International Symposium on Circuits and Systems VLSI*, May 1999, pp. 206–209.
- [61] T. Rahkonen, T. Kankaala, M. Neitola, "A programmable analog polynomial predistortion circuit for linearising radio transmitters," in *Proc. of the 24th European Solid-State Circuits Conference*, Sep. 1998, pp. 276–279.
- [62] P. Andreani and L. Sundstroem, "Chip for wideband digital predistortion RF power amplifier linearisation," *Electronics Letters*, vol. 33, pp. 925–926, May 1997.
- [63] L. Sundstroem, M. Faulkner, and M. Johansson, "Quantization analysis and design of a digital predistortion linearizer for RF power amplifiers," *IEEE Transactions on Vehicular Technology*, vol. 45, pp. 707–719, Nov. 1996.

- [64] K. J. Muhonen, R. Krishnamoorthy, and M. Kavehrad, "Look-up table techniques for adaptive digital predistortion, A development and comparison," *IEEE Transactions on Vehicular Technology*, vol. 49, pp. 1995–2002, Feb. 2000.
- [65] G. Baudoin, P. Jardin, "Adaptive polynomial pre-distortion for linearization of power amplifiers in wireless communications and WLAN," in *Proc. of the International Conference on Trends in Communications*, Jul. 2001, pp. 157–160.
- [66] R. Bauernschmitt, T. Bitzer, G. Woelfle, "Digital predistortion for the linearization of power amplifiers in W-CDMA basestations," in *Conference on Microwaves, Radio Communication and Electromagnetic Compatibility*, May 2001, pp. 350–355.
- [67] K. C. Lee, P. Gardner, "Comparison of different adaptation algorithms for adaptive digital predistortion based on EDGE standard," in *MTT-S International Microwave Symposium Digest*, May 2001, pp. 1353–1356.
- [68] Y. Nagata, "Linear amplification technique for digital mobile communications," in *39th Vehicular Technology Conference*, May 1989, pp. 159–164.
- [69] S. Boumaiza, and F. M. Ghannouchi, "Realistic power-amplifiers characterization with application to baseband digital predistortion for 3G base stations," *IEEE Transactions on Microwave Theory and Techniques*, vol. 50, pp. 3016–3021, Dec. 2002.
- [70] P. Andreani and L. Sundstroem, "A chip for linearization of RF power amplifiers using predistortion based on a bit-parallel complex multiplier," in *Proc. of the International Symposium on Circuits and Systems*, May-Jun. 1999, pp. 25–30.
- [71] J. K. Cavers, "Optimum table spacing in predistorting amplifier linearizers," *IEEE Transactions on Vehicular Technology*, vol. 48, pp. 1699–1705, Sep. 1999.
- [72] J. K. Cavers, "The effect of quadrature modulator and demodulator errors on adaptive digital predistorters for amplifier linearization," *IEEE Transactions on Vehicular Technology*, vol. 46, pp. 456–466, May 1997.
- [73] Q. Wu, J. Qiu, J. Fu, Y. Qin and H. Xing, "High precision RF linearizer by digital predistortion technique," in *Conference on Precision Electromagnetic Measurements Digest*, Jun. 2002, pp. 76–77.
- [74] E. G. Jeckeln, F. M. Ghannouchi and M. Sawan, "An L band adaptive digital predistorter for power amplifiers using direct I-Q modem," in *MTT-S International Microwave Symposium Digest*, Jun. 1998, pp. 719–722.
- [75] A. R. Mansell and A. Bateman, "Adaptive predistortion with reduced feedback complexity," *Electronics Letters*, vol. 32, pp. 1153–1154, Jun. 1996.
- [76] G. Baudoin, P. Jardin, "A new adaptive baseband pre-distortion algorithm for linearization of power amplifiers, Application to EDGE-GSM transmitters," in *Proc. of the European Conference on Wireless Technology*, Oct. 2000, pp. 163–166.

- [77] J. K. Cavers, “New methods for adaptation of quadrature modulators and demodulators in amplifier linearization circuits,” *IEEE Transactions on Vehicular Technology*, vol. 46, pp. 707–716, Aug. 1997.
- [78] A. Brilliant, D. Pezo, “Modulation imperfections in IS54/136 dual-mode cellular radio,” *Microwave Journal, Euro-Global Edition*, vol. 43, pp. 300–312, 2000.
- [79] Q. Ren and I. Wolff, “Influence of some imperfect system performances on linearizers,” in *MTT-S International Microwave Symposium Digest*, Jun. 1998, pp. 973–976.
- [80] L. Sundstroem, M. Faulkner, and M. Johansson, “Effects of reconstruction filters in digital predistortion linearizers for RF power amplifiers,” *IEEE Transactions on Vehicular Technology*, vol. 44, pp. 131–139, Feb. 1995.
- [81] W. Shan, L. Sundstroem, “Effect of anti-aliasing filters in feedback path of adaptive predistortion,” in *MTT-S International Microwave Symposium Digest*, Jun. 2002, pp. 469–472.
- [82] P. Manninen, “Effect of feedback delay error on adaptive digital predistortion,” *Electronics Letters*, vol. 35, pp. 1124–1126, Jul. 1999.
- [83] J. H. K. Vuolevi, T. Rahkonen, and J. P. A. Manninen, “Measurement technique for characterizing memory effects in RF power amplifiers,” *IEEE Transactions on Microwave Theory and Techniques*, vol. 94, pp. 1383–1389, Aug. 2001.
- [84] J. Vuolevi, T. Rahkonen, *Distortion in RF power amplifiers*, Artech House, Boston, London, 2003.
- [85] E. Aschbacher and M. Rupp, “Modeling and identification of a nonlinear power-amplifier with memory for nonlinear digital adaptive pre-distortion,” in *Proc. of the SPAWC Workshop*, Jun. 2003, pp. 555–559.
- [86] H. Ku, M. D. McKinley, and J. S. Kenney, “Quantifying memory effects in RF power amplifiers,” *IEEE Transactions on Microwave Theory and Techniques*, vol. 50, pp. 2843–2849, Dec. 2002.
- [87] W. Boesch and G. Gatti, “Measurement and simulation of memory effects in predistortion linearizers,” *IEEE Transactions on Microwave Theory and Techniques*, vol. 37, pp. 1885–1890, Dec. 1989.
- [88] A. A. Moulthrop, C. J. Clark, C. P. Silva and M. S. Muha, “A dynamic AM/AM and AM/PM measurement technique,” in *MTT-S Digest*, Jun. 1997, pp. 1455–1458.
- [89] M. Eron, E. Martony, Y. Fogel, E. Jeckeln and M. Hrybenko, “Accurate, mid-band characterization and optimization of high power LDMOS amplifier memory properties,” in *MTT-S International Microwave Symposium Digest*, Jun. 2003, pp. 1729–1732.

- [90] Y. Yang, J. Yi, J. Nam and B. Kim, "Behavioral modeling of high power amplifiers based on measured two-tone transfer characteristics," *Microwave Journal*, pp. 90–104, Dec. 2000.
- [91] T. Reveyrand, C. Maziere, J. M. Nebus, R. Quere, A. Mallet, L. Lapierre, J. Sombrin, "A calibrated time domain envelope measurement system for the behavioral modeling of power amplifiers," in *Gallium Arsenide Applications Symposium*, Sep. 2002, pp. 237–240.
- [92] C. Maziere, T. Reveyrand, S. Mons, D. Barataud, J. M. Nebus, R. Quere, A. Mallet, L. Lapierre and J. Sombrin, "A novel behavioral model of power amplifier based on a dynamic envelope gain approach for the system level simulation and design," in *MTT-S International Microwave Symposium Digest*, Jun. 2003, pp. 769–772.
- [93] S. Boumaiza, and F. M. Ghannouchi, "An accurate complex behavior test bed suitable for 3G power amplifiers characterization," in *MTT-S International Microwave Symposium Digest*, Jun. 2002, pp. 2241–2244.
- [94] E. G. Jeckeln, H.-Y. Shih, E. Martony and M. Eron, "Method for modeling amplitude and bandwidth dependent distortion in nonlinear RF devices," in *MTT-S International Microwave Symposium Digest*, Jun. 2003, pp. 1733–1736.
- [95] J. Vuolevi, J. Manninen, T. Rahkonen, "Cancelling the memory effects in RF power amplifiers," in *International Symposium on Circuits and Systems*, May 2001, pp. 57–60.
- [96] J. S. Kenney, W. Woo, L. Ding, R. Raich, H. Ku, and G. T. Zhou, "The impact of memory effects on predistortion linearization of RF power amplifiers," in *Proc. of the 8th International Symposium on Microwave and Optical Tech.*, Jun. 2001, pp. 189–193.
- [97] P. B. Kenington, M. Cope, R. M. Bennett and J. Bishop, "A GSM-EDGE high power amplifier utilizing digital linearization," in *MTT-S International Microwave Symposium Digest*, May 2001, pp. 1517–1520.

Curriculum vitae

PERSONAL DETAILS:

Name: Nazim Ceylan
Date of Birth: 22 October 1976
Place of Birth: Kurtalan/Turkey
Nationality: Turkish
Sex: male
Marital Status: married
No. of Children: 1
Address: Wirtstr. 14, D-81539 Munich, Germany
E-mail: nceylan@gmx.de

EDUCATION:

- 2001-2005: **Philosophy of Doctorate** (Ph.D.) degree from the University of Erlangen-Nuremberg, Germany.
- Subject: “*Linearization of terminal power amplifiers by means of digital predistortion*”
 - Studies done at Infineon Technologies Munich in conjunction with the University of Erlangen-Nuremberg (Prof. Robert Weigel).
- 1998-2000: **Master of Science** (M.Sc.) degree from the University of Kassel, Germany.
- High Frequency Techniques
 - Thesis: “*Design, modelling and simulation of a highly linear power amplifier operating between 2.1-2.2 GHz*”
This thesis has been supported by Alcatel Corp. Research Center, Stuttgart, Germany.
 - The best student with overall grade of 1.5 (the best:1.0 - the worst:5.0)
- 1994-1998: **Bachelor of Science** (B.Sc.) degree from the Middle East Technical University (METU) in Electrical and Electronics Engineering, Ankara, Turkey.
- Microwave and Antenna Engineering
 - Thesis: “*Parameter extraction of a field effect transistor and modelling*”
 - Honour Student with CumGPA of 3.01
- 1993-1994: English Course at METU Language School.

PROFESSIONAL EXPERIENCE:

October 2004 to present

Concept Engineer at Infineon Technologies AG, Munich, Germany

- Research on power amplifier efficiency improvement techniques
- Simulation and measurement of innovative TX-Architectures
- Automation of a PA characterization, linearization and performance verification setup

October 2001 to September 2004

PhD Student (Researcher) at Infineon Technologies AG, Munich, Germany

- Research on power amplifier (PA) linearization techniques, especially digital predistortion.
 - Investigations on possible simplifications in the conventional digital predistortion architectures in order to have simple systems with good performance in terminal PAs.
 - Measurement of memoryless digital predistortion performance in WCDMA transmitters using an FPGA.
 - Investigation of the applicability of memoryless digital predistortion in EDGE terminal PAs with and without adaptation.
 - Quantization analysis of digital predistortion systems by means of simulations.
- Simulation and measurement of innovative TX-Architectures for multi-mode terminal applications
 - Investigations on linearity, efficiency, stability against load mismatch etc. of different signal amplification structures like linear PA, EER, linear PA with DC-DC converter.
 - System level simulation of mobile communication systems (WCDMA, EDGE) using behavioural and transistor level PA models with and without digital predistortion.
 - Simulation and measurement of a highly efficient transmitter architecture called Envelope Elimination and Restoration (EER) with and without digital predistortion.
- Characterization of power amplifier AM-AM and AM-PM nonlinearities by measurements and behavioural modeling.
- Defining various tasks related to the research subjects and coaching students and interns working on these tasks.

November 2000 to September 2001

Application Design Engineer at Infineon Technologies AG, Munich, Germany

- Design, PCB layout and measurement of GSM application boards using Infineons transceiver ICs.
- Measurement of application board samples using automated test setups (done with Labview) and preparation of the related application notes for customers.
- Simulation and Design of PLL loop filters for GSM synthesizers in order to improve lock-in time and optimize phase noise.

May 1999 to February 2000

Student assistant on part time basis at the University of Kassel, Germany

- Simulation of a frequency tripler in HP MDS.
- Supervising new coming foreign students accepted to the International M.Sc. Program in EE: finding rooms, registering to german foreigner authorities, university matriculation, german-english interpreter etc.

April 1998 to September 1998

RF Engineer at MIKES A.S., Ankara, Turkey

- Simulation and measurement of radar systems.
- Endurance tests of the components used in radar systems.

Fall term 1997

Student assistant in the Microwave Course Laboratory on part time basis at METU, Ankara, Turkey

- Preparing experiment setups.
- Supervision during student experiments.

SKILLS:

Languages: Fluent in English and German, Turkish as native language.

Computer:

Circuit Simulation: HP ADS (Digital & Analog) and MDS, Matlab, CADENCE (little),
Modelsim, Xilinx ISE.

Layout: PROTEL

Programming: Turbo Pascal, VHDL

PC: Windows 95/98/2000/XP, MS Office, Visio, Adobe

INTERESTS:

Playing chess and soccer, also interested in watching both. Cinema and listening to music.

PUBLICATIONS:

1. N. Ceylan, J.-E. Mueller, T. Pittorino and R. Weigel, “*Mobile phone power amplifier linearity and efficiency enhancement using digital predistortion*”, in Proc. of the 33rd European Microwave Conference, Oct. 2003, vol. 1, pp. 269-272.
2. N. Ceylan, J.-E. Mueller and R. Weigel, “*Optimization of EDGE terminal power amplifiers using memoryless digital predistortion*”, in Proc. of the Radio Frequency Integrated Circuits Symposium, Jun. 2004, pp. 373-376.
3. N. Ceylan, J.-E. Mueller and R. Weigel, “*A new addressing method for LUT based digital predistortion linearizers*”, in Proc. of the International Symposium on Signals, Systems and Electronics, Aug. 2004.
4. N. Ceylan, J.-E. Mueller and R. Weigel, “*Optimization of EDGE terminal power amplifiers using memoryless digital predistortion*”, IEEE Transactions on Microwave Theory and Techniques, vol. 53, pp. 515-522, Feb. 2005.

Inhaltsverzeichnis

1. Einleitung	1
1.1 Gliederung der Dissertationsarbeit	2
2. Leistungsverstärker	4
2.1 Grundlagen der Leistungsverstärker	4
2.1.1 Verstärkung und Ausgangsleistung	4
2.1.2 Linearität	4
2.1.3 Wirkungsgrad	8
2.1.4 Back-off	10
2.1.5 Anpassung	11
2.2 Verstärker Klassen	12
2.2.1 Klasse A Verstärker	13
2.2.2 Klasse B Verstärker	14
2.2.3 Klasse AB Verstärker	15
2.2.4 Klasse C Verstärker	17
2.2.5 Klasse D Verstärker	17
2.2.6 Klasse E Verstärker	18
2.2.7 Klasse F Verstärker	19
2.3 Verstärker Topologien	20
2.3.1 Single-ended Leistungsverstärker	20
2.3.2 Differential Leistungsverstärker	21
2.3.3 Balancierte Leistungsverstärker	21
2.4 Die untersuchte Leistungsverstärker	22
3. Mobilfunk	23
3.1 Digitale Modulationsarten	23
3.1.1 Amplitudenumtastung (ASK)	24
3.1.2 Phasenumtastung (PSK)	24
3.1.3 Quadratur-Amplitudenmodulation (QAM)	26
3.1.4 Gauss'sche Minimumumtastung (GMSK)	26
3.2 Zellular Systeme	27
3.2.1 GSM/EDGE	28
3.2.2 WCDMA/CDMA2000	30
4. HF Sender	33
4.1 Sender Architekturen	33
4.1.1 Direkt-Konvertierung (homodyne) Architektur	33
4.1.2 Zwei-Schritt-Konvertierung (heterodyne) Architektur	35
4.1.3 Modulationsschleife	36
4.1.4 Polar-Modulator	37
4.2 Nichtlineare Sender	37
4.3 Lineare Sender	38
4.3.1 Linearer Sender mit linearem Leistungsverstärker	39
4.3.2 Envelope-Elimination and Restoration (EER) / Polar-Sender (PTx)	39
4.3.3 Polar-Loop-Sender (PLTx)	43
4.3.4 Hüllkurvenfolger	44
4.3.5 Leistungsverfolgung	45

5. Linearisierungsmethoden der Leistungsverstärker	47
5.1 Rückkopplung (Feedback)	47
5.1.1 HF-Rückkopplung	48
5.1.2 Polar-Schleife	49
5.1.3 Kartesische-Schleife	50
5.2 Feedforward	51
5.3 Vorverzerrung	53
5.3.1 Analoge Vorverzerrung	54
5.3.2 Digitale Vorverzerrung	56
5.4 Gedächtnislose digitale Vorverzerrung (MDP)	58
5.4.1 Look-up Tabelle (LUT) basierte Vorverzerrung	59
5.4.2 Polynomische Vorverzerrung	68
5.4.3 Effekte von Systemunvollkommenheiten	71
5.5 Vorverzerrung der Leistungsverstärkern mit Gedächtnis	74
6. Gedächtnislose digitale Vorverzerrung für Terminals	78
6.1 Leistungsverstärker Charakterisierung	79
6.2 Anwendung der MDP in EDGE	87
6.2.1 Systemleistung	89
6.2.2 Quantisierungsanalyse	93
6.2.3 Effekte von Antennenfehlanpassung	95
6.2.4 Benötigte Systemmodifikationen	97
6.3 Anwendung der MDP in WCDMA	101
6.4 MDP für Leistungsverstärker mit DC-DC Wandler	105
6.5 Symbol Adressierung	109
6.6 MDP Implementierung als offene und geschlossene Schleife	115
6.6.1 Offene Schleife	116
6.6.2 Geschlossene Schleife	117
6.7 Anwendung der MDP in Polar-Sender-Konzept	120
6.7.1 PA Charakterisierung	120
6.7.2 Systemleistung	123
7. Zusammenfassung	125
7.1 Ausblick	126

Einleitung

Produkte im Bereich der mobilen Kommunikation gewannen im letzten Jahrzehnt immer mehr an Bedeutung in unserem Alltagsleben. Diese Entwicklung scheint sich weiter fortzusetzen. Hersteller versehen ihre Produkte mit neuen Funktionalitäten und Diensten, um neue Kunden zu gewinnen. Das zwingt sie, neue Systemtopologien zu benutzen, den Energieverbrauch zu senken, die Systemintegration zur Verlängerung der Batterielebensdauer zu verbessern und die Größe und die Kosten ihrer Produkte zu reduzieren.

Mehr Teilnehmer und neue Dienste erfordern größere Bandbreiten im Frequenzspektrum, die wegen der momentanen Auslastung des Spektrums eingeschränkt verfügbar sind. Die Lösung besteht darin, Modulationsformate zu implementieren, die das Frequenzspektrum effizient ausnutzen, wie sie in mobilen Kommunikationssystemen der Generation 2.5 und 3 (2.5G, 3G) eingesetzt werden. Bekannte Beispiele sind EDGE (Enhanced Data for GSM Evolution) und UMTS (Universal Mobile Telecommunications System) in Europa. Gegenüber Systemen der zweiten Generation (2G), wie z.B. GSM (Global System for Mobile Communications), in denen die Phase des Trägers moduliert und seine Einhüllende konstant gehalten wird, wird in 2.5G und 3G Systemen die Amplitude des Trägers (Signaleinhüllende) zusätzlich moduliert. Durch diese Erweiterung stellt sich eine Effizienzsteigerung des Spektrums (übertragene Bits/Hz) im Vergleich zu 2G Systemen ein. Dieser Gewinn an Bandbreite bringt neue Herausforderungen für die Entwicklung von Leistungsverstärkern.

Durch den Umstand, dass die Signale eine nichtkonstante Einhüllende haben, sind mobile Kommunikationssysteme der neuen Generation ggü. Nichtlinearitäten in ihrem Transmitterpfad sehr empfindlich. Signifikante Nichtlinearitäten werden bei einem Transmitter meistens durch den Leistungsverstärker am Ende der Verarbeitungskette erzeugt. Um die gewünschte Linearität zu erhalten, wird der Leistungsverstärker im sog. Back-off, d.h. im linearen Bereich seiner Kennlinie, betrieben. Dies hat zur Folge, dass der Leistungsverstärker jedoch mit geringem Energiewirkungsgrad arbeitet, was bei phasenmodulierten 2G Systemen mit einer konstanten Einhüllenden nicht der Fall ist. Falls die Anforderungen an die Systemlinearität streng sind, wird der Wirkungsgrad dadurch schlechter ausfallen, weil der Leistungsverstärker noch weiter im Back-off betrieben werden muss. Da der Leistungsverstärker die Komponente mit dem höchsten Leistungsverbrauch bei einem Mobilfunksender ist, hat jede kleine Änderung an seinem Wirkungsgrad eine signifikante Auswirkung auf die Effizienz des Gesamtsystems. Eine geringere Effizienz reduziert die Gesprächszeit. Eine lange Gesprächszeit ist insbesondere bei batteriebetriebenen mobilen Endgeräten sehr wichtig. Außerdem wird bei Systemen mit niedrigem Wirkungsgrad ein signifikanter Teil der Energie als Wärme abgegeben, welches hohe Gehäusetemperaturen verursachen kann.

Hohe Anforderung an die Linearität einer Senderarchitektur macht das Design von Leistungsverstärkern schwierig, weil es gleichzeitig linear und hocheffizient sein soll. Linearisierungstechniken können angewendet werden, um die Linearität zu erhöhen, den Umfang des benötigten Back-off zu reduzieren und somit den Wirkungsgrad des Leistungsverstärkers zu verbessern. Es gibt unterschiedliche Arten von Linearisierungstechniken, die unter drei Hauptgruppen klassifiziert werden können: Feedback, Feedforward und Vorverzerrung. Im Rahmen dieser Arbeit wird die Linearisierung von Leistungsverstärkern auf die Untersuchung von sog. "Look-up"-Tabellen basierter, gedächtnisloser digitaler Vorverzerrung (MDP) eingeschränkt. Dieser ist wegen seiner Einfachheit, seinem geringem Energieverbrauch, seiner Zuverlässigkeit und Flexibilität, auf Leistungsverstärker von Mobiltelefonen (auch Endgerät genannt) anwendbar. Desweiteren verursacht dieses Verfahren niedrige Kosten, ist flächensparend und erzielt im Ganzen eine signifikante Leistungsverbesserung.

In heutigen mobilen Kommunikationssystemen ist die Gesamtssystemleistung wichtig. Das bedeutet; die einzelnen integrierten Schaltkreise (IC) müssen nicht unbedingt hochleistungsfähig sein aber die Systeme, die aus diesen ICs bestehen und innerhalb eines entsprechenden Architekturansatzes eingebettet sind, erfordern Hochleistungsfähigkeit im Hinblick auf Linearität und Wirkungsgrad. Das macht digitale Vorverzerrung (DP) attraktiv, weil Leistungsverstärker hinsichtlich ihrer hohen

Leistungsfähigkeit entworfen werden können, und die Linearität gleichzeitig durch DP verbessert werden. Die Kombination von beidem sorgt also für Designflexibilität beim Erreichen guter Linearität und hoher Effizienz. Die zusätzlichen Bemühungen für den Prozessor werden langfristig durch eine schnelle und kontinuierliche Verbesserung der digitalen IC Technologie begünstigt, da deren Leistungsfähigkeit Nutzen aus der Geräteskalierung zieht. Durch sinkenden Energieverbrauch, weiter ansteigende erreichbare Taktfrequenzen, sind digitale ICs flexibler und robuster im Vergleich zu analogen ICs. DP ist eine vielversprechende Linearisierungstechnik, weil in Zukunft immer mehr Aufgaben im digitalen Einsatzgebiet viel einfacher zu lösen sein werden.

Gliederung der Dissertationsarbeit

In Kapitel 2 wird ein allgemeiner Überblick zu Leistungsverstärkern gegeben. Die grundlegenden Begriffe wie Verstärkung, Linearität, Wirkungsgrad usw. werden erklärt, unterschiedliche Leistungsverstärkerklassen und Topologien werden besprochen. Die Leistungsverstärker, die bei der Arbeit zum Einsatz kamen, werden diskutiert.

Kapitel 3 stellt die 2G, 2.5G und 3G mobilen Kommunikationssysteme GSM, EDGE, CDMA200 (Code Division Multiple Access 2000) und WCDMA (Wideband CDMA) dar. Ihre Systemkapazität, ihre Vor- und Nachteile werden erwähnt und ihre Spezifikationen insbesondere hinsichtlich angrenzender Channel Power Ratio und Fehlervektorbeträge werden erklärt; die Folgen der Nichtlinearitäten von Leistungsverstärkern werden diskutiert.

Verschiedene Transmitterarchitekturen werden im Kapitel 4 im Hinblick auf ihre Vor- und Nachteile für zukünftige Transmitterarchitekturen von hochleistungsfähigen Endgeräten beschrieben. Diese sind nichtlineare Transmitter, wie bei GSM, lineare Transmitter, wie bei EDGE, WCDMA oder CDMA200, aber auch polare Transmitter, die sowohl mit linearen als auch nichtlinearen Systemen gleichzeitig umgehen können.

Linearisierungsmethoden werden im Detail in Kapitel 5 erläutert. Diese können hauptsächlich als Feedback-, Feedforward- und Vorverzerrungssysteme klassifiziert werden, wobei verschiedene Implementierungsarten (polar, kartesisch, digital, analog) möglich sind. DP Systeme mit der Fähigkeit, Memory-Effekte zu korrigieren, sind komplex und können in Basisstationen angewendet werden. MDP hat in Leistungsverstärkern von Endgeräten, wegen ihres geringen Memory-Effektes, eine gute Leistungsfähigkeit und ist mit ihrem geringen Energieverbrauch, ihrer Zuverlässigkeit und ihrer Flexibilität einfach zu implementieren. Weiterhin ist sie preiswert und nimmt kleine Räume ein. Dieses Kapitel konzentriert sich damit auf die Vorverzerrung und erläutert sie ausführlich.

Im Kapitel 6 werden AM/AM und AM/PM Charakterisierungsmethoden von statischen und dynamischen Leistungsverstärkern verglichen. Die Anwendung von MDP in EDGE und WCDMA Endgeräten mittels Leistungsverstärkern in linearer Betriebsart wird untersucht. Notwendige Systemmodifikationen in verfügbaren Systemen und eine mögliche Leistungsverbesserung mit einem DC-DC Wandler werden auch betrachtet. Eine neue Adressierungsmethode, die in Transmittern mit kartesischen Basisbandsignalen brauchbar ist, wird vorgeschlagen und ist erfolgreich getestet worden. Es werden auch einige neuartige open- und closed-loop MDP Implementierungen vorgeschlagen, die in Endgeräteapplikationen anwendbar sind. Außerdem wird auch die Anwendung von MDP in EER untersucht.

Kapitel 7 schließt die Arbeit ab und weist auf mögliche zukünftige Tätigkeiten hin, um die vorgeschlagene Methode in mobilen Kommunikationssystemen zu implementieren.

Zusammenfassung

Der Einsatz von Spektrum-Effizienten Modulationsmethoden in neuen Generationen von mobilen Kommunikationssystemen ist unentbehrlich. Jedoch erfordern sie zum einwandfreien Betrieb, wegen der nicht-konstanten Hüllkurven ihrer Signale, eine hohe Linearität in ihren Senderarchitekturen. Der Großteil der Nichtlinearitäten in einem Sender wird durch den Leistungsverstärker verursacht. Deshalb sind die PA-Linearisierungstechniken sehr wichtig und werden häufig in neueren Systemen verwendet. MDP ist, wegen ihrer Überschaubarkeit, ihren guten Leistungsmerkmalen hinsichtlich ihres Wirkungsgrades, ihrer geringen Größe und den niedrigen Kosten, eine der interessantesten Linearisierungsmethoden für Terminal-Anwendungen. In dieser Arbeit wird die Leistung der auf LUT basierten MDP in Mobiltelefon-Anwendungen untersucht. Die Ergebnisse dieser Untersuchung ergaben übereinstimmende Charakteristika zu realen Leistungsverstärkern, was in einer hohen Leistungsfähigkeit der Linearisierungsmethode resultiert.

Zusammenfassung der wichtigsten Ergebnisse

- Statische und dynamische Leistungsverstärker AM/AM- und AM/PM-Charakterisierungsmethoden wurden verglichen und eine genaue und einfache dynamische PA-Charakterisierungsmethode wurde vorgeschlagen. Die Anzahl der erforderlichen analogen Komponenten im konventionellen Messaufbau wurde dadurch reduziert. Verhaltensmodelle wurden entwickelt, die auf Groß-signal S-Parameter basieren und in der Systemsimulationen verwendbar sind [1, 2]. Resultierende Verhaltensmerkmale passen zu tatsächlichen Leistungsverstärkern, welche wiederum eine gute Leistungsfähigkeit der Linearisierung mit sich bringt.
- Verschiedene Aspekte von MDP für EDGE und WCDMA Terminal-Anwendungen wurden untersucht. Ein nichtlineares GSM- Leistungsverstärker wurde linearisiert und für EDGE getestet. Die maximal erreichbare lineare Ausgangsleistung wurde um 3,5 dB (von 25 dBm zu 28,5 dBm) erhöht. Das bedeutet eine Verbesserung des Wirkungsgrads von 15% auf 23% [2]. Die Wirkungsgrad-steigerung auf 23% bei einer Ausgangsleistung von 28,5 dBm ist mit kommerziellen EDGE Leistungsverstärkern vergleichbar. Aber der Wirkungsgrad ist im back-off besser. Bei Anwendung der MDP in WCDMA mit einem FPGA anstelle eines DSP zeigt, dass diese Methode geeignet ist, die maximal erzielbare lineare Verstärker-Ausgangsleistung um 2 dB zu steigern und, im Vergleich zu verfügbaren linearen Leistungsverstärkern, den durchschnittlichen Systemwirkungsgrad um 20% zu erhöhen [3]. Die mögliche Wirkungsgradverbesserung mit einem DC-DC-Wandler und die minimalen Systemanforderungen auf Wortlänge und LUT Größe wurden untersucht.
- Für Terminal-Anwendungen wurde eine neue LUT-Adressierungsmethode (die sog. Symboladressierung) vorgeschlagen und erfolgreich getestet[4]. Diese Methode bewirkt eine deutliche Reduktion der erforderlichen Systemtaktfrequenz und der Anzahl von mathematischen Vorgängen, womit gleichzeitig der Stromverbrauch in digitalen Schaltkreisen verringert wird. Die Methode ist vom Modulationsformat abhängig. Die notwendige Speichergröße nimmt mit der Komplexität der Modulation und der Linearisierungsgenauigkeit zu. Messungen und Simulationen mit WCDMA Signalen zeigen eine deutliche Verbesserung der ACPR. Für ein QPSK-Signal mit vier Konstellationspunkten wurde eine Verbesserung von 8 dB für den ersten und 3 dB für den zweiten Nachbarkanal erreicht. Nach der Erhöhung der Anzahl der Konstellationspunkte auf acht (8-PSK), wurde eine Verbesserung von 11 dB für den ersten und 2 dB für die zwei benachbarten Kanäle erreicht. Die erforderliche Speichergröße beträgt für 4-PSK (QPSK) 4k-Worte und für 8-PSK 512 k-Worte.
- Es wurde gezeigt, dass die auf LUT basierende MDP dazu fähig ist, die Linearität der hoch-effizienten Senderarchitektur EER in EDGE Mobiltelefonen zu verbessern. Für Messungen wurde dazu eine handelsübliche GSM- Leistungsverstärker eingesetzt. Ein Messaufbau für Leistungsverstärker-Beschreibung wurde vorgeschlagen, wobei der PA in Sättigungsbereich

betrieben wurde. Durch die Modulation der Versorgungsspannung wurden EDGE-Spezifikationen für 20 bis 29,5 dBm Ausgangsleistung erfüllt, was ohne DP nicht möglich war.

Für einen optimalen Betrieb ist nicht die Leistung der einzelnen Systemkomponente, sondern die Leistung des gesamten Systemverbundes ausschlaggebend. Deshalb kann mit dem Konzept, zunächst ein hocheffizientes, aber nicht-lineares Leistungsverstärker entworfen werden, um dann die MDP zur Linearisierung einzusetzen, womit die Systemleistung bedeutend verbessert wird. Beispielsweise ist es sehr schwierig, hocheffiziente und lineare Breitband Leistungsverstärker zu implementieren, was eine sehr wichtige Anwendung für zukünftige Multi-Mode und Multi-Band Systeme sein wird. Für solche Systeme ist die MDP, wegen ihrer Leistung, Zuverlässigkeit und ihrer Flexibilität, besonders attraktiv. Aufgrund ihrer Flexibilität kann die MDP, ein- oder ausgeschaltet werden, je nachdem, ob die Spezifikationen (ohne Vorverzerrung) erfüllt wird oder nicht. Außerdem können Methoden, die auf digitalen Implementierungen basieren, von der kontinuierlichen Weiterentwicklung von digitalen ICs, die an Geschwindigkeit und Effizienz verbessert werden, profitieren. Obwohl die DP das Ansehen hat, ein hoher Stromverbraucher und zugleich eine komplizierte Linearisierungsmethode zu sein, die nur für spezifische Anwendungen (z.B. Basisstationen mit extrem hoher Linearitätsanforderung) wirtschaftlich ist, zeigen die Studien, dass sie mit einem sorgfältigen und optimierten Systementwurf auch in mobilen Endgeräten einsetzbar ist und zu einer bedeutsamen Linearitäts- und Effizienzverbesserung führt.

Ausblick

Das Verstehen der Beschränkungen von MDP für verschiedene Systeme und eine Anpassung für die zuverlässige Operation sind wichtige Aufgaben, die weiter untersucht werden sollten. Die Umweltbedingungen wie z.B. Parameterschwankungen, das Altern, Temperatur- und Versorgungsspannungs-Schwankungen können die Systemleistung beeinflussen. Für ein marktreifes Produkt sollten deswegen adaptive Systeme bevorzugt werden. Jedoch ist der Einsatz von herkömmlichen Anpassungsmethoden, die einen Empfänger-Pfad benötigen, wegen der zusätzlichen Komplexität, Kosten und Größe nur bedingt möglich. Deshalb sind in Mobiltelefon-Anwendungen einfache Anpassungsmethoden erforderlich, die ein Kompromiss zwischen System-Komplexität und -Leistung finden. Eine andere interessante Aufgabe ist die Untersuchung der Anwendbarkeit von MDP bei nichtlinearen CMOS Leistungsverstärkern. Diese sind interessant wegen ihrer niedrigen Kosten und der hohen Integrationsfähigkeit.

PTx ist sehr attraktiv wegen seinem hohen Wirkungsgrad und der Multi-Mode Fähigkeit mit einer niedrigen Anzahl von eingesetzten Bausteinen. Der Entwurf eines zuverlässigen PTx Systems für Multi-Mode-Systeme stellt eine große Herausforderung dar. Hierzu müssen verschiedene Probleme gelöst werden. Ein breitbandiger und effizienter Versorgungsspannungs-Modulator ist für Amplituden-Modulation erforderlich. Die Verzögerungsfehlanspassung zwischen Amplituden- und Phasen-Pfad, der Nulldurchgang des Amplituden-Signals sind hierbei die Hauptaufgaben. Ein großer Schritt zur PTx Implementierung ist die Erstellung eines PA Charakterisierungs- und Leistungsüberprüfungs-Aufbau, damit System-Beschränkungen und -Verhalten unter verschiedenen Bedingungen untersucht werden können.